



**University of
Reading**

Neuroestrogens in the Mouse
Hypothalamus: Synthesis, Regulation,
and Behavioural Implications Using
Novel *Ex Vivo* Slice Culture and *In Vivo*
Models

This dissertation is submitted for the degree of

Doctor of Philosophy

School of Biological Sciences

University of Reading

Janine L Dovey

October 2023

Declaration

I, Janine L Dovey, confirm that the work presented in this thesis is my own. Where information has been derived from other sources, I confirm that this has been indicated and fully acknowledged.

Janine L Dovey

October 2023

Abstract

17 β -oestradiol significantly influences several physiological processes, many of which are linked to the central nervous system. Oestrogen receptors (ERs) are widespread throughout the brain, including the social behaviour network (SBN): a conserved set of hypothalamic and limbic nuclei underlying sexually dimorphic social behaviours. Previous research has shown confirmed the brain's capacity to synthesise its own oestrogens, termed neuroestrogens, albeit with a focus on the hippocampus. The hypothalamus has garnered less attention in this regard. Despite evidence that hypothalamic aromatase is active, direct quantification of neuroestrogens in this region or in the nodes of the social behaviour network have not been performed. This highlights a significant gap in knowledge, as neuroestrogens bear the potential to serve as critical modulators within the SBN. Furthermore, how neuroestrogen synthesis is regulated in the female in the face of abundant gonadal oestrogens is unknown.

To address this gap, we developed a novel method to measure neuroestrogens within the SBN, allowing us to understand how neuroestrogen synthesis is regulated in two major hypothalamic SBN nuclei. We have demonstrated that neuroestrogens were still measurable in ovariectomised mice, underscoring the autonomous steroidogenic capacity of the SBN. We also demonstrated the presence of a novel, androgen-dependent regulatory pathway that regulates neuroestrogen synthesis in the female medial preoptic area (mPOA) but not in the ventromedial hypothalamus (VMH), suggesting nuclei-specific regulation of neuroestrogen production. We have demonstrated that disruption of this pathway *in vivo* has a subtle anxiogenic effect, correlated with dendritic atrophy and reduced spine density in the female mPOA, akin to that observed in ovariectomised mice. Finally, we used a unique conditional aromatase knockout mouse to understand how neuroestrogen synthesis within discrete hypothalamic SBN nuclei contributes to behaviour. In doing this, we showed hypothalamo-limbic aromatase regulates anxiety but not sex or aggressive behaviours in the male mouse.

Acknowledgements

Thank you to my supervisors, Dr Nandini Vasudevan and Prof Phil Knight, for their guidance, supervision, and valuable inputs to my research that have undoubtedly made me a better scientist. Thank you also to Dr Tim Wells of Cardiff University, who put me on the path of a PhD in the first place. I would also like to thank my collaborators at the University of Tsukuba for their hospitality and patience during my visit. I'm so grateful to have had the experience of working in Japan and I've made many wonderful memories. Japan now holds a special place in my heart, and I can't wait to go back one day.

I am indebted to my lab gals and soon to be Drs, DeAsia Davis and Ruby Vajaria, without whom I would probably not have made it to this point of my PhD. The best thing I've taken from these four years is our friendship. Thank you for your unending support (both emotionally and academically!). I can't wait to see you both do great things in the future. I would be remiss not to mention Leah Napier and Meg Donnelly, with whom it has been a pleasure to share Hopkins lab. Thank you also to Gio and Rosie, who have been instrumental in the data collection during the last year of my research.

I would like to express my deepest appreciation to my friends outside of academia, for being a great source of distraction and reminding me that there's so much more to life outside of my PhD. Specific thanks to Kate and Gee, my bestest friends, and Maddy and Avrelina, who were once strangers in an HMO but are now like sisters. Thank you also to my mom and nan, for always being at the other end of the phone after a long day of experiments.

Finally, I could not have undertaken this journey without my partner and best friend, Rhys. Even when we were living 100+ miles away from each other, you were my main source of encouragement and support through all the highs and lows. Thank you for your unwavering love, understanding, patience, and nice times during the most stressful period of my life. You probably deserve this PhD just as much as me for all the times you've listened to me talk about it! I would also like to thank our cats, Beans, Twts, and Lilu for providing much needed emotional support as I have written this thesis.

To Dad, who I miss every day, and Mom.

You always told me to work hard in school. This is for you.

Table of Contents

xi	LIST OF FIGURES
xv	LIST OF TABLES
xvi	ABBREVIATIONS
1	CHAPTER 1: INTRODUCTION
2	1.1 Neurosteroids
2	1.1.1 Steroid hormones
3	1.1.2 Steroid hormone synthesis
6	1.1.3 Aromatase
8	1.1.4 Neuroestrogens
10	1.2 Oestrogen receptors
11	1.2.1 Genomic oestrogen receptor signalling
12	1.2.2 Nongenomic oestrogen receptor signalling
16	1.3 The social behaviour network
18	1.3.1 The organisation-activation hypothesis
20	1.3.2 Organisation and activation of the medial preoptic area (mPOA)
22	1.3.3 Organisation and activation of the ventromedial hypothalamus (VMH)
23	1.4 Behavioural effects of neuroestrogen
23	1.4.1 Contribution of E ₂ to reproductive behaviour in male and female mice
25	1.4.2 Contribution of E ₂ to aggression in rodents
26	1.4.3 Contribution of E ₂ to anxiety in rodents
29	1.4.4 Oestrogen-mediated spinogenesis
31	1.5 Experimental rationale
34	CHAPTER 2: MATERIALS AND METHODS
35	2.1 Mice
36	2.1.1 Aromatase-flox (Aro ^{fl/fl}) mice
38	2.2 Surgical procedures
38	2.2.1 Ovariectomy
38	2.2.2 Hormone priming
38	2.2.3 Intraperitoneal injections
39	2.2.4 Stereotaxic surgery
42	2.2.5 Olfactory bulbectomy
42	2.3 Behavioural experiments

42	2.3.1 Open field test (OFT)
44	2.3.2 Elevated plus maze (EPM)
45	2.3.3 Light-dark test (LDT)
45	2.3.4 Social investigation test (SIT)
47	2.3.5 Running wheel
47	2.3.6 Sexual behaviour
47	2.3.7 Aggressive behaviour
48	2.4 Perfusion fixation
48	2.5 Oestrous staging
50	2.6 Plasma collection
50	2.7 Preparation of ex vivo brain slices
54	2.8 Brain slice viability
54	2.9 Palkovits punch technique (micropunch dissection)
56	2.10 Solid phase extraction
57	2.11 Hormone immunoassays
57	2.11.1 17 β -oestradiol (E ₂) ELISA
61	2.11.2 Testosterone ELISA
65	2.12 Gene expression analysis
65	2.12.1 Total RNA extraction
65	2.12.2 cDNA synthesis
65	2.12.3 RT-qPCR
67	2.13 Golgi staining
68	2.13.1 Image acquisition and analysis
69	2.14 Immunohistochemistry for the aromatase protein
69	2.14.1 Optimisation of staining protocol
72	2.14.2 Characterisation of aromatase antibody in mouse ovary sections
75	2.15 Statistical analyses
77	CHAPTER 3: MEASURING NEUROSTEROIDS IN THE SOCIAL BEHAVIOUR NETWORK OF THE MOUSE USING A NOVEL EX VIVO SLICE CULTURE TECHNIQUE
78	3.1 Introduction
78	3.1.1 Expression of steroidogenic enzymes
79	3.1.2 The role of neurosteroids
80	3.2 Methods
80	3.2.1 Materials: animals and chemicals

80	3.2.2 Preparation of slice culture
80	3.2.3 Determination of slice viability
81	3.2.4 Blood collection and plasma preparation
81	3.2.5 Palkovits punch technique for extraction of steroids and RT-qPCR
81	3.2.6 Determination of steroid concentration by ELISA
81	3.2.7 Statistical analyses
81	3.3 Results
81	3.3.1 The brain produces neurosteroids ex vivo
83	3.3.2 The capacity to synthesise neurosteroids in the social behaviour network is sexually dimorphic
85	3.3.3 Neurosteroids are locally regulated across the social behaviour network and are significantly higher than plasma steroids
89	3.3.4 Expression of steroidogenic enzymes varies between regions and is sexually dimorphic
95	3.4 Discussion
95	3.4.1 Timeline of neurosteroid production in the SBN
96	3.4.2 Sexual dimorphism in neurosteroid concentrations in the SBN
98	3.4.3 Sexual dimorphism in the steroidogenic pathway in the SBN
101	3.5 Summary
102	3.6 Supplementary information
102	3.6.1 E ₂ ELISA
102	3.6.2 Testosterone ELISA
105	CHAPTER 4: REGULATION OF NEUROSTEROID PRODUCTION BY EX VIVO HYPOTHALAMIC BRAIN SLICES FROM THE ADULT FEMALE MOUSE
106	4.1 Introduction
108	4.2 Methods
108	4.2.1 Animals
109	4.2.2 Preparation of ex vivo brain slices
109	4.2.3 Drug treatments
109	4.2.4 Palkovits punch technique for extraction of steroids and RT-qPCR
109	4.2.5 Hormone immunoassays
109	4.2.6 Statistical analysis
110	4.3 Results

110	4.3.1 E ₂ production is not increased by providing an androgenic substrate nor decreased by the aromatase inhibitor letrozole in the female mouse mPOA and VMH
113	4.3.2 Inhibiting DHT production in conjunction with letrozole reduces E ₂ production in the adult female mouse mPOA, but not the VMH
120	4.3.3 3 β -diol reinstates neurosteroid production that is blocked by letrozole and dutasteride in the mPOA
125	4.3.4 The induction of E ₂ synthesis by 3 β -diol may be ligand specific
131	4.3.5 Ovariectomy does not seem to impede neurosteroid production
136	4.4 Discussion
136	4.4.1 The 3 β -diol pathway in the mPOA
140	4.4.2 Regional specificity of the 3 β -diol pathway
141	4.4.3 Functional significance of 3 β -diol in the mPOA
142	4.4.4 Effect of ER modulators
144	4.4.5 Gonadal status does not affect neurosteroidogenesis in the female mouse hypothalamus
146	4.5 Summary
147	4.6 Supplementary information
154	CHAPTER 5: BEHAVIOURAL AND NEUROARCHITECTURAL RELEVANCE OF NEUROESTROGENS AND 3β-DIOL IN THE ADULT FEMALE MOUSE
155	5.1 Introduction
157	5.2 Methods
157	5.2.1 Animals
158	5.2.2 Samples for Golgi staining and hormone measurements
159	5.2.3 Statistical analysis
159	5.3 Results
159	5.3.1 Treatment can cross the blood brain barrier to alter hypothalamic E ₂ concentration
161	5.3.2 Systemically blocking the 3 β -diol pathway does not affect anxious behaviours in the adult female mouse
168	5.3.3 Systemically blocking the 3 β -diol pathway causes significant changes in neuroarchitecture

173	5.4 Discussion
173	5.4.1 The influence of ovarian hormones on behaviours that denote anxiety
175	5.4.2 3 β -diol and anxiety
176	5.4.3 The mPOA is implicated in behaviours that denote anxiety
177	5.4.4 Neuroarchitectural changes associated with blockade of steroid hormones
179	5.5 Summary
180	5.6 Supplementary information
187	CHAPTER 6: BEHAVIOURAL SIGNIFICANCE OF NEUROESTROGENS ORIGINATING FROM THE HYPOTHALAMUS: OBSERVATIONS FROM A NOVEL CONDITIONAL AND SITE-SPECIFIC AROMATASE KNOCKOUT MOUSE (ARO^{FL/FL})
188	6.1 Introduction
190	6.2 Methods
190	6.2.1 Animals and behavioural tests
192	6.2.2 Hormone measurements
192	6.2.3 Statistical analysis
192	6.3 Results
192	6.3.1 Confirmation of injection site
193	6.3.2 Site-specific ArKO does not affect plasma E ₂ concentrations
194	6.3.3 Running wheel activity is significantly decreased by site-specific ArKO without affecting bodyweight in hypo-ArKO
197	6.3.4 Site-specific ArKO in the mPOA/BNST alone or in conjunction with adjacent limbic regions does not affect sex or aggressive behaviour
200	6.3.5 hypo-lim-ArKO increases anxiety in the light-dark test
202	6.4 Discussion
204	6.4.1 Physiological characteristics and voluntary running wheel activity
205	6.4.2 Sexual behaviour
206	6.4.3 Aggressive behaviour
208	6.4.4 Anxiety
210	6.5 Summary
212	6.6 Supplementary information
213	CHAPTER 7: GENERAL DISCUSSION

215	7.1 Limitations
216	7.2 Concluding statement
219	APPENDIX
224	BIBLIOGRAPHY

List of Figures

- 4 **Figure 1.1** Rodent steroidogenic pathway
- 15 **Figure 1.2** Oestrogen signalling mechanisms
- 33 **Figure 1.3** Aims of this thesis
- 37 **Figure 2.1** Generation of *Aro^{fl/fl}* mice
- 41 **Figure 2.2** Location of stereotaxic injections in the medial preoptic area (mPOA)
- 44 **Figure 2.3** Open field test (OFT) arena
- 46 **Figure 2.4** Social investigation test apparatus
- 49 **Figure 2.5** Vaginal cytology of mouse oestrous stages
- 51 **Figure 2.6** Adjacent, potentially neurosteroidogenic regions within hypothalamic slices
- 61 **Figure 2.7** Typical standard curve obtained for the 17 β -oestradiol ELISA
- 64 **Figure 2.8** Typical standard curve obtained for the testosterone ELISA
- 71 **Figure 2.9** Corrected total cell fluorescence (CTCF) using two different staining methods during the optimisation of immunostaining with the Novus Biologicals anti-aromatase antibody (AB_10000919)
- 73 **Figure 2.10** Representative images to show the effects of antigen retrieval time on aromatase staining of 10 μ m mouse ovary sections
- 74 **Figure 2.11** Representative images to show the effects of wash times on aromatase staining of 10 μ m mouse ovary sections
- 82 **Figure 3.1** Neurosteroid concentrations in hypothalamic brain slices from adult male and female mice incubated for different time points
- 83 **Figure 3.2** Viability of hypothalamic brain slices incubated for different time points measured by the Trypan Blue exclusion assay
- 84 **Figure 3.3** Neurosteroid concentrations in pooled SBN nuclei of adult male and female mice
- 87 **Figure 3.4** Neuroestrogen concentrations in individual SBN nuclei of adult male and female mice
- 88 **Figure 3.5** Neurotestosterone concentrations in individual SBN nuclei of adult male and female mice
- 89 **Figure 3.6** E₂ concentrations in plasma vs aCSF in female mice at different oestrous stages
- 90 **Figure 3.7** Expression of *Stard1* and *Cyp11a1* in the adult male and female SBN nuclei at 0 h and 24 h slice incubation timepoints, measured by RT-qPCR

- 92 **Figure 3.8** Expression of *Hsd3b1* and *Hsd17b1* in adult male and female SBN nuclei at 0 h and 24 h slice incubation timepoints, measured by RT-qPCR
- 94 **Figure 3.9** Expression of *Cyp19a1* in adult male and female SBN nuclei at 0 h and 24 h slice incubation timepoints, measured by RT-qPCR
- 104 **Supplementary Figure S3.1** Comparison of steroidogenic enzyme levels in adult male and female pooled SBN nuclei at 0 h and 24 h incubation timepoints, compared to ovary, measured by RT-qPCR
- 111 **Figure 4.1** Effect of letrozole and testosterone on E₂ concentrations in adult female mouse medial preoptic area and ventromedial hypothalamus
- 112 **Figure 4.2** Effect of letrozole and testosterone on T concentrations in adult female mouse medial preoptic area and ventromedial hypothalamus
- 115 **Figure 4.3** Effect of the inhibition of aromatase and 5 α -reductase on steroid hormone concentrations and enzyme expression in the adult female mouse medial preoptic area
- 116 **Figure 4.4** Effect of the inhibition of aromatase and 5 α -reductase on aromatase and ER expression in the adult female mouse medial preoptic area
- 118 **Figure 4.5** Effect of the inhibition of aromatase and 5 α -reductase on steroid hormone concentrations and enzyme expression in the adult female mouse ventromedial hypothalamus
- 119 **Figure 4.6** Effect of the inhibition of aromatase and 5 α -reductase on aromatase and ER expression in the adult female mouse ventromedial hypothalamus
- 121 **Figure 4.7** The effect of 3 β -diol on steroid hormone concentrations and enzyme expression in the adult female mouse mPOA
- 122 **Figure 4.8** The effect of 3 β -diol on aromatase and ER expression in the adult female mouse mPOA
- 124 **Figure 4.9** The effect of 3 β -diol on steroid hormone concentrations and enzyme expression in the adult female mouse VMH
- 125 **Figure 4.10** The effect of 3 β -diol on aromatase and ER expression in the adult female mouse VMH
- 126 **Figure 4.11** Effect of oestrogen receptor modulators on steroid hormone concentration in the adult female mouse mPOA
- 127 **Figure 4.12** Effect of oestrogen receptor modulators on oestrogen receptor expression and *Cyp19a1* expression in the adult female mouse mPOA

- 129 **Figure 4.13** Effect of oestrogen receptor modulators on steroid hormone concentration in the adult female mouse VMH
- 130 **Figure 4.14** Effect of oestrogen receptor modulators on oestrogen receptor expression and *Cyp19a1* expression in the adult female mouse VMH
- 132 **Figure 4.15** Effect of ovariectomy on E₂ and testosterone production in punch dissected medial preoptic area and ventromedial hypothalamus from the adult female mouse
- 134 **Figure 4.16** Effect of ovariectomy on steroidogenic enzyme expression in the adult female mouse hypothalamus
- 135 **Figure 4.17** Effect of ovariectomy on oestrogen receptor expression and steroidogenic enzyme expression in the adult female mouse hypothalamus
- 138 **Figure 4.18** The mechanism of the 3β-diol pathway in *ex vivo* slice culture
- 147 **Supplementary Figure S4.1** Effect of the inhibition of aromatase and 5α-reductase on steroid enzyme expression in the adult female mouse medial preoptic area
- 148 **Supplementary Figure S4.2** Effect of the inhibition of aromatase and 5α-reductase on steroid enzyme expression in the adult female mouse ventromedial hypothalamus
- 149 **Supplementary Figure S4.3** The effect of 3β-diol on steroid enzyme expression in the adult female mouse mPOA
- 150 **Supplementary Figure S4.4** The effect of 3β-diol on steroid enzyme expression in the adult female mouse VMH
- 151 **Supplementary Figure S4.5** Effect of oestrogen receptor modulators on steroid enzyme expression in the adult female mouse mPOA
- 152 **Supplementary Figure S4.6** Effect of oestrogen receptor modulators on steroid enzyme expression in the adult female mouse VMH
- 153 **Supplementary Figure S4.7** Effect of ovariectomy on the expression of steroidogenic enzymes related to the 3β-diol pathway in the adult female mouse hypothalamus
- 158 **Figure 5.1** Experimental timeline
- 160 **Figure 5.2** Hormone concentrations in plasma and hypothalamic extractions from adult female mice treated with steroidogenic enzyme inhibitors
- 162 **Figure 5.3** Open field test
- 163 **Figure 5.4** Elevated plus maze (i)
- 164 **Figure 5.5** Elevated plus maze (ii)
- 165 **Figure 5.6** Light-dark test

167	Figure 5.7	Social investigation test
170	Figure 5.8	Neuroarchitectural analysis (i)
171	Figure 5.9	Neuroarchitectural analysis (ii)
173	Figure 5.10	Dendritic spine analysis
181	Supplementary Figure S5.1	Hormone concentrations in plasma vs hypothalamic extractions
182	Supplementary Figure S5.2	Social investigation test empty cone data
183	Supplementary Figure S5.3	Representative 20X images of neuroarchitecture in the medial preoptic area of adult female mice treated with steroidogenic enzyme inhibitors
184	Supplementary Figure S5.4	Representative 100X image of spine density of a neurone in the medial preoptic area in vehicle-treated intact female mice
185	Supplementary Figure S5.5	Representative 100X image of spine density of a neurone in the medial preoptic area in vehicle-treated ovariectomised mice
186	Supplementary Figure S5.6	Representative 100X image of spine density of a neurone in the medial preoptic area in letrozole-treated intact female mice
187	Supplementary Figure S5.7	Representative 100X image of spine density of a neurone in the medial preoptic area in letrozole- and dutasteride-treated intact female mice
192	Figure 6.1	Experimental timeline
195	Figure 6.2	Plasma E ₂ concentrations
196	Figure 6.3	Running wheel activity
197	Figure 6.4	Body weight
199	Figure 6.5	Sexual behaviour
200	Figure 6.6	Aggressive bouts
201	Figure 6.7	Aggressive behaviours
202	Figure 6.8	Light-dark test (i)
203	Figure 6.9	Light-dark test (ii)
213	Supplementary Figure S6.1	Sexual behaviour
218	Figure 7.1	Findings of this thesis

List of Tables

- 17 **Table 1.1** Oestrogen receptor and aromatase expression in the social behaviour network and behaviourally relevant nodes of the hypothalamus of male and female rodents across development
- 52 **Table 2.1** Slice distribution across three treatment groups
- 53 **Table 2.2** Slice distribution across four treatment groups
- 56 **Table 2.3** Number and volume of punches for each nucleus of interest in the social behaviour network and hypothalamus
- 59 **Table 2.4** Crossreactivity of physiologically relevant steroid hormones with the 17 β -estradiol ELISA
- 60 **Table 2.5** % crossreactivity of drugs used in brain slice incubation with the 17 β -oestradiol ELISA
- 63 **Table 2.6** Crossreactivity of physiologically relevant steroid hormones with the testosterone ELISA
- 64 **Table 2.7** % crossreactivity of drugs used in brain slice incubation with the testosterone ELISA
- 67 **Table 2.8** Primer sequences for RT-qPCR
- 194 **Table 6.1** Location of Cre injection sites
- 221 **Appendix Table S1** List of specific reagents for each experiment

Abbreviations

(m)POA	(Medial) preoptic area
3 β -diol	5 α -androstane-3 β , 17 β -diol
aCSF	Artificial cerebrospinal fluid
AH	Anterior hypothalamus
AP-1	Activator protein-1
ARC	Arcuate nucleus
ArKO	Aromatase knockout
BNST	Bed nucleus of stria terminalis
cAMP	Cyclic adenosine monophosphate
DHT	Dihydrotestosterone
DPN	Diarylpropionitrile
E ₂	17 β -oestradiol
EB	Oestradiol benzoate
EPM	Elevated plus maze
ER	Oestrogen receptor
ERE	Oestrogen response element
ERK	Extracellular signal-related kinase
ERKO	Oestrogen receptor knockout
GnRH	Gonadotropin releasing hormone
GPCR	G protein-coupled receptor
GPER1	G protein-coupled oestrogen receptor 1
i.p.	Intraperitoneal
LDT	Light-dark test
LS	Lateral septum
meA	Medial amygdala
mER	Membrane oestrogen receptor
NCM	Caudal medial nidopallium
OBX	Olfactory bulbectomy/olfactory bulbectomised
OFT	Open field test
OVX	Ovariectomy/ovariectomised
P450scc	Cytochrome P450 side chain cleavage enzyme
PPT	Propylpyrazoletriol
PSD-95	Postsynaptic density protein-95
PVN	Paraventricular nucleus
SBN	Social behaviour network

SIT	Social investigation test
StAR	Steroidogenic acute regulatory protein
VMH	Ventromedial hypothalamus
WT	Wildtype

Publications

Dovey, J. L. and Vasudevan, N. (2020). Does GPER1 Play a Role in Sexual Dimorphism? *Front Endocrinol (Lausanne)*. 11, 595895.

Davis, D., Dovey, J., Sagoshi, S., Thaweepanyaporn, K., Ogawa, S., and Vasudevan, N. (2023). Steroid hormone-mediated regulation of sexual and aggressive behaviour by non-genomic signalling. *Steroids*. 200, 109324.

Davis, D., Dovey, J., Vajaria, R., Nasuto, S., Delivopoulos, E., Tamagnini, F., and Vasudevan, N. Steroid secretion from the mouse brain. *Submitted as a methodology primary research paper to Steroids, subsequent to a talk by D. Davis and N. Vasudevan at Rapid Response to Steroid Hormones, Paris, Sept 2022.*

Dovey, J., Davis, D., Knight, P. G., and Vasudevan, N. Neurosteroids in the social behaviour network of the mouse. *Submitted to Endocrinology, Oct 2023.*

Chapter 1
Introduction

1.1 Neurosteroids

1.1.1 Steroid hormones

Oestrogens, a class of sex steroid hormones including oestrone, 17β -oestradiol (E_2), oestriol, and oestetrol, display a broad range of physiological functions. These functions are mediated through cognate oestrogen receptors (ERs) belonging to the nuclear receptor family which activate transcriptional processes and/or signalling events upon ligand binding (Fuentes and Silveyra, 2019). Steroid hormones are synthesised from cholesterol in peripheral steroid glands, such as the ovaries, which primarily produce and secrete oestrogens and progestins; the testes, which primarily produce and secrete androgens including testosterone; and the adrenal cortex, which produces and secretes a range of steroid hormones including glucocorticoids, mineralocorticoids, androgens, progestins and oestrogens (Payne and Hales, 2004). Since all steroid hormones share a common precursor, they can be transformed into other steroid hormones in the steroidogenic pathway (section 1.1.2). For example, the adrenal cortex is a rich source of dehydroepiandrosterone (DHEA), which can weakly bind androgen receptors or be transformed into androgens or oestrogens (Beck and Handa, 2004).

Steroid hormones exert transient effects that have the potential to cause permanent tissue-specific alterations in anatomy and physiology (Wilson and Davies, 2007), alter physiological processes (Charkoudian et al., 2017), and modulate behaviours (Schulz and Sisk, 2016). Often steroid hormones induce these effects in series. For example, E_2 -stimulated progesterone synthesis triggers the surge in luteinising hormone which regulates ovulation (Micevych and Sinchak, 2011). Conversely, progesterone inhibits E_2 synthesis by inhibiting the expression and activity of aromatase, the enzyme responsible for E_2 synthesis (Yilmaz et al., 2011). The lipophilic nature of steroid hormones means that they are unable to be stored in intracellular vesicles and are typically synthesised when required (Holst et al., 2004). Their properties make them ideal chemical messengers that can act on a wide range of tissues as well as pass through the blood brain barrier (Banks, 2012). The neuroendocrine actions of steroid hormones were originally thought to be mediated solely through their endocrine mode of signalling from the periphery. However, the discovery of steroidogenic enzyme expression in the central nervous system (CNS) (Wehrenberg et al., 2001) and the ability of primary cell cultures to synthesise steroids (Hojo et al., 2004a) led to a re-evaluation of the relationship between steroid hormone synthesis and brain function. It is now appreciated that neurones and glial cells synthesise “neurosteroids”, a term

referring to steroids synthesised from haematogenous precursors or *de novo* in the brain. Neurosteroids are critical mediators of CNS development and function, including the differentiation, proliferation, and survival of neurones (Dovey and Vasudevan, 2020), and regulate physiology. For example, neuroprogesterone synthesis within the hypothalamus triggers the surge in luteinising hormone which regulates ovulation and oestrous cyclicity (Micevych and Sinchak, 2011). Alterations in neurosteroid concentrations are a factor in pathological states including anxiety and depression (Walf and Frye, 2006), epilepsy (Miziak et al., 2020), and neurodegenerative disease (Luchetti et al., 2011).

1.1.2 Steroid hormone synthesis

All steroid hormones are derived from a common cholesterol precursor. The steroidogenic pathway is shown in **Fig. 1.1**. The rate-limiting step is the transport of free cholesterol across the aqueous intermembrane space of the mitochondria by transporter proteins, the most acknowledged being the steroidogenic acute regulatory protein (StAR) (King et al., 2002). Other transport proteins – the translocator protein, the voltage-dependent anion channel, and the adenine nucleotide transporter – are also necessary for the initial synthesis step (Miller and Bose, 2011). The cytochrome P450 side chain cleavage enzyme (P450_{scc}, encoded by the CYP11A1 gene), located on the inner mitochondrial membrane, converts cholesterol to pregnenolone, initiating steroidogenesis (Miller and Bose, 2011). Pregnenolone is the final common branch point for corticoids, progestogens, and androgens. Sex steroid hormones (androgens and oestrogens) are synthesised through a complex series of enzymatic conversions that produce intermediary progestogens: progesterone, dihydroxyprogesterone, and allopregnanolone. Hydroxysteroid dehydrogenase (HSD) enzymes 3 β -HSD and 17 β -HSD (encoded by the HSD3B1 and HSD17B1 genes, respectively) synthesise androgens, which are the precursors for oestrogen synthesis, with the exception of dihydrotestosterone (DHT), which is non-aromatisable. Among the oestrogens, E₂ is the most physiologically relevant due to its abundance and potency (Thomas and Potter, 2013).

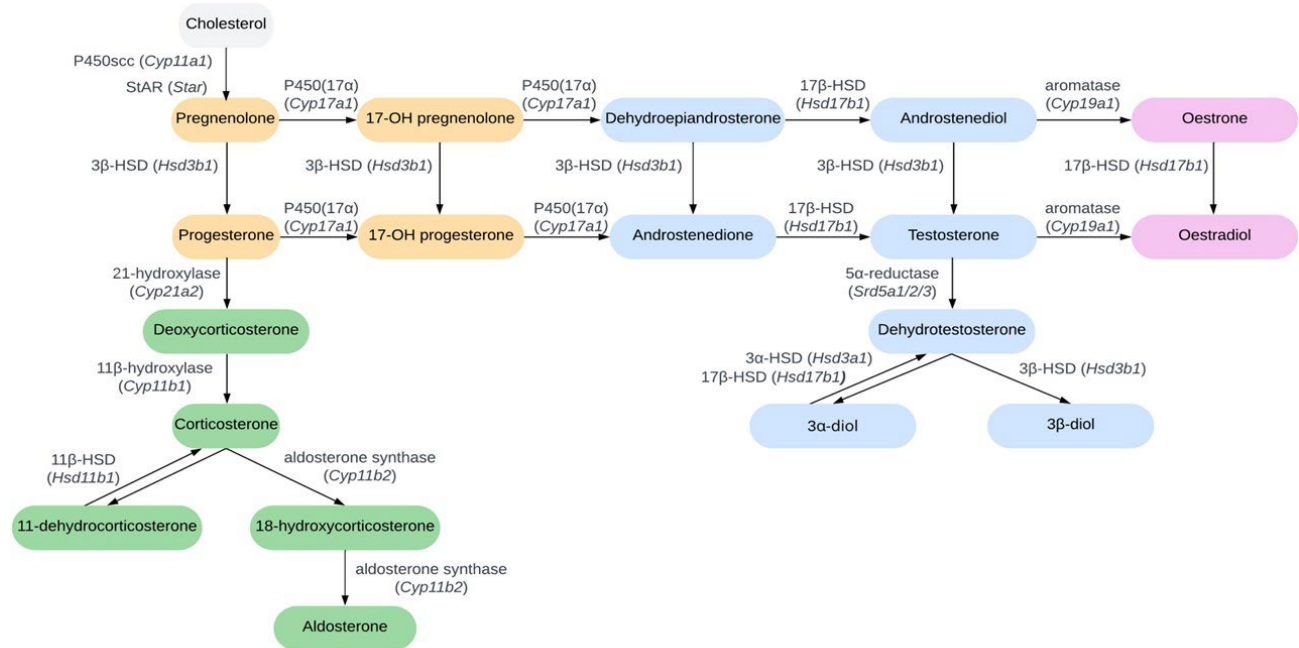


Figure 1.1. Rodent steroidogenic pathway. Oestrogens (pink), androgens (blue), progestogens (yellow) and corticosteroids (green) are all synthesised from cholesterol (grey). Enzymes are shown next to arrows, and gene names for each enzyme are shown in italics.

Steroidogenic enzymes are widely expressed across the brain (Do Rego et al., 2009). One of the best studied steroidogenic regions is the hippocampus, where neurosteroids have been associated with learning and memory (Hojo and Kawato, 2018). However, other brain regions, including the hypothalamus and cerebral cortex, have also been shown to express all of the steroidogenic enzymes necessary for *de novo* steroid synthesis in rodents (Strömstedt and Waterman, 1995). Rodents, birds, and primates express steroidogenic enzymes in neurones and glia (Do Rego et al., 2009), suggesting neurosteroidogenesis is the result of a synergy of enzymatic reactions between cell types. Indeed, in the rat brain, oligodendrocytes primarily produce pregnenolone; astrocytes produce progesterone and androgens; neurones produce progesterone and oestrogen, but do not produce testosterone (Zwain and Yen, 1999). For *de novo* synthesis of neurosteroids, cells must coexpress StAR and P450scc (King et al., 2002). StAR is widely expressed throughout the brain and coexpression with P450scc has been shown in the hypothalamus (King et al., 2002), hippocampus, and Purkinje cells (Furukawa et al., 2002). Purkinje cells also express 3 β -HSD (Furukawa et al., 2002), alongside cultured primary rat astrocytes

(Emanuelsson et al., 2018). The existence of 17β -HSD in the brain has long been inferred from the presence of androgens and oestrogens in brain tissue (Pérez et al., 1975), but expression is restricted to astrocytes in the neonatal rat brain (Zwain and Yen, 1999) and glial cells in the adult male rat (Pelletier et al., 1995). 5α -reductase exists in three isoforms, types I-III, yet type I is the most abundant isoform in the brain of rodents (Melcangi et al., 1993, Pelletier et al., 1994). Expression has been shown in both neurones and glial cells obtained from primary cultures from neonatal rat (Melcangi et al., 1993). Despite the abundance of steroid enzyme expression in the brain, it is receptive to peripheral steroid precursors from the circulation or even other brain areas. It is not entirely clear which areas function as independent steroidogenic microenvironments and if or how this is balanced with availability of peripheral precursors.

Neurosteroid synthesis is not fully understood due to the complexities of enzyme expression and activity throughout the brain, which are simultaneously site-specific (Strömstedt and Waterman, 1995), sexually dimorphic (Roselli et al., 1998), developmentally regulated (Kohchi et al., 1998), contextually regulated (Liu et al., 2011), and species-specific (Pelletier, 2010). For example, 3β -HSD mRNA is expressed across the rat brain, including the olfactory bulb, thalamus, hypothalamus, and hippocampus, but the highest levels are observed in the cerebellum (Guennoun et al., 1995). The concentration of hippocampal 3β -HSD mRNA decreases between birth and adulthood in the male rat (Ibanez et al., 2003), though in the cerebellum, expression peaks at postnatal day 10 in male and female rats (Kohchi et al., 1998). In quail, 3β -HSD mRNA has been detected in the diencephalon and at high levels in the cerebellum (Matsunaga et al., 2002), though enzyme activity is higher in the diencephalon (Ukena et al., 1999). In zebra finches, 3β -HSD activity is sexually dimorphic, with females showing more activity in telencephalic regions than males (Soma et al., 2004). However, acute restraint stress rapidly reverses the sex dimorphism, such that activity is higher in the male telencephalon (Soma et al., 2004).

Another complicating factor is the differences between studies that measure mRNA expression, protein expression, and enzymatic activity. mRNA is not always correlated with protein level and enzymatic activity may be regulated by post-translational modifications (Russell et al., 1995). Furthermore, there are no studies that show a comprehensive expression profile of the major steroidogenic enzymes across the brain, or in discrete brain regions in a particular species. This is something we have addressed in this thesis.

1.1.3 Aromatase

Aromatase, encoded by the CYP19A1 gene, converts testosterone and other C19 androgens into oestrogens. In the brain, expression and activity is typically highest in the medial preoptic area (mPOA), anterior hypothalamus (AH), ventromedial hypothalamus (VMH) and medial amygdala (meA) of adult rats (Roselli et al., 1985b). Aromatase protein and synaptic activity have also been reported in synaptic boutons in vertebrates (Peterson et al., 2005). A single functional isoform is present in rodents (Terashima et al., 1991) and humans (Corbin et al., 1988), whereas fish express multiple functional isoforms (Callard and Tchoudakova, 1997, Chiang et al., 2001). In the mouse, aromatase expression is under the control of four different promoters specific to the brain, adipose tissue, ovary, and testis, each of which contributes more than 85% of *Cyp19* transcripts to its particular tissue (Golovine et al., 2003, Zhou et al., 1996). In mHypo-E42 mouse embryonic hypothalamic cell lines (N42), activity of the brain-specific promoter is regulated by E₂ and progesterone acting via their cognate receptors (Yilmaz et al., 2009, Yilmaz et al., 2011). Oestrogen receptor (ER) α complexes with c-Jun at distinct activator protein (AP)-1 regions in the *Cyp19a1* gene to induce expression of aromatase via promoter I.f. (Yilmaz et al., 2009). Conversely, aromatase expression is inhibited when the progesterone receptor is recruited to promoter I.f. (Yilmaz et al., 2011). E₂-mediated positive feedback on aromatase expression has also been reported in cancer cell lines (Catalano et al., 2014) and primary cultures of amygdala neurones (Cisternas et al., 2017), though how this mechanism is downregulated is not well understood. Furthermore, the synthetic oestrogen diethylstilbestrol was shown to slightly increase aromatase activity in the mPOA, VMH and bed nucleus of stria terminalis (BNST) of the adult female rat, though to a much lesser extent than androgens (Roselli and Klosterman, 1998b).

Aromatase is post-translationally regulated by phosphorylation, which reduces catalytic activity and promotes protein degradation (Hayashi and Harada, 2014). Androgens have also been shown to regulate aromatase protein expression and activity. In the adult male rat, castration significantly reduced both expression and activity of aromatase in the preoptic area (POA) (Abdelgadir et al., 1994). Testosterone treatment restored levels to those seen in intact male rats (Abdelgadir et al., 1994), suggesting that the expression and activity of aromatase depends on its substrate. Testosterone also increases aromatase activity in the female rat mPOA, VMH, and BNST (Roselli and Klosterman, 1998b). Interestingly, treatment with the non-aromatisable androgen DHT increased expression and activity in castrated male rats (Abdelgadir et al., 1994). Whether this was mediated by the androgen receptor was unclear, although recent

studies have shown that DHT and its metabolite 5 α -androstane-3 β ,17 β -diol (3 β -diol) can increase aromatase expression in amygdala cultures (Cisternas et al., 2017). This was shown to be mediated via ER β (Cisternas et al., 2017), for which 3 β -diol shows a strong affinity (Handa et al., 2011).

The aromatase protein is notoriously difficult to immunostain, likely due to the subcellular localisation of the enzyme (Cornil, 2018). Therefore, visualisation is typically achieved by engineering the expression of detectable proteins, such as green fluorescent protein (GFP), in transgenic mice (Stanic et al., 2014), and localisation is typically derived from expression of the mRNA transcript (Roselli et al., 1998). These methods have shown that aromatase is primarily expressed in the hypothalamus, hippocampus, and amygdala of vertebrates (Tabatadze et al., 2014b, Stanic et al., 2014, Zhao et al., 2007), though expression has also been detected in the olfactory bulb and cerebral cortex (Stanic et al., 2014). Like the other steroidogenic enzymes, the expression and regulation of aromatase is both region-dependent and sexually dimorphic (Roselli, 1991). The embryonic mouse hypothalamus houses a network of ~6000 aromatase-expressing neurones from E13.5 (Wartenberg et al., 2021). By birth at postnatal day (P)0, the expression becomes sexually dimorphic, with higher levels of aromatase expression in the female mPOA, whilst the male arcuate nucleus (ARC) expresses higher levels of aromatase than the female (Wartenberg et al., 2021).

Since the ovary represents the major source of oestrogens in the female, the role of brain aromatase in behaviour and its effect on the underlying neurophysiological circuitry is often overlooked, with studies typically only reporting the role of central aromatase in male knockout animals (Brooks et al., 2020b). Whilst female rodents show lower enzymatic activity than males across several brain regions (Roselli and Klosterman, 1998b), the affinity of brain aromatase for its substrate is similar between the sexes (Konkle and Balthazart, 2011), and higher than the affinity of ovarian aromatase (Hutchison et al., 1992). In the rat, aromatase activity within the mPOA does not fluctuate across the oestrous cycle, nor is it significantly altered by ovariectomy (OVX) (Roselli et al., 1984), suggesting that brain aromatase activity may be constitutive and independent of ovarian aromatase. In line with this, concentrations of hippocampal E₂ are significantly greater than plasma concentrations in the female rat (Kato et al., 2013). Thus, brain aromatase activity could be important for maintaining local levels of E₂ for proper neuronal function (Pareto et al., 2013).

The aromatase knockout (ArKO) mouse, which is deficient in aromatase activity because of a targeted mutation in the *Cyp19a1* gene, shows severe impairments in

reproductive behaviour and olfaction (Bakker et al., 2002). Female ArKO mice possess functional ERs, yet olfaction is not rescued by E₂ treatment (Bakker et al., 2002). Whilst a non-conditional knockout model does not define the contribution of brain vs ovarian aromatase to resulting behaviours, it suggests a role for aromatase in female brain development. As discussed in section 1.2.1, the majority of neural circuitry that underlies sexually dimorphic and innate behaviours is set up perinatally. At this stage, the ovaries are quiescent and remain this way until puberty (McCarthy, 2008). This has led to the belief that the female brain develops in the absence of E₂. However, the behavioural phenotype of ArKO mice suggests that the neural circuitry was not properly organised perinatally. Furthermore, androgenised females, a model in which a single exposure of a neonatal female to androgen causes permanent sterilisation and masculinisation of the behavioural profile (Arai and Gorski, 1968), a known result of E₂, indicates that brain aromatase is present and catalytically active in the brain during the quiescence of the ovaries. Together, this points to a role for central aromatase in female brain development. A more suitable genetic model for understanding brain aromatase in the female is the brain-specific conditional ArKO mouse (Brooks et al., 2020b). However, this has only been used for the investigation of male sexual behaviour, which was significantly impaired compared to WT controls (Brooks et al., 2020b). More recently, a forebrain-specific ArKO mouse was generated, in which males and females both showed significant deficits in forebrain spine and synaptic density, hippocampal-dependent spatial memory, recognition memory, and contextual fear memory (Lu et al., 2019). Social behaviours were not investigated. A better model for understanding the contributions of brain aromatase to behaviours would be a site-specific conditional knockout model, which has been utilised in this thesis.

1.1.4 Neuroestrogens

The synthesis of neuroestrogens is widely accepted and has been shown in cell culture (Prange-Kiel et al., 2003), slice culture (Kretz et al., 2004a), and *in vivo* across many species including rodents (Hojo and Kawato, 2018), fish (Callard et al., 1995), frogs (Chakraborty and Burmeister, 2015), and primates (Maclusky et al., 1986), though it is best studied in birds (Jalabert et al., 2022, Saldanha et al., 2013b, Schlinger and Arnold, 1992). Intracerebral injection of tritiated androstenedione to male zebra finch resulted in the detection of tritiated E₂ in the jugular plasma leaving the brain after 5 minutes (Schlinger and Arnold, 1992). Microdialysis has also shown rapid fluctuations in the zebra finch forebrain during social behaviours (Ramage-Healey et al., 2008). Micropunches taken from the male zebra finch brain show varying concentrations of E₂, with the caudal medial nidopallium (NCM), an auditory area

related to song behaviour, showing the highest levels (Charlier et al., 2010b). In rodents, neuroestrogen synthesis is typically studied in areas known to produce high concentrations of neuroestrogens, such as the hippocampus (Hojo and Kawato, 2018). In rat hippocampal slice cultures, the concentration of E₂ measured in culture medium is significantly decreased with the aromatase inhibitor letrozole in a dose-dependent manner (Kretz et al., 2004a). Studies in mice tend to focus on the localisation and activity of aromatase rather than measuring neuroestrogens themselves (Brann et al., 2022). It is also important to note that neuroestrogen synthesis is typically studied in males, perhaps due to higher aromatase activity (Roselli et al., 1985b) lending itself to a better ability to detect neuroestrogens.

Neuroestrogens play a pivotal role in modulating the physiology and architecture of neurones (Romanò et al., 2008, Di Mauro et al., 2015, Kretz et al., 2004a) by acting in a paracrine, autocrine, or synaptocrine manner (Saldanha et al., 2011).

Neuroestrogens mediate their effects in the same way as peripheral oestrogens: binding to their cognate receptors. Steroid hormones are typically viewed as freely diffusing molecules due to their lipophilic properties (Holst et al., 2004), yet neuroestrogens are thought to be spatially restricted by nearby enzymes and receptors (Schlinger et al., 2014). Transgenic mice that express enhanced (E)GFP following the physiological activation of the *Cyp19a1* gene have shown that, in many cases, ER-expressing cells are in close proximity to aromatase-positive cells, and many cells co-express the two (Stanic et al., 2014). In primary cultures from adult male rat hippocampus, neuroestrogen released into the culture medium acts in a para/autocrine manner to increase ER α expression in cells (Prange-Kiel et al., 2003). In areas abundant in aromatase-positive soma (**Table 1.1**), there is also an abundance of aromatase-positive fibres, which typically project to regions that possess aromatase-negative cells (Saldanha et al., 2000). This leads to some areas being rich in aromatase-positive fibres with a scarcity of aromatase-positive soma (Stanic et al., 2014). Therefore, one brain region may be able to control E₂ concentrations in other brain areas through its afferent projections. Dendritic aromatase and production of neuroestrogens at or near the synapse (Saldanha et al., 2011) is controlled by depolarisation-sensitive, calcium-dependent events in the presynaptic terminal (Remage-Healey et al., 2011). Therefore, E₂ produced at or near the synapse can act as a neurotransmitter, docking membrane receptors on the postsynaptic terminal to rapidly modulate long-term potentiation and fast excitatory postsynaptic potentials (Di Mauro et al., 2015, Foy et al., 1999). E₂ can also act on the presynaptic neurone, suppressing GABAergic currents synapsing on gonadotropin-releasing hormone

(GnRH) neurones (Romanò et al., 2008). It is in this manner that neuroestrogen regulates GnRH neurosecretion (Kenealy et al., 2013). These actions are typically rapid and therefore rely on the expression of nongenomic receptors in particular regions, which helps to limit the actions of E₂ to discrete neural circuits. Spatial specificity of neuroestrogens may be further controlled by hormone-binding globulins that sequester E₂, or by catabolism to limit actions in discrete neural circuits (Schlinger et al., 2014, Cornil et al., 2006). These mechanisms have received very little attention.

E₂ has a myriad of effects on the structural plasticity of the brain, and these may depend on the receptor it activates. The hypothalamic cell lines RCF-6 and RCF-12 express ER β but not ER α , whilst RCF-8 cells express both ERs (Nilsen et al., 2000). When grown in steroid-deficient media and treated with E₂ with or without the ER antagonist tamoxifen, RCF-6 and RCF-12 cells show decreased viability in the presence of E₂ but not tamoxifen; RCF-8 cells show increased viability in the presence of E₂ but not tamoxifen. Furthermore, when grown in steroid-deficient media with E₂ added, RCF-8 cells show increased expression of the anti-apoptotic gene bcl-2; RCF-12 and RCF-6 cells show increased numbers of TUNEL-positive cells, indicating apoptotic DNA fragmentation (Nilsen et al., 2000). This strongly suggests ER β mediates apoptosis whilst ER α is neuroprotective, at least in cell lines. On the contrary, treating neonatal female and androgenised female rats with antisense oligonucleotides against ER α reduces the volume of the SDN-POA (McCarthy et al., 1993). In dopaminergic neurones expressing ER α and the G protein-coupled oestrogen receptor (GPER)1, activation of GPER1 is necessary for neuroprotection (Bourque et al., 2015). Thus, it seems that the neuroprotective or apoptotic effects of E₂ may also depend on multiple receptors and signalling mechanisms.

1.2 Oestrogen receptors

ERs are densely expressed in both the male and female reproductive tract (Chen et al., 2022). In the male, ER α is primarily located in the efferent ductile epithelium, where its expression is even more abundant than in the female reproductive tract (Hess, 2003). ERs are also expressed in a vast array of tissues including bone, liver, adipose tissue, skin, and the brain at similar levels in both sexes (Hutson et al., 2019), although regional differences in expression levels within the brain have been noted (Dovey and Vasudevan, 2020).

The brain is widely responsive to sex hormones due to the expression of ERs in neurones and glial cells (Crespo-Castrillo and Arevalo, 2020). As a result, the brain

shows considerable hormone-regulated plasticity (Woolley and McEwen, 1992). The effects of E₂ are largely dependent upon the receptor activated and the relative density of its expression (Chen et al., 2022). Brain regions with lower ER expression levels might have limited responses to E₂, or may require higher concentrations provided by targeted, local E₂ synthesis (discussed in section 1.4). The localisation of ERs within cells also determines the involvement of signalling pathways causing changes in gene expression or the initiation of signalling cascades (Hall et al., 2001). Together, these signalling mechanisms coordinate the pleiotropic effects of E₂ in the brain, such as neurogenesis (Fowler et al., 2008), neurodevelopment (Dovey and Vasudevan, 2020, Crider and Pillai, 2017), and neuroprotection (Brann et al., 2007).

1.2.1 Genomic oestrogen receptor signalling

As a lipophilic steroid hormone, E₂ can freely enter cells and bind to nuclear ERs in the cytoplasm. ER α is a 66 kDa protein encoded by the ESR1 gene and was first cloned from the human breast cancer cell line MCF-7 (Green et al., 1986). ER β (ESR2) is a 59 kDa protein that was discovered 10 years later in the prostate and ovary (Kuiper et al., 1996) and is assumed to have arisen as a gene duplication event early in evolution (Handa et al., 2012). Both ERs have a similar structural organisation, consisting of an N-terminal/activation function-1 domain, DNA binding/activation function-2 domain, hinge domain, and a C-terminal region containing the ligand-binding domain (Kumar et al., 1987). The binding of ligand induces a conformational change in the receptor that promotes homo- or heterodimerisation (Tamrazi et al., 2002). Dimers translocate to the nucleus and bind DNA at conserved oestrogen response elements (EREs), which are cis-acting enhancers found within the regulatory regions of target genes (Klinge, 2001). The activation function regions of the receptor dimer bind to coactivators to drive a positive or negative effect on the downstream target gene (Hall et al., 2001). ERs can also be activated in the absence of ligand by phosphorylation of specific serine and tyrosine residues in the receptors themselves, or by associating with coactivators and corepressors (Bennesch and Picard, 2015). Nuclear oestrogen receptors can also induce the expression of genes containing non-ERE elements, such as those containing activator protein (AP)-1 sites (Fuentes and Silveyra, 2019). AP-1 is composed of proteins belonging to the c-Fos, c-Jun, and Jun dimerisation partner families, and ER α can interact with c-Fos and c-Jun to induce the expression of genes (O'Lone et al., 2004). The transcriptional effects of genomic signalling take place over the course of hours to days (Lai et al., 2017).

Small differences in sequence homology elicit functional differences between the receptors. ER α and ER β share up to 95% sequence homology in their DNA-binding domain, 55% in their ligand-binding domain, and 15% in their N-terminal domain (Kumar et al., 2011). Although the DNA binding domains of the nuclear ERs are highly homologous, ER α and ER β show different binding affinities for natural EREs that have one or more nucleotide changes from a “core” sequence (Hyder et al., 1999). Thus, the binding affinity of ER β may be two-fold lower than ER α for a specific ERE (Yi et al., 2002). Functionally, this makes ER α a more potent activator of transcription than ER β (Loven et al., 2001), though ER β shows an increased affinity for phytoestrogens (Kuiper et al., 1998). The two receptors overlap in their expression patterns across the brain with a few exceptions where one receptor is expressed at higher levels than the other (Merchenthaler et al., 2004). ER α is the prevailing receptor in the ventromedial hypothalamus (VMH) (Mitra et al., 2003) whereas ER β is more abundantly expressed in the hippocampus (Shughrue et al., 1997). Though there is a relative lack of sex differences in brain ER expression (Hutson et al., 2019), the genomic targets of ERs are sexually dimorphic (Chen et al., 2016). For example, in human breast tissue, the immunoglobulin gene *I_{GLV4-69}* showed increased targeting by ESR1 in males compared to females (Chen et al., 2016). In females, *MYOT*, encoding a cytoskeletal protein involved in muscle contraction showed greater ESR1 targeting in females (Chen et al., 2016).

1.2.2 Nongenomic oestrogen receptor signalling

Not all oestrogenic signalling can be attributed to ER α and ER β . Transcriptionally regulated proteins are not detected for hours, which is not consistent with some of the rapid effects of E₂ (Watters et al., 1997, Sheppard et al., 2018). Membrane ERs (mERs) initiate rapid nongenomic responses by activating protein kinases, modulating calcium flux, and altering the electrical properties of neuronal membranes (Foy et al., 1999, Chaban et al., 2004, Wade et al., 2001). This is important for enhancing fast excitatory postsynaptic potentials and facilitating long-term potentiation for the strengthening of synapses (Babayán and Kramár, 2013).

Approximately 5-10% of ER α is trafficked to the membrane of all cells studied to date (Levin, 2009). Extra-nuclear ER α is detected in dendrites and axon terminals in the hypothalamus (Blaustein et al., 1992), in dendritic spines in the hippocampus (Milner et al., 2001), and in within vesicles of GABAergic neurones that are triggered to move towards the axonal membrane within 24 h of E₂ application (Hart et al., 2007). Membrane ER α exists as a 66 kDa protein that can mediate transcriptional responses

to E₂ and a truncated 46 kDa protein that mediates acute responses to E₂ (Figtree et al., 2003), though the 46 kDa variant has not been described in the brain (Toran-Allerand, 2004). In hypothalamic neurones and astrocytes cultured from male and female rats, a 52 kDa variant of ER α has been detected (Dominguez and Micevych, 2010). Palmitoylation by cellular proteins is required to traffic ERs to the plasma membrane (Pedram et al., 2007), though E₂ has been shown to increase the amount of the 52 and 66 kDa ER α at neuronal and astrocytic membranes within 30 min (Dominguez and Micevych, 2010). The role of the ER variants has been discussed in (Rainville et al., 2015).

Other novel mERs exist as G protein-coupled receptors (GPCRs) (Filardo et al., 2002). The G protein-coupled oestrogen receptor (GPER)1 is a former orphan GPCR that was shown to bind E₂ and increase adenylyl cyclase activity and cyclic AMP (cAMP) in breast cancer SKBR3 cells (Thomas et al., 2005). GPER1 can signal via both the G α_s and G $\beta\gamma$ subunits to transactivate the epidermal growth factor receptor leading to downstream activation of the extracellular signal-regulated kinase (ERK) pathway (Filardo et al., 2002). In the hippocampus, GPER1 associates with postsynaptic density protein-95 (PSD-95) to localise to the membrane independently of E₂ (Akama et al., 2013). Activation of neuronal GPER1 promotes the activity of pro-survival kinases and attenuates the pro-apoptotic JNK pathway (Tang et al., 2014). The GPER1 agonist G-1 increases cAMP in hippocampal neurones and initiates signal transduction cascades in a dose-dependent manner (Evans et al., 2016). GPER1 has been observed in the rat hypothalamus, particularly in the paraventricular nucleus (PVN) and supraoptic nucleus, with lower expression levels in the arcuate nucleus (ARC) (Brailoiu et al., 2007). In the mouse, there are no sex differences in GPER1 expression throughout the brain (Hazell et al., 2009, Dovey and Vasudevan, 2020).

Evidence suggests that genomic and nongenomic signalling are integrated and this may be important for regulating social behaviours and memory (Hadjimarkou and Vasudevan, 2018). ER α and GPER1 may interact to either contribute to or agonise the same output via pathways that are ordered in series or take place in parallel (Hadjimarkou and Vasudevan, 2018). Specific examples include COS7 cells, in which overexpression of ER α led to an increase in calcium that was dependent on phospholipase C, and overexpression of GPER1 led to the same output but this was dependent on epidermal growth factor (Revankar et al., 2005). In prostate stromal cells, overexpression of GPER1 promoted cell differentiation into cancer-associated fibroblasts, an outcome that could also be promoted by ER α knockdown (Jia et al., 2016).

The mechanisms of oestrogen signalling are shown in **Fig. 1.2**.

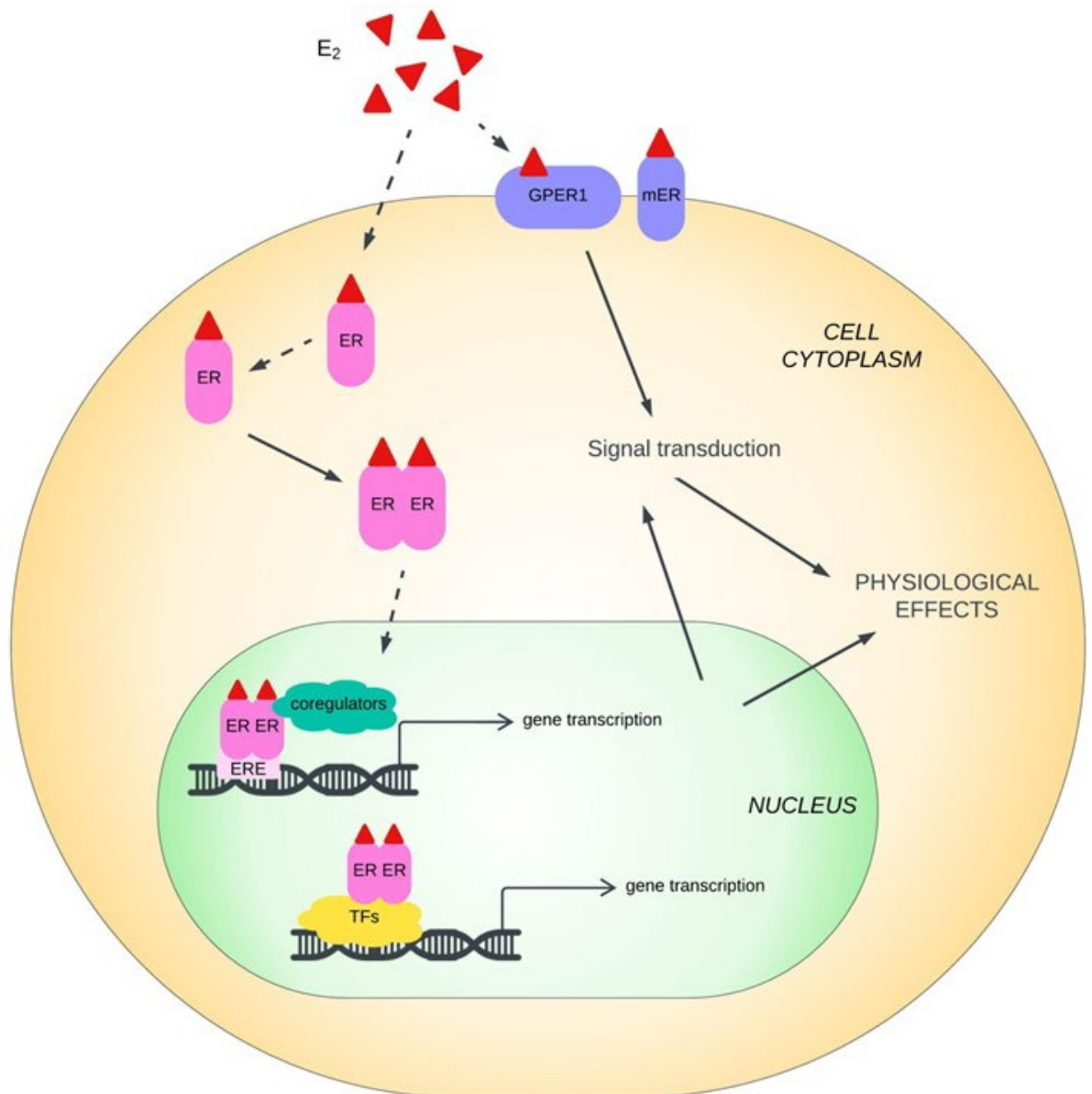


Figure 1.2. Oestrogen signalling mechanisms. As a lipophilic steroid hormone, 17 β -oestradiol (E_2) can diffuse through plasma membranes to activate nuclear oestrogen receptors (ER), such as ER α and ER β that exist within the cytoplasm. Upon hormone binding, E_2 initiates dimerisation and translocation to the nucleus. Receptor dimers can act as transcription factors, binding oestrogen response elements (ERE) in the promoter regions of target genes. This is direct genomic signalling. Alternatively, activated ER dimers can modulate the expression of genes through protein-protein interactions with transcription factors that can bind genes without EREs in an indirect genomic signalling mechanism. E_2 may also bind to membrane ERs (mER); isoforms of ERs α and β that exist within the membrane due to post-translational modifications such as palmitoylation. E_2 may also bind to GPER1, a G-protein coupled oestrogen

receptor. Activation of these membrane-bound receptors in nongenomic signalling can lead to signal transduction through the activation of protein kinases or induction of calcium release. These transduction cascades may also be induced by genomic signalling, effectively linking the two signalling mechanisms together. Collectively, these mechanisms give rise to physiological effects that may be evident within seconds (nongenomic signalling) or hours to days (genomic signalling).

1.3 The social behaviour network

The social behaviour network (SBN) is a conserved set of interconnected hypothalamic and limbic nuclei that are responsible for the facilitation and expression of sexually dimorphic behaviours (Newman, 1999). The SBN is comprised of six nodes: the extended amygdala (the medial amygdala, meA) and the bed nucleus of stria terminalis, (BNST), the lateral septum (LS), the preoptic area (POA), the anterior hypothalamus (AH), the ventromedial hypothalamus (VMH), and the midbrain (Newman, 1999). Each node responds to a variety of stimuli in a distinct pattern across the nodes depending on social contexts (Newman, 1999). In vertebrates, sex hormones are potent modulators of social behaviour (Laredo et al., 2014). The nodes of the SBN are generally rich in sex hormone receptors and aromatase (**Table 1.1**) and are sites of steroid hormone synthesis (Morrell and Pfaff, 1978, Balthazart and Ball, 1998), making the SBN a prime focal point for neuroendocrine activity. The SBN, establishment of sex differences, and the contribution of sex hormones has been reviewed extensively in Dovey and Vasudevan (2020).

Table 1.1. Oestrogen receptor and aromatase expression in the social behaviour network and behaviourally relevant nodes of the hypothalamus of male and female rats and mice across development. Relative expression of oestrogen receptors (ER) α and β and aromatase during perinatal (Pn), pubertal (Pb), and adult (A) periods in the medial preoptic area (mPOA), lateral septum (LS), paraventricular nucleus (PVN), ventromedial hypothalamus (VMH), anteroventral periventricular nucleus (AVPV), arcuate nucleus (ARC), bed nucleus of the stria terminalis (BNST), and medial amygdala (meA). “F” denotes a greater expression in females, “M” a greater expression in males, “=” an equal expression between males and females, and “X” indicates undetectable expression. Gaps in the table are due to data not being found for mRNA or protein expression in the area; a gap does not mean that there is no expression. All referenced research uses mouse or rat (*) models. References 1-4 measured mRNA expression; references 6-11 measured protein expression; reference 5 measured both protein and mRNA expression. 1, Kanaya et al. (2014). 2, Tabatadze et al. (2014). 3, Cao and Patisaul (2011). 4, (Lauber et al., 1997). 5, Ikeda et al. (2003). 6, Yokosuka et al. (1997). 7, (Brock et al., 2015). 8, Kelly et al. (2013). 9, (Chakraborty et al., 2005). 10, Stanic et al. (2014). 11, Zhang et al. (2002). 12, Hazell et al. (2009).

Area		ER α			ER β			Aromatase			GPER1		
		Pn	Pb	A	Pn	Pb	A	Pn	Pb	A	Pn	Pb	A
Hypothalamus	mPOA	= 6,7	F 6,7		= 3	F 3	M* 11	X* 4		M 2, 10			=12
	LS	= 6	= 6										=12
	PVN		= 6				=* 11			= 10			
	VMH	= 6,7	F 6		F 5	= 5	=* 11	=* 4					=12
	AVPV	F 1,8		F 8	X 1	X 9							=12
	ARC	= 6,7	= 6		X 3	= 3				= 10			=12
Medial and extended amygdala	BNST	F 1,8	= 6,8	F 8	= 1		M* 11	= 1 M* 4		M 2			=12
	meA		= 6				F* 11	=* 4		M 2			=12

1.3.1 The organisation-activation hypothesis

The neural networks underlying the SBN are believed to be organised around birth by sex hormones via molecular mechanisms including neurogenesis (Ahmed et al., 2008), programmed cell death (Waters and Simerly, 2009), synaptogenesis (Hutton et al., 1998), and pruning (Zehr et al., 2006). Organisational events are precisely timed and can be influenced by hormone exposure during critical periods that are defined by organ-specific morphogenetic timetables. For example, the neonatal testosterone surge is unique to males due to the activation of the testes whilst the ovaries remain quiescent until puberty (McCarthy, 2008). That is not to say that other tissues are incapable of producing sex hormones during this period; direct measurement of sex hormones in neonatal rats indicates that hypothalamic E₂ is independent of gonadal status in both sexes (Konkle and McCarthy, 2011b). The organisation of the perinatal brain is permanent, establishing sex-specific patterns of neural connectivity (McCarthy, 2008). These neural differences provide the foundation for sexually dimorphic behaviours that are activated by sex hormones in adults. In contrast, the activational effects of sex hormones are transient and temporarily modulate preexisting neural circuitry to facilitate the expression of sexually dimorphic behaviours (Newman, 1999, Schulz et al., 2009). Thus, whilst organisational and activational effects are separate, they are also linked: activational responses are conditioned by earlier organisational exposure to sex hormones during development.

The critical period for organisation of the brain is generally believed to be constrained to the neonatal and perinatal periods, where the brain displays a heightened sensitivity to sex hormones (McCarthy, 2008). For example, male rats castrated 1 h postpartum show female sexual behaviour in adulthood, and this behaviour is less pronounced in rats castrated 6, 12, or 48 h after birth (Thomas and Gerall, 1969). On the other hand, prenatal exposure to testosterone masculinises behaviour in the female guinea pig (Phoenix et al., 1959), implying that neonatal exposure to gonadal steroids is necessary for development of the male brain but not the female. The idea of neonatal brain organisation is caveated by puberty, which presents a second period of brain sensitivity to sex hormones (Schulz and Sisk, 2016). In male Syrian hamsters, prepubertal gonadectomy results in significantly fewer mounts, intromissions, and ejaculations than in males gonadectomised after puberty (Schulz et al., 2004), suggesting pubertal testosterone is required for the complete masculinisation of the developing male brain. In novel environments, male rats exhibit low levels of aggression and reduced social interaction, but this response is prevented by prepubertal gonadectomy (Primus and Kellogg, 1990). This organisational effect is

mediated by E_2 , as treatment with fadrozole, an inhibitor of the aromatase enzyme responsible for the synthesis of E_2 , prevents the typical masculine response to a novel environment (Kellogg and Lundin, 1999). In females, prepubertal E_2 is capable of feminising (enhancing female-typical), masculinising (enhancing male-typical), or defeminising (suppressing female-typical) behaviours (Schulz and Sisk, 2016). A genetic manipulation that prevents the synthesis of E_2 (aromatase knockout, ArKO) results in fewer displays of lordosis and defeminised reproductive behaviour (Bakker et al., 2002). Systemic administration of E_2 to ArKO female mice during prepuberty increases lordosis behaviour in adulthood, but administration during the perinatal period had no effect on adult reproductive behaviour (Brock et al., 2011). Ovariectomy (OVX) of Syrian hamsters prepubertally, but not postpubertally, increases the overall lordosis response in adulthood, suggesting that in this species, E_2 exposure during puberty defeminises reproductive behaviour (Schulz and Sisk, 2006). This is in stark contrast to the literature on female mice. The organisational effects of sex hormones during puberty may be determined by the neonatal hormonal environment. For example, pubertal ovarian hormones have little effect on the reproductive behaviour of neonatally androgenised female rats (de Jonge et al., 1988).

Pubertal organisation by sex hormones also occurs outside of the SBN in areas that display adult neurogenesis such as the dentate gyrus and olfactory bulb, and this contributes to the development of circuitry related to cognitive and executive functions (Laube et al., 2020). Rates of neurogenesis peak during adolescence and decline thereafter (Curlik II et al., 2014), coinciding with a surge in gonadal hormones. The integration of new inhibitory interneurons in the olfactory bulb modulates the output to downstream circuits to influence the neural correlates underlying reproductive behaviour (Peretto et al., 2014). In line with this, impairments in adult neurogenesis have detrimental effects on sex-specific behaviours, such as mate choice and opposite-sex preference (Schellino et al., 2016).

Thus, puberty offers another organisational window for the establishment of sexually dimorphic behaviours and their neural correlates. However, the organisational contribution of sex hormones synthesised in extragonadal tissues, such as the brain, remains underexplored. Whilst ArKO models have proven useful in understanding the organisational deficits that result from a lack of E_2 , a non-conditional knockout masks both a) the contribution of aromatase to normal behaviours in adulthood in a model that has developed with archetypal hormone exposure, and b) the specific contribution of aromatase in the brain. This is something we have explored in this thesis.

1.3.2 Organisation and activation of the medial preoptic area (mPOA)

In mammals, the medial POA (mPOA) is located in the anterior part of the hypothalamus and is derived from proliferative zones from the diencephalon and telencephalon (Paredes, 2003). The mPOA is a central node in the SBN, integrating environmental and neuronal signals and coordinating outputs via a multitude of efferent and afferent inputs (Balthazart et al., 1994). Morphological sex differences further enrich the multifaceted roles of the mPOA. This convergence facilitates its involvement in a variety of physiological functions and behaviours, the most well-studied including thermoregulation (Nakamura and Morrison, 2008), feeding behaviour (Qian et al., 2022), maternal behaviour (Fang et al., 2018), and sexual behaviour (Dominguez and Hull, 2005, Wei et al., 2018).

The rat mPOA is rich in androgen receptors and ERs (Simerly et al., 1990) and is sensitive to perinatal organisation by sex steroids which give rise to morphological sex differences. For example, the perinatal androgen surge at embryonic day 18 (E18) and subsequent aromatisation to E₂ protects dopaminergic cells in the rat mPOA from apoptosis (Davis et al., 1996). Therefore, the male mPOA contains approximately two-fold more dendritic spine synapses than in females, which is believed to play an important role in male mouse sexual behaviour (Bharadwaj et al., 2013). Interestingly, this is established through the convergence of neuroendocrine and immune systems. E₂ is a well-known mediator of dendritic spine plasticity (discussed in further detail in section 1.4.1), whilst immune mast cells and microglia activate protein kinase A which phosphorylates a subunit of the AMPA glutamate receptor, promoting the trafficking of the receptor to the membrane and stimulating the formation and stabilisation of dendritic spine synapses (Lenz et al., 2011). The sexually dimorphic nucleus of the rat POA (SDN-POA) exhibits male-biased sex differences in its number of neurones, and therefore, volume (Gorski et al., 1980). A cluster of neurones in the SDN-POA express calbindin-D28K (calb) (Sickel and McCarthy, 2000), a calcium-binding protein that has a critical role in maintaining calcium homeostasis and preventing neuronal death (Kook et al., 2014). This calb-positive cluster is larger in male rats than in females (Sickel and McCarthy, 2000). The physiological significance of this is not fully understood, though calb-positive neurones are activated during male sexual behaviour (Yamaguchi et al., 2018). A genetic mutation that destroys the tethering of ER α to the membrane decreases the number of calb-immunoreactive neurones in male mice (Khbouz et al., 2020), suggesting a critical role for nongenomic signalling in the sexual differentiation of the SDN-POA, though the E₂-dependent mechanism that underlies the larger volume in males is still unknown.

The mPOA is central to sexually dimorphic behaviours and this has been investigated extensively in rodents through means of lesion studies. In female rats, the mPOA is essential for the onset and early expression of maternal behaviour, integrating sensory feedback from the pups with outputs to the mesolimbic dopamine system (Pereira and Morrell, 2009). Maternal behaviour that is induced by pup stimulation in virgin females is disrupted by lesions in the mPOA (Numan et al., 1977). In lactating females, small lesions outside of the dorsal mPOA abolished nest building and pup retrieval (Jacobson et al., 1980), implicating a subregion-specific component of mPOA-driven maternal behaviour. In males, lesions in the frontal part of the mPOA reduce intermale aggression (Bermond, 1982).

During sexual behaviour, peripheral olfactory signals are received by sensory neurones that process and relay the information to the olfactory bulbs and then to the meA before finally being integrated in the mPOA (Hull and Dominguez, 2007, Simerly and Swanson, 1986). In turn, the mPOA activates a premotor network that leads to a sexual response. In males, lesions to the mPOA result in permanent disruption of copulation, but not sexual motivation (Paredes, 2003). Male rats with mPOA lesions continue to show noncontact erections (Liu et al., 1997) and continue to press a lever to gain access to a sexually receptive female, without copulating (Everitt and Stacey, 1987). Contrarily, mPOA lesions in female Syrian hamsters facilitate lordosis (Rodriguez-Sierra and Terasawa, 1979), and electrical stimulation of the mPOA interrupts the lordosis reflex in female rats (Takeo et al., 1993). The lordosis reflex is under the control of a complex and multiregional circuit encompassing the ARC, mPOA, and VMH. E₂ signalling in the ARC rapidly promotes the release of neuropeptide Y which activates β -endorphin neurones that project to the mPOA. β -endorphin causes the activation and subsequent internalisation of μ -opioid receptors in the mPOA, producing a transient inhibition of the mPOA. The activation of μ -opioid receptors in turn relays to the VMH to activate motor neurones necessary for the display of lordosis behaviour (Micevych and Meisel, 2017). Reproductive behaviours, and the contributions of E₂, are discussed further in section 1.5.1.

Despite clear sex differences, the mPOA of the sexually mature adult mouse maintained the ability to drive either male-typical mounting or female-typical pup retrieval regardless of sex (Wei et al., 2018). Optogenetic stimulation of ER α -positive neurones in the mPOA can bypass hormonal and sensory constraints to drive similar displays of behaviour in male and female mice, strongly implicating mPOA ER α -positive neurones as the key neuronal population underlying sexually dimorphic behaviours dependent on the mPOA (Wei et al., 2018). The precise distinctions in

wiring or gene expression within this neuronal subset in wildtype (WT) animals that lead to sexually dimorphic behaviours remain unclear, yet the implication of E₂ as a central factor is evident.

1.3.3 Organisation and activation of the ventromedial hypothalamus (VMH)

The VMH is a critical site of sex hormone action that displays morphological and neurochemical sex differences. Nissl stain analysis estimates that the volume of the adult VMH is approximately 25% larger in male rodents compared to female (Flanagan-Cato, 2011). This is due to increased soma size and a higher density of spine synapses compared with females, as opposed to having a greater total number of neurones (Dulce Madeira et al., 2001). The ventrolateral subdivision of the VMH (VMHvl) contains a pool of neurones that express ERs (Correa et al., 2015). ER α is expressed at greater levels than ER β in the VMHvl, though the female expresses more of both subtypes than the male (Flanagan-Cato, 2011, Krause and Ingraham, 2017). The male, on the other hand, expresses higher levels of the androgen receptor and aromatase (Roselli and Klosterman, 1998b, Roselli et al., 1985b). The expression of aromatase in the VMHvl is thought to be critical for the masculine organisation of the male brain via E₂ (Yang and Shah, 2014). Receptor expression in the VMH is plastic between the organisational and activational periods. In adulthood, ER α is the predominant ER isoform present in the VMHvl of either sex (Correa et al., 2015). Yet, immunohistochemical studies have shown that in both male and female rats, ER β is expressed in the VMHvl during early postnatal development at remarkably higher levels than in adulthood, though expression is still lower than ER α regardless of age (Ikeda et al., 2003). ER β expression in the VMH may be determined by E₂, since neonatal female rats, which develop in the absence of ovarian E₂, express greater amounts of ER β in the VMH than males (Orikasa and Sakuma, 2004). Treatment of neonatal females with E₂ or neonatal castration of males reversed the sex difference in ER β expression (Orikasa and Sakuma, 2004). Furthermore, there was no difference in ER β expression between control males and males administered oestradiol benzoate (EB) neonatally (Ikeda et al., 2003). Together, this suggests a central involvement of E₂ in regulating the sexually dimorphic neurochemistry in the developing rodent brain.

The topography and density of receptors in the female VMHvl have been intricately linked to female sexual receptivity (Musatov et al., 2006, Xu et al., 2011). Indeed, the VMH is the final neural output of the lordosis reflex, and lesions in this area result in permanent deficits in reproductive behaviour (Mathews et al., 1983). In males, the VMHvl is heavily implicated in aggression-seeking behaviours, as neurones become

active during a task where male mice repeatedly self-initiate trials to seek opportunities to attack (Falkner et al., 2016). Reversible genetic suppression of electrical excitability in VMHvl neurones can reversibly inhibit aggressive behaviour (Lin et al., 2011). ER α knockdown in the VMH, but not in the mPOA or meA, significantly decreased aggressive behaviours, indicating that aggression is dependent on E₂ signalling in the VMH (Sano et al., 2013). Whilst the VMH is not traditionally considered an important node in male sexual behaviour, ER α knockdown in the VMH was associated with fewer attempted mounts and fewer intromissions (Sano et al., 2013). One study has identified a neuronal population distinct from the pool of neurones active during aggression that are active during mating (Lin et al., 2011). The role of these neurones remains unclear, though one line of thought is that these neurones inhibit the firing of aggression-related neurones in the VMHvl (Lin et al., 2011).

Aside from social behaviour, the VMH is also important in metabolism, thermoregulation, and locomotor activity in both sexes (Xu et al., 2011, Musatov et al., 2007, Narita et al., 2016). The functional and behavioural pleiotropy of this hypothalamic node despite the somewhat heterogeneous molecular environment is intriguing and is no doubt a reflection of a complex integration of hormonal, sensory, and neural signals.

1.4 Behavioural effects of neuroestrogen

The SBN is the generative site of behaviour that is organised by E₂, as discussed in section 1.3. In adulthood, the SBN is activated by E₂ signalling via its genomic and nongenomic receptors (Laredo et al., 2014).

In this section, the contributions of E₂ to the behaviours relevant to this thesis will be discussed. It is important to note that the actions of E₂ are not exclusive to the behaviours discussed here; effects on other behaviours are discussed in Bridges (2015) (maternal behaviour), Walf and Frye (2006) (depression), and Rivera and Stincic (2018) (feeding behaviour).

1.4.1 Contribution of E₂ to reproductive behaviour in male and female mice

Sex dimorphisms in reproductive behaviour are easily identified and are intricately influenced by E₂. Female sexual behaviour can be broadly divided into two components: proceptivity (readiness to mate) and receptivity (acceptance of mating) (Beach, 1976). OVX abolishes both proceptive and receptive sexual behaviour, and hormonal priming with subcutaneous injections of E₂ and progesterone to simulate

oestrous is effective at restoring sexual behaviours (Jennings and de Lecea, 2020). Because of this, hormone-primed OVX mice are commonly used as stimulus mice in the investigation of male sexual behaviour, as their sexual responsiveness can be accurately timed to coincide with experimentation (Cummings and Becker, 2012). Previous research has used hormonal implants to localise the effects of E₂ to the POA and VMH (Barfield and Chen, 1977, Davis et al., 1979). Sexual behaviour was activated with EB implants in the POA, but to a greater extent in animals with EB implants in the VMH (Barfield and Chen, 1977). Stereotaxic implantations of the anti-oestrogen CN-69,725-27 in subcutaneously primed OVX rats inhibited lordosis, and this was reversed following the removal of the CN-69,725-27 cannulas (Luttge, 1976). E₂ is believed to act via both genomic and nongenomic mechanisms to facilitate lordosis behaviour. Silencing of ER α in the VMH abolishes the transcriptional upregulation of the progesterone receptor that is required for proceptive behaviours and lordosis in female mice (Musatov et al., 2006). Meanwhile, administration of the GPER1 agonist G-1 prior to progesterone in an E₂-progesterone priming paradigm results in increased lordosis behaviour and decreased rejective responses in OVX rats (Anchan et al., 2014). One of the outputs of nongenomic signalling is the activation of protein kinases (Filardo et al., 2002). Direct administration of protein kinase inhibitors to the VMH blocked the facilitation of lordosis that was induced by infusions of E₂ into the VMH (Domínguez-Ordóñez et al., 2019). This suggests that nongenomic signalling in the VMH is required for female reproductive behaviour. Interestingly, ArKO mice show little lordosis behaviour when primed with E₂ and progesterone that is behaviourally effective in WT controls (Bakker et al., 2002). This suggests that E₂ is required not only for the activation of the lordosis neural circuit, but for its organisation. This is contrary to the widely held belief that the female brain develops in the absence of E₂ due to a quiescence of the ovaries, suggesting a role for locally produced E₂ in the organisation of the sexually dimorphic brain.

A central role for E₂ in male sexual behaviour was established in male mice injected with an AAV against ER α in the mPOA, resulting in reduced sexual behaviour (Sano et al., 2013). In castrated rats, bilateral infusions of E₂ to the mPOA are more effective than testosterone in the resumption of male sexual behaviour (Christensen and Clemens, 1974), though behaviour was not completely restored. Indeed, the full and complete expression of male sexual behaviour requires both androgens and E₂ (Hull and Dominguez, 2007, Baum and Vreeburg, 1973). Unlike females, the actions of E₂ in male sexual behaviour are mainly localised to the mPOA (Dominguez and Hull, 2005). ER α -expressing neurones in the mPOA become active during social investigation with

a proceptive female, and activity of these neurones further increases during mounting (Wei et al., 2018). E₂ was demonstrated to rapidly (within 35 min) induce mounting behaviour in sexually naïve rats and reduced the latency to mount in sexually experienced castrated rats (Cross and Roselli, 1999). Roles for nongenomic E₂ signalling have been further highlighted by the observation of increased levels of phosphorylated ERK in the male mPOA when introduced to a sexually receptive female (Taziaux et al., 2007), and levels were shown to remain elevated after the display of copulatory behaviour (Jean et al., 2017). In ArKO male mice, E₂ administration rapidly restores most aspects of sexual behaviour, but the effect is best observed in mice that are sexually experienced and pretreated with a small dose of EB (Taziaux et al., 2007). This effect of pre-dosing suggests that some priming is required for the full expression of male reproductive behaviour.

1.4.2 Contribution of E₂ to aggression in rodents

Aggressive behaviour in rodents is typically measured as intermale aggression in the resident-intruder paradigm (Koolhaas et al., 2013), though aggression relating to parenthood is shown in both sexes (Bridges, 2015, Trainor et al., 2008a). The neuroanatomical pathway of aggression includes several SBN nuclei, including the AH, BNST, LS, and meA (Nelson and Trainor, 2007). Several biochemical signals influence aggression (Nelson and Trainor, 2007), but of the steroid hormones, testosterone and E₂ have been studied in the most detail. Androgens have a central effect on the organisation of aggressive neural correlates, as neonatal castration significantly reduces the expression of aggressive behaviour in adulthood (Peters et al., 1972). This was further refined to be an effect of E₂ using ArKO mice, which show a complete loss of aggressive behaviour in adulthood that is prevented if E₂ is supplemented on the day of birth (Toda et al., 2001). E₂ signalling in adulthood is an important influence on aggressive behaviour, which is positively correlated with ER α expression levels in the LS, BNST, and AH, but not the mPOA (Trainor et al., 2006). Despite this, lesion studies have demonstrated an important role for the mPOA in suppressing aggression (Albert et al., 1986). The suppressive action of the mPOA is mediated through ER α -positive GABAergic cells that project to the VMHvl that, upon optogenetic activation, caused a reduction in intermale aggression (Karigo et al., 2021). Optogenetic inactivation of the pathway between ER α -positive mPOA neurones and the VMHvl increased aggression (Wei et al., 2023). Conversely, knockdown of ER α in the VMH was shown to reduce aggressive behaviour (Sano et al., 2013), suggesting that a) ER α is central to the normal expression of male aggressive behaviour, and b) the effect mediated by ER α is dependent upon the subregion of the brain in which it is expressed. The effect of ER β

on aggression, though less well studied, is believed to be dependent on age. ERK α mice showed increased aggressive behaviour and shorter latency periods to attack compared to WT mice during puberty (Nomura et al., 2002), but normal levels of aggression during adulthood (Ogawa et al., 1999). Secondary to E₂ signalling, a role for GABA transmission has been elucidated: deletion of ER α from GABAergic, but not glutamatergic, neurones in the BNST and mPOA was found to attenuate aggressive behaviour in male mice (Wu and Tollkuhn, 2017), suggesting that non-genomic signalling makes an important contribution to the facilitation of aggression in male rodents.

Seasonal or photoperiod sensitive animals, such as rodents, respond to altered day length with changes in their physiology and behaviour to adapt to their environment. In many rodent species, winter-like short day photoperiods induce aggression to a greater degree than summer-like long day photoperiods (Silva et al., 2010), and this has region-specific effects on ER expression (Trainor et al., 2007b). For example, ER α -immunoreactivity in the lateral septum increased on short days in old field mice and deer mice, and this was positively correlated with aggression in old field mice (Trainor et al., 2007b). Meanwhile, ER β -immunoreactivity was decreased in the BNST, meA, and VMH (Trainor et al., 2007b). In castrated old field mice housed under short or long days that received an injection of E₂ or saline, E₂ was shown to increase the number of offensive attacks by short day mice after 15 min (Trainor et al., 2007a), suggesting a role for nongenomic E₂ signalling in aggressive behaviour. This was supported by the fact that cycloheximide, a protein synthesis inhibitor, did not alter the rapid facilitation of aggression in castrated mice housed in short photoperiods with E₂ supplementation (Laredo et al., 2013).

1.4.3 Contribution of E₂ to anxiety in rodents

E₂ has been shown to affect nonreproductive behaviours in rodents, such as anxiety, a sexually dimorphic behaviour that is determined by organisational and activational E₂ (Domonkos et al., 2018). For example, offspring of rats with maternal hypergonadism are more likely to develop anxiety, and this is seen especially in female offspring (Hu et al., 2015). Administration of testosterone to female mice on the day of birth increased marble burying when tested in adulthood, indicative of increased anxiety (Goel and Bale, 2008). Prepubertal castration of male rats was found to increase the time spent in the open arms of the elevated plus maze (EPM) and increase the amount of time spent in the light section of the light-dark test (LDT) (Brown et al., 2015). Contrarily, castration of adult male rodents is associated with

increased anxiety in the open field (OFT), EPM, and burying tests (Carrier et al., 2015, Frye and Seliga, 2001). Sex differences in the display of anxious behaviour and the contributions of E₂ are conflicting and often inconsistent between studies. Female rats in proestrous display more exploratory behaviour in a novel environment, more time in the open arms of the EPM, and interact for longer with an unfamiliar social partner compared to females in other stages of their oestrous cycle or other males (Frye et al., 2000). Similarly, OVX rats receiving E₂ injections displayed increased exploration of the open arms of the EPM (Nomikos and Spyraiki, 1988). OVX rodents that do not receive exogenous E₂ show increased anxiety (de Chaves et al., 2009, Puga-Olguín et al., 2019). However, these actions are not always consistent, and may depend upon the nature of the test used. For example, treating OVX rats with E₂ has been reported to increase (Morgan and Pfaff, 2001) and decrease (Palermo-Neto and Dorce, 1990) locomotor activity in the OFT. In the EPM, a non-social anxiety test, males are typically more anxious than females, but tend to be less anxious in social investigation tests (Scholl et al., 2019). A recent approach that utilised a conflicting dark (preferred) vs light dilemma with a weaker but increasingly aversive hyperthermic condition showed that in more complex multi-dimensional tests of anxiety behaviours, females are more anxious than males (Lee et al., 2022).

One of the predominant brain areas involved in anxious behaviours is the paraventricular nucleus (PVN). The PVN is subdivided into the anterior and posterior divisions which are both anatomically and chemically unique from one another, implying the existence of distinct functional differences across a singular nucleus (Barson et al., 2020). The anterior PVN projects widely to limbic areas, with dense projections to the suprachiasmatic nucleus, associated with circadian rhythm, and the dorsomedial accumbens shell, associated with appetitive behaviours (Dong et al., 2017). The posterior PVN harbours dense projections towards the BNST and amygdala, which are involved in anxiety and fear (Dong et al., 2017). Efferent fibres travel within the PVN, from anterior to posterior regions, though fibres travelling in the opposite direction have not been found, suggesting that information flow may be unidirectional in the PVN (Vertes and Hoover, 2008). Some of these intra-PVN efferent fibres originate from magnocellular neuroendocrine neurones that reside in the anterior PVN. The PVN also integrates a variety of signals that contribute to anxiety. For example, the prelimbic cortex is critical for the retrieval of remote fear memories and promotes conditioned fear responses that contribute to fear generalisation and anxiety (Kirouac, 2021a). The PVN is one of the few brain regions that expresses greater levels of ER β than ER α (Shughrue et al., 1997), and activation of these receptors is

believed to either decrease or increase anxiety, respectively. The dichotomous effect of each of these receptors may account for the inconsistencies in the literature regarding the role of E₂ signalling in anxiety. Subcutaneous injections of the ER β -specific agonist diarylpropionitrile (DPN) were shown to reduce anxiety-related behaviours in the OFT, LDT, and EPM and were associated with decreased plasma corticosterone compared to OVX rats treated with vehicle control or the ER α agonist propylpyrazoneetriol (PPT) 1 h after removal from the maze (Lund et al., 2005). Other studies have also corroborated the reduction in plasma corticosterone associated with ER β signalling, as well as increased reactivity of the hypothalamic-pituitary-adrenal (HPA) axis with ER α signalling (Weiser and Handa, 2009, Weiser et al., 2009). Consistent with this, gonadally intact ERKO β female mice show increased anxiety in the EPM compared to WT controls (Krężel et al., 2001). ER β may mediate its anxiolytic effects via non-traditional ligands such as 3 β -diol, an androgenic metabolite of DHT (Ando et al., 2016). Wax pellets containing 3 β -diol and implanted directly above the PVN were effective in reducing plasma corticosterone in male rats 30 min after restraint stress (Lund et al., 2006). It has been suggested that ER α has no effect on anxiety since behaviours in gonadally intact ERKO α female mice were no different to WT controls (Krężel et al., 2001). However, some studies have reported anxiogenic effects in animals treated with PPT (Lund et al., 2005). ER α is found at low levels in the rodent PVN (Suzuki and Handa, 2005) and is less abundant than ER β in the amygdala (Shughrue et al., 1997), yet a subpopulation of cells in the peri-PVN express ER α and GAD-67, the rate-limiting enzyme for the production of GABA (Weiser and Handa, 2009). The glucocorticoid-induced negative feedback on PVN activity is mediated through increased GABA release onto parvocellular neurones of the PVN (Di et al., 2005), and this negative feedback is impaired by the administration of PPT (Weiser and Handa, 2009). Magnocellular neurones of the PVN produce oxytocin, which has classically been associated with parturition and lactation, but has also demonstrated negative correlation with anxiety (Borrow and Handa, 2017). Oxytocin and ER β are colocalised within the PVN, and the ER β -specific agonist 3 β -diol increased oxytocin mRNA in a mouse hypothalamic cell line (Hiroi et al., 2013). GPER1 has also been localised in magnocellular neurones in the PVN (Hadjimarkou and Vasudevan, 2018). The parvocellular neurones of the PVN secrete corticotropin-releasing hormone, a central regulator of the HPA axis, and there is significant overlap between ER β and AVP-immunoreactivity specific to parvocellular neurones (Kanaya et al., 2019). Thus, both genomic and nongenomic ERs are strategically positioned to modulate anxiety via the PVN.

The expression of GPER1 in the hippocampus and amygdala implicates nongenomic signalling in the regulation of anxious behaviours (Hazell et al., 2009). Signalling through ERK, which can be induced by GPER1, (Filardo et al., 2002) has been shown to be anxiogenic in mice (Sato et al., 2011), and treating OVX female or gonadally intact male mice with G-1 led to increased anxious behaviour in the EPM, LDT, and OFT (Kastenberger et al., 2012). However, this study administered treatment 2 h prior to testing, which could encapsulate both genomic and nongenomic signalling time frames. Another study, which administered G-1 30 min prior to behavioural testing, showed that G-1 was anxiolytic in castrated male, but not OVX female, mice tested in the EPM (Hart et al., 2014). The disparity in these results could be due to differences in gonadal status, drug dosages, and time between injection and behavioural testing. GPER1 is expressed in the paraventricular nucleus, though there have been no functional connections between activation of the receptor and anxiety. Activation of GPER1 in the PVN has been shown to promote anti-inflammatory effects in the early stages of colitis in mice (Jiang et al., 2019) and decrease fluid intake in female rats (Santollo and Daniels, 2015). However, given the importance of E₂ signalling and PVN activation in anxious behaviours, it is possible that GPER1 signalling also plays a contributory role. Clearly, further efforts are required to understand the role and molecular actions of ERs in regulating non-social behaviours such as anxiety.

1.4.4 Oestrogen-mediated spinogenesis

The structural plasticity of dendrites and dendritic spines is an important neural effect of E₂ that may act as the interface between neuroendocrine physiology and behaviour (Gorman and Docherty, 2010, Woolley and McEwen, 1993). Changes in E₂ across the 5-day oestrous cycle of the rat have been shown to rapidly modulate hippocampal spine density (Woolley and McEwen, 1992), and OVX has been associated with a gradual loss of dendritic spines that nadirs roughly six weeks post-surgery (Woolley and McEwen, 1993). A single injection of E₂ benzoate increases dendritic spine density within 24 h, with peak densities reached within 2-3 days, and a gradual decline in density over the following 7 days (Woolley and McEwen, 1993), suggesting this is mediated by genomic signalling. Previous studies have indicated divergent roles of ER α and ER β in spinogenesis: in hippocampal neurones, activation of ER α , but not ER β , significantly increased spine density within 2 h of drug application (Mukai et al., 2007). However, in cortical neurones, the ER β agonist WAY-200070 increased spine density within 30 min (Srivastava et al., 2010, Sellers et al., 2015). Increases in dendritic spine density have been correlated with activation of kinases, such as ERK (Srivastava et al., 2010). MAP kinase inhibitors are effective in

suppressing spinogenesis in the face of E_2 (Mukai et al., 2007). GPER1 can also activate these kinases, and recent reports have suggested that nongenomic signalling via this receptor has a positive effect on spine density in the hippocampus (Kim et al., 2019, Li et al., 2021). In the ARC, nongenomic signalling was proposed to mediate dendritic spine plasticity, as E_2 was able to increase density of immature filopodial spines within 4 h (Christensen et al., 2011). The study further showed that, in animals injected with EB and perfused 1 h later, phosphorylated cofilin, a marker for remodelling of the actin cytoskeleton, was increased. However, in animals that received an mGluR1a inhibitor 1 h before EB injection, phosphorylated cofilin levels were no different to that of vehicle-treated controls (Christensen et al., 2011). This suggests that nongenomic E_2 signalling initiated by the $ER\alpha$ -mGluR1a complex regulated dendritic spine plasticity. Genomic signalling may be more important for the maintenance and maturation of spines, as mature mushroom-shaped spines increased from 20 h after EB injection (Christensen et al., 2011).

The contribution of neuroestrogens to spinogenesis is an experimental conundrum since it is difficult to separate the actions of central and systemic E_2 by OVX. OVX resulted in decreased spine density in hippocampal CA1 neurones (Woolley and McEwen, 1993), suggesting that neuroestrogens do not contribute to spinogenesis. However, other studies have found no effect of OVX on dendritic spine density in CA3 neurones (Mendell et al., 2017), suggesting either a) dendritic spines in the CA3 layer are not regulated by E_2 or progesterone, or b) neuroestrogens play a greater role than ovarian E_2 in the regulation of CA3 spines. Aromatase has been detected in synaptic terminals, positioning it perfectly to mediate rapid signalling mechanisms that could lead to outputs that include spinogenesis (Srivastava et al., 2010). However, many *in vivo* experiments have supplied aromatase inhibitors peripherally (Zhao et al., 2018, Liu et al., 2019, Zhou et al., 2010), and although these are given at concentrations that cross the blood brain barrier, they may affect the function of peripheral aromatase making it difficult to disseminate the effects of brain and peripheral aromatase inhibition. Aromatase inhibition in hippocampal slice cultures results in a reduction in spine density (Kretz et al., 2004a), and in cortical neurones, aromatase is colocalised with PSD-95 (Srivastava et al., 2010). In the forebrain-specific ArKO mouse, spine density was significantly decreased in the CA1 region and cortex, but the morphology of spines affected were dependent on sex (Lu et al., 2019). In adult male forebrain-specific ArKO mice, immature thin spines were significantly decreased, whereas in adult OVX mice of the same genotype, mature mushroom spines showed the greatest decrease in comparison to OVX WT controls (Lu et al., 2019). Thus, not only do

neuroestrogens have a temporal effect on spine maturation as discussed above, but also a sexually dimorphic effect on dendritic spine maintenance that has been associated with cognitive function (Lu et al., 2019).

Studies have revealed that alterations in spinogenesis can have profound effects on behaviour. Dendritic spines play a role in the regulation of mood and emotion, and chronic stress is associated with decreased dendritic spines and synaptic plasticity in the hippocampus (Chen et al., 2008). In the ARC, dendritic spine morphology is critical for the display of lordosis behaviour in female rats, and disruption of E₂-induced spinogenesis attenuated lordosis (Christensen et al., 2011).

1.5 Experimental rationale

E₂ is critical for the organisation and activation of the brain, specifically the nodes of the SBN, which contribute to the expression of sex typical behaviours. The brain can synthesise E₂ from haematogenous precursors or *de novo* in neurones, astrocytes, and glia. It is thought that neuroestrogens are important to increase local concentrations of E₂ to support rapid signalling processes which underlie many physiological processes from spinogenesis to behaviour. Despite this, there is a relative lack of literature documenting direct measurements of E₂ in discrete regions of the rodent brain. This gap in knowledge hinders a comprehensive understanding of the spatial distribution of neuroestrogen and the precise regulatory mechanisms governing its production. Numerous studies have shown that aromatase expression and/or activity is regulated by ERs (Yilmaz et al., 2009) and the progesterone receptor in hypothalamic neuronal cell lines (Yilmaz et al., 2011), and androgens (Abdelgadir et al., 1994) in the male and female rat brain. However, the intricate details of these regulatory interactions, particularly within the SBN, remain unclear. As a result, there exists a compelling need for further research to unravel the complexities of neuroestrogen synthesis and its regulation, specifically within those regions that are activated by E₂ to facilitate behaviour.

The purpose of the research herein is to understand how hormone synthesis is regulated in two key nodes of the mouse SBN: the mPOA and the VMH. This has been investigated primarily in female mice to dissect the relative contributions of ovarian and central E₂ to neuroendocrine physiology. We also aimed to understand how the process of neuroestrogen production is regulated in each of these nuclei, given the evidence that aromatase expression and neurosteroid production is region specific. We also investigated how the regulation of neuroestrogen production affected

neuroarchitecture in the female mouse hypothalamus. Finally, we investigated how this contributes to behaviours in the male and female mouse. This thesis represents a well-rounded body of research into both the molecular mechanisms and behavioural function of neuroestrogen production, as summarised in **Fig. 1.3**.

Figure 1.3. Aims of this thesis. In this thesis, we aim to understand neuroestrogen synthesis within the medial preoptic area and ventromedial hypothalamus, two key hypothalamic nodes of the social behaviour network, and how this is regulated. We also wish to explore how this affects neuroarchitecture underlying anxious behaviours, and how neuroestrogens themselves contribute to sex and aggressive behaviours.

Chapter 2

Materials and Methods

Consumables and materials used in this thesis are shown in **Appendix Table S1**.

2.1 Mice

All animal experimental procedures described in this thesis conformed to institutional and national ethical guidelines and were approved by the University of Reading, UK, and the Animal Care and Use Committee at the University of Tsukuba, Japan. All efforts were made to minimise the number of animals and their suffering. All efforts were made to ensure adequate enrichment of animals, as described below. Power analysis (section 2.15) was performed to ensure the correct number of animals used and prevent unnecessary wastage of animal life. Although alternative methods can be utilised for neuroendocrine experiments without the need for live animals (e.g., primary cell culture or using hypothalamic cell lines such as N42 cells), there is a considerable lack of literature addressing sex differences in neuroendocrine function in intact, non-hormone-primed animals. This gap not only perpetuates the sex bias in biomedical research but also implies the existence of unidentified therapeutic targets for human medicine (see Chapter 7).

For experiments carried out at the University of Reading UK: Female C57/BL6J mice were purchased at 6-8 weeks old (Charles River and Envigo, UK) and group housed (maximum of 5 mice/cage of same-sex animals) in plastic cages (17 x 33.5 x 12cm) with white paper for nesting and plastic toys (ball, tunnel) for enrichment, provided by the Bioresource Unit at the University of Reading. Food (SDS RM3 (P) mouse diet, LBS Biotechnology, UK) and water were provided *ad libitum* and animal housing rooms were maintained on a 12 h light/12 h dark cycle (lights off at 19:00) at a constant temperature ($23 \pm 2^\circ\text{C}$). No live animals received any drugs or modified diets that would require the use of a project license. Mice were killed by Schedule 1 procedures (cervical dislocation); these are not regulated procedures and therefore did not require a project license. The researcher undertaking these procedures (JD) was fully trained and named on the University of Reading's Schedule 1 register.

For experiments carried out at the University of Tsukuba, Japan: All mice were maintained in breeding colonies by technicians at the Laboratory Animal Resource Centre at the University of Tsukuba. At the time of weaning at 3 weeks old, mice were transferred to the animal housing facility in Research Building D at the University of Tsukuba. Here, mice were group housed in plastic cages with cornhusk bedding for enrichment provided by the Laboratory Animal Resource Centre (3-5 mice/cage of same-sex animals) and provided with food (standard MF, Oriental Bioservice, Japan)

and water *ad libitum*. Animal housing rooms were maintained on a 12 h light/12 h dark cycle (lights off at noon) at a constant temperature ($23 \pm 2^\circ\text{C}$). All procedures carried out on mice in Japan were reviewed by the Animal Care and Use Committee at the University of Tsukuba and complied with the national Guidelines for Proper Conduct of Animal Experiments issued by the Science Council of Japan.

2.1.1 Aromatase-flox (*Aro^{fl/fl}*) mice

Aro^{fl/fl} mice, in which the aromatase allele was floxed to allow conditional and site-specific knockdown of the aromatase gene, was constructed at MRC Harwell (funding from NSF CAREER grant IOS-105371 to Dr Nandini Vasudevan) and maintained and bred at Laboratory Animal Resource Centre at the University of Tsukuba.

For the generation of *Aro^{fl/fl}* mice, which was carried out by researchers at MRC Harwell, a targeting vector (**Fig. 2.1A**) containing the neomycin resistance gene (*neo*) and lacZ reporter gene flanked by two FRT sites and three loxP sites was constructed. The vector was introduced into the WT aromatase gene at a critical site between exons 1 and 2 in C57Bl/6N embryonic stem cells to generate a “knockout-first” allele (tm1a) using electroporation (**Fig. 2.1B**). The embryonic stem cells that successfully incorporated the targeting vector were selected in the presence of neomycin. Probes were then used to identify the presence of hybridisation bands corresponding to the loxP-flanked aromatase gene. The correctly targeted cells were transfected with an FLP recombinase expression plasmid to delete the FRT-flanked *neo* cassette to generate a conditional allele (tm1c) (**Fig. 2.1B**), in which aromatase exon 2 is flanked by loxP sites. The resulting DNA was used to generate chimeric mice at the University of Tsukuba that successfully transmitted the gene in the germ line. Mice homozygous for the floxed aromatase gene (*Aro^{fl/fl}*) were born at the expected Mendelian ratios and presented with no obvious abnormalities. At the time of weaning at 3 weeks old, tail tissue of tm1c mice was collected for gel-based genotyping by research technicians at the University of Tsukuba before the mice were transferred to the animal housing facility in Research Building D at the University of Tsukuba. The PCR cycling conditions were: 1 min hold at 95°C ; 30 cycles of denaturation at 95°C for 10 sec, annealing and extension at 60°C for 10 sec and 72°C for 1 sec; 72°C for 30 sec; infinite hold at 16°C . The PCR mix for genotyping consisted of 5 μl KAPA2G Fast Hotstart Readymix (Roche, Sigma-Aldrich), 2.5 μl nuclease free water, 1 μl (~30 ng) DNA template, and 0.5 μl of each primer at a final concentration of 20 μM . The primers used were the Cyp19a1-5arm-WTF (TATCCTCGCAGACCCTCTC), Cyp19a1-Crit-WTR

(GAAGCATGGCTTCAAAGTTGC) and 5mut-R1 (GAACTTCGGAATAGGAACTTCG). WT and tm1c mice both produce PCR products from the Cyp19a1-5arm-WTF and Cyp19a1-Crit-WTR, although the tm1c product (472 bp) is 200 bp bigger than the WT product (272 bp) due to the presence of the FRT-loxP part of the cassette. Only tm1c mice produce a mutant-specific product of 186 bp from Cyp19a1-5arm-WTF and 5mut-R1 (Fig. 2.1C-D).

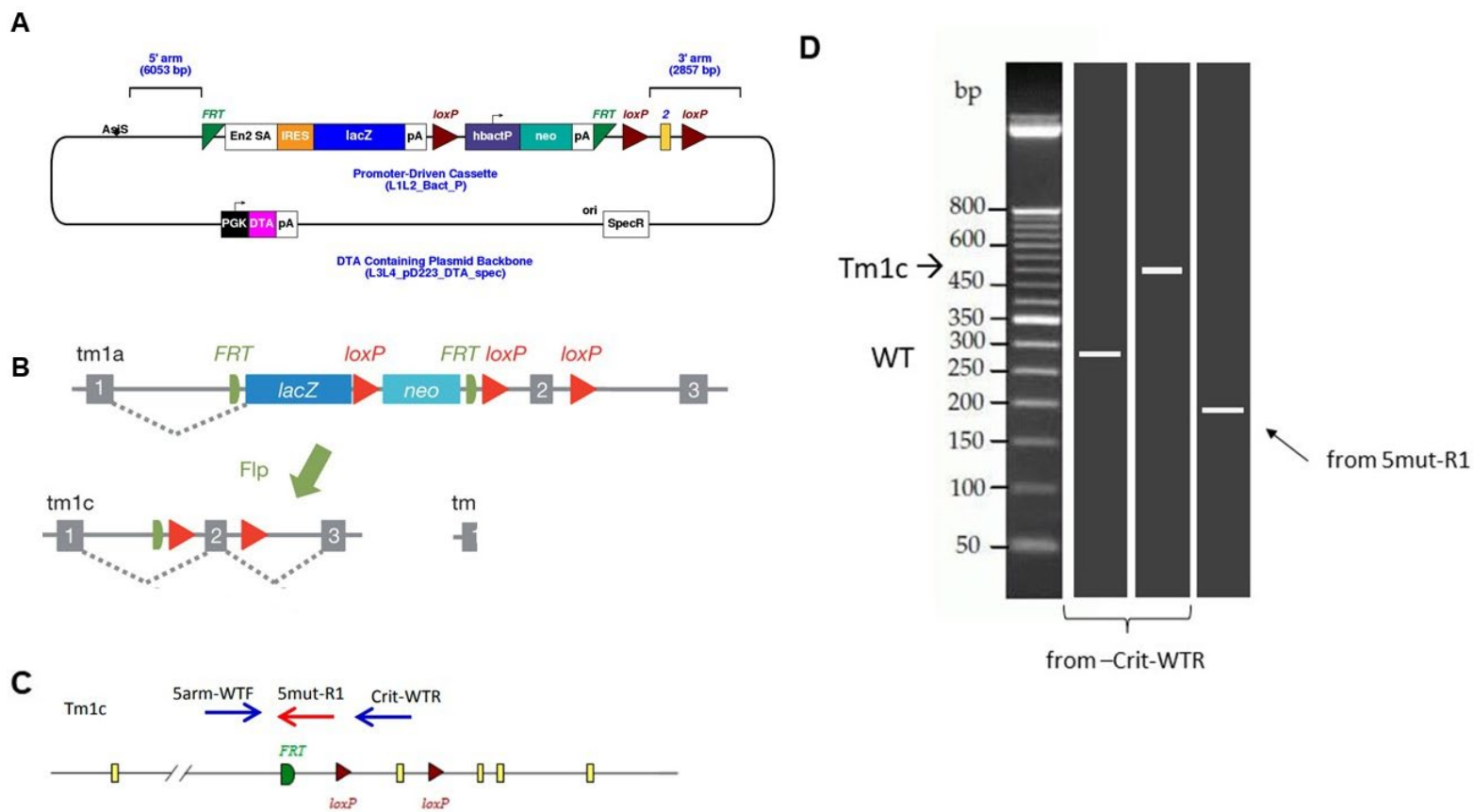


Figure 2.1. Generation of *Aro*^{fl/fl} mice. The targeting vector (**A**) contained three loxP sites and two FRT sites that flanked the neomycin resistance gene (*neo*) and the lacZ reporter gene. The vector was electroporated into mouse embryonic stem cells, thereby introducing the vector to the aromatase gene at a critical site between exons 1 and 2, shown by the numbered grey bars (**B**). This created a “knockout-first” allele (tm1a). Embryonic stem cells with the tm1a allele were selected in the presence of neomycin. Probes were used to identify the presence of hybridisation bands corresponding to the loxP-flanked aromatase gene. Correctly targeted cells were transected with an Flp recombinase expression plasmid, which deleted the FRT-

flanked *neo* cassette to generate a conditional allele (tm1c), in which aromatase expression is restored (**B**). Aromatase can later be conditionally knocked out by injecting a Cre-expressing vector, which deletes the floxed exon of the tm1c allele to generate a frameshift mutation. Tm1c mice were genotyped using three primers, Cyp19a1-5arm-WTF, designed to the 5' homology arm, Cyp19a1-Crit-WTR, and 5mut-R1 (**C**). **D** shows an example representative gel in which WT produces a 272 bp product from Cyp19a1-5arm-WTF and Cyp19a1-Crit-WTR. These same primers produce a 472 bp product in tm1c. Tm1c mice produce a mutant-specific product of 182 bp from the Cyp19a1-5arm-WTF and 5mut-R1 primers.

2.2 Surgical procedures

Every effort was made to use aseptic technique during surgical procedures to circumvent infection and further unnecessary pain caused to animals.

2.2.1 Ovariectomy

Female mice were bilaterally ovariectomised (OVX) under anaesthesia with isoflurane inhalation (1.5-3%). Fur was shaved off the flank area and a dorsolateral incision was made in the area between the last rib and hips, where the musculature was separated from the skin. The ovarian fat pad was carefully pulled out of the incision and the region below the ovary was clamped. The ovary was excised with scissors and the fat pad was returned before the incisions were sutured. After surgery, the animals were group housed ($n = 4$ per cage) with other OVX female mice and allowed 7 days to recover before use in experiments.

2.2.2 Hormone priming

10 μ g oestradiol benzoate (EB) in sesame oil was administered to female mice by subcutaneous injection 2 and 1 days prior to experimentation using a 26-gauge sterile needle. 500 μ g progesterone in sesame oil was administered by subcutaneous injection 4-6 h prior to experimentation using a 26-gauge sterile needle. Hormone priming was used specifically for sexual behaviour tests involving a male test mouse. One experiment used OVX test mice that received EB injections only. These were administered in the same protocol as described here, with the omission of the progesterone injection.

2.2.3 Intraperitoneal injections

In our experiments, we delivered drugs using intraperitoneal (i.p.) injections. I.p. injections were delivered bilaterally to adult female mice using a 27-gauge sterile

needle, dosed at 0.1 ml/10 g bodyweight, delivering 1 mg/ml letrozole and/or 12 mg/ml dutasteride and/or vehicle control (10% Tween-80 in sterile saline (v/v) for letrozole; 0.3% gelatine in sterile saline (w/v) for dutasteride). On average, mice received an injection volume of 0.2 ml bilaterally with no adverse effects. These drug concentrations and vehicles have been used previously and have been shown to cross the blood-brain barrier, resulting in behavioural effects (Litim et al., 2017, Chaiton et al., 2019). Mice receiving only vehicle controls were injected with the vehicle for letrozole in one side and the vehicle for dutasteride in the other. Mice receiving only letrozole were injected with letrozole in one side and the vehicle for the dutasteride in the other. Mice receiving both letrozole and dutasteride were injected with one treatment per side. All injections were administered during the light phase at approximately the same time each day. Animals were injected once a day for a total of 16 days, receiving 6 injections before behavioural testing commenced. On days of behavioural experimentation, experiments were carried out during the dark phase, at least 2 h after the animal received the injections.

2.2.4 Stereotaxic surgery

Stereotaxic surgery was carried out on adult male *Aro^{fl/fl}* mice, anaesthetised with inhalational isoflurane (1.5-3%) and placed in a stereotaxic frame with non-puncture ear bars (Model 900, David Kopf Instruments, USA). Fur was shaved from the top of the head and a petroleum-based lubricant was applied over the eyes. A sagittal cut was made in the skin to expose the skull, and Bregma was identified as the reference point to locate the medial preoptic area (mPOA). A burr hole was drilled into the skull on either side of the midline, and a 10 µl Hamilton syringe (gauge 26S, 2-inch needle length) was aimed at the mPOA using the coordinates ± 0.2 mm ML, +0.2 mm AP, -5.3 mm DV from the Bregma starting point, identified using the Paxinos Mouse Brain Atlas (Paxinos and Franklin, 2001) (**Fig. 2.1**). Each mouse was injected bilaterally with either 0.6 µl of pENN.AAV.hSyn.HI.eGFP-Cre.WPRE.SV40 (10^{13} packaged particles, 0.3 µl/hemisphere; James M. Wilson, Addgene plasmid #105540-AAV9; <http://n2t.net/addgene:105540>; RRID: Addgene_105540) or 0.6 µl of pAAV-hSyn-EGFP (10^{12} packaged particles, 0.3 µl/hemisphere; Bryan Roth, Addgene plasmid #50465-AAV2; RRID: Addgene_50465) over 3 min using a micropump injector (World Precision Instruments Inc., Sarasota, FL). The needle was left in place for additional 20 min following infusion before being withdrawn gently by 1 mm and being left in place for a further 5 min. After removal of the needle, the skin was silk sutured, and the mice were individually housed in running wheel cages. The location of the stereotaxic injection was confirmed by immunocytochemistry. Briefly, mice were

sacrificed by perfusion fixation (section 2.4) and brains were immediately isolated and post-fixed in 4% paraformaldehyde overnight at 4°C. The brains were washed in 0.1 M PBS before they were transferred to 30% sucrose in 0.1 M PB (w/v) for 24 h, or until the brains had sunk to the bottom of the tube. All brains were coronally sections at 60 µm on a freezing microtome (Leica Biosystems). Free-floating sections were washed in 0.2% Triton X-100 in 0.1 M PBS (v/v), (PBS-X) pH 7.2, followed by a further wash in 0.1% hydrogen peroxide in PBS-X (v/v) for 20 min to inhibit endogenous peroxidase activity. After 3 more washed in PBS-X, slices were incubated in blocking buffer (3% BSA (v/v) and 3% skim milk powder (w/v) in PBS-X) for 2 h. Sections were stained with the goat anti-GFP antibody (ab6673, Abcam) at 1:6000 dilution in blocking buffer overnight at 4°C. The avidin-biotin-peroxidase complex (Vectastain ABC Elite Kitm Vector Laboratories) was visualised with 0.03% 3,3-diaminobenzidine (DAB) and 0.0003% hydrogen peroxide in TBS for 10 min. Sections were mounted on gelatin-coated slides and air dried. The slides were dehydrated through an ascending alcohol series, cleared with xylene, and coverslipped with Permount. Staining was visualised using a fluorescent microscope (Zeiss AxioSkop) and GFP-positive cells were scored manually confirm the site of stereotaxic injection for each mouse.

2.2.5 Olfactory bulbectomy

Olfactory bulbectomised (OBX) Jcl:ICR mice were used as stimulus animals for the resident-intruder paradigm (see section 2.3.7). For the OBX procedure, male mice were anaesthetised with inhalational isoflurane (1.5-3%) and placed in a stereotaxic frame with non-puncture ear bars (Model 900, David Kopf Instruments, USA). A petroleum-based lubricant was applied over the eyes. Fur was shaved from the top of the head and a sagittal cut was made in the skin to expose the skull. A burr hole was drilled into each side of the skull covering the olfactory bulbs. The olfactory bulbs were removed using a vacuum pump and a sterile flat-ended 23-gauge needle, taking care to minimise damage to the vasculature and forebrain tissue. The incision was closed with a silk suture. Animals were group housed ($n = 4$ per cage) with other same-sex OBX mice and allowed at least 7 days to recover before use in experiments. OBX ensures lack of aggression by intruders so that the behaviour of the resident can be monitored without confound. This has been used routinely in Sano et al. (2013) and Ogawa et al. (2000).

2.3 Behavioural experiments

Timeline for behavioural testing will be given in the relevant chapters.

Behavioural experimentation (apart from running wheel analyses) took place 2 h after lights off and mice in the test were moved from housing rooms to behavioural rooms 1 h prior to lights off. This ensured that mice could acclimitise to the behavioural testing rooms prior to testing. Cage changes were not performed 48 h prior to each test. Mice were typically weighed after each behaviour test and prior to sacrifice.

2.3.1 Open field test (OFT)

Mice were tested for 10 min in an open field apparatus (60 x 60 cm, 28.5 cm-high wall), which was illuminated with white light at 19 lux and a recording camera directly above the arena. Activity and position in the arena were automatically monitored and analysed on a Macintosh computer using Image OFC 2.03 (O'Hara & Co., Ltd.), modified software based on the public domain NIH Image programme (developed at the U.S. National Institute of Health). The software split the arena into 25 squares (left to right, top to bottom), where squares 7-9, 12-14, and 17-19 were classed as the centre of the arena (illustrated in **Fig. 2.3**). At the beginning of the test,

the mouse was placed in the bottom right of the arena with its nose pointing towards the corner. The total ambulatory distance, total movement duration, movement speed, and centre duration were recorded automatically for each mouse. The first three measurements primarily indicated general exploratory activity levels in a novel environment, whereas the total duration in the centre of the arena was interpreted to be related to anxiety and fear. After completion of the test, mice were returned to the home cage. Between each test, the apparatus was thoroughly wiped clean with 70% ethanol.


1	2	3	4	5
6	7	8	9	10
11	12	13	14	15
16	17	18	19	20
21	22	23	24	25 

Figure 2.3. Open field test (OFT) arena. The Image OFC 2.03 (O'Hara & Co., Ltd) software, based on the public domain NIH Image programme (developed at the U.S. National Institute of Health) split the OFT area into 25 squares as shown. Mice were placed in the bottom right corner (square 25), facing the corner of the arena, at the beginning of the test. The total duration spent in the centre squares of the arena (highlighted in yellow), was interpreted to be related to anxiety and fear, where mice that spent more time in the centre were considered less anxious.

2.3.2 Elevated plus maze (EPM)

Mice were tested for 10 min in a maze consisting of a 5 x 5 cm centre platform from which extended four acrylic arms in a cross formation, with two opposing arms enclosed by side walls and two left open. Arms were 25 x 5 cm, with the enclosed arms having 15 cm-high transparent acrylic walls. The entire maze was elevated 59 cm from the ground and illuminated by a red light, with a recording camera placed directly over

the maze. Activity was automatically monitored and analysed on a Macintosh computer using Image OFC 2.03 (O'Hara & Co., Ltd.), modified software based on the public domain NIH Image programme (developed at the U.S. National Institute of Health). At the beginning of the test, mice were placed into the centre of the maze, facing one of the closed arms. Total ambulatory distance, movement duration, time spent in the open and closed arms, number of open arm entries, latency to enter open arms, time spent in the centre square, and time spent immobile were recorded automatically. These measurements were taken to analyse anxiety-related behaviour in the animals. Between each test, the apparatus was thoroughly wiped clean with 70% ethanol.

2.3.3 Light-dark test (LDT)

Apparatus consisted of an opaque black "dark" box (18.5 x 38.5 x 25 cm) with a doorway to a transparent "light" box (18.5 x 38.5 x 25 cm) which was illuminated at 20 lux. The dark box also had an entrance doorway, where mice were placed at the beginning of the test. Once mice had entered the dark box, the doorway to the light box was automatically opened 2 sec after movement was detected. Movements were recorded for 10 min on a Windows computer using Image J LD2 (O'Hara & Co., Ltd.) modified software based on the public domain NIH Image programme (developed at the U.S. National Institute of Health). For each mouse, the following activities were recorded: distance travelled in light and dark boxes, total distance travelled, time spent in light and dark boxes, number of transitions between light and dark boxes, and latency to the first entrance to the light box. These measurements were taken to analyse anxiety-related behaviour in the animals. Between each test, the apparatus was thoroughly wiped clean with 70% ethanol.

2.3.4 Social investigation test (SIT)

Two days before the test, extra bedding was added to each of the home cages. On the day of the test, the surplus soiled bedding was transferred to a larger housing cage (31 x 36.5 x 17 cm) which was used for testing, to allow the subject to establish territory in the larger cage quickly. The test was carried out in a soundproof box illuminated at 25 lux with a camera placed directly above the cage. Testing apparatus is shown in **Fig. 2.4**. Mice were tested individually in test cages that contained their own home bedding. A gonadally intact male stimulus mouse of C57Bl/6J strain was placed in a perforated plexiglass cone (6.4 cm base x 4.3 cm top x 16 cm height) for 5 min before the test. A male mouse was used to evoke more anxiety in the female test mouse. For the test, female mice were placed in the test cage with an empty plexiglass cone for 5 min. The plexiglass cone was then replaced with the cone containing the

male stimulus mouse and the test continued for 15 min. The total ambulatory distance, average moving speed, immobile time, and the count and duration of contact with the social investigation cone was recorded automatically using an independently licensed software (O'Hara& Co., Ltd.) for the Ogawa Lab, University of Tsukuba. Between each test, the stimulus mouse was swapped out and each plexiglass cone was thoroughly wiped clean with 70% ethanol.

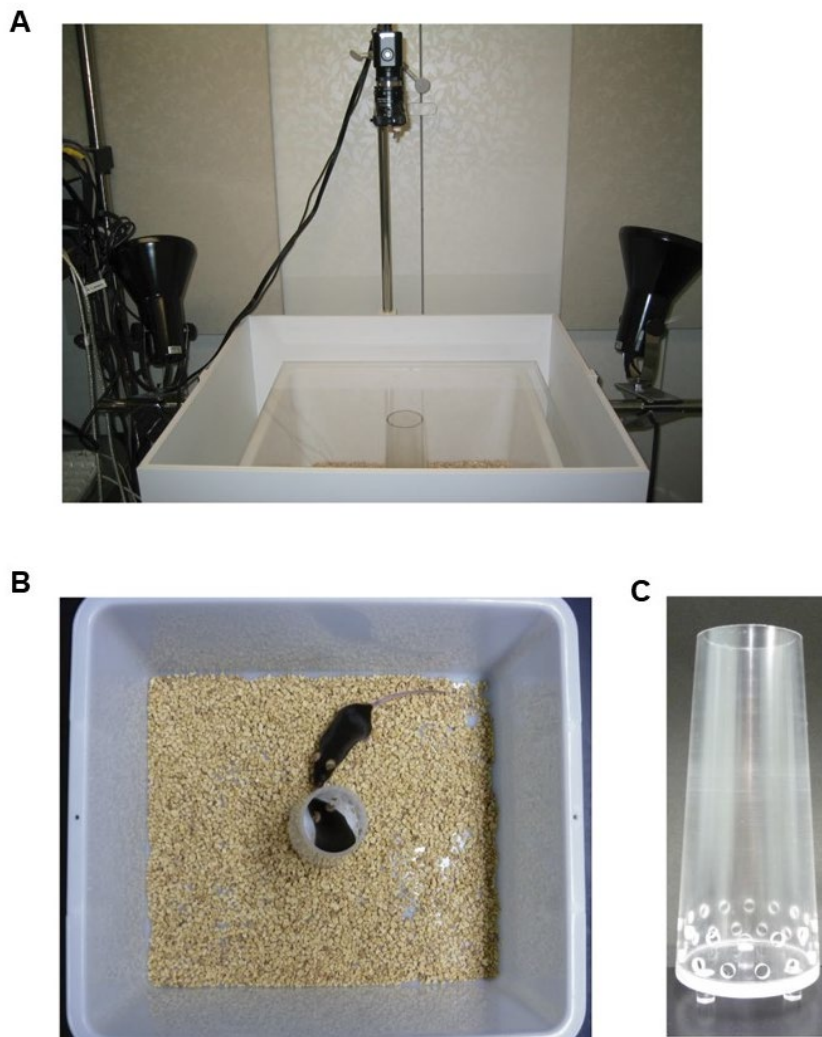


Figure 2.4. Social investigation test apparatus. The test apparatus (**A**) consisted of a camera placed over a white plastic testing cage (**B**) and a transparent plexiglass cylinder (**C**). The test apparatus was housed within a soundproof box which was illuminated under 25 lux white light. The cone was placed in the centre of the testing cage as shown in **B**, either empty or with a stimulus mouse inside. The test mouse was able to pick up on odour cues through the small holes in the plexiglass tube. This figure is modified from (Tsuda and Ogawa, 2012) Tsuda and Ogawa (2012).

2.3.5 Running wheel

Aromatase-flox mice were individually housed in plastic cages (29.8 x 19m x 12 cm) equipped with a running wheel (25 cm diameter). Each revolution of the wheel was registered by a laser beam, which was connected to a counter. The number of revolutions was recorded daily for 15 days (data starting on day 3 were included for analysis so that stable data may be analysed). After the last recording day, the running wheel apparatus was removed, and mice remained individually housed.

2.3.6 Sexual behaviour

Two sexual behaviour tests were conducted one week apart. Sexual behaviour was measured in the home cage. Subject male *Aro^{flox}* mice were placed with an OVX female stimulus mouse that was in hormone-primed oestrous (described above in section 2.2.1). Testing for sexual behaviour took place 4-6 h after the progesterone injection was given to the female stimulus mouse. Male test mice were paired with a novel stimulus mouse for each test, so that behaviour was not dependent on specific male-female interactions. After placing the female in the cage, interactions were recorded for 30 min using a camera placed in front of the cage. The cumulative duration and number of bouts of following, sniffing, attempted mounts, mounts, and head grooming attempted by the male mouse were measured *post hoc* using a digital event recorder programme (Recordia 1.0b, O'Hara & Co., Ltd.). Between each test, the surface upon which the cage was placed was thoroughly wiped clean with 70% ethanol.

2.3.7 Aggressive behaviour

Aggressive behaviour tests were conducted in the home cage over 3 consecutive days following sexual behaviour using a resident-intruder paradigm with an OBX intact male stimulus mouse (Section 2.2.5). Because aggression is primarily governed by olfactory signals, OBX mice rarely show aggression (Ogawa et al., 1997). However, since their gonads are still intact, they can evoke aggression from the resident test mouse (Denenberg et al., 1973). This allows the measurement of aggression in test mice that have not been influenced by any experience of defeat. After the stimulus mouse was placed in the cage, behaviours were recorded for 15 min using a camera placed in front of the cage. Behavioural events were measured using a digital event recorder programme (Recordia 1.0b, O'Hara & Co., Ltd.).

The three consecutive tests were then repeated one week later. This is because aggression can be a learned reward-based behaviour in male mice (Golden et al., 2019). For each test, the test mouse was paired with a new OBX intruder.

2.4 Perfusion fixation

At the end of behavioural testing, mice were deeply anaesthetised by i.p. injection of ketamine/xylazine dosed at 0.1 ml/10 g bodyweight, delivering 10 mg/ml ketamine and 1 mg/ml xylazine. Once anaesthetised, the mice were transcardially perfused with 0.1 M PBS for 10 min followed by 4% paraformaldehyde for a further 10 min, both delivered at a speed of 2 ml/min. The brains were immediately isolated and post-fixed in 4% paraformaldehyde overnight at 4°C. The brains were washed in 0.1 M PBS and transferred to 30% sucrose in 0.1 M PB (w/v) for at least 24 h, until the brains had sunk to the bottom of the tube.

Perfusion fixation was the method of sacrifice for *Aro^{fl/fl}* animals, unless otherwise stated.

2.5 Oestrous staging

The oestrous stage of female mice was assessed *post-mortem* both visually and using vaginal cytology. Visual assessment was performed by evaluating the vaginal opening based on criteria described by Champlin et al. (1973). Vaginal cytology was assessed by means of a vaginal lavage. Any secretions covering the entrance of the vagina after sacrifice were removed with a cotton bud dampened with physiological saline (0.9% NaCl (w/v) in double distilled H₂O). A Pasteur pipette was used to gently flush the vagina with physiological saline and the final flush was dispensed into a 24-well plate. The material was observed, unstained, under a light microscope with a 10X objective (**Fig. 2.5**) and compared to the criteria detailed in (Byers et al., 2012).

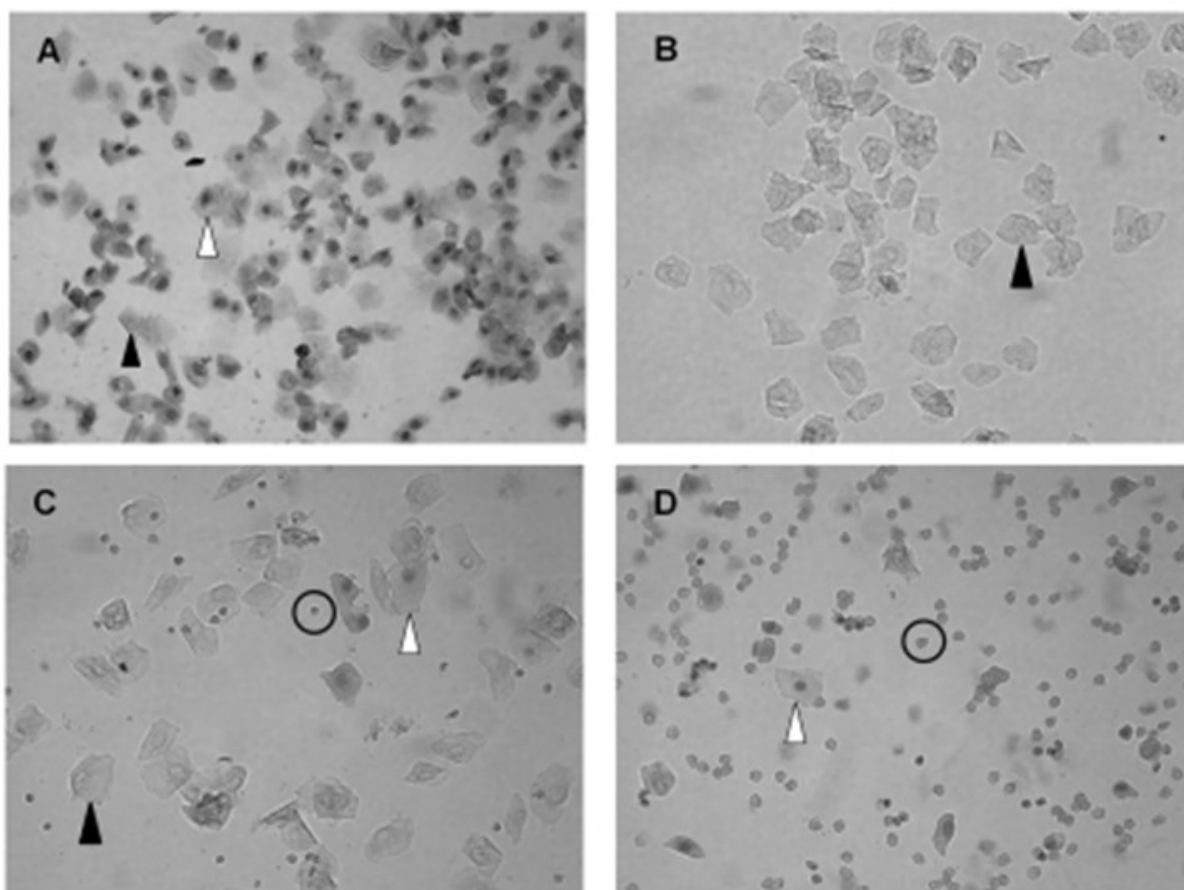


Figure 2.5. Vaginal cytology of mouse oestrous stages. Cornified epithelial cells (black arrow) and nucleated epithelial cells (white arrow) are characteristic of prooestrous (**A**). Cornified epithelial cells in the absence of any other cell type are characteristic of oestrous (**B**). Leukocytes (black circle) in the presence of cornified and nucleated epithelial cells is characteristic of metoestrous (**C**). Leukocytes and nucleated epithelial cells, in the absence of cornified epithelial cells, is characteristic of dioestrous (**D**). *From: Byers et al. (2012).*

Post-mortem assessment of oestrous stage prevented unnecessary stress being caused to animals. However, given that access to the animal housing facility was restricted and animals were delivered to experimentation rooms at designated times of day, we were not able to guarantee the oestrous stage of the mice upon experimentation. For this reason, it was decided to pool female mice regardless of oestrous stage, as obtaining enough mice in each individual stage to meet statistical power would have required a larger number of animals, contravening the principles of the 3Rs. We acknowledge that pooling animals may have caused insignificant findings, despite power being achieved (see section 2.15).

2.6 Plasma collection

1.5 ml microfuge tubes were coated with 0.5 M sterile filtered EDTA and an additional 10 μ l of EDTA was added to prevent blood clotting. Trunk blood of sacrificed mice was collected in the coated microfuge tubes. The tube was inverted several times to mix and placed on ice until plasma preparation. Samples were centrifuged for 10 min at 10,000 \times g 4°C. Supernatant (plasma) was transferred to a new microfuge tube and stored at -80°C until further processing.

2.7 Preparation of *ex vivo* brain slices

For animal experiments carried out at the University of Reading, UK, surgery and dissection equipment was kindly provided by Dr Francesco Tamagnini, University of Reading. Following cervical dislocation and decapitation, the brain was rapidly removed and immediately submerged in oxygenated ice-cold sucrose solution (189 mM sucrose, 10 mM glucose, 26 mM NaHCO₃, 3 mM KCl, 5 mM MgCl₂·6H₂O, 12.5 mM NaH₂PO₄·2H₂O, and 0.1 M CaCl₂) in a 5 ml collection tube. After 2 min, the brain was removed and blotted dry on filter paper before the cerebrum was removed with a razor blade. The remaining brain was placed onto a magnetic stage with Super Glue (caudal edge facing down) and resubmerged in oxygenated ice-cold sucrose. The stage and its container were placed on the vibratome (Leica Biosystems) and 200 μ m coronal sections throughout the hypothalamus were made. Individual slices were collected in glass bijoux containing 5 ml freshly made artificial cerebrospinal fluid (aCSF; 129 mM NaCl, 3 mM KCl, 1.2 mM MgSO₄, 0.4 mM K₂HPO₄, 25 mM HEPES, 10 mM glucose, 1.4 mM CaCl₂, 0.4 mM ascorbic acid, pH 7.6, sterile filtered using a 22 μ m filter). aCSF was oxygenated in carbogen (95% O₂/5% CO₂) for 15 min at 37°C prior to slice collection. The bijoux containing the brain slices were transferred to an incubator (37°C, 95% O₂/5% CO₂), and left to recover for 1 h. The recovery aCSF was used as the 0 h timepoint. After recovery, slices were transferred to 12-well plates containing pre-warmed oxygenated aCSF and placed back in the incubator for various timepoints either with or without treatment, depending on the study aims.

Although hypothalamic brain slices containing the SBN were collected, all brain slices contained adjacent brain regions which may have contributed to measurements made from the whole slice. These are shown in **Fig 2.6**.

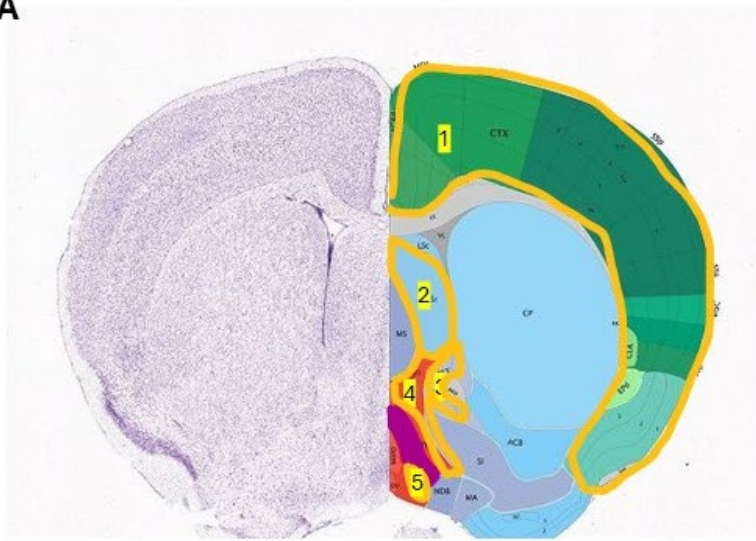
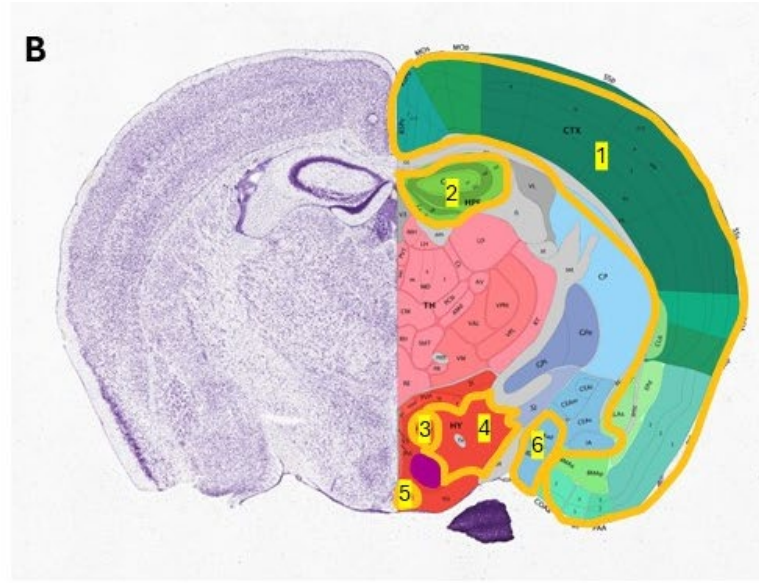
A**B**

Fig. 2.6. Adjacent, potentially neurosteroidogenic regions within hypothalamic slices. Slices containing the mPOA (**A**) also contain the cortex (1), lateral septum (2), lateral preoptic area (3), bed nucleus of stria terminalis (4), and anteroventral periventricular nucleus (5). Slices containing the VMH (**B**) also contain the cortex (1), hippocampus (2), anterior hypothalamus (3), lateral hypothalamus (4), arcuate nucleus (5), and medial amygdala (6). There also exists the possibility that other non-labelled regions are steroidogenic.

To avoid skewing the data, brain slices were counterbalanced across treatment groups by exposing different slices from different animals to each treatment. This is shown in **Table 2.1** and **2.2**.

Table 2.1. Slice distribution across three treatment groups. Animals are denoted by letters; slice number is as shown. Five slices containing the mPOA were obtained for each animal. They were counterbalanced across treatments as shown to obtain $n = 15$ slices per treatment from a total of 9 animals. Three slices containing the VMH were obtained for each animal. They were counterbalanced across treatments as shown to obtain $n = 9$ slices per treatment from a total of 9 animals. This is across all chapters.

	mPOA			VMH		
	Treatment I	Treatment II	Treatment III	Treatment I	Treatment II	Treatment III
Animal [letter], Slice #	A1	A2	A3	A1	A2	A3
	A4	A5	B1	B2	B3	B1
	B2	B2	B3	C3	C1	C2
	B5	C1	C2	D1	D2	D3
	C3	C4	C5	E2	E3	E1
	D1	D2	D3	F3	F1	F2
	D4	D5	E1	G1	G2	G3
	E2	E3	E4	H2	H3	H1
	E5	F1	F2	I3	I1	I2
	F3	F4	F5			
	G1	G2	G3			
	G4	G5	H1			
	H2	H3	H4			
	H5	I1	I2			
	I3	I4	I5			

Table 2.2. Slice distribution across four treatment groups. Animals are denoted by letters; slice number is as shown. Five slices containing the mPOA were obtained for each animal. They were counterbalanced across treatments as shown to obtain $n = 15$ slices per treatment from a total of 12 animals. Three slices containing the VMH were obtained for each animal. They were counterbalanced across treatments as shown to obtain $n = 9$ slices per treatment from a total of 12 animals. For RT-qPCR (section 2.12), slices for each treatment were pooled as shown by the highlighting, and SBN nuclei were punched out. Pooling was necessary to obtain sufficient RNA concentrations from the small amount of tissue collected in punching. Pooling resulted in a biological $n = 5$ for the mPOA, where each biological replicate was made up of punches from 1 brain slice each of 3 animals. The VMH, the biological replicates were $n = 3$, where each biological replicate was made up of punches from 1 brain slice each of 3 animals. All samples were run in triplicate to give a technical replicate of $n = 3$. This is across all chapters.

	mPOA				VMH			
	Treatment I	Treatment II	Treatment III	Treatment IV	Treatment I	Treatment II	Treatment III	Treatment IV
	I	II	III	IV	I	II	III	IV
Animal [letter], Slice #	A1	A2	A3	A4	A1	A2	A3	B1
	A5	B1	B2	B3	B2	B3	C1	C2
	B4	B5	C1	C2	C3	D1	D2	D3
	C3	C4	C5	D1	E1	E2	E3	F1
	D2	D3	D4	D5	F2	F3	G1	G2
	E1	E2	E3	E4	G3	H1	H2	H3
	E5	F1	F2	F3	U1	I2	I3	J1
	F4	F5	G1	G2	J2	J3	K1	K2
	G3	G4	G5	H1	K3	L1	L2	L3
	H2	H3	H4	H5				
	I1	I2	I3	I4				
	I5	J1	J2	J3				
	J4	J5	K1	K2				
	K3	K4	K5	L1				
	L2	L3	L4	L5				

2.8 Brain slice viability

Brain slice viability was assessed using the Trypan Blue exclusion test (Strober, 2001). Slices were collected and incubated as described above for timepoints of 2, 8, 24, and 48 h ($n = 3$ slices per timepoint from 3 different animals), before being briefly rinsed in PBS and fixed in 4% paraformaldehyde with 0.4% Trypan Blue Solution (v/v) for 30 min at room temperature. Slices were then rinsed with PBS and carefully mounted on microscope slides for imaging. 10X brightfield images of four separate areas of each slice were acquired using a Zeiss Axiolmager Epifluorescence microscope (Carl Zeiss MicroImaging GmbH) under identical exposure times. Stained cells were identified using the ImageJ Particle Analyser plugin (version 1.52u, 17 March 2020).

2.9 Palkovits punch technique (micropunch dissection)

Following incubation (section 2.7) 200 μm brain slices were rinsed in 0.1 M PBS and fixed in 4% PFA (w/v) for 30 min. Slices were washed with PBS for 1 min before being placed on a 0.01 mm microscope calibration slide over dry ice for a few seconds until the slice was firm but not frozen. A dissection microscope was used to identify nuclei of interest to closely match the Paxinos Mouse Brain Atlas (Paxinos and Franklin, 2001). A 0.5 mm stainless steel cannula (Fine Science Tools, USA) was used to dissect out each nucleus. The resulting micropunches were pooled into Eppendorf tubes ready for further processing by solid phase extraction and hormone analysis or RNA isolation (see sections 2.10 – 2.12).

An alternative method of micropunch dissection was also used for mice tested at the University of Tsukuba, Japan, where *ex vivo* slices could not be prepared and incubated. Mice were sacrificed by cervical dislocation and brains were immediately isolated. After removal of the cerebellum, the brains were snap frozen in ice-cold isopentane and stored at -80°C until further processing. Brains were placed in a brain mould and embedded in OCT before 200 μm sections were taken on a cryostat (Leica Biosystems, Japan). Sections were placed on a cooled microscope slide on a bed of dry ice under a dissection microscope and nuclei of interest were identified to closely match the Paxinos Mouse Brain Atlas (Paxinos and Franklin, 2001). A 0.5 mm stainless steel cannula (Fine Science Tools, USA) was used to dissect out each nucleus. The resulting micropunches were pooled into Eppendorf tubes ready for further processing by solid phase extraction and hormone analysis (see sections 2.10 – 2.11).

For either method, punches could be stored at -20°C prior to solid phase extraction. The number of punches and punch volume for each brain nucleus is shown in **Table 2.3**.

Table 2.3. Number and volume of punches for each nucleus of interest in the social behaviour network and hypothalamus. Slices were 200 µm thick, but one nucleus may span several slices. Therefore, the height of the nucleus was determined by 200 µm multiplied by the number of slices the nucleus spanned. Number of punches and punch volume are for both hemispheres combined. Punch volume was determined by:

$$V (mm^3) = \pi \times 0.5^2 \times (0.2 \times \text{the number of slices the nucleus spans})$$

In instances where the area of a nucleus in a particular slice was too diminutive to sample independently, it was omitted from the collection.

Nucleus	# Punches from both hemispheres	Nucleus volume from both hemispheres (mm³)
Medial preoptic area	10	0.785
Anterior hypothalamus	6	0.471
Ventromedial hypothalamus	6	0.471
Arcuate nucleus of the hypothalamus	4	0.314

2.10 Solid phase extraction

Brain tissue and plasma samples were homogenised in Eppendorf tubes with ice-cold 85% HPLC-grade methanol, which was gently agitated with a pipette until the slice was homogenised and left at 4°C overnight. Non-end capped 1 ml C18 columns were used to extract steroids from plasma and homogenised brain tissue. Columns were primed with 3 ml absolute ethanol and equilibrated with 2.5 ml deionised water. Homogenised samples were diluted 1/5 in deionised water and loaded to the C18 column. The column was washed twice more with 2.5 ml deionised water and steroids were eluted with 1.5 ml 90% HPLC-grade methanol. Steroid eluates were spin-dried on a SpeedVac and resuspended in 350 µl of 0.1 M phosphate buffer containing 0.1% (w/v) gelatine and 0.7% (v/v) ethanol. The composition of the resuspension solution was optimised previously by Charlier et al. (2010b).

2.11 Hormone immunoassays

The steroid hormone assays used in this thesis are competitive enzyme-linked immunosorbent assays (ELISAs) that rely on competition between the sample and an enzyme-conjugated competing antigen in binding to the limited amount of antibody that coats the plate. For all ELISAs, the competing antigen was bound to horseradish peroxidase (HP), and the assay buffer used was gelatine-phosphate buffer (GPB), consisting of 0.1% (w/v) gelatine in PBS and 0.5% (v/v) ProClin 300 as a biocide. Standards in the range of 0-10,000 pg/ml 17 β -oestradiol (E₂) or testosterone were prepared as 3-fold serial dilutions in GPB and stored at -4°C (not beyond 3 months) prior to running the assay. All samples were run in triplicate to give 3 technical replicates per biological replicate.

Detection limits of the E₂ (section 2.11.1) and testosterone (section 2.11.2) ELISAs were 10 and 15 pg/ml, respectively. Mean within- and between-plate coefficients of variability were <10% and <15%, respectively for both assays.

Steroids were measured either in aCSF that bathed the slices during *ex vivo* slice preparation or in punch dissected brain tissue. For punch samples, concentrations were normalised to pg/mm³ to reflect the size of each nucleus. This was calculated by the following equation:

$$V \text{ (mm}^3\text{)} = \pi \times 0.5^2 \times (0.2 \times \text{the number of slices the nucleus spans})$$

where 0.5 is the diameter of the punch (mm) and 0.2 is the thickness of each slice (mm). Refer to **Table 2.3** (section 2.9) for the number and volume of punches from each nucleus.

2.11.1 17 β -oestradiol (E₂) ELISA

The 510/6 goat anti-oestradiol serum (kindly gifted by the late Prof G. S. Pope, National Institute for Research in Dairying, Shinfield, Berkshire, UK) was diluted 1/10,000 in 0.05 M carbonate buffer, pH 9.6 and stored at 4°C for no longer than 1 month prior to use. Greiner Bio-One high binding capacity 96-well ELISA plates were coated with 100 μ l/well of the diluted anti-oestradiol antibody and incubated overnight at room temperature in a moist, sealed box. The following day, the antibody coating was removed with 3 washes of a PBS wash buffer containing 0.1% (v/v) Tween-20 and any free binding sites on the plates were blocked with GPB at 250 μ l/well. The plates were stored overnight in a moist, sealed box at 4°C.

For the assay, plates were washed 3 times with wash buffer and banged dry on a paper towel immediately before use. 60 µl of standards (diluted 5:1 in GPB) or 60 µl sample (diluted 1:5 in GPB) were added to wells in duplicate. Blank wells and negative control wells containing aCSF in GPB (1:5) were also ran in duplicate. 50 µl of E₂-HP, (stored neat at 4°C for no longer than 1 week prior to use) diluted 1/2000 in GPB, was added as the competing antigen to all wells except the blank wells. The plate was mixed thoroughly on a plate shaker and incubated for 3 h at room temperature in a moist, sealed box.

After incubation, the plate was washed 3 times with wash buffer and 100 µl/well of freshly prepared o-phenylenediamine (OPD), diluted 1 mg/ml in 0.05 M citrate buffer, pH 5.0, with 1 µl/ml 30% hydrogen peroxide, was added as the HP substrate. The plates were incubated at room temperature in the dark for 30 min to allow the yellow colour to develop. The reaction was stopped by adding 50 µl/well of 1 M hydrochloric acid before the absorbance was read at 450 nm (600 nm reference filter) on a microplate reader (Emax Microplate Reader, Molecular Devices, USA). A standard curve was constructed using SoftMax Pro V5 software (Molecular Devices, USA) and sample concentrations were interpolated using R (version 4.0.2m, The R Foundation for Statistical Computing, Vienna, Austria).

The crossreactivity of other physiologically relevant hormones with the anti-oestradiol serum was tested previously by Dr W. Cheewasopit (**Table 2.4**). Briefly, hormones were diluted in standard concentrations of E₂ at a concentration of 100 pg/ml. Absorbance readings of standards containing each hormone were compared to the absorbance readings of the E₂ standards. % crossreactivity was calculated by:

$$\% \text{ crossreactivity} = \left(\frac{\text{Absorbance of E}_2 \text{ standard with hormone}}{\text{Absorbance of E}_2 \text{ standard}} \right) \times 100$$

Table 2.4. Crossreactivity of physiologically relevant steroid hormones with the 17 β -oestradiol ELISA. All steroids were tested at a concentration of 100 pg/ml.

Steroid hormone	% crossreactivity
17 β -oestradiol	100
Aldosterone	0.106
Androstenedione	0.050
Corticosterone	0.047
Dehydroepiandrosterone	0.132
Deoxycorticosterone	0.180
Dihydrotestosterone	0.210
Estrone	7.489
Progesterone	0.056
Testosterone	0.097

Table 2.5 shows the % crossreactivity of drug treatments that were added to aCSF and incubated with the brain slices. Drugs were run in a series of concentrations, diluted in E₂ standards, to determine appropriate concentrations for experimentation. Crossreactivity was determined as above.

Table 2.5. % crossreactivity of drugs used in brain slice incubation with the 17 β -oestradiol ELISA. A range of concentrations for each drug were tested over 10-fold dilutions based on relevant literature. The concentrations used for experiments are highlighted in **bold**.

Drug	Concentration	% crossreactivity
Letrozole	10⁻⁸ M	6.22
	10 ⁻⁷ M	26.41
	10 ⁻⁶ M	52.21
Dutasteride	10⁻⁸ M	3.02
	10 ⁻⁶ M	25.99
	10 ⁻⁴ M	17.72
Finasteride	10⁻⁸ M	4.45
	10 ⁻⁶ M	8.66
	10 ⁻⁴ M	18.73
Propylpyrazoletriol (PPT)	10⁻⁹ M	4.27
	10 ⁻⁸ M	10.60
	10 ⁻⁷ M	13.10
Diarylpropionitrile (DPN)	10⁻⁹ M	1.89
	10 ⁻⁸ M	4.98
	10 ⁻⁷ M	13.48
ICI 182,780	10⁻⁸ M	12.41
5 α -androstane-3 β , 17 β -diol (3 β -diol)	10⁻⁸ M	6.33
	10 ⁻⁷ M	8.55

The minimum detection limit of the assay was approximately 10 pg/ml and the inter- and intra-assay CVs were <15%.

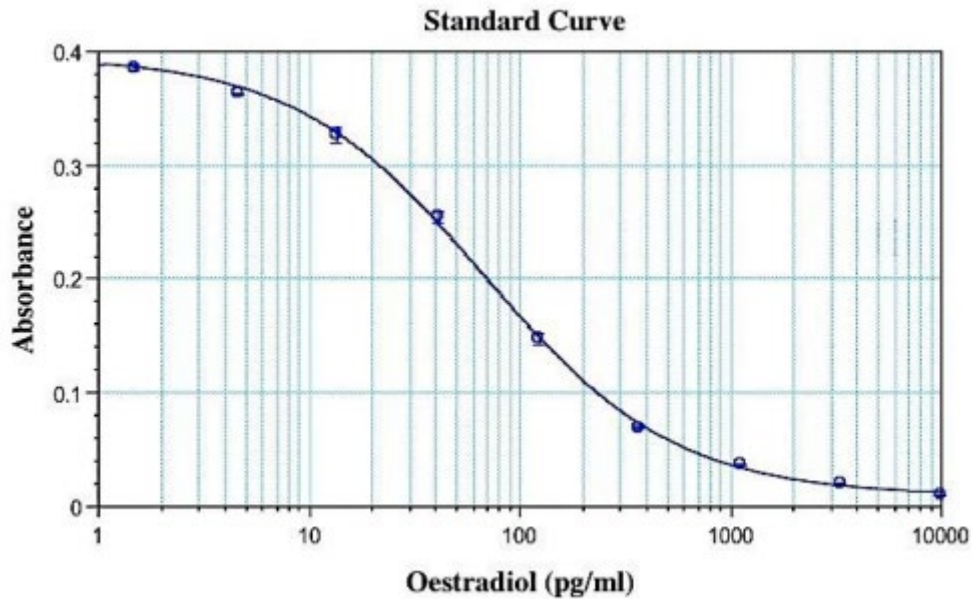


Figure 2.7. Typical standard curve obtained for the 17 β -oestradiol ELISA.

2.11.2 Testosterone ELISA

The S505 sheep anti-testosterone serum (National Institute for Research in Dairying, Shinfield, Berkshire, UK) was diluted 1/30,000 in 0.05 M carbonate buffer (pH 9.6) and stored at 4°C for no longer than 1 month prior to use. Greiner Bio-One high binding capacity 96-well ELISA plates were coated with 100 μ l/well of the diluted anti-testosterone antibody and incubated overnight at room temperature in a moist, sealed box. The following day, the antibody coating was removed with 3 washes of a PBS wash buffer containing 0.1% (v/v) Tween-20 and any free binding sites on the plates were blocked GPB, 250 μ l/well. The plates were stored overnight in a moist, sealed box at 4°C.

For the assay, plates were washed 3 times with wash buffer and banded dry on a paper towel immediately before use. 60 μ l of standards (diluted 5:1 in GPB) or 60 μ l sample (diluted 1:5 in GPB) were added to wells in duplicate. Blank wells containing aCSF in GPB (1:5) were also ran in duplicate. 50 μ l of testosterone-HP (stored neat at 4°C for no longer than 1 week prior to use) diluted 1/6000 in GPB, was added as the competing antigen to all wells except the blank wells. The plate was incubated for 4 h at room temperature in a moist, sealed box.

After incubation, the plate was washed 3 times with wash buffer and 100 μ l/well of freshly prepared OPD, diluted 1 mg/ml in 0.05 M citrate buffer, pH 5.0, with 1 μ l/ml 30%

hydrogen peroxide, was added as the HP substrate. The plates were incubated at room temperature in the dark for 30 min to allow the yellow colour to develop. The reaction was stopped by adding 50 µl/well of 1 M hydrochloric acid before the absorbance was read at 450 nm (600 nm reference filter) on a microplate reader (Emax Microplate Reader, Molecular Devices, USA). A standard curve was constructed using SoftMax Pro V5 software (Molecular Devices, USA) and sample concentrations were interpolated using R (version 4.0.2m, The R Foundation for Statistical Computing, Vienna, Austria).

The crossreactivity of other physiologically relevant hormones with the anti-testosterone serum was tested previously by Dr W. Cheewasopit (**Table 2.6**) by following a similar procedure as in Section 2.11.1.

Table 2.6. Crossreactivity of physiologically relevant steroid hormones with the testosterone ELISA. All hormones were tested at a concentration of 100 pg/ml.

Steroid hormone	% crossreactivity
Testosterone	100
17 β -oestradiol	0.385
Aldosterone	0.005
Androstenedione	1.322
Corticosterone	0.001
Dehydroepiandrosterone	0.071
Deoxycorticosterone	0.008
Dihydrotestosterone	9.497
Estrone	0.011
Progesterone	0.004

Table 2.7 shows the crossreactivity of drug treatments that were added to aCSF and incubated with the brain slices. Drugs were run in a series of concentrations to determine appropriate concentrations for experimentation.

Table 2.7. % crossreactivity of drugs used in brain slice incubation with the testosterone ELISA. The desired concentration was first ascertained by % crossreactivity with the 17 β -oestradiol ELISA, since that was the hormone of interest. The chosen drug concentration was then tested for % crossreactivity with the testosterone ELISA.

Drug	Concentration	% crossreactivity
Letrozole	10 ⁻⁷ M	5.11
Dutasteride	10 ⁻⁸ M	10.87
Finasteride	10 ⁻⁸ M	13.58
Propylpyracoletriol (PPT)	10 ⁻⁹ M	1.37
Diarylpropionitrile (DPN)	10 ⁻⁹ M	0.75
ICI 182,780	10 ⁻⁸ M	1.71
5 α -androstane-3 β , 17 β -diol (3 β -diol)	10 ⁻⁸ M	20.6

The assay detection limit was approximately 15 pg/ml and inter- and intra-assay CVs were <15%.

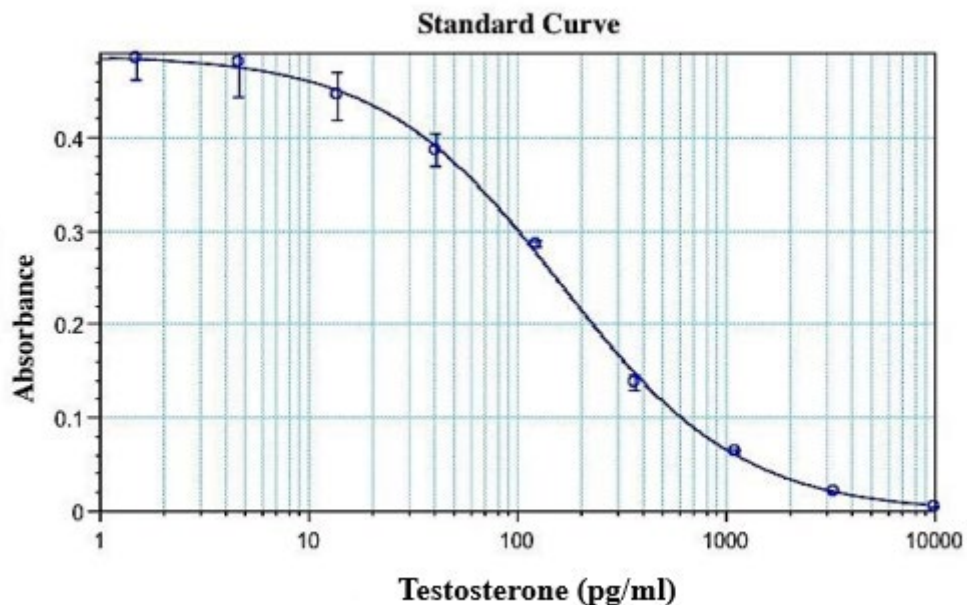


Figure 2.8. Typical standard curve obtained for the testosterone ELISA.

2.12 Gene expression analysis

2.12.1 Total RNA extraction

Tissue was submerged in 5 volumes of RNA^{later} Stabilization Solution in a 24-well plate and stored at 4°C. Samples were processed within 3 weeks of collection for optimal RNA recovery.

Total RNA was extracted using a Qiagen RNeasy Plus Mini Kit, following manufacturer's instructions. Absorbance at A₂₆₀ and A₂₈₀ nm was measured using the NanoDrop™ 2000 Spectrophotometer (Thermo Fisher Scientific) to determine RNA concentration and purity. Isolated RNA was temporarily stored up to 3 months at -20°C in nuclease-free water and more permanently at -80°C. Punches from a single social behaviour network (SBN) nucleus/animal yielded approximately 100-120 ng of RNA and hence RNA from 3-4 animals per treatment per SBN nucleus were pooled for use in RT-qPCR experiments.

2.12.2 cDNA synthesis

100 ng total RNA was reverse transcribed in a 20 µl reaction mixture using the High Capacity cDNA Reverse Transcription kit (Applied Biosystems, Thermo Fisher Scientific), following manufacturer's instructions. A single reaction mixture contained 2 µl reverse transcription buffer, 2 µl random primers, 0.8 µl deoxyNTP mixture, and 1 µl MultiScribe reverse transcriptase. The StepOne™ Real-Time PCR System (Applied Biosystems, Thermo Fisher Scientific) was used to create the following reaction conditions: annealing at 25°C for 10 min, reverse transcription at 37°C for 120 min, RNA denaturation at 85°C for 5 min. cDNA was temporarily stored (no longer than 1 month) at -20°C.

2.12.3 RT-qPCR

RT-qPCR was performed with the StepOne™ Real-Time PCR System (Applied Biosystems). The cDNA was amplified in a reaction volume of 14 µl, consisting of 7 µl 2X PowerSYBR® Green Master Mix (Thermo Fisher Scientific) and primers at a final concentration of 360 nM. The primer sets were designed by Integrated DNA Technologies Primer 3 tool and checked against NCBI Primer-Blast for duplex formation with other species or other genes. Primer sequences for all target genes are shown in **Table 2.8**. For each cDNA sample, PCR amplification of the housekeeping gene *ActB* (encoding β-actin) was determined to allow normalisation between the samples. Targets and controls were run in separate wells under the following reaction conditions: an initial holding step of 95°C for 10 min, 40 cycles of denaturation at 94°C

for 15 sec, followed by annealing and extension at 60°C for 1 min. A melt curve was also included. Cycle thresholds (C_T) were automatically determined by the StepOne™ Software (Applied Biosystems). Three reactions were performed for each cDNA sample ($n = 3$ technical replicates), and a no template control, in which molecular-grade water was included instead of cDNA template, was included for each target gene in each assay.

Relative gene expression was determined using the $2^{-\Delta\Delta C_T}$ method (Livak and Schmittgen, 2001) with β -actin as the housekeeping control gene. β -actin was chosen due to its high conservation and hypothalamic insensitivity to dietary changes that affect other housekeeping genes such as GAPDH (Sellayah et al., 2008). Furthermore, β -actin has been the housekeeping gene of choice in previous literature measuring steroidogenic enzyme expression in the rodent hypothalamus (Soma et al., 2005). C_T values from triplicate samples were normalised to the average C_T of the endogenous control gene *ActB* to obtain ΔC_T . ΔC_T values were normalised to the corresponding ΔC_T value for 0 h samples or the ovary, depending on the experiment. $\Delta\Delta C_T$ values were then converted to fold-differences using the formula: fold-difference = $2^{-\Delta\Delta C_T}$.

Table 2.8. Primer sequences for RT-qPCR. Primers were designed by Integrated DNA Technologies Primer 3 tool and duplex formation with other species or genes was checked against NCBI Primer-Blast.

Gene name	Forward sequence (5' → 3')	Reverse sequence (3' → 5')
<i>ActB</i>	TGTGCTGTCCCTGTATGCCTCTG G	GGGAGAGCATAGCCCTCGTAGAT GG
<i>StAR</i>	GGAACCCAAATGTCAAGGAGATC AAGG	AGGCCCCACCAGGTTGCC
<i>Cyp11a1</i>	AGTCCTGGCTGCCCGGCG	GGTGGAGTCTCAGTGTCTCCTTG ATGC
<i>Hsd3b1</i>	CACCCAGTACCTGAGGAGAGCTT GC	GGCACACTGGCTTGGATACAGGC
<i>Hsd17b1</i>	GTGCGAGAGTCTGGCGATCCTGC	CGCCCACCAGCTTTTCATAGAAG G
<i>Cyp19a1</i>	GGACACCTCTAACATGCTCTTCCT GGG	TGATGAGGAGAGCTTGCCAGGC
<i>Srd5a1</i>	GCCGATACTTGAGCCAGTTTGC	CTCAGATTCCGCAGGATGTGGT
<i>Srd5a2</i>	CATCCACAGTGACTIONCATGCTG	AAGGCTGGAACAGACCAAGTGG
<i>Srd5a3</i>	GGAGCACCTTTTCCAAACTGGC	ACCAAGAAGGCAGACAGAGCCA
<i>Esr1</i>	TCTGCCAAGGAGACTCGCTACT	GGTGCATTGGTTTGTAGCTGGAC
<i>Esr2</i>	GGTCCTGTGAAGGATGTAAGGC	TAACTTGC GAAGTCGGCAGG

2.13 Golgi staining

The sliceGolgi Kit protocol was used to impregnate neurones for Golgi analysis, with some modifications.

Mice used for Golgi staining were transcardially perfused as described in section 2.4, but with the aldehyde fixative supplied *in sliceGolgi* kit, Bioenno Tech 003760.

Following perfusion fixation, the brains were cut into hemispheres so that one hemisphere could be used in solid phase extraction and hormone analysis (see Sections 2.10-2.11) and the other hemisphere was post-fixed in the aldehyde fixative (volume = 10x volume of tissue) for 5 h and used for Golgi staining. The fixative was

replaced after 30 min. After post-fixing, the brains were stored in 0.1 M PB at 4°C for no longer than 3 days, until ready for further processing.

Brains were removed from the 0.1 M PB and sectioned at 200 µm on a vibratome (Leica Biosystems) in room temperature 0.1 M PB. The slices were collected using a paintbrush and placed in a 12-well plate (3 slices/well) containing 0.1 M PB (3 ml/well). Under a fume hood, the 0.1 M PB was removed carefully with a Pasteur pipette, making sure not to damage any of the slices in the well. 2 ml of 1X impregnation solution (diluted from 5X stock following instructions in the sliceGolgi protocol) was added to each well. The slices were incubated in the dark for 4 days at room temperature, refreshing the impregnation solution after 1 day. The slices were rinsed in double-distilled H₂O and washed in 0.01 M PBS with 0.3% Triton X-100 (v/v) 5 min, 3 times. 2 ml of the Solution C stain was added to the slices for 4 min and the slices were again rinsed with double-distilled H₂O. 2 ml of the Solution D post-stain was applied for 1 min and the slices were washed 3 times in 0.01 M PBS with 0.3% Triton X-100 (v/v), 5 min each wash. The slices were then carefully mounted onto gelatin-coated microscope slides and left overnight to dry slightly. Gelatin-coated microscope slides were prepared by dipping slide racks into slide jars containing filtered gelatin solution (5 g gelatin and 0.5 g chromium potassium sulphate in 1 L deionised H₂O). Slides were left to dry completely before use. Finally, the mounted slices were dehydrated in increasing concentrations of ethanol (50%, 70%, 90%, 100%, 100%, 100%) in slide jars and defatted 3 times in xylene (also in a slide jar). The slides were covered with a 76 x 26 x 1 mm rectangular coverslip with Permount mounting medium and left in the dark until dry.

2.13.1 Image acquisition and analysis

An inverted microscope (Nikon TiE) was used to take a series of z stacks (0.5 µm step size) at 100X magnification to visualise dendritic spines ($n = 50$ per animal) in the mPOA resulting from i.p. injections. 20X images were also taken for Sholl analysis (Sholl, 1953), $n = 50$ neurones/treatment evenly distributed across each of the 4-5 animals per treatment group. ImageJ (v 1.8.0) was used to analyse the images and measure arbourisation, dendrite length, soma size, and spine density and morphology. Briefly, pixel-to-micron scale was set, and the line drawing tool was used to measure dendrite lengths and the width of the soma. Spine morphology was determined by measuring the length and width of each spine using the line drawing tool and categorised as according to the criteria in Risher et al. (2014). Filopodial spines were characterised by a length >2 µm, long thin spines were characterised by a length <2

μm , and thin spines were characterised by a length $<1 \mu\text{m}$. Stubby spines were characterised by a length:width ratio <1 . Mushroom spines were characterised by a width $>0.6 \mu\text{m}$. Branched spines were characterised by having 2 or more heads. During analysis, microscope slides were coded using an alphabetical system by an independent researcher (Ruby Vajaria, RV) who was not involved in the experimental procedures. The analysts (JD and Rosie Moore, RM) were unaware of the treatment received by the brain slices on the slides until after the image analysis was completed.

2.14 Immunohistochemistry for the aromatase protein

Aromatase is a microsomal cytochrome P450 enzyme that resides largely in the endoplasmic reticulum (Chan et al., 2016) but is also found at synapses and presynaptic terminals (Hojo et al., 2004a, Srivastava et al., 2010). Due to its limited expression in specific subcellular compartments, the aromatase protein is notoriously difficult to immunostain (Cornil, 2018). Though several antibodies have been used to immunostain aromatase, they are limited by insufficient characterisation and no scoring or grading system for immunoreactivity (Hong et al., 2009). Previously, unpublished data from our laboratory utilised a specific aromatase antibody that is unfortunately no longer available from the commercial supplier. Therefore, a closely related rabbit polyclonal antibody (rabbit anti-aromatase, Novus Biologicals, AB_10000919) was used in an immunostaining optimisation protocol with the end goal of localising the aromatase protein in brain slices.

2.14.1 Optimisation of staining protocol

In an initial method adapted from Hornsby et al. (2020), testes were dissected from adult male mice and snap frozen in ice-cold isopentane. Frozen tissue was stored at -80°C until sectioning. Tissue was embedded in OCT for sectioning at $20 \mu\text{m}$ on a cryostat (Bright Instruments, UK) and collected on SuperFrost Plus Adhesion slides (EpreDia, UK). Slides were placed in a slide jar and washed 3 times with 0.1 M PBS, 5 min per wash. The tissue was permeabilised with ice-cold methanol for 2 min and washed as previous. The slide jar was placed in a water-bath heated to 70°C and pre-heated antigen retrieval buffer (0.1 M sodium citrate buffer + 0.05% Tween 20 (v/v), pH 6.0) was added to the jar. The slides were incubated in this solution for 1 h. Slides were removed from the jar and SuperBlock Blocking Buffer (ThermoFisher Scientific, UK) was applied to each section. Slides were incubated in a dark, moist box at room temperature for 1 h. Excess blocking solution was removed and the primary antibody was applied at a 1:500 or a 1:200 dilution in 0.1 M PBS with 0.1% Triton X-100 (v/v) for

24 h in a dark, moist box at 4°C. Negative control samples were incubated in the same solution, but the primary antibody was omitted. Slides were washed as previous before application of the secondary antibody (goat anti-rabbit AlexaFluor 568, diluted 1:300 in 0.1 M PBS with 0.1% Triton X-100 (v/v), and incubated in a dark, moist box for 2 h at room temperature. Slides were washed as previous and coverslipped with Fluoromount-G mounting medium with DAPI (Invitrogen, UK).

A second protocol, designed to reduce background staining and enhance visualisation of the immunostain, was adapted from Rosas-Arellano et al, (2016). This method was identical to the method above except for the composition of the blocking solution and the primary antibody incubation solution. Sections were blocked in 50 mM glycine, 0.05% Tween-20 (v/v), 0.1% Triton X-100 (v/v) and 0.1% BSA (v/v) in SuperBlock Blocking Buffer. The primary antibody was diluted at 1:500 or 1:200 in 10 mM glycine, 0.05% Tween-20 (v/v), 0.1% Triton X-100 (v/v) and 0.1% hydrogen peroxide (v/v) in 0.1 M PBS. Negative control samples were incubated in the same solution, but the primary antibody was omitted. The addition of glycine and hydrogen peroxide aims to quench any autofluorescence, enhance specific signals, and reduce background noise (Rosas-Arellano et al., 2016).

Sections were imaged on a fluorescent microscope (Zeiss Axioskop) at 10X and 20X and images were analysed in ImageJ (v 1.8.0). Each image was segmented in to four quadrants which were analysed separately using thesholding tools in ImageJ. Corrected total cell fluorecence (CTCF) was calculated for each image as shown below:

$$CTCF = \text{integrated density of immunostained area} - (\text{area of immunostained selection} \times \text{mean integrated density of unstained background})$$

The CTCF of each primary antibody dilution in each method is shown in **Fig. 2.9**. The method modified from Rosas-Arellano et al. (2016) gave a stronger signal, and was used for all subsequent staining.

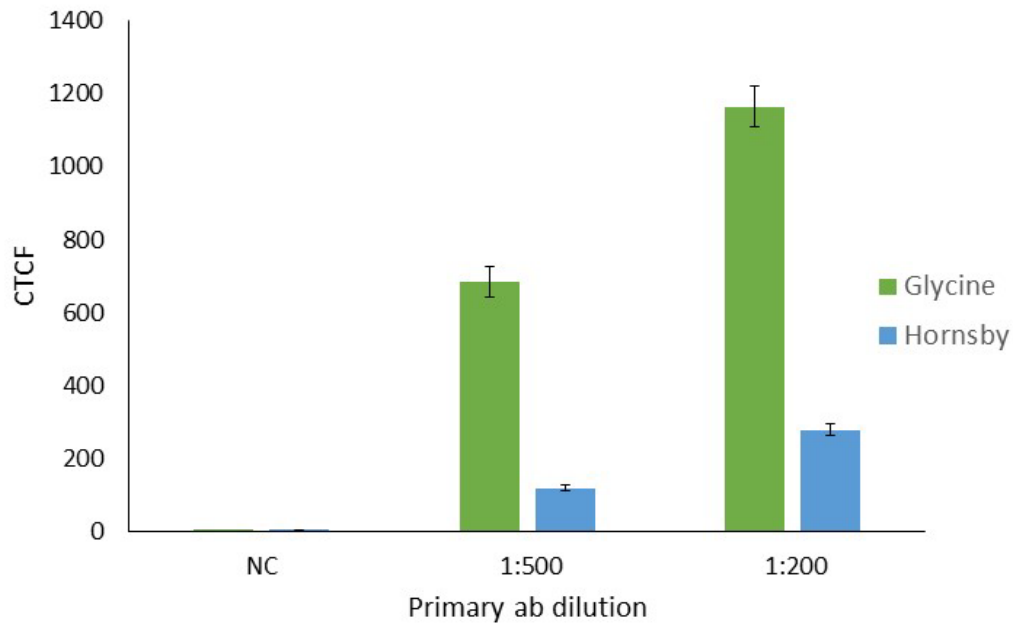


Figure 2.9. Corrected total cell fluorescence (CTCF) using two different staining methods during the optimisation of immunostaining with the Novus Biologicals anti-aromatase antibody (AB_10000919). Following cryostat sectioning, two methods were employed to determine the best protocol for aromatase staining in tissue sections. Both methods were identical except for the composition of the blocking solution and primary antibody incubation solution. In a method adapted from Hornsby et al. (2020) (blue bars), SuperBlock Blocking Buffer (ThermoFisher Scientific, UK) was used as the blocking solution. The primary antibody incubation solution in this method was 0.1 M PBS with 0.1% Triton X-100 (v/v). A second method, designed to reduce background staining and enhance visualisation of the immunostain, adapted from Rosas-Arellano et al. (2016) (green bars), used a blocking solution consisting of 50 mM glycine, 0.05% Tween-20 (v/v), 0.1% Triton X-100 (v/v) and 0.1% BSA (v/v) in SuperBlock Blocking Buffer. The primary antibody incubation solution was 10 mM glycine, 0.05% Tween-20 (v/v), 0.1% Triton X-100 (v/v) and 0.1% hydrogen peroxide (v/v) in 0.1 M PBS. Sections were either incubated with no primary antibody (negative control, NC), or the primary antibody diluted at 1:500 or 1:200. All sections were incubated with the secondary antibody (goat anti-rabbit AlexaFluor 568, diluted 1:300 in 0.1 M PBS with 0.1% Triton X-100 (v/v) and coverslipped with Fluoromount-G mounting medium with DAPI (Invitrogen, UK). The resulting CTCF of each method is shown.

2.14.2 Characterisation of aromatase antibody in mouse ovary sections

The immunostaining method with the anti-aromatase antibody was further optimised using ovaries. Ovarian tissue consists of thecal cells, which do not express aromatase, and granulosa cells, where aromatase is exclusively expressed (Stocco, 2008) making it an ideal positive and negative staining control.

Ovaries were dissected out of adult female mice in dioestrous and snap frozen in ice-cold isopentane. Frozen tissue was stored at -80°C until sectioning. Tissue was embedded in OCT for sectioning at 10 µm on a cryostat (Bright Instruments, UK) and collected on SuperFrost Plus Adhesion slides (EpreDia). Section thickness was reduced to improve the resolution of the images. The method adapted from Rosas-Arellano et al. (2016) described above was used with a 1:200 primary antibody dilution. Antigen retrieval times were further optimised to maintain the integrity of the sections on the slides. Retrieval times of 0, 10, 30, and 60 min were used, and resulting images are shown in **Fig. 2.10**. Antigen retrieval was also performed for 120 min, but this resulted in sections peeling away from the slides. 60 min led to significant deformation of the sections on the slides, whilst no antigen retrieval step resulted in no visible immunostain (**Fig. 2.10**). Therefore, antigen retrieval was necessary to visualise immunostaining. Section morphology was best with 10 min antigen retrieval, whilst also providing clear staining. Negative controls (primary anti-aromatase antibody omitted; secondary antibody only) showed large blotches of colour across the tissue whilst all experimental samples showed non-specific staining across the theca and stroma, where aromatase is not expressed (Stocco, 2008) (**Fig. 2.10**). To ensure this was not due to ineffectual wash times, wash times were increased to 3x 20 min with a 10 min antigen retrieval. This was effective at removing colour blotches in the negative controls, though staining continued to be observed outside the granulosa layer (**Fig. 2.11**). Due to the non-specific staining of the antibody, aromatase immunostaining was not pursued further.

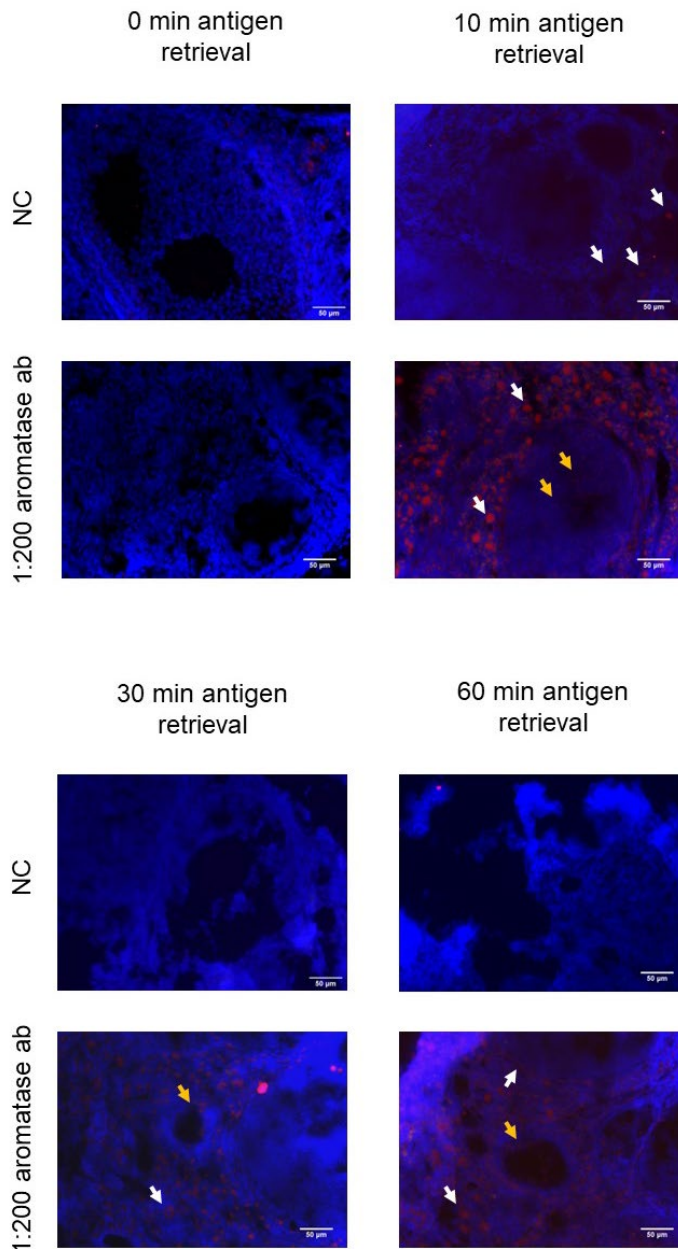


Figure 2.10. Representative images to show the effects of antigen retrieval time on aromatase staining of 10 μm mouse ovary sections. Slices underwent a 0, 10, 30, 60, or 120 min antigen retrieval time. Antigen retrieval for 120 min resulted in samples peeling away from slides, therefore these samples are not shown. Negative control (NC) sections (first and third rows) were incubated with the primary antibody incubation solution with the primary antibody omitted, followed by incubation with the secondary antibody (goat anti-rabbit AlexaFluor 568, diluted 1:300 in 0.1 M PBS with 0.1% Triton X-100 (v/v)). The second and fourth rows show sections stained with the primary antibody at a 1:200 dilution and the secondary antibody. Images show expected staining of aromatase in the granulosa layer (yellow arrows) and non-specific staining in the stroma and theca (white arrows).

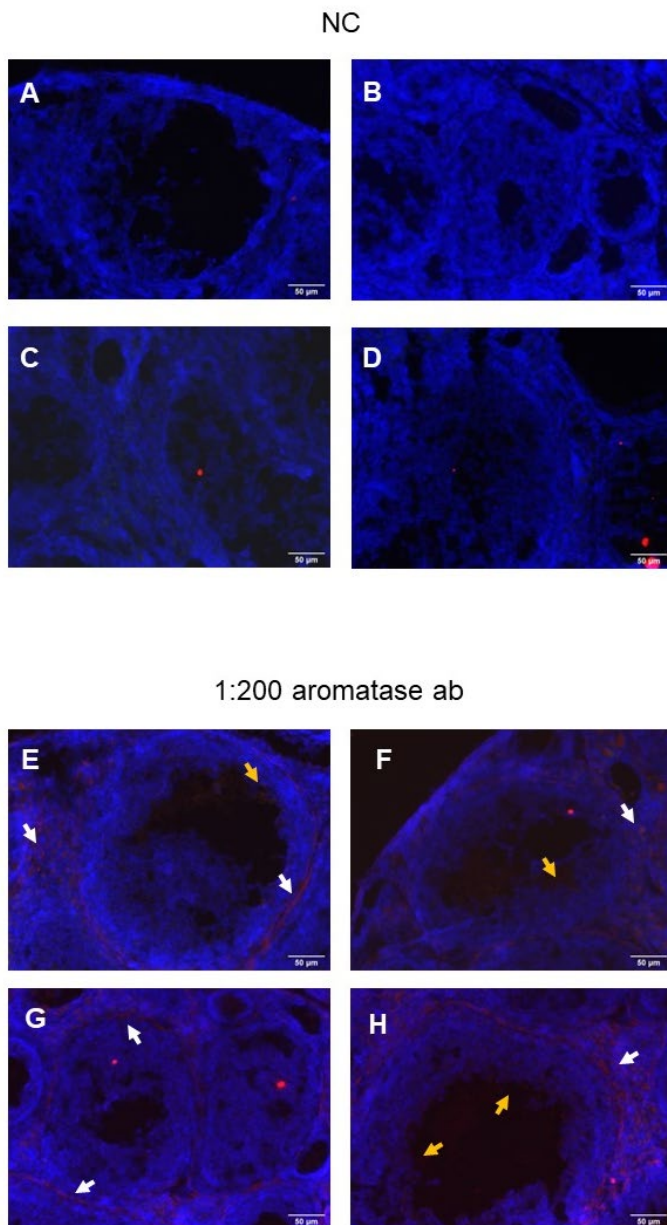


Figure 2.11. Representative images to show the effects of wash times on aromatase staining of 10 μ m mouse ovary sections. Negative control (NC) sections (A-D) were incubated with the primary antibody incubation solution with the primary antibody omitted, followed by incubation with the secondary antibody (goat anti-rabbit AlexaFluor 568, diluted 1:300 in 0.1 M PBS with 0.1% Triton X-100 (v/v)). E-F shows sections stained with the primary antibody at a 1:200 dilution followed by the secondary antibody. Images show expected staining of aromatase in the granulosa layer (yellow arrows) and non-specific staining in the stroma and theca (white arrows).

2.15 Statistical analyses

For the measurement of steroid hormones, it was estimated that 10 slices per treatment group would be required to reach power of 80%. This estimation was based on our initial measurements of E₂ from 6 samples, where the 24 h group had a mean of 218 pg/ml and the 0 h group had a mean of 80 pg/ml.

$$k = \frac{n_2}{n_1} = 1$$
$$n_1 = \frac{(\sigma_1^2 + \sigma_2^2/K)(z_{1-\frac{\alpha}{2}} + z_{1-\beta})^2}{\Delta^2}$$
$$n_1 = \frac{(111^2 + 111^2/1)(1.96 + 0.84)^2}{138^2}$$
$$n_1 = 10$$
$$n_2 = K \times n_1 = 10$$

where:

$\Delta = |\mu_2 - \mu_1|$ = absolute difference between two means

σ_1, σ_2 = variance of mean #1 and #2

n_1 = sample size for group #1

n_2 = sample size for group #2

α = probability of type I error (0.05)

β = probability of type II error (0.2)

z = critical Z value for a given α or β

k = ratio of sample size for group #2 to group #1

Power was achieved in all experiments, however lack of statistical differences could be a consequence of oestrous cycle stage, as animals were pooled across stages (see section 2.5).

Results are expressed as mean \pm SEM, and data was tested for normality using the Shapiro-Wilk test. For parametric datasets, differences established by Student's *t* test and one-way ANOVA with Bonferroni *post hoc* test for multiple comparisons. For nonparametric datasets, differences were established by a Kruskal-

Wallis test with Dunn's multiple comparisons *post hoc*. This is indicated in the figure legends. *P* values of <0.05 were considered statistically significant. Statistical testing and graphing were carried out using GraphPad Prism version 8.0 for Windows, GraphPad Software, Boston, Massachusetts, USA.

Chapter 3

Measuring Neurosteroids in the Social Behaviour Network of the Mouse Using a Novel Ex Vivo Brain Slice Culture Technique

This chapter was originally written as a manuscript submitted to Endocrinology, October 2023 and co-authored by Janine Dovey (JD) and DeAsia Davis (DD). All male data were collected by DD; all female data was collected by JD. Both authors contributed to the manuscript equally. For this thesis, all data obtained by DD were reanalysed and redrawn by JD.

3.1 Introduction

Steroid hormones have widespread effects on sexually dimorphic behaviours via nuclear hormone receptors that are abundantly expressed in the brain. The neural circuits underlying behaviour are found within the social behaviour network (SBN); a conserved, sexually dimorphic network of brain nuclei (Newman, 1999). The hypothalamus contributes several nuclei to the SBN, including the medial preoptic area (mPOA), anterior hypothalamus (AH), and ventromedial hypothalamus (VMH), and is a critical mediator of lordosis behaviour in female rodents (Pfaff, 1998) and aggressive behaviour in male rodents (Sano et al., 2013) (Unger et al., 2015) when activated by sex hormones.

3.1.1 Expression of steroidogenic enzymes

Sex hormones not only originate from the gonads or adrenals but can be produced by the brain itself in de novo synthesis from cholesterol or in situ from haematogenous precursors (Giatti et al., 2019). De novo neurosteroidogenesis requires the expression of both steroidogenic acute regulatory protein (StAR), which mediates the transfer of cholesterol to the inner mitochondrial membrane, and the mitochondrial enzyme cytochrome P450 side-chain cleavage (P450_{scc}), which converts cholesterol into pregnenolone. RT-PCR has demonstrated the regional and sexually dimorphic distribution of Cyp11a1 (encoding P450_{scc}) in the rat brain, where cortical expression is high amongst both male and female rats, but hippocampal expression is much higher in the female than the male (Mellon and Deschepper, 1993). Discrete cell populations in the mouse brain express P450_{scc} and StAR proteins, suggesting that only a few cells can synthesise neurosteroids de novo, though co-immunoreactivity has been observed in the hypothalamus of both male and female mouse brains (King et al., 2002). Enzymes involved in further steroid metabolism, including 3 β -hydroxysteroid dehydrogenase (3 β -HSD), encoded by Hsd3b1, 17 β -hydroxysteroid dehydrogenase (17 β -HSD), encoded by Hsd17b1, and cytochrome P450 aromatase, encoded by the Cyp19a1 gene, have also been demonstrated in the mammalian brain by means of immunohistochemistry, in situ hybridisation, Western blot, RT-PCR, and transgenes (Stanic et al., 2014) (Pelletier, 2010). Many of the steroidogenic enzymes show regional and sex differences in expression across the cerebral cortex, cerebellum, and hypothalamus. For example, female rats tend to express higher levels of Stard1 mRNA (encoding StAR) in the cerebellum and Hsd3b1 mRNA in the cerebral cortex (Giatti et al., 2019). Meanwhile, the female mouse hypothalamus expresses less Hsd3b1 than the male (Nishida et al., 2005). In contrast, in the male hypothalamus, the bed nucleus

of stria terminalis (BNST), preoptic area, and amygdala exhibit higher levels of aromatase expression than in the female (Tabatadze et al., 2014a) (Stanic et al., 2014) (Wu et al., 2009). However, the dorsal hippocampus and cingulate cortex did not show any sex dimorphisms in aromatase expression (Tabatadze et al., 2014a).

3.1.2 *The role of neurosteroids*

Steroids made within the brain, i.e., neurosteroids, contribute to rapid signalling functions to exert a variety of effects on the nervous system, including myelin formation in peripheral nerves (Schumacher et al., 2001), synapse formation and maintenance in the hippocampus (Kretz et al., 2004b, Prange-Kiel and Rune, 2006), dendritic spine formation in the hippocampus (Murakami et al., 2018) (Kato et al., 2013), and promotion of GABAergic transmission in the VMH (Uddin et al., 2020). Many of these cellular or network effects have behavioural consequences. For example, neuroestrogens rapidly modulate auditory processing circuits in the songbird brain to enhance song memory (Vahaba and Remage-Healey, 2018). In the mouse, neuroestrogen in the medial amygdala (meA) drives aggressive behaviour (Unger et al., 2015) and sexual motivation in male quail (Seredynski et al., 2013). In ovariectomised (OVX) female mice, both intracerebroventricular and intra-VMH injections of E2-benzoate (EB) can drive lordosis in a protein kinase-dependent pathway (Domínguez-Ordóñez et al., 2019), suggesting hypothalamic neuroestrogen is important for female sexual behaviour. In male mice with a forebrain-specific aromatase knockout (ArKO), sexual behaviour is decreased despite high levels of testosterone (Brooks et al., 2020a). In the female rat hippocampus, neuroestrogens fluctuate across the oestrous cycle, following a similar cyclicity in concentration to that in the plasma (Kato et al., 2013). However, the relative contribution of ovarian oestrogen and neuroestrogen to the overall concentrations measured in the brain remains unclear.

Concentrations of circulating sex hormones are not a direct representation of the concentrations present in the brain because of regional and sexually dimorphic changes in aromatase activity under certain physiological conditions. In the newborn rat, high aromatase activity in the hypothalamus correlates with higher levels of oestradiol and low levels of aromatase activity in the hippocampus and cortex correlates with lower levels of brain-derived oestradiol (Konkle and McCarthy, 2011a). Neurosteroids have been measured to a greater extent in the songbird (Jalabert et al., 2022) (Charlier et al., 2010b) (Saldanha et al., 2013a), which contains the same SBN regions along with the caudal medial nidopallium (NCM); a steroid-responsive brain

region important for song processing and social behaviours (Vahaba and Ramage-Healey, 2018). In the rodent, neurosteroids have been measured mostly in the hippocampus (Hojo et al., 2004a, Hojo et al., 2009, Hojo and Kawato, 2018, Kretz et al., 2004a), where they play an important role in learning and memory (Frick and Kim, 2018). Neurosteroids exist in higher concentrations than that of plasma steroids in both the songbird brain and the rodent hippocampus (Charlier et al., 2010b) (Kato et al., 2013).

However, absolute concentrations of sex hormones and the regulation of their production within the adult SBN have not yet been demonstrated in the rodent.

Using a novel *ex vivo* slice culture method, we show differential expression between the sexes of steroidogenic enzymes and differences in local sex hormone concentrations that are important for the dynamics of neuroestrogen signalling *in vivo*, in response to stimuli. Since this research was carried out by two independent researchers (JD and DD) at different stages of their PhDs, all analysis was carried out *post hoc*. Thus, there exists some inconsistencies in brain regions used in analysis. JD, who gathered data from female mice, was primarily interested in behaviourally relevant regions involved in female typical behaviour. DD, who gathered data from male mice, conducted research on the whole SBN. Whilst it is acknowledged that differences in the brain regions studied by each researcher do not lend themselves to direct comparisons, it should be noted that there is significant overlap in the behaviourally relevant brain areas for female behaviour and the SBN. Overall, the aim of this work was to contribute to a greater understanding of the paracrine roles of locally produced hormones in sexually dimorphic brain processes.

3.2 Methods

3.2.1 Materials: animals and chemicals

All animals were housed at the University of Reading as described in section 2.1. Oestrous stage was determined as described in section 2.5.

3.2.2 Preparation of slice culture

Ex vivo brain slices were prepared as described in section 2.7.

3.2.3 Determination of slice viability

Slice viability was determined with Trypan Blue, as described in section 2.8.

3.2.4 Blood collection and plasma preparation

Blood was collected and plasma prepared as described in section 2.6.

3.2.5 Palkovits punch technique for extraction of steroids and for RT-qPCR

The Palkovits punch method (described in section 2.9) was used to micropunch regions of interest which were used for solid phase extraction (section 2.10) or RT-qPCR (section 2.12).

3.2.6 Determination of steroid concentration by ELISA

Concentrations of E₂ and testosterone in aCSF samples, and from punches and serum (which had been subject to solid phase extraction) were measured using competitive in-house ELISAs, described in section 2.11. It should be noted that hormones measured from aCSF may not be a direct reflection of the neurosteroidogenic capacity of the brain regions of interest alone, as each slice contains several other brain regions that have the capability to produce neurosteroids. Please see section 2.8 and **Fig. 2.5**.

3.2.7 Statistical analyses

Statistical analysis was carried out as described in section 2.15.

3.3 Results

3.3.1 The brain produces neurosteroids ex vivo

The concentrations of sex hormones E₂ and testosterone in *ex vivo* hypothalamic brain slices following incubation at different time points are shown in **Fig. 3.1**. Neurosteroids were measured in the incubation media, in females (**Fig. 3.1A** and **3.1C**) and males (**Fig. 3.1B** and **3.1D**). In female hypothalamic slices, E₂ concentration was significantly increased by 8 h (**Fig. 3.1A**, 0 h vs 8 h, $P = 0.0291$). In both females and males, there was a significant increase in E₂ between 0 h and 24 h (**Fig 3.1A**, females, $P = 0.0373$; **Fig. 3.1B**, males, $P = 0.0456$), but no increase at 48 h (**Fig. 3.1A**, females, 0h vs 48h, $P > 0.999$; **Fig. 3.1B**, males, 0 h vs 48 h, $P > 0.999$). In female hypothalamic slices, testosterone concentration increased significantly from 0 h after 2 h incubation (0h vs 2h, $P = 0.0067$), showing a continued increase at 8 h (0 h vs 8 h, $P < 0.0001$) (**Fig. 3.1C**). After 24 h incubation testosterone had increased significantly from 0 h in both females (**Fig. 3.1C**, $P = 0.0109$) and males (**Fig. 3.1D**, $P = 0.0257$) but did not increase significantly from 0 h after 48 h (0 h vs 48 h, $P > 0.999$ for both

females [Fig. 3.1C] and males [Fig. 3.1D]). Since there was a significant increase in the concentration of both E₂ and testosterone at 24 h in both males and females alongside satisfactory slice viability (Fig. 3.2), a 24 h incubation period was used for all subsequent experiments.

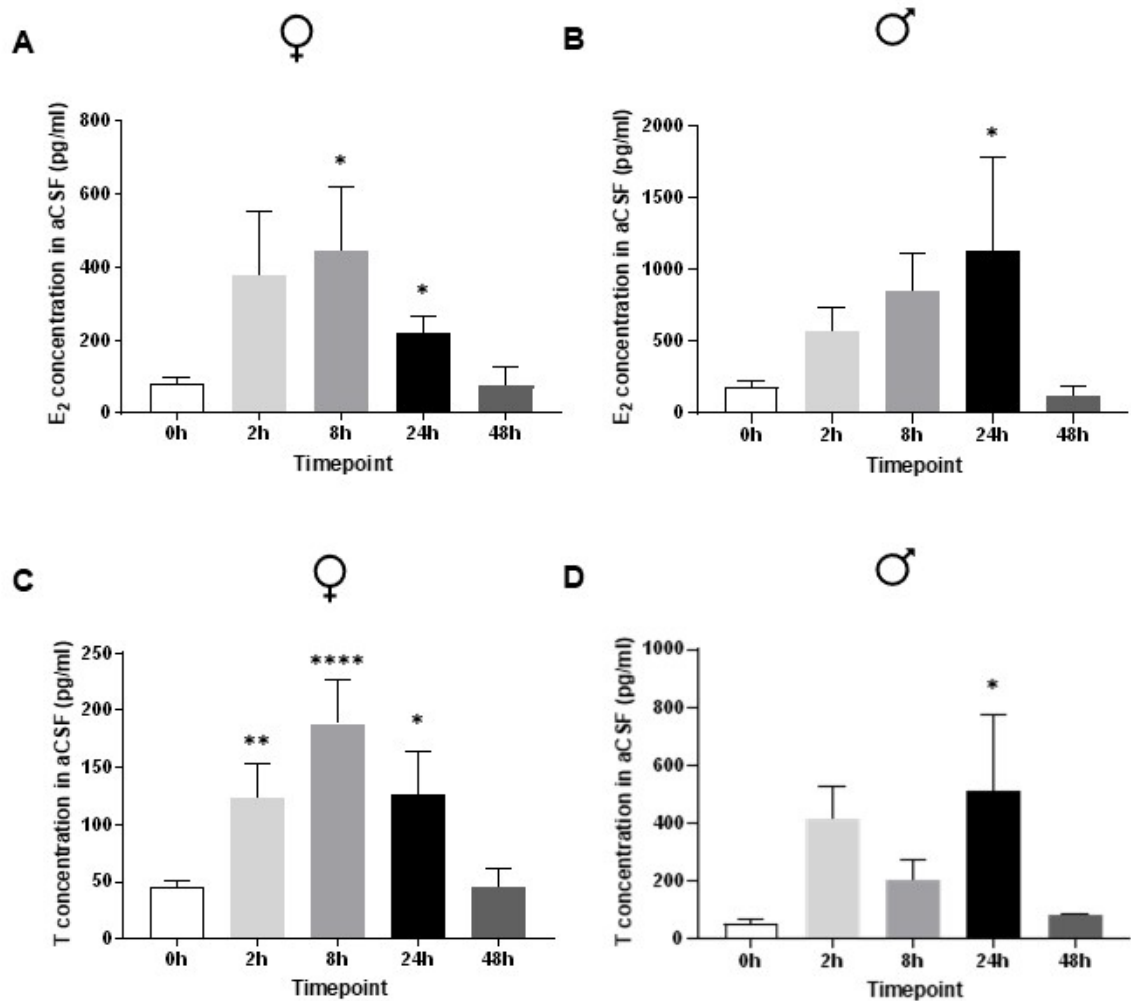


Figure 3.1. Neurosteroid concentrations in hypothalamic brain slices from adult male and female mice incubated for different time points. Concentrations of neuroestrogen (A, B) and neurotestosterone (C, D) in female (left) and male (right) animals. $n = 6$ slices from 6 animals for all timepoints except 48 h where $n = 3$ slices from 3 animals, and 0 h where $n = 24$ slices from 6 animals. Differences were established by the Kruskal Wallis test with Dunn's multiple comparisons test *post hoc* (A and C), or by a one-way ANOVA with Bonferroni's multiple comparisons test *post hoc* (B and D), * $P < 0.05$ vs 0 h, ** $P < 0.01$ vs 0 h, **** $P < 0.0001$ vs 0 h.

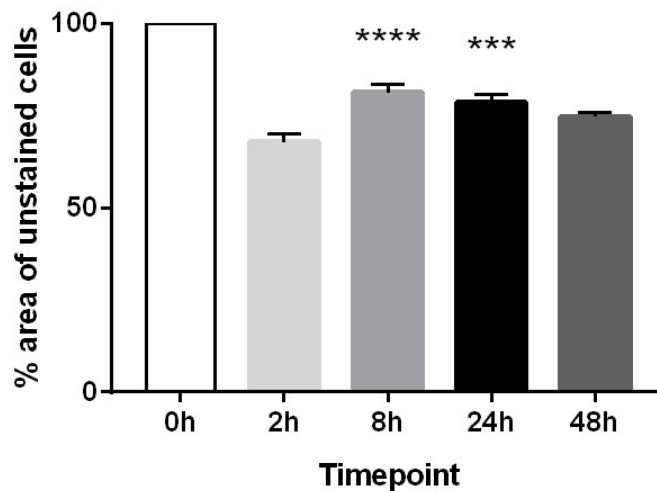


Figure 3.2. Viability of hypothalamic brain slices incubated for different time points measured by the Trypan Blue exclusion assay. A vibratome was used to take 200 μm slices from hypothalamic brain regions of P38-44 C57Bl/6 mice, which were incubated in aCSF for different time points. Following incubation, slices were incubated with 0.4% Trypan Blue Solution and fixed in 4% w/v paraformaldehyde before being mounted on microscope slides and imaged under a light microscope. 10X images of four separate areas of each slice were taken, and each image was then divided into quadrants. The % area of unstained tissue is plotted, where 0 h was assumed 100% viability. $n = 1$ slice per time point, where each slice contributed 16 images. Differences were established by a one-way ANOVA with Bonferroni's multiple comparisons test *post hoc*. *** $P < 0.001$ vs 2 h, **** $P < 0.0001$ vs 2 h.

3.3.2 The capacity to synthesise neurosteroids in the social behaviour network is sexually dimorphic

To understand if males differed from females in neurosteroid synthesis, we investigated E_2 and testosterone concentration at 0 h and 24 h across all SBN nuclei (**Fig. 3.3**). For both E_2 (**Fig. 3.3A**) and testosterone (**Fig. 3.3C**), there was a significant effect of sex ($P < 0.0001$ for E_2 and testosterone), timepoint ($P < 0.0001$ for E_2 and testosterone), and the interaction between sex and timepoint ($P = 0.0002$ for E_2 , $P < 0.0001$ for testosterone). To compare punch dissected SBN nuclei between males and females, the concentrations of neurosteroids from the female mPOA, AH, and VMH was averaged and compared to the concentration of neurosteroids from the SBN nuclei of the male (**Fig 3.3B**). There was a significant effect of sex ($P = 0.001$), timepoint ($P = 0.0005$), and the interaction between sex and timepoint ($P = 0.001$) on

E₂ concentration in SBN punches (Fig. 3.3B). There was a significant effect of timepoint on the concentration of testosterone in SBN nuclei ($P = 0.0002$), but no effect of sex or the interaction between sex and timepoint (Fig. 3.3D).

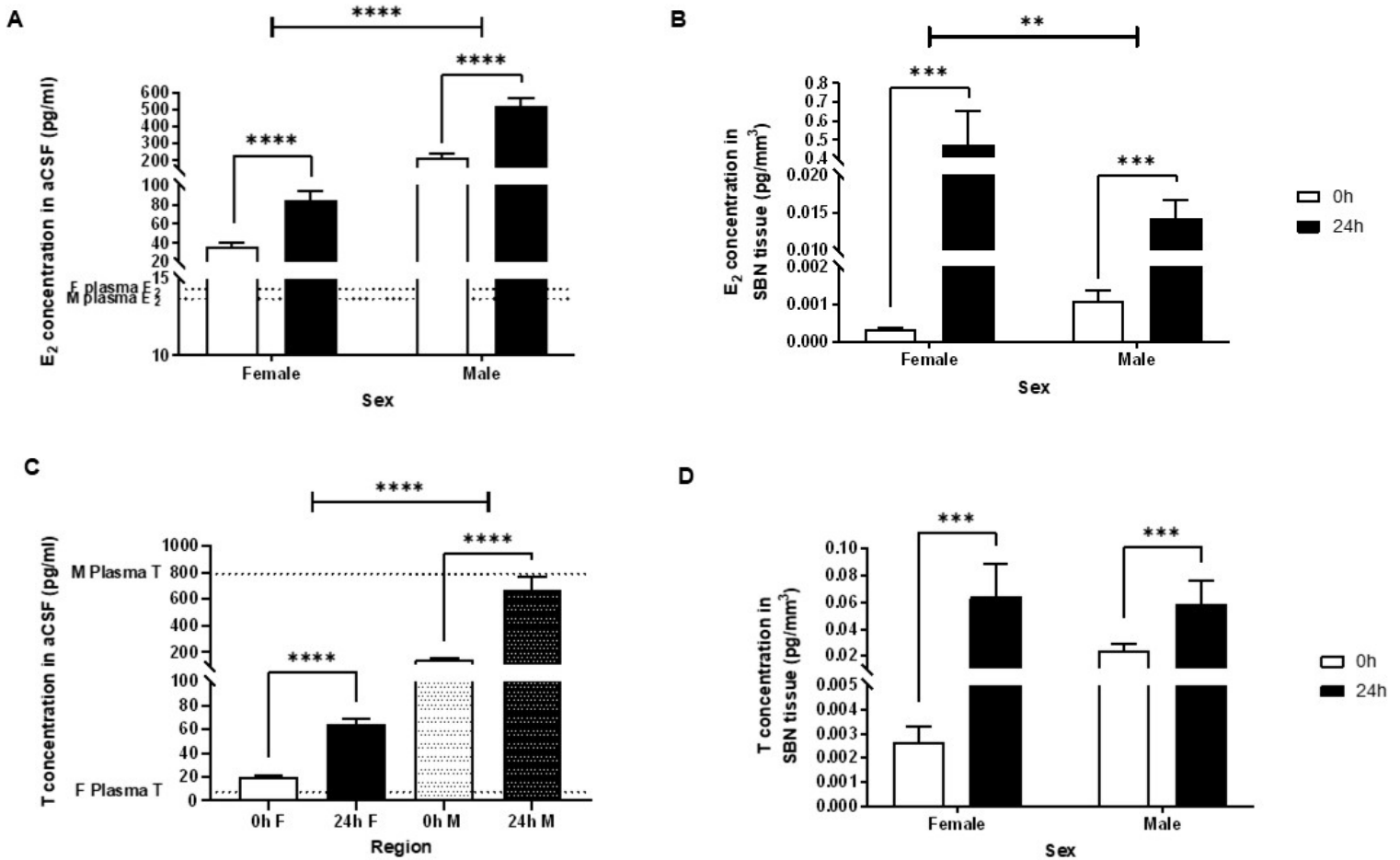


Figure 3.3. Neurosteroid concentrations in pooled SBN nuclei of adult male and female mice. Concentrations of neuroestrogen (A) and neurotestosterone (C) in pooled aCSF bathing male and female slices comprising the lateral septum, medial preoptic area, bed nucleus of stria terminalis, anterior hypothalamus, medial amygdala, and ventromedial hypothalamus after either 0 h or 24 h incubation. Individual SBN nuclei were punch dissected from their slices after either 0 h or 24 h incubation in aCSF before being processed by C18 extraction to extract steroids for measurement of neuroestrogen (B) or neurotestosterone (D) contents. Note that SBN nuclei pooled from male and female mice were used for this analysis. Differences were established by a Kruskal-Wallis test with Dunn's multiple comparisons *post hoc*. * $P < 0.05$ vs 0 h, ** $P < 0.01$ vs 0 h, *** $P < 0.001$ vs 0 h, **** $P < 0.0001$ vs 0 h.

3.3.3 Neurosteroids are locally regulated across the social behaviour network and are significantly higher than plasma steroids

Across the SBN, neurosteroid production in *ex vivo* slices is locally regulated. Neurosteroids were measured from the incubation aCSF bathing hypothalamic slices containing SBN nuclei (**Fig. 3.4A, 3.4C, 3.4E, and 3.4G**). In females, there was a significant increase in E₂ between 0 h and 24 h in all slices except those containing the mPOA/BNST (**Fig. 3.4A**, 0 h vs 24 h, LS/mPOA, $P = 0.0097$; AH/meA, $P < 0.0001$, meA/VMH, $P = 0.0253$; mPOA/BNST, $P = 0.0939$). E₂ measured in aCSF at any timepoint was at least 1.9x higher than that measured in plasma, shown by the dotted line (14.33 ± 1.71 pg/ml) (**Fig. 3.4A**). Plasma steroids were lower than neurosteroids measured in aCSF regardless of oestrous stage (**Fig. 3.6**). In male slices, there was a significant increase in E₂ between 0 h and 24 h in all slice regions (**Fig. 3.4C**, 0 h vs 24 h, LS/mPOA, $P < 0.0001$; mPOA/BNST, $P = 0.0061$; AH/meA, $P = 0.0014$, meA/VMH, $P < 0.0001$). E₂ measured in aCSF was considerably greater than that measured in plasma (13.7 ± 0.07 pg/ml, shown by the dotted line), with a minimum difference of 11-fold (**Fig. 3.4C**).

For testosterone, there was a significant increase between 0 h and 24 h for all slice regions in both female (**Fig 3.5A**, 0 h vs 24 h, LS/mPOA, $P < 0.0001$; mPOA/BNST, $P = 0.0007$; AH/meA, $P < 0.0001$; meA/VMH, $P = 0.0079$) and male (**Fig. 3.5C**, 0 h vs 24 h, LS/mPOA, $P < 0.0001$; mPOA/BNST, $P = 0.0004$; AH/meA, $P = 0.0157$; meA/VMH, $P = 0.0048$) *ex vivo* slices. This was most predominantly seen in male slices, where testosterone concentrations increased by up to 3.6-fold (**Fig 3.5C**). Plasma testosterone concentrations (shown by the dotted line) were less than that measured in aCSF in both females (7.49 ± 1.34 pg/ml) (**Fig. 3.5A**) and males (660.21 ± 15.07 g/ml) (**Fig 3.5C**).

Since *ex vivo* hypothalamic slices contain steroid-producing cells outside of the SBN nuclei, individual nuclei were punch dissected and steroids were extracted by C18 extraction (**Fig. 3.4 and Fig. 3.5, panels C-D**). In the female, only 3 SBN nuclei were dissected, along with the ARC, a non-SBN region that is important for the expression of lordosis during female reproductive behaviour. There was a significant increase in E₂ between 0 h and 24 h in the female AH (0 h vs 24 h, $P = 0.0095$) and VMH (0 h vs 24 h, $P = 0.0270$) (**Fig. 3.4B**). In males, there was a significant increase in E₂ between 0 h and 24 h for all regions except the VMH (**Fig 3.3D**, 0 h vs 24 h, LS, $P = 0.0357$; mPOA, $P = 0.0109$; BNST, $P = 0.0388$; AH, $P = 0.0135$; meA, $P = 0.0163$; VMH, $P = 0.1509$).

Testosterone concentrations within mPOA punch dissections showed a significant increase in females (**Fig 3.5B**, 0 h vs 24 h, $P = 0.0152$) and males (**Fig. 3.5D**, 0 h vs 24 h, $P = 0.0477$). In male SBN punches, there was also a significant increase in testosterone between 0 h and 24 h in the VMH (**Fig. 3.5D**, 0 h vs 24 h, $P < 0.0001$).

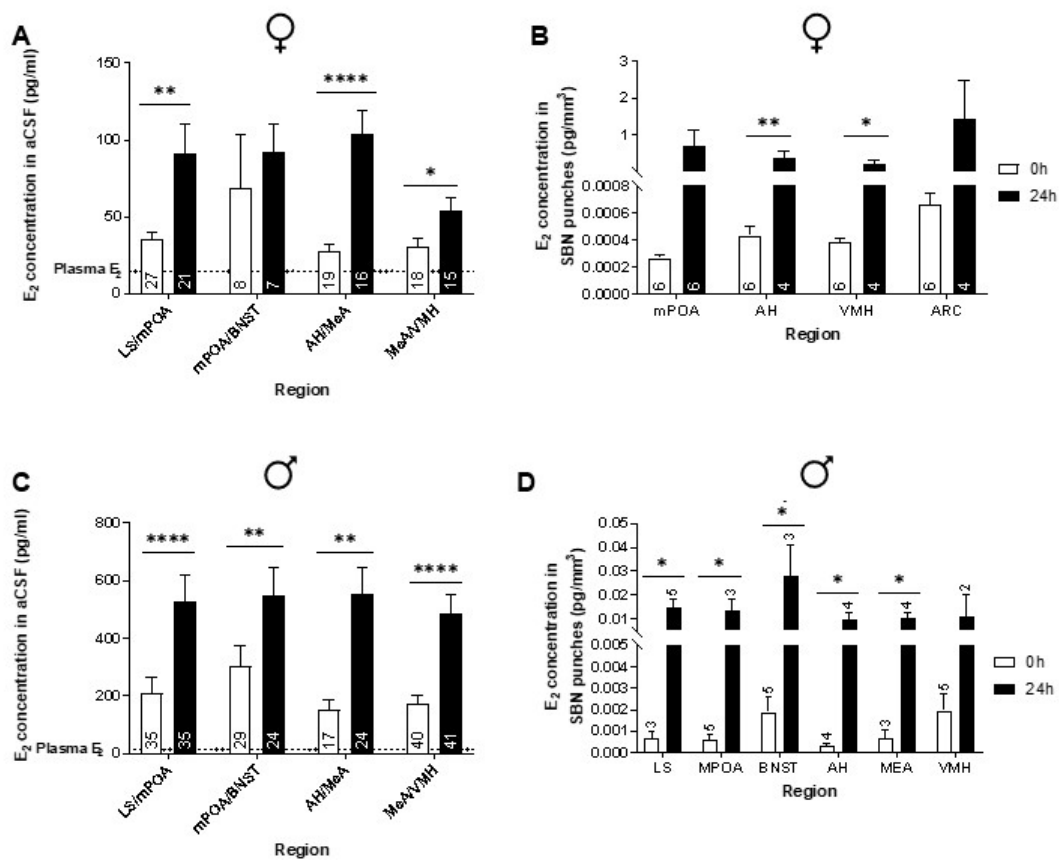


Figure 3.4. Neuroestrogen concentrations in individual SBN nuclei of adult male and female mice. *Left side:* Neuroestrogen concentrations were measured in aCSF bathing female (**A**) and male (**C**) slices after either 0 h or 24 h incubation. Dotted lines represent the average plasma steroid levels in the animals used for neurosteroid analysis. *Right side:* Six different SBN nuclei were punch dissected from their slices after either 0 h or 24 h incubation in aCSF before being processed by C18 extraction to extract steroids to measure neuroestrogen in female (**B**) and male (**D**) SBN nuclei. Slice *n* is shown in bars for **A-B**, contributed by at least 5 animals per group. Animal *n* is shown in bars for **C-D**, where one animal contributed one whole SBN nucleus. Differences were established by a two-way ANOVA comparing time, region, and the interaction between time and region. Parametric datasets for 0 h vs 24 h were compared by an unpaired *t*-test; nonparametric datasets for 0 h vs 24 h were compared by a Mann-Whitney test. * $P < 0.05$ vs 0 h, ** $P < 0.01$ vs 0 h, **** $P < 0.0001$ vs 0 h.

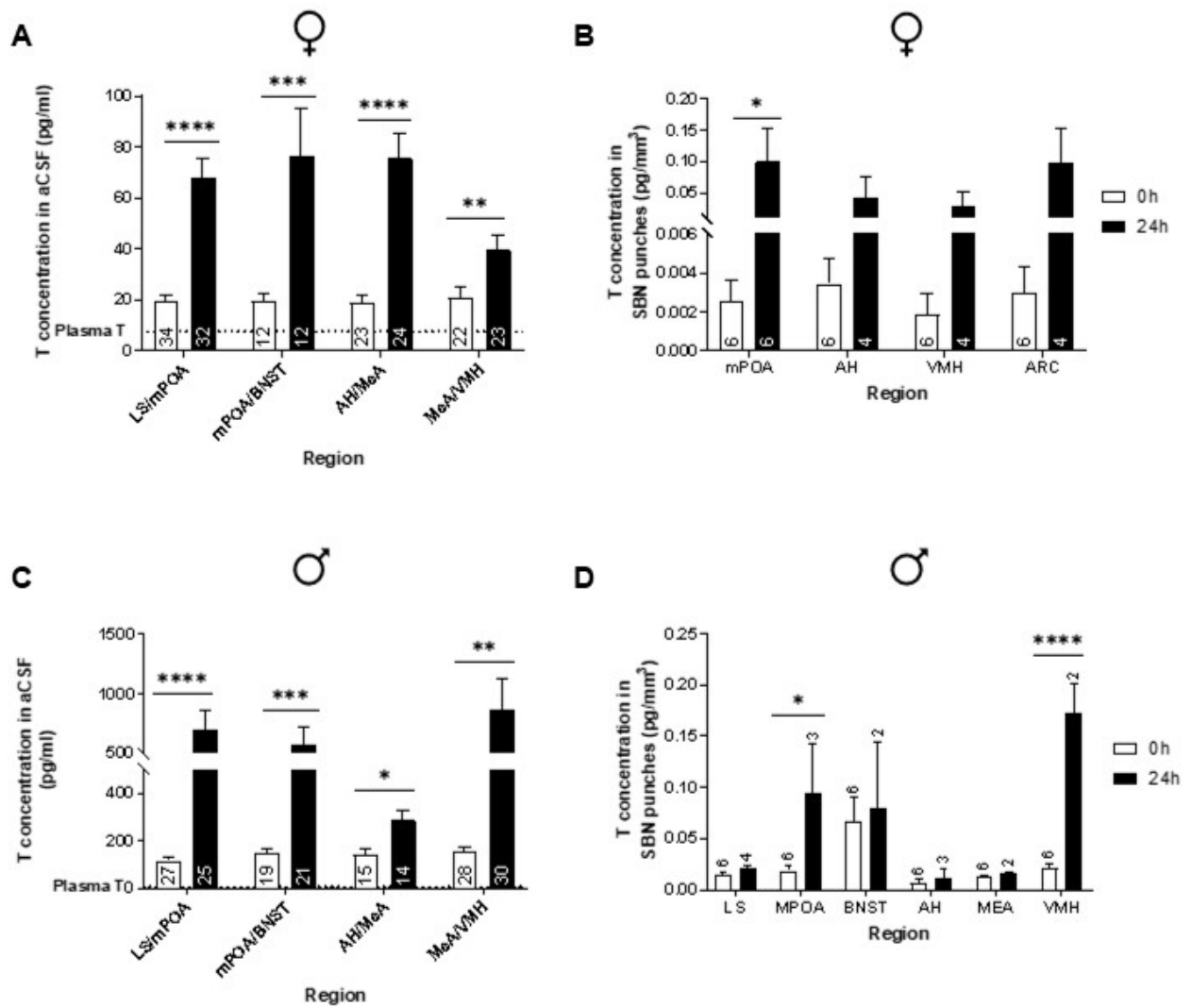


Figure 3.5. Neurotestosterone concentrations in individual SBN nuclei of adult male and female mice. *Left side:* Neurotestosterone concentrations were measured in aCSF bathing female (**A**) and male (**C**) slices after either 0 h or 24 h incubation. Dotted lines represent the average plasma steroid levels in the animals used for neurosteroid analysis. *Right side:* Six different SBN nuclei were punch dissected from their slices after either 0 h or 24 h incubation in aCSF before being processed by C18 extraction to extract steroids to measure neurotestosterone in female (**B**) and male (**D**) SBN nuclei. Slice *n* is shown in bars for **A-B**, contributed by at least 5 animals per group. Animal *n* is shown in bars for **C-D**, where one animal contributed one whole SBN nucleus. Differences were established by a two-way ANOVA comparing time, region, and the interaction between time and region. Parametric datasets for 0 h vs 24 h were compared by an unpaired *t*-test; nonparametric datasets for 0 h vs 24 h were compared by a Mann-Whitney test. * $P < 0.05$ vs 0 h, ** $P < 0.01$ vs 0 h, **** $P < 0.0001$ vs 0 h.

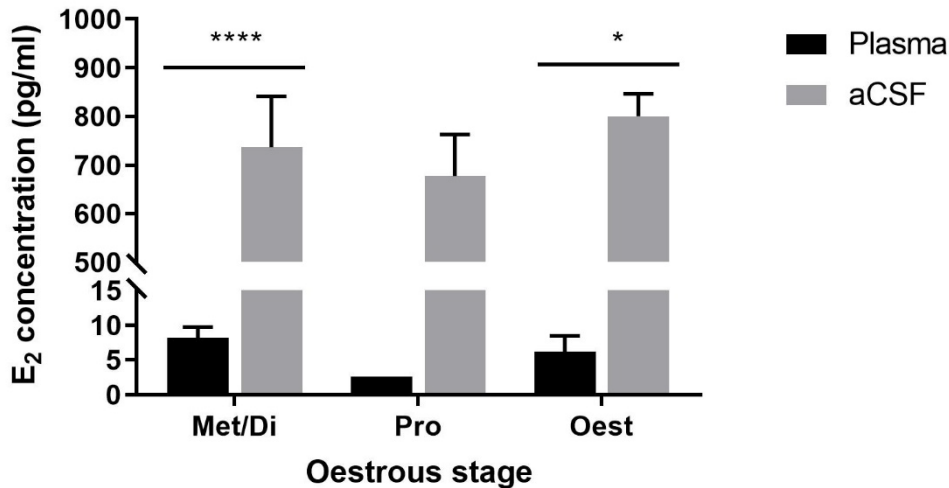


Figure 3.6. E₂ concentrations in plasma vs aCSF in female mice at different oestrous stages. Mice were staged *post mortem* by assessing vaginal cytology following vaginal lavage. $n = 11$ animals in metoestrous/dioestrous (Met/Di), and $n = 2$ animals in oestrous (Oest). Due to the relatively short proestrous window and the timing of animal delivery and sacrifice, only one animal was obtained in proestrous (Pro). Therefore, statistics could not be performed for this group. Differences were established by a two-way ANOVA with Bonferroni's multiple comparisons *post hoc*. * $P < 0.05$, **** $P < 0.0001$.

3.3.4 Expression of steroidogenic enzymes varies between regions and is sexually dimorphic

Stard1 and Cyp11a1: Expression of *Stard1* mRNA encoding the cholesterol transport protein StAR and *Cyp11a1*, encoding cytochrome P450_{scc}, was measured in punch dissections of the SBN of male and female brain slices that had been incubated for 0 h and 24 h (**Fig. 3.5**), using RT-qPCR. In the female, there was a significant increase in *Stard1* expression in the LS (0 h vs 24 h, $P = 0.0266$), BNST (0 h vs 24 h, $P = 0.2179$), AH (0 h vs 24 h, $P = 0.0025$), and meA (0 h vs 24 h, $P = 0.0125$) (**Fig. 3.7A**). *Cyp11a1* expression increased significantly between 0 h and 24 h in the female BNST (0 h vs 24 h, $P = 0.0179$) and AH (0 h vs 24 h, $P < 0.0001$) (**Fig. 3.7B**).

In male SBN punches, there was no significant difference in expression of either *Stard1* (**Fig. 3.7C**) or *Cyp11a1* (**Fig. 3.7D**) between 0 h and 24 h. However, the male SBN expressed significantly more *Stard1* than the female SBN at both time points (male vs female, 0 h, $P = 0.0056$; 24 h, $P < 0.0001$) (**Supp. Fig. S3.1A**). The same was

true for *Cyp11a1* (male vs female, 0 h, $P = 0.0134$; 24 h, $P = 0.0031$) (Supp. Fig. S3.1B).

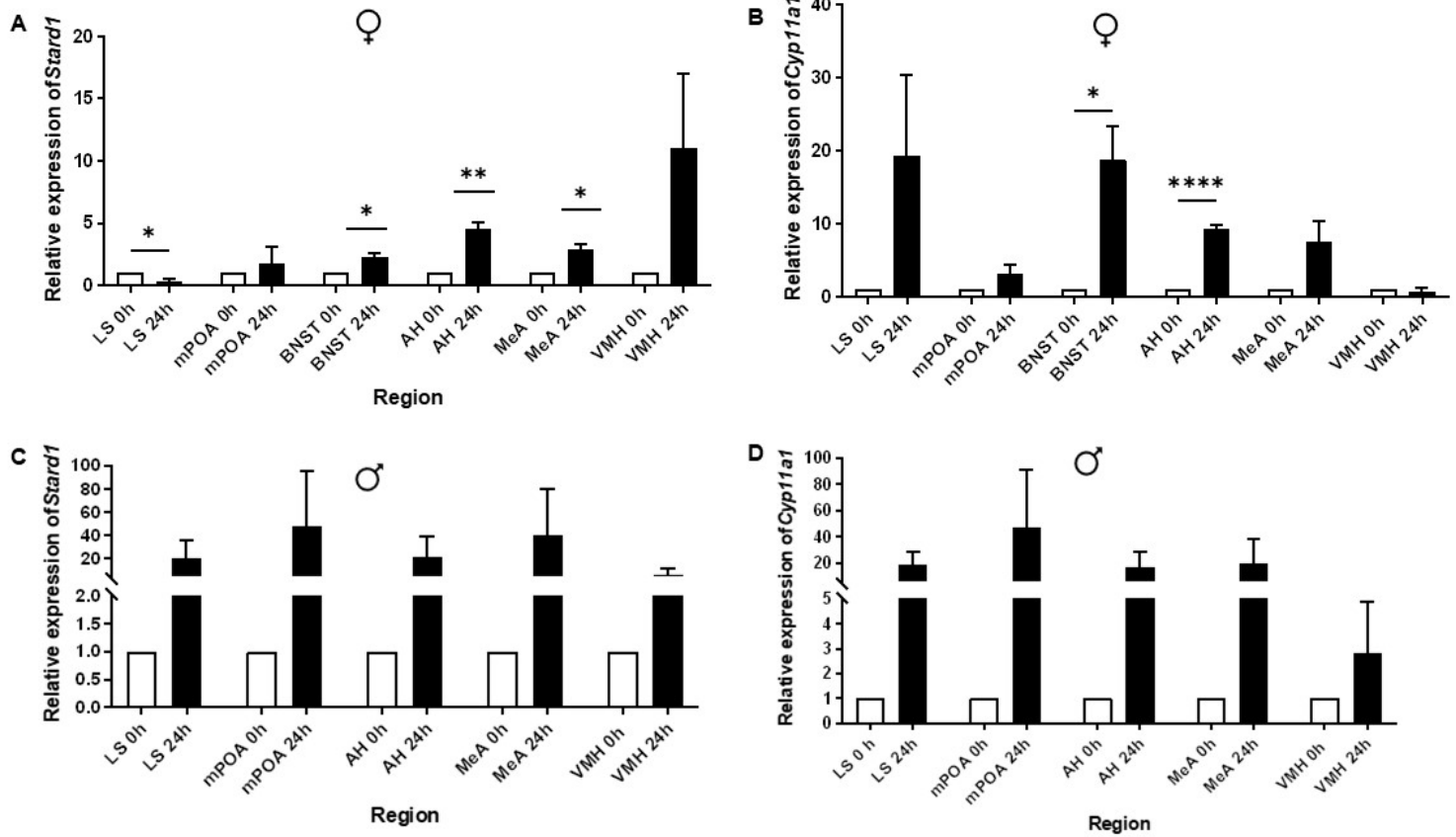


Figure 3.7. Expression of *Stard1* and *Cyp11a1* in adult male and female SBN nuclei at 0 h and 24 h slice incubation timepoints, measured by RT-qPCR.

Following incubation of slices for 0 h or 24 h, six different SBN nuclei were punch dissected, and nuclei from 4 animals were pooled into one, such that $n = 3$ from a total of 12 animals for **A** and **B**, and $n = 2$ from a total of 6 animals for **C** and **D**. Following RNA extraction, cDNA was synthesised and used for RT-qPCR analysis. Expression levels, relative to the housekeeping gene (*Actb*), are shown for *Stard1* (**A**, **C**) and *Cyp11a1* (**B**, **D**) in female and male mice, respectively. Differences were established by a two-way ANOVA comparing region, time, and the interaction between time and region. Parametric datasets for 0 h vs 24 h were compared by an unpaired *t*-test; nonparametric datasets for 0 h vs 24 h were compared by a Mann-Whitney test. * $P < 0.05$ vs 0 h, ** $P < 0.01$ vs 0 h, **** $P < 0.0001$ vs 0 h.

Hsd3b1 and *Hsd17b1*: In the female SBN, a significant increase in *Hsd3b1* expression was observed in the LS (0 h vs 24 h, $P = 0.0056$), AH (0 h vs 24 h, $P = 0.0027$), and VMH (0 h vs 24 h, $P = 0.0023$) (**Fig. 3.8A**). There was a tendency for increase in the female BNST (0 h vs 24 h, $P = 0.0509$) (**Fig. 3.8A**). The female BNST, AH, and meA all showed a significant increase in *Hsd17b1* expression between 0 h and 24 h (BNST, $P = 0.0035$; AH, $P = 0.0093$; meA, $P = 0.0285$) (**Fig. 3.8B**).

The male mPOA showed a significant increase in *Hsd3b1* expression between 0 h and 24 h (0 h vs 24 h, $P = 0.0177$), but this was not observed elsewhere in the SBN (**Fig. 3.8C**). There were no significant changes in *Hsd17b1* expression between 0 h and 24 h in the male SBN (**Fig. 3.6D**). Sexual dimorphisms in enzyme expression were clear when the SBN nuclei were pooled per time point (**Supp. Fig. S3.1**). At 0 h and 24 h, the male SBN expressed more *Hsd3b1* than the female SBN (0 h, $P = 0.0004$; 24 h, $P = 0.0001$) (**Supp. Fig. S3.1C**). For *Hsd17b1*, expression was also significantly higher in the male SBN at 24 h (male vs female, $P = 0.0001$) (**Supp. Fig. S3.1D**).

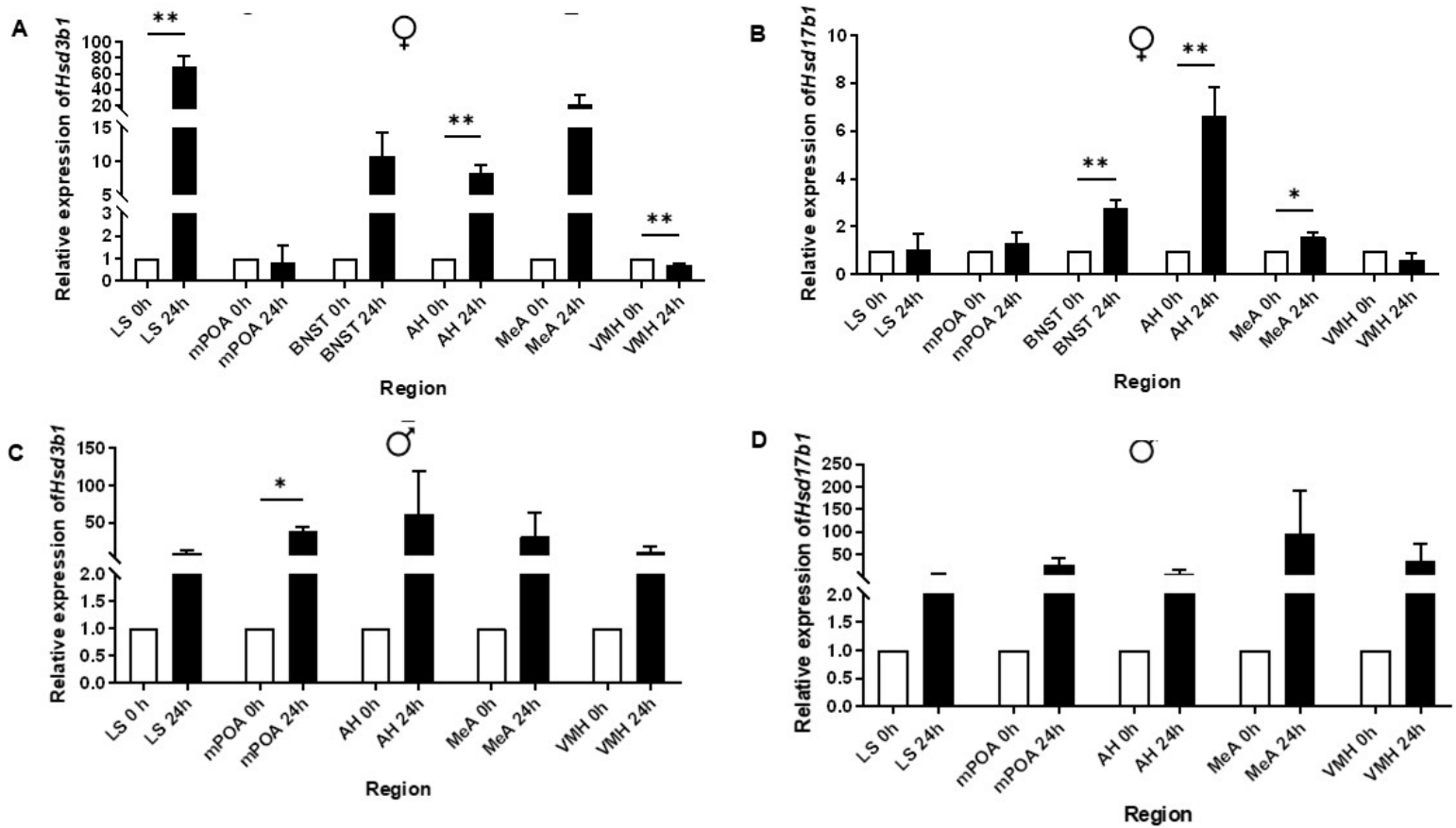


Figure 3.8. Expression of *Hsd3b1* and *Hsd17b1* in adult male and female SBN nuclei at 0 h and 24 h slice incubation timepoints, measured by RT-qPCR.

Following incubation of slices for 0 h or 24 h, six different SBN nuclei were punch dissected, and nuclei from 4 animals were pooled into one, such that $n = 3$ from a total of 12 animals for **A** and **B**, and $n = 2$ from a total of 6 animals for **C** and **D**. Following RNA extraction, cDNA was synthesised and used for RT-qPCR analysis. Expression levels, relative to the housekeeping gene (*Actb*), are shown for *Hsd3b1* (**A**, **C**) and *Hsd17b1* (**B**, **D**) in female and male mice, respectively. Differences were established by a two-way ANOVA comparing time, region, and the interaction between time and region. Parametric datasets for 0 h vs 24 h were compared by an unpaired *t*-test; nonparametric datasets for 0 h vs 24 h were compared by a Mann-Whitney test. * $P < 0.05$ vs 0 h, ** $P < 0.01$ vs 0 h.

Cyp19a1: Finally, the expression of *Cyp19a1*, encoding the aromatase enzyme that converts androgens to oestrogens, was measured in SBN punches, shown in **Fig. 3.9**. In the female SBN, expression increased significantly in the mPOA (0 h vs 24h, $P = 0.0025$), AH (0 h vs 24 h, $P = 0.0013$), and meA (0 h vs 24 h, $P = 0.0265$) (**Fig. 3.9A**). There was no significant difference in expression between 0 h and 24 h in any SBN

regions in the male (**Fig. 3.9B**), but sex dimorphisms in expression were clear when SBN punches were pooled per time point (**Supp. Fig. S3.1E**). At both 0 h and 24 h, males expressed significantly more *Cyp19a1* than females at matched time points (**Supp. Fig. S3.1E**, $P < 0.0001$ for both 0 h and 24 h).

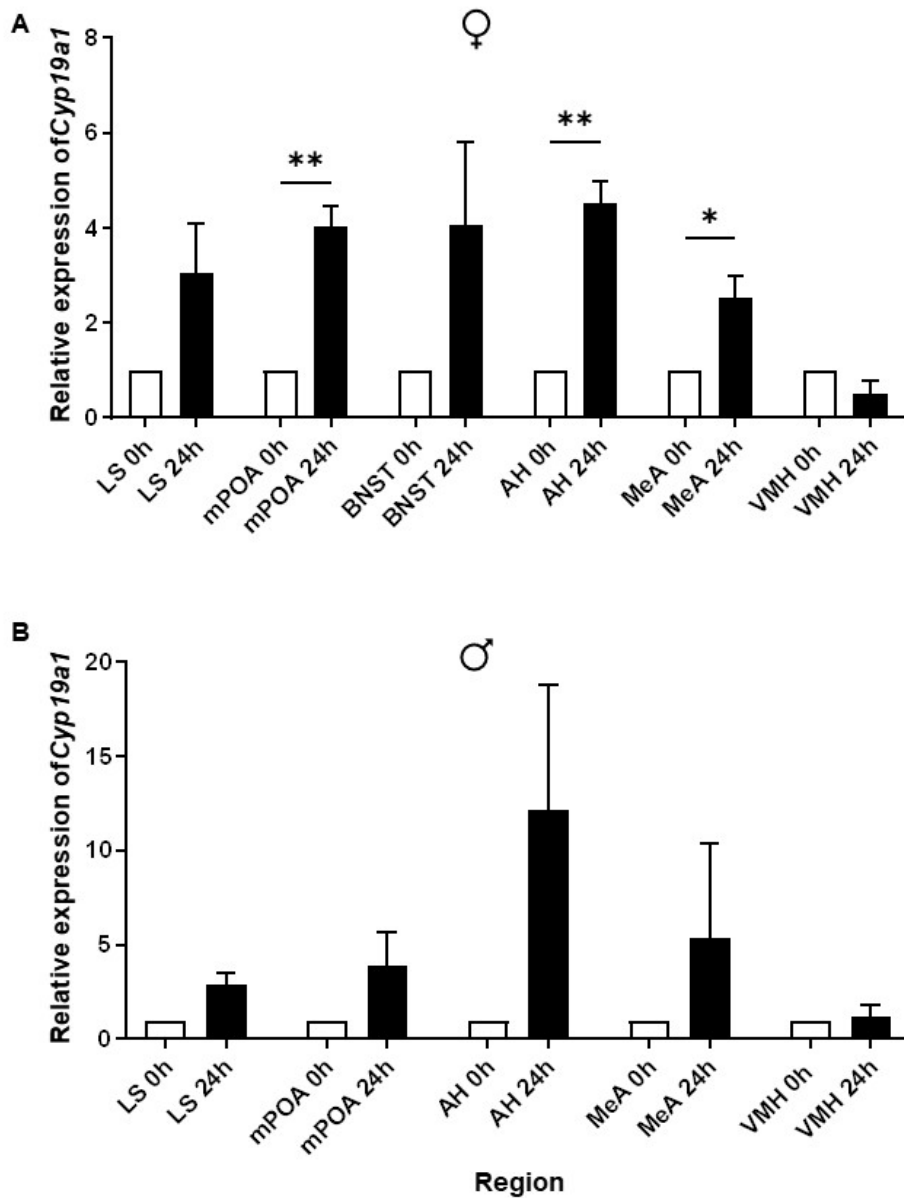


Figure 3.9. Expression of *Cyp19a1* in adult male and female SBN nuclei at 0 h and 24 h slice incubation timepoints, measured by RT-qPCR. Following incubation of slices for 0 h or 24 h, six different SBN nuclei were punch dissected, and nuclei from 4 animals were pooled into one, such that $n = 3$ from a total of 12 animals. Following RNA extraction, cDNA was synthesised and used for RT-qPCR analysis. Expression levels, relative to the housekeeping gene (*Actb*), are shown for *Cyp19a1* in female (**A**) and male (**B**) mice. Differences were established by a two-way ANOVA comparing time, region, and the interaction between time and region. Parametric datasets for 0 h vs 24 h were compared by an unpaired t -test; nonparametric datasets for 0 h vs 24 h were compared by a Mann-Whitney test. * $P < 0.05$ vs 0 h, ** $P < 0.01$ vs 0 h.

3.4 Discussion

In the present study, we used a novel method to measure steroid production by *ex vivo* hypothalamic brain slices from male and female mice. We punch-dissected specific nodes of the hypothalamus and SBN and found substantial sex differences in steroid production and expression of steroidogenic enzymes. In support of previous literature, the male brain was much more active in synthesising steroid hormones, as shown by higher levels of enzyme expression and greater concentrations of oestrogen and testosterone within the brain areas investigated (Stanic et al., 2014, Hojo and Kawato, 2018, Roselli et al., 1984, Wu et al., 2009, Tabatadze et al., 2014b).

We investigated the synthesis of neurosteroids in male and female slices of the SBN using a modified method outlined in Loryan et al. (2013), followed by a sensitive in-house assay for neurosteroids. This modified brain slice incubation model allows for the determination of neurosteroid concentration, not only in brain tissue, but also from the aCSF that served as the incubation media. It has been shown previously that, under optimal conditions that encapsulate the control of temperature, pH, bacterial growth and bacterial-induced glial nitric oxide production, acute brain slices can stay viable in aCSF for up to 36 h (Buskila et al., 2014). In a series of optimization studies, we found that the volume of aCSF used initially during brain slice recovery has a high impact on viability and neurosteroid output. Using our system where we oxygenated 200 μm brain slices in 5 ml aCSF, we demonstrate that not only are hypothalamic brain slices viable up to 48 h, but they are also functional with secretion of steroids.

3.4.1 Timeline of neurosteroid production in the SBN

We have utilised an incubation system to show that steroid hormones can be measured from brain slices *ex vivo* after 24 h in culture. Moreover, steroid hormone concentration increased over time in the absence of endocrine glands and peripheral steroid precursors. Steroid hormones are lipophilic and therefore cannot be stored in vesicles from which they would easily diffuse (Holst et al., 2004); this eliminates the possibility that the steroids measured were simply those that had originated from the periphery and were stored in the brain, thereby indicating true *de novo* synthesis. In male hypothalamic slices, both E_2 and testosterone had increased by 24 h incubation but in female hypothalamic slices, testosterone concentration increased significantly after 2 h incubation. 3β -HSD catalyses the biosynthesis of both progesterone from pregnenolone, and androstenedione from DHEA (Schlinger et al., 2008). The synthesis of both steroids is required for testosterone production, catalysed by 17β -HSD (Labrie et al., 1997). In zebra finches, the baseline activity of 3β -HSD is higher in females than

males (Soma et al., 2004). This could explain, at least in part, our observation of a much earlier increase in testosterone in female hypothalamic slices compared to males. Despite an early increase in testosterone, E₂ concentration in female hypothalamic slices did not significantly increase until 8 h incubation, which could be due to the time required to synthesise *de novo* aromatisable precursors, which exist in much lower concentrations in the female brain and plasma (Konkle and McCarthy, 2011a, Caruso et al., 2013). This delayed increase in E₂ was observed in a similar slice culture method using male rat brain, where application of tritiated (³H-) DHEA to slice culture medium resulted in the production of ³H-E₂ after 5 h (Hojo et al., 2004b, Hojo et al., 2004a). DHEA is an intermediate product between pregnenolone and testosterone. Therefore, it makes sense that in a slice without exogenously applied steroid precursors, concentrations of E₂ and testosterone (further down the steroidogenic pathway) increase significantly after 8 h, because they may be being synthesised *de novo* from cholesterol. Additionally, the sex differences in dynamics of steroid hormone production by brain slices could be due to differences in steroid hormone metabolism. For example, testosterone is metabolised by the 5 α -reductase enzymes, which are expressed at much higher levels in the male brain (Giatti et al., 2019)

3.4.2 Sexual dimorphism in neurosteroid concentrations in the SBN

We found profound sex differences in E₂ and testosterone concentrations across the SBN. Both E₂ and testosterone measured from incubation aCSF were significantly higher in males compared to females at both 0 h and 24 h, and there was a significant increase over time within the same sex (**Fig. 3.2**). This highlights not only that the slices continued to synthesise steroids over time in incubation, but also that the basal levels of steroids and the capacity to produce and secrete them over time is significantly greater in male mouse hypothalamic slices. Using an EGFP transgene that is transcribed following the physiological activation of the aromatase gene in male and female mice, it was shown that there are significantly more aromatase-positive fibres in the male BNST, posterodorsal and posteroventral medial amygdaloid nucleus, AH and mPOA of male mice (Stanic et al., 2014). This would provide more avenues for steroid secretion; a possible reason for our observation of higher steroids in aCSF incubating male slices.

In the hippocampus, which is steroidogenically active (Hojo et al., 2004b) and responsive to neurosteroids (Kretz et al., 2004a), sophisticated LC-MS techniques revealed that the levels of basal testosterone and E₂ were higher in male than in female rats at any stage of the oestrous cycle (Hojo and Kawato, 2018), consistent

with the data that we see at the 0 h timepoint. However, another study showed higher levels of testosterone in male hippocampus, cerebral cortex and cerebellum than in females but higher levels of E₂ in these areas in females than in male rats (Caruso et al., 2013). This opposing sex dimorphism may highlight regional and/or species differences to our data or could be due to methodological differences. Consistent with previous reports, we observed much higher concentrations of neurosteroids (E₂ and testosterone) compared to concentrations of steroids measured in plasma (Charlier et al., 2010b, Nilsson et al., 2015, Caruso et al., 2013, Hojo et al., 2009, Charlier et al., 2010a).

Few studies have made similar sex comparisons in the rodent SBN, but in a study comparing neurosteroid levels in male and female rats following acute swim stress, there was no significant difference in hypothalamic levels of corticosterone, deoxycorticosterone, dihydrodeoxycorticosterone, pregnenolone, or progesterone in non-stressed subjects (Sze et al., 2018). E₂ was not measured, and testosterone could not be measured because concentrations in the female rat brain fell below the lower limit of quantification in all brain regions examined (Sze et al., 2018). Following swim stress testing, hypothalamic pregnenolone and progesterone increased to a significantly greater level in stressed female rats compared to stressed males (Sze et al., 2018), though this only highlights context-dependent changes in neurosteroids and not constitutive levels or typical synthesis rates in a non-stressed state.

When SBN regions were analysed separately, we found regional differences in steroid production in the male and female mouse brain (**Fig. 3.3**). E₂ production increased significantly between 0 h and 24 h in both male and female hypothalamic slices corresponding to the LS/mPOA, AH/meA, and meA/VMH, and male slices corresponding to the mPOA/BNST. Testosterone production increased significantly in all slice regions of both male and female mice between 0 h and 24 h. In steroid extractions from punch dissections, the male SBN showed a significant increase in testosterone in both the mPOA and VMH and a significant increase in E₂ across the whole SBN except the VMH, though there was a trend for increase. The female SBN showed a significant increase in E₂ in AH and VMH punches, and a significant increase in testosterone in mPOA punches. Taken together, this suggests that some mouse SBN nuclei synthesise their own neurosteroids. Typically, neurooestrogen synthesis in the rodent is analysed by means of aromatase activity, which can be measured indirectly through the production of ³H₂O in brain homogenates incubated with [1β-³H] androstenedione (Roselli et al., 1984). Hypothalamic preoptic area homogenates from male rats showed higher aromatase activity than homogenates of female rats,

regardless of oestrous stage (Roselli et al., 1984). The same method has also shown that aromatase activity is greater in the male VMH, BNST, and meA (Roselli et al., 1985a) consistent with our observations of greater levels of E₂ in these very same areas of the male mouse brain compared to females. To our knowledge, there are no detailed reports of neurosteroid concentrations in the intact, non-hormone-primed female rodent SBN available to compare with our data.

Neurosteroid concentrations have been investigated more thoroughly in the bird SBN and NCM: a node outside the SBN but responsive to steroid hormones and significant in the expression of complex and sexually dimorphic avian behaviour (Vahaba and Remage-Healey, 2018). Palkovits punch and C18 steroid extraction from behaviourally significant brain areas of sexually naïve male zebra finches also revealed regional differences in E₂ concentration (Charlier et al., 2010b). The NCM expresses high levels of aromatase (Saldanha et al., 2000), and unsurprisingly displayed the highest levels of E₂, though this was not significantly different to the levels observed in the mPOA (Charlier et al., 2010b). In male breeding song sparrows, E₂ concentrations in microdissected mPOA and AH did not differ from levels in the NCM, and whilst E₂ was significantly lower in the VMH compared to the NCM and AH, it did not differ from levels observed in the mPOA (Jalabert et al., 2022). Despite the species difference, there is similarity in the regional steroidogenic activity in the SBN, at least in the male mouse where all regions of the SBN studied displayed higher levels of E₂ at 24 h.

Sex dimorphism is most easily visible when comparing secreted neurosteroids in the aCSF rather than punches of a SBN area, possibly due to methodological constraints of extraction or because of synthesis from overlapping brain regions in the slice. One caveat when comparing data, however, are the methodological differences and the units in which concentrations are measured. Studies measuring neurosteroids by LC-MS/MS or GC-MS/MS may present data as pg/mg protein (Charlier et al., 2010b, Caruso et al., 2013, Hojo et al., 2004a). Other studies have expressed neurosteroid concentrations in nM values (Kato et al., 2013). Our steroid concentrations were presented as pg/ml, given the liquid phase of incubation (aCSF) and pg/mm³ tissue, given the technical difficulty of accurately weighing 'wet' mouse brain punches. This further highlights the importance of having such comparisons between regions and sex carried out in one study.

3.4.3 Sexual dimorphism in the steroidogenic pathway in the SBN

Most studies investigate aromatase localisation and regulation as the main end enzyme that generates E₂, possibly from circulating testosterone in males. However,

some studies have shown that other steroidogenic enzymes are present in the brain. In the male rat hippocampus, the presence of 5 α -reductase, StAR, P450_{scc}, 3 β -HSD, 17 β -HSD, P450(17 α) and aromatase proteins have been localised using immunohistochemistry to the dentate gyrus granule cells and to hippocampal neurons in the CA1-CA3 (Mellon and Deschepper, 1993, Furukawa et al., 2002, Agís-Balboa et al., 2006, Kawato et al., 2002, Shibuya et al., 2003). Consistent with this, our data shows the presence of several steroidogenic enzymes, ranging from Cyp11a1 to Cyp19a1 in both male and female mouse hypothalami. Comparison to the ovary shows that the female hypothalamus possesses lower levels of *Hsd3b1*, *Hsd17b1*, *Stard1*, and *Cyp11a1* but similar levels of *Cyp19a1* as the ovary (**Supp. Fig. S3.3**). In addition, levels of mRNA of steroidogenic enzymes in the male at baseline (0 h) are higher than in the female for all steroidogenic enzymes except *Hsd17b1*, suggesting that this might be a reason for higher steroidogenic capacity in the male brain. Transcriptomics data from the whole hypothalamus also shows that P450_{scc} and 3 β -HSD steroidogenic enzymes are lower in the female than the male, consistent with our data (Nishida et al., 2005).

Though our data suggests that none of the steroidogenic enzymes measured in the whole hypothalamus show differences in mRNA level from the 0 h to the 24 h timepoint in either sex, sexual dimorphism is evident when individual SBN nuclei are investigated. There is both node-specific and enzyme-specific regulation in females. For example, *Stard1* mRNA increases within 24 h in the AH, BNST, and meA, though such increases are not seen in the male. The AH and BNST also show increases of *Cyp11a1* and *Hsd17b1* mRNA at 24 h in the female but not in the male. This is in contrast to the hippocampus where there appears to be no differences in *Stard1*, *Hsd17b1* and *Cyp19a1* expression between males and females (Kato et al., 2013). In hippocampal dissociated cultures derived from mixed male and female pups, provision of cholesterol increases the amount of E₂ produced, to a much larger extent than the provision of testosterone; this could be decreased with letrozole and by the knockdown of *Stard1* with siRNA. These suggest that hippocampal cultures can synthesise E₂ *de novo* from cholesterol and this is not sex-specific (Fester et al., 2009), in parallel with the lack of sexual dimorphism in steroidogenic enzymes. Similarly, in the cerebral cortex of the rat, there were no sex differences in the expression of several steroidogenic enzymes though *Stard1* mRNA was higher in the female cerebellum than in the male rat cerebellum (Giatti et al., 2019). Consistent with these studies, our study also shows region and sex-specific levels of expression of steroidogenic enzymes.

In addition, there is very low expression of mRNA for the enzymes *Cyp11a1* and *Hsd3b1* when compared to the ovary and intermediate level of *Cyp19a1* expression in adult male rat hippocampus (Hojo et al., 2004b). This is not true for the hypothalamus where expression levels of *Cyp11a1*, *Stard1*, *Hsd3b1* and *Hsd17b1* are equivalent to the ovary in the male hypothalamus; this may be due to differences in methodology used in the previous study compared to ours, or differences between mouse and rat.

We found a regional difference in *Cyp19a1* expression in the female mouse mPOA over 24 h incubation times, though there was a tendency for increase in the AH ($P = 0.0818$) and meA ($P = 0.1$). It is interesting to note that, in steroids measured in the aCSF, E_2 increased significantly between 0 h and 24 h in slices corresponding to the LS/mPOA, AH/meA, and meA/VMH. Regional differences were not observed in the male SBN, though there was a tendency for increase in the LS ($P = 0.0977$). This indicates that aromatase expression increases over time in incubation, though the mechanism underlying this is unclear. High levels of *Cyp19a1* expression have also been found in the meA, BNST, and mPOA (Tabatadze et al., 2014a) consistent with our data. Aromatase mRNA (Tabatadze et al., 2014a) and protein (Stanic et al., 2014) have been identified at high levels in the BNST and meA, expressed in cell bodies and fibres (Wu et al., 2009). These studies have also shown a clear sex dimorphism in aromatase expression within these areas, where males typically express more aromatase mRNA and protein than females (Tabatadze et al., 2014a, Stanic et al., 2014, Roselli et al., 1998), consistent with our data.

In male and female mice that express EGFP under the physiological activation of *Cyp19a1* (Stanic et al., 2014), low densities of EGFP-positive cell bodies were found in the AH (male > female), ARC (male = female), and mPOA (male > female). EGFP-positive cell bodies were not detected at all in the VMH of male or female mice (Stanic et al., 2014). Protein expression levels do not always correlate with mRNA expression levels, and aromatase activity is known to be post-translationally modified by phosphorylation and dephosphorylation (Hayashi and Harada, 2014). *Cyp19a1* mRNA has been found in the rodent VMH, but it is worth noting that this was in male rats that had been treated with testosterone propionate for 1 week before sacrifice (Roselli and Klosterman, 1998a).

Notably, most previous studies have been performed in males due to the complications inherent in cycling females. One caveat is that we used very young mice with most females in diestrous since it was difficult to source the required number of females in each phase of the cycle for such analyses. This was especially difficult when RNA

amounts obtained from each SBN nucleus of individual animals is very low, meaning that we need to pool several animals together to obtain enough RNA for accurate analyses. However, mRNA levels of steroidogenic enzymes in the hippocampus do not change depending on the oestrous cycle phase, though the neuroestrogen levels show a peak in proestrous and a nadir at diestrous in the female (Kato et al., 2013). Similarly, the increase in neurotestosterone and neuroestrogen levels in SBN nuclei at 24 h in our study is not paralleled by an increase in the expression of steroidogenic enzymes. However, protein was not measured in these studies or ours and it is possible that activity levels are modulated independent of mRNA levels during this period.

3.5 Summary

This study is the first of its kind to measure steroid levels within nuclei of the mouse SBN and make direct comparisons in steroid synthesis and enzyme expression between age-matched, intact, and non-hormone-primed male and female subjects. We show that all SBN nuclei can show increased secretion of both E₂ and testosterone within 24 h, suggesting *de novo* synthesis. This is similar in both males and females (with the exception of slices that comprise the mPOA and BNST in the female) with levels of steroid secreted higher in males than in females for every SBN nucleus tested. In the hippocampus, increase in the concentration of E₂, DHT and DHEA by addition of radiolabeled pregnenolone to hippocampal neurons, upon NMDA stimulation, suggests *de novo* steroidogenesis takes place specifically in neurons (Hojo et al., 2004b). The role of neurosteroids has been explored using both pharmacological and genetic manipulations, typically in the hippocampus. Aromatase inhibitor treatment to female rat hippocampal slice culture decreases synapse density, spine density and long term potentiation (LTP) (Kretz et al., 2004b, Prange-Kiel and Rune, 2006). *In vivo*, central administration of an aromatase inhibitor decreased spatial memory in mice (Zhao et al., 2018) and the songbird (Bailey et al., 2013) and also decreased consolidation of novel object recognition memories in mice (Tuscher et al., 2016). Supporting this, conditional forebrain ArKO male and OVX female mice showed reduced LTP, spine density, novel object recognition memory, and spatial memories (Lu et al., 2019). Our study provides a foundation to explore the physiological relevance of neuroestrogen synthesized in SBN nuclei to social behaviours in the mouse.

3.6 Supplementary information

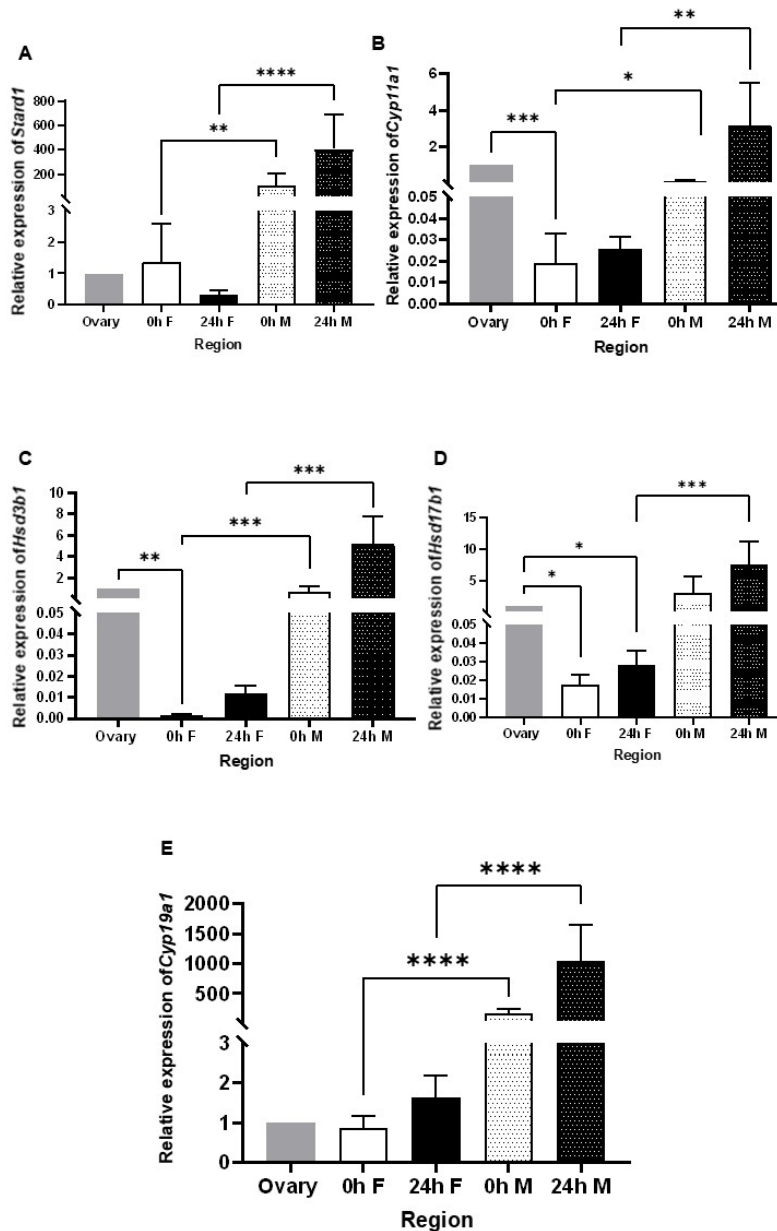
3.6.1 *E₂* ELISA

Concentrations of *E₂* were determined by an in-house competitive ELISA using goat anti-oestradiol-17 β antiserum (510/6) kindly provided by Dr G. S. Pope (National Institute for Research in Dairying, Shinfield, Berkshire, UK). Briefly, 96-well plates (Nunc Maxisorb; Fisher Scientific) were coated overnight with 100 μ l antiserum diluted 1/10,000 in 0.05 M sodium hydrogen carbonate solution, washed 3x with wash buffer (PBS with 0.1% (v/v) Tween-20), blocked overnight with 250 μ l assay diluent (PBS containing 0.1% (w/v) gelatin and 0.05% (v/v) Proclin-2000), and stored for <5 days at 4°C. Standards (1.5 pg/ml to 10 ng/ml; serial 3-fold dilutions) were diluted in assay diluent and 50 μ l added to wells together with 10 μ l sample medium blank and 50 μ l horseradish peroxidase (HP)-labeled oestradiol-6-CMO (1:5000; Fitzgerald Industries, USA). Samples (10 μ l) were added to wells with 50 μ l assay diluent and 50 μ l HP-labelled oestradiol tracer. Plates were mixed and incubated for 3 h at room temperature before washing 3x and adding 200 μ l substrate solution (prepared by dissolving 10 mg o-phenylenediamine in 25 ml 0.05 M citrate-phosphate buffer, pH 5.0, and adding 10 μ l H₂O₂). After incubating in the dark for ~1 h, absorbance values at 450 nm (600 nm reference) were read using a microwell plate reader (Emax, Molecular Devices, UK). Calibration curve fitting and calculation of 'unknowns' was carried out using the PC-based Softmax program (Molecular Devices) linked to the plate reader. The assay detection limit was ~10 pg/ml and mean intra- and inter-assay CVs were <9% and <12% respectively. The specificity of the assay was confirmed by determining the percentage cross-reactivity relative to the oestradiol standard (100%) of a range of steroids including pregnenolone (0.69%), progesterone (0.06%), dehydroepiandrosterone (0.13%), testosterone (0.10%), androstenedione (<0.05%), dihydrotestosterone (0.21%), oestrone (7.5%), deoxycorticosterone (<0.18%), cortisol (<0.05%), corticosterone (<0.05%) and aldosterone (0.11%).

3.6.2 *Testosterone* ELISA

Concentrations of testosterone were determined by an in-house competitive ELISA developed using S505 sheep anti-testosterone serum (National Institute for Research in Dairying, Shinfield, Berkshire, UK) used at a coating dilution of 1:30,000 dilution. The tracer was testosterone-6-CMO-HP (Fitzgerald Industries) used at a 1:6000 dilution. Testosterone standards prepared by 3-fold serial dilutions ranged from 1.5 pg/ml to 10 ng/ml (50 μ l/well). Other features of the assay methodology were essentially the same as those described above for the *E₂* ELISA. The assay detection

limit was ~15 pg/ml and mean intra- and inter-assay CVs were <10% and <15% respectively. The specificity of the assay was confirmed by determining the percentage cross-reactivity relative to the testosterone standard (100%) of a range of steroids including pregnenolone (0.02%), progesterone (<0.01%), dehydroepiandrosterone (0.05%), androstenedione (1.32%), dihydrotestosterone (6.25%), oestradiol-17 β (0.61%), oestrone (0.04%), deoxycorticosterone (<0.18%), cortisol (<0.01%), corticosterone (<0.01%) and aldosterone (<0.01%).



Supplementary Figure S3.1. Comparison of steroidogenic enzyme levels in adult male and female pooled SBN nuclei at 0 h and 24 h slice incubation timepoints, compared to ovary, measured by RT-qPCR. Following incubation, SBN nuclei were punch dissected, and nuclei from 4 animals were pooled into one, such that $n = 3$ from a total of 12 animals for female, and $n = 2$ from a total of 6 animals for male. Following RNA extraction, cDNA was synthesised and used in an RT-qPCR analysis. In this analysis, all SBN nuclei for each particular timepoint from male and female mice were pooled together. Relative expression to the housekeeping gene, *Actb*, is shown for *Stard1* (A) *Cyp11a1*, encoding cytochrome P450 side-chain cleavage enzyme (B) *Hsd3b1* (C), *Hsd17b1* (D), and *Cyp19a1* (E), as compared to ovary. Differences were established by a non-parametric one-way ANOVA between groups with Dunn's multiple comparisons *post hoc*, * $P < 0.05$, ** $P < 0.01$, *** $P < 0.001$, **** $P < 0.0001$.

Chapter 4

Regulation of Neurosteroid Production by Ex Vivo Hypothalamic Brain Slices from the Adult Female Mouse

4.1 Introduction

It is now widely recognised that the vertebrate brain expresses the steroidogenic enzymes required for *de novo* production of 17β -oestradiol (E_2) (King et al., 2002, Mellon and Deschepper, 1993, Kohchi et al., 1998, Soma et al., 2004, Takase et al., 2002, Strömstedt and Waterman, 1995, Gottfried-Blackmore et al., 2008). The nuclear oestrogen receptors (ERs) α and β are abundantly expressed in the brain, particularly the hypothalamus, hippocampus, and amygdala (Mitra et al., 2003, Merchenthaler et al., 2004, Zhang et al., 2002, Moëne et al., 2019), giving rise to several organisational and activational effects that are both region-dependent and sexually dimorphic in nature (McCarthy et al., 2009).

Neuroestrogens – i.e., oestrogens produced from cholesterol *de novo* in the brain or those synthesised centrally from haematogenous precursors – have several important functions in the brain that may be independent of E_2 from the periphery (Giatti et al., 2019). Neuroestrogen synthesised in the hippocampus has been implicated in hippocampal spine formation and plasticity (Kretz et al., 2004a, Murakami et al., 2018). In the hypothalamus, neuroestrogen contributes to the regulation of the hypothalamic-pituitary-gonadal axis by stimulating gonadotropin-releasing hormone (GnRH) release (Kenealy et al., 2013), in turn leading to the surge in luteinising hormone (Kenealy et al., 2017). Neuroestrogen induces GABAergic transmission in the ventromedial hypothalamus (VMH) to activate a protein kinase-mediated response to hypoglycaemia (Uddin et al., 2020). E_2 can modulate membrane excitability in the male songbird brain (Ramage-Healey et al., 2011) and can potentiate the excitation of neurones in the rat ventrolateral VMH within 5 min (Kow et al., 2006). These rapid actions indicate that neurosteroids can function as neurotransmitters, binding to membrane-bound receptors at the synapse to stimulate second messengers, bypassing the lengthy process of gene transcription associated with classical nuclear ER signalling. Together, these neuroestrogen-driven mechanisms give rise to sexually dimorphic behaviours, including reproduction (Cornil et al., 2013), aggression (Trainor et al., 2008b), and learning and memory (Sheppard et al., 2018). For example, brain aromatase in the male mouse is essential for the complete expression of male sexual behaviour (Brooks et al., 2020b), whereas intracerebroventricular E_2 restores the expression of lordosis in ovariectomised (OVX) mice (Domínguez-Ordóñez et al., 2019). ER α -expressing neurones in the ventrolateral VMH regulate territorial aggression in male mice (Yang et al., 2013) and maternal aggression in female mice (Hashikawa et al., 2017). Female rats and mice have a greater abundance of synaptic ER α in the hippocampus and a

greater threshold for the induction of long-term potentiation compared to males, which contributes to sex differences in encoding specific types of memories (Wang et al., 2018). This shows that both ligand and receptor may be differentially produced or expressed between sexes.

Brain aromatase and neuroestrogen have predominantly been studied in male vertebrates (Cornil, 2018), whereas the female behavioural phenotype is typically thought to arise from fluctuations in ovarian E_2 (Schlinger et al., 2014, Gerall et al., 1973) which confound the importance of neuroestrogens. However, there is substantial evidence that brain aromatase is expressed and active in the female vertebrate brain, though typically at much lower levels than in males (Saldanha et al., 2000, Wu et al., 2009, Stanic et al., 2014). We have shown a sex dimorphism in the capacity to synthesise neuroestrogen (Chapter 3), which could be attributed to the higher levels of circulating androgens (Caruso et al., 2013, Sonnweber et al., 2022) in conjunction with the aforementioned higher aromatase activity in the male mouse. Despite low circulating androgens in the female, the high affinity of aromatase allows it to bind testosterone effectively (Konkle and Balthazart, 2011). Local production of neuroestrogen may be important for elevating regional E_2 to sufficient concentrations to activate neural circuits either independently or in the presence of ovarian E_2 (Schlinger et al., 2014).

Regulation of aromatase – and consequently, neuroestrogen production – involves complex interactions between sexually dimorphic mechanisms, including photoperiod (Trainor et al., 2008b), neural activity (Charlier et al., 2013), and behavioural stimuli (Ramage-Healey et al., 2008). Moreover, evidence suggests that gonadal hormones may further influence aromatase expression and activity in both males and females, adding another layer of complexity to the regulation of aromatase and neuroestrogen production. In male rats, aromatase expression in the medial preoptic area (mPOA), bed nucleus of stria terminalis (BNST), and the medial amygdala (meA) is increased following administration of testosterone propionate via a subcutaneous silastic capsule for 1 week (Roselli et al., 1998). Castration was found to reduce aromatase activity to a level similar to that observed in intact female rats (Roselli et al., 1985b) while testosterone delivery could restore hypothalamic aromatase activity, making them no different to intact controls (Roselli et al., 1985b). However, aromatase activity does not appear to be under the influence of gonadal hormones in the meA of the male rat, as there is no difference in activity between intact males, castrated males, and castrated males treated with testosterone, dihydrotestosterone (DHT), or E_2 (Abdelgadir et al.,

1994, Roselli et al., 1985b). In primary amygdala neuronal cultures from female mouse embryos, aromatase expression is significantly increased by both E₂ and the non-aromatisable androgen DHT (Cisternas et al., 2017). In oestrogen response element (ERE)-Luciferase reporter mice, OVX did not alter ERE-dependent gene transcription across brain regions in the short-term (10 days) but decreased transcription in the long-term (70 days), suggesting a dependence of neuroestrogen on gonadal hormones (Baumgartner et al., 2019). *In vitro*, E₂ shows a biphasic effect on aromatase expression that depends on the duration of E₂ exposure with a decrease at 12 h and an induction in 24 h (Yilmaz et al., 2009) that is dependent on ER α in the N42 hypothalamic cell line (Yilmaz et al., 2009). These studies show that neuroestrogen production is itself E₂- and/or androgen-dependent in a nuclei and sex-specific manner.

Despite these studies, the regulation of aromatase and neuroestrogen production in the female mouse brain has been underexplored, particularly in specific brain regions and nuclei. The mPOA and VMH are critical for female reproductive behaviour (Micevych and Christensen, 2012), express aromatase (Stanic et al., 2014, Roselli et al., 1998), and express ERs (Dovey and Vasudevan, 2020). The mPOA expresses both ER α and ER β (Merchenthaler et al., 2004), whereas ER α is the predominant ER isoform in the VMH (Correa et al., 2015). In previous work, we demonstrated a novel slice incubation method that confirmed the continued production of neurosteroids by the brain *ex vivo* (Chapter 3). In this study, we build on this method to investigate the regulation of aromatase expression and neuroestrogen production in the female mouse mPOA and VMH, revealing a region-specific androgen-driven pathway of regulation in the female mouse hypothalamus.

4.2 Methods

4.2.1 Animals

Animals were housed as described in section 2.1. All mice were housed at the University of Reading apart from the mice that were used in OVX experiments, which were housed at the University of Tsukuba. In OVX experiments, surgical procedures were carried out as in section 2.1.1 and mice were hormonally primed as described in section 2.2.2, with the omission of progesterone injection.

4.2.2 Preparation of ex vivo brain slices

Ex vivo brain slices were prepared as described in section 2.7. Slice viability using this method has been confirmed previously (Chapter 3).

4.2.3 Drug treatments

Enzyme inhibitors, hormones, ER modulators, and their corresponding vehicles were added to aCSF prior to filtering. Over a series of experiments, brain slices were incubated in aCSF containing 10^{-8} M letrozole (DMSO vehicle, final DMSO concentration 0.01%), 10^{-9} M testosterone (ethanol vehicle, final ethanol concentration 0.0001%), 10^{-8} M dutasteride (DMSO vehicle, final DMSO concentration 0.01%), 10^{-8} M finasteride (DMSO vehicle, final DMSO concentration 0.01%), 10^{-8} M 5α -androstane- 3β , 17β -diol (3β -diol) (DMSO vehicle, final DMSO concentration 0.01%), 10^{-9} M propyl pyrazole triol (PPT; DMSO vehicle, final DMSO concentration 0.01%), 10^{-9} M diarylpropionitrile (DPN, DMSO vehicle, final DMSO concentration 0.01%), 10^{-8} M ICI 182,780 (DMSO vehicle, final DMSO concentration 0.01%). Slices from each animal were counterbalanced between treatments to account for biological and slice-dependent variability.

These concentrations were chosen based on previous literature (Phan et al., 2015, Smejkalova and Woolley, 2010, Kretz et al., 2004a) and levels of crossreactivity with ELISAs (section 2.11).

4.2.4 Palkovits punch technique for extraction of steroids and RT-qPCR

Palkovits punch and RT-qPCR was performed as described in sections 2.9 and 2.12.

4.2.5 Hormone immunoassays

ELISAs for E_2 and T were carried out as described in section 2.11. Steroid hormones were measured in either aCSF or steroid eluates from brain punches (procedure detailed in section 2.10). It should be noted that hormones measured from aCSF may not be a direct reflection of the neurosteroidogenic capacity of the brain regions of interest alone, as each slice contains several other brain regions that have the capability to produce neurosteroids. Please see section 2.8 and **Fig. 2.5**.

4.2.6 Statistical analysis

Statistical analysis and presentation of results is as described in section 2.15.

4.3 Results

4.3.1 *E₂ production is not increased by providing an androgenic substrate nor decreased by the aromatase inhibitor letrozole in the female mouse mPOA and VMH*

Female mouse brain slices containing the mPOA and VMH were incubated in aCSF containing 10^{-9} M testosterone, 10^{-8} M letrozole, or vehicle control. **Fig. 4.1** and **4.2** show the resulting concentrations of E_2 and testosterone measured from the aCSF (panels **A-B**) or within punch dissections of each region (panels **C-D**) at 0 h and after 24 h incubation. There was a significant effect of time on the concentration of E_2 measured in aCSF bathing mPOA-containing slices (mPOA-aCSF) (**Fig. 4.1A**, $P < 0.0001$) and VMH-aCSF (**Fig. 4.1B**, $P = 0.0049$), similar to what we have observed previously (Chapter 3). However, there was no significant effect of treatment (mPOA-aCSF, $P = 0.3349$; VMH-aCSF, $P = 0.8040$) or the interaction between treatment and time (mPOA-aCSF, $P = 0.2608$; VMH-aCSF, $P = 0.4753$) on E_2 measured in aCSF (**Fig. 4.1A-B**). Bonferroni's multiple comparisons test between 0 h and 24 h timepoints showed a significant increase in E_2 measured in mPOA-aCSF with vehicle control ($P = 0.0002$) and, unexpectedly, letrozole ($P = 0.0172$) (**Fig. 4.1A**). In VMH-aCSF, E_2 concentration increased only with vehicle control ($P = 0.0431$) (**Fig. 4.1B**). Likewise, treatment had no significant effect on E_2 measured in mPOA and VMH punches (**Fig. 4.1C-D**).

For testosterone measured in aCSF, there was again a significant effect of time (mPOA-aCSF, $P = 0.0010$ [**Fig. 4.2A**] VMH-aCSF, $P = 0.0001$ [**Fig. 4.2B**]), but no significant effect of treatment or the interaction between treatment and time. Letrozole treatment led to a significant increase in testosterone in VMH-aCSF ($P = 0.0142$ [**Fig. 4.2B**]), but not mPOA-aCSF ($P > 0.9999$ [**Fig. 4.2A**]). For both mPOA-aCSF and VMH-aCSF, the concentration of testosterone was less than the concentration of testosterone added, indicating that the steroid had been taken up and/or metabolised by the slice. There was no significant effect of treatment on testosterone concentrations in punch dissections of the mPOA or VMH (**Fig. 4.2C-D**), similar to what was observed for E_2 .

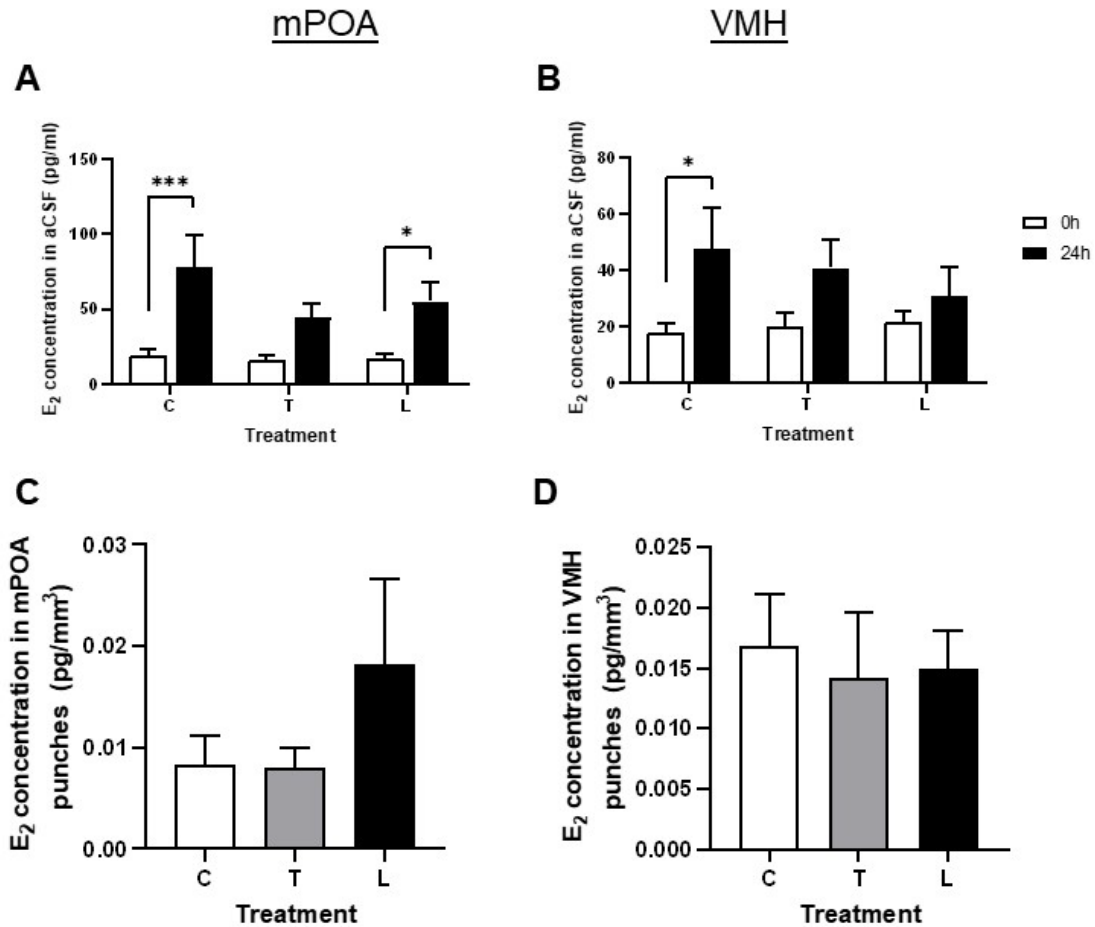


Figure 4.1. Effect of letrozole and testosterone on E₂ concentrations in adult female mouse medial preoptic area and ventromedial hypothalamus. E₂ was measured in aCSF bathing slices containing the medial preoptic area (mPOA, left column) and ventromedial hypothalamus (VMH, right column) at 0 h and 24 h timepoints after treatment with 10⁻⁹M testosterone (T), 10⁻⁸ M letrozole (L) or vehicle control (C). Concentrations of neuroestrogen in aCSF are shown in **A-B**; for mPOA, *n* = 15 slices per treatment group, and for VMH, *n* = 9 slices per treatment group, from a total of 9 animals. Punch dissections of the mPOA and VMH were used to measure neuroestrogen (**C-D**) after 24 h incubation. Punches were pooled across animals and treatment groups such that *n* = 9 pooled punch groups from 9 animals. Differences were established by a two-way ANOVA with Bonferroni's multiple comparisons test *post hoc* (**A-B**) or by a one-way ANOVA with Bonferroni's multiple comparisons test *post hoc* (**C-D**). * *P* < 0.05, *** *P* < 0.001.

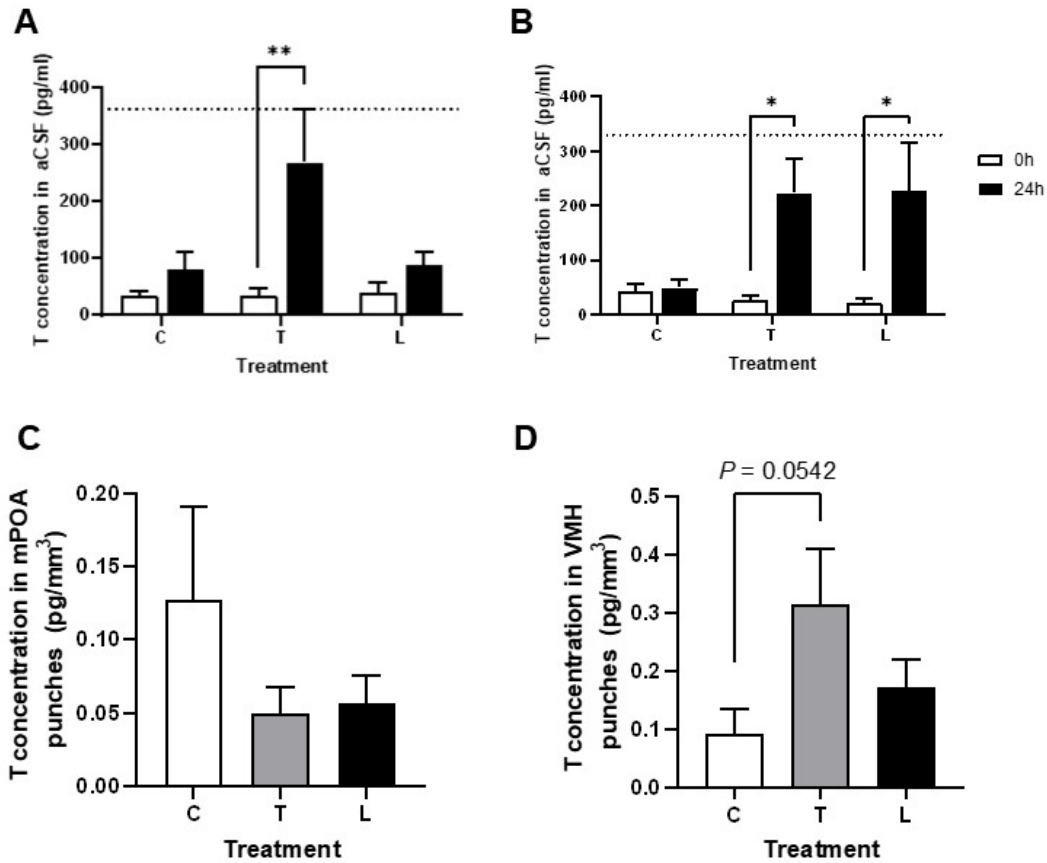


Figure 4.2. Effect of letrozole and testosterone on T concentrations in adult female mouse medial preoptic area and ventromedial hypothalamus. T was measured in aCSF bathing slices containing the medial preoptic area (mPOA, left column) and ventromedial hypothalamus (VMH, right column) at 0 h and 24 h timepoints after treatment with 10^{-9} M testosterone (T), 10^{-8} M letrozole (L) or vehicle control (C). Concentrations of neurotestosterone in aCSF are shown in **A-B**; for mPOA, $n = 15$ slices per treatment group, and for VMH, $n = 9$ slices per treatment group, from a total of 9 animals. Punch dissections of the mPOA and VMH were used to measure neurotestosterone (**C-D**) after 24 h incubation. Punches were pooled across animals and treatment groups such that $n = 9$ pooled punch groups from 9 animals. Differences were established by a two-way ANOVA with Bonferroni's multiple comparisons test *post hoc* (**A-B**) or by a one-way ANOVA with Bonferroni's multiple comparisons test *post hoc* (**C-D**). * $P < 0.05$, ** $P < 0.01$.

4.3.2 Inhibiting DHT production in conjunction with letrozole reduces E₂ production in the adult female mouse mPOA, but not the VMH

Testosterone is aromatised to E₂ via aromatase but can also be converted to the non-aromatisable androgen, DHT, via the 5 α -reductase enzymes, encoded by *Srd5a1-3* (Zhu and Sun, 2005). 5 α -androstane-3 β , 17 β -diol (3 β -diol), a metabolite of DHT, can increase aromatase expression by acting on ER β (Cisternas et al., 2017). To investigate if activation of this pathway was preventing the expected decrease in E₂ with letrozole, we incubated slices with letrozole and the 5 α -reductase inhibitors dutasteride (L + D) and finasteride (L + F) (**Fig. 4.3 - 4.6**).

mPOA: E₂ measured in mPOA-aCSF was significantly reduced when incubated with letrozole and dutasteride compared with all other treatment groups (L + D vs C, $P = 0.0332$; vs L, $P = 0.0306$; vs L + F, $P = 0.024$) (**Fig. 4.3A**). There was no significant difference between incubations with letrozole and vehicle control ($P > 0.9999$) (**Fig. 4.3A**). Testosterone measurements in mPOA-aCSF were significantly less with letrozole treatment compared to vehicle control ($P = 0.0193$) (**Fig. 4.3B**). There was no difference between vehicle control, letrozole + dutasteride, or letrozole + finasteride treatment groups (C vs L + D, $P > 0.9999$; vs L + F, $P = 0.3615$) (**Fig. 4.3B**).

Srd5a1 expression in mPOA punches was significantly increased with letrozole + finasteride treatment compared to vehicle control ($P = 0.0444$) (**Fig. 4.3C**). *Srd5a2* expression tended to increase with letrozole + dutasteride treatment ($P = 0.0616$) and letrozole + finasteride treatment ($P = 0.0845$) compared to vehicle control (**Fig. 4.3D**). Letrozole + finasteride decreased *Srd5a3* expression compared to letrozole treatment ($P = 0.0084$), but expression with letrozole nor letrozole + finasteride was significantly different to vehicle control ($P = 0.7094$ and 0.2675 , respectively) (**Fig. 4.3E**). *Esr1*, encoding ER α , was significantly increased with letrozole + finasteride treatment compared to letrozole alone ($P = 0.0165$), though expression levels with letrozole or letrozole + finasteride treatment were not significantly different to vehicle control ($P = 0.5650$) (**Fig. 4.4A**). Letrozole + finasteride treatment also increased *Esr2* expression (encoding ER β) compared to letrozole ($P = 0.0423$) and letrozole + dutasteride treatments ($P = 0.0165$). However, no treatment changed expression to a level that was significantly different to vehicle control (**Fig. 4.4B**). There was no difference in *Cyp19a1* expression (encoding aromatase) between letrozole and vehicle control ($P > 0.9999$) (**Fig. 4.3C**), reaffirming the notion that letrozole was ineffective in reducing E₂ production in mPOA-aCSF (**Fig. 4.1A** and **4.3A**). Incubation with letrozole + dutasteride and letrozole + finasteride decreased *Cyp19a1* expression compared to

letrozole alone ($P = 0.0423$ and 0.0165 , respectively), though no treatment changed expression levels compared to vehicle control (**Fig. 4.4C**).

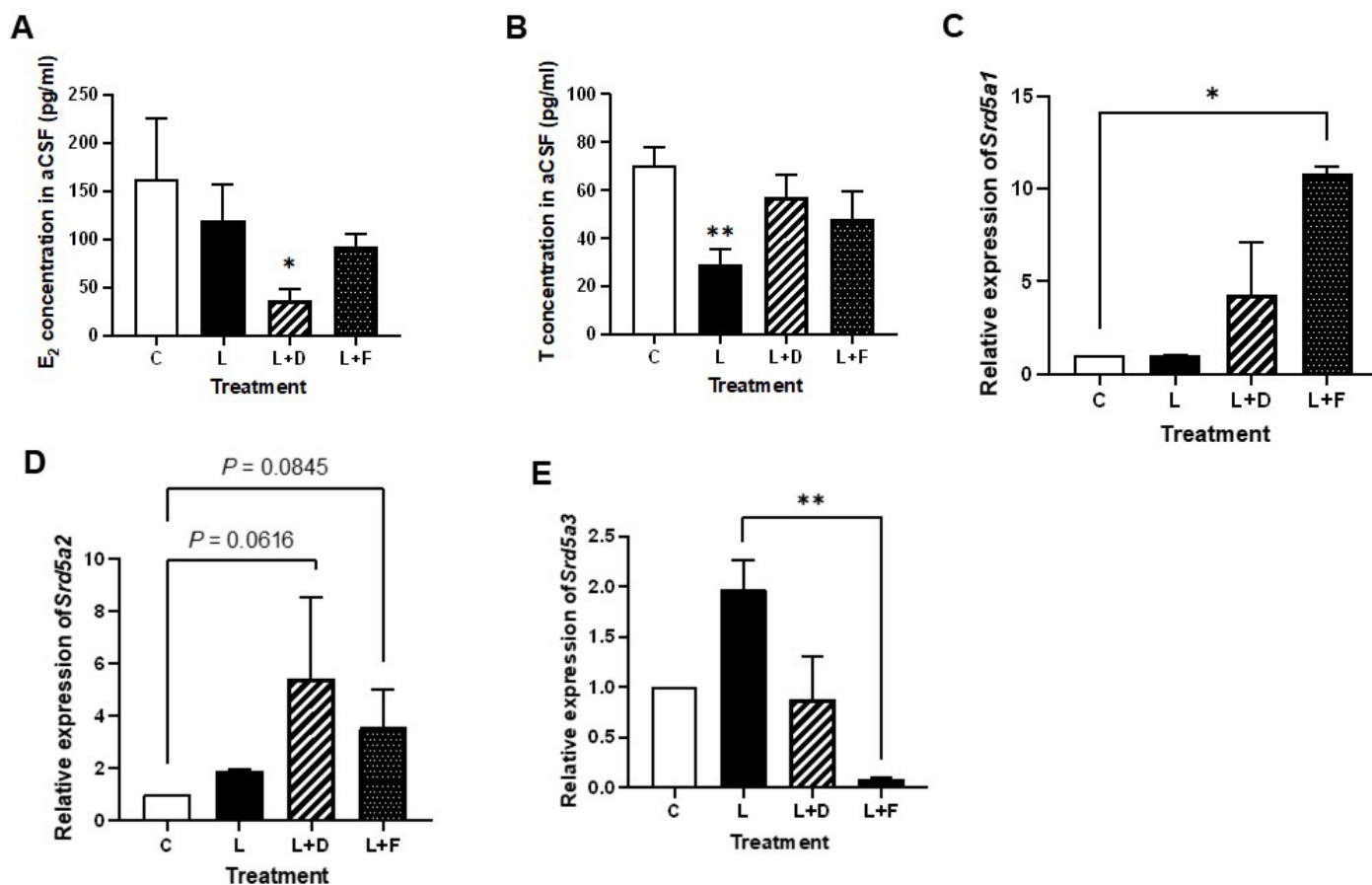


Figure 4.3. Effect of the inhibition of aromatase and 5 α -reductase on steroid hormone concentrations and enzyme expression in the adult female mouse medial preoptic area. Slices were incubated for 24 h with vehicle control (C), 10⁻⁸ M letrozole (L), with and without 10⁻⁸ M dutasteride (L + D) or 10⁻⁸ M finasteride (L + F). aCSF bathing medial preoptic area (mPOA)-containing slices was used to measure neuroestrogen (A) and neurotestosterone (B). *n* = 15 slices per treatment group from a total of 9 animals. Punch dissections of the mPOA from 3 animals were pooled into one, such that *n* = 3 from a total of 12 animals, which were used to measure gene expression. Expression levels, relative to the housekeeping gene (*Actb*) are shown for *Srd5a1* (C), *Srd5a2* (D), *Srd5a3* (E). For parametric datasets, differences were established by a one-way ANOVA with Bonferroni's multiple comparisons *post hoc*; nonparametric datasets were compared by a Kruskal-Wallis test with Dunn's multiple comparisons *post hoc*. * *P* < 0.05, ** *P* < 0.01.

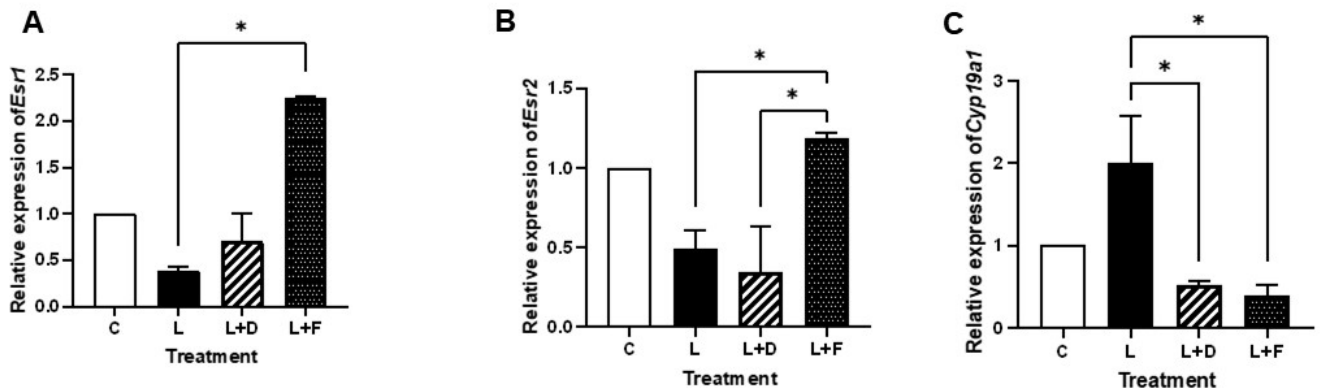


Figure 4.4. Effect of the inhibition of aromatase and 5 α -reductase on aromatase and ER expression in the adult female mouse medial preoptic area. Slices were incubated for 24 h with vehicle control (C), 10⁻⁸ M letrozole (L), with and without 10⁻⁸ M dutasteride (L + D) or 10⁻⁸ M finasteride (L + F). $n = 15$ slices per treatment group from a total of 9 animals. Punch dissections of the mPOA from 3 animals were pooled into one, such that $n = 3$ from a total of 12 animals, which were used to measure gene expression. Expression levels, relative to the housekeeping gene (*Actb*) are shown for *Esr1* (A), *Esr2* (B), *Cyp19a1* (C). For parametric datasets, differences were established by a one-way ANOVA with Bonferroni's multiple comparisons *post hoc*; nonparametric datasets were compared by a Kruskal-Wallis test with Dunn's multiple comparisons *post hoc*. * $P < 0.05$, ** $P < 0.01$.

Expression of other steroidogenic enzymes (*Stard1*, *Cyp11a1*, *Hsd3b1*, *Hsd17b1*) is shown in **Supp. Fig. S4.1**. There was no significant effect of any treatment of the expression of *Cyp11a1* (encoding cytochrome P450 side chain cleavage enzyme) (**Supp. Fig. S4.1B**), *Hsd3b1* (encoding 3 β -HSD) (**Supp. Fig. S4.1C**), or *Hsd17b1* (encoding 17 β -HSD); though *Hsd17b1* expression tended to increase with letrozole + dutasteride compared to letrozole + finasteride treatment ($P = 0.0755$) (**Supp. Fig. S4.1D**). Letrozole + dutasteride treatment significantly increased *Stard1* expression (encoding steroidogenic acute regulatory protein, StAR) compared to letrozole + finasteride ($P = 0.0118$), though neither were significantly different to vehicle control (**Supp. Fig. S4.1A**).

VMH: There was no significant effect of treatment on E₂ (**Fig. 4.5A**) or testosterone concentration (**Fig. 4.5B**) in VMH-aCSF. *Srd5a1* and *Srd5a2* expression

were not significantly affected by treatment (**Fig. 4.5C** and **4.5D**, respectively), though letrozole + dutasteride significantly increased *Srd5a3* expression compared to vehicle control ($P = 0.0334$) (**Fig. 4.5E**). ER mRNA expression in the VMH was not affected by treatment (**Fig. 4.6A-B**); the same was true for *Cyp19a1* (**Fig. 4.6C**), consistent with the lack of significant differences in E₂ concentrations measured in VMH-aCSF (**Fig. 4.2A**).

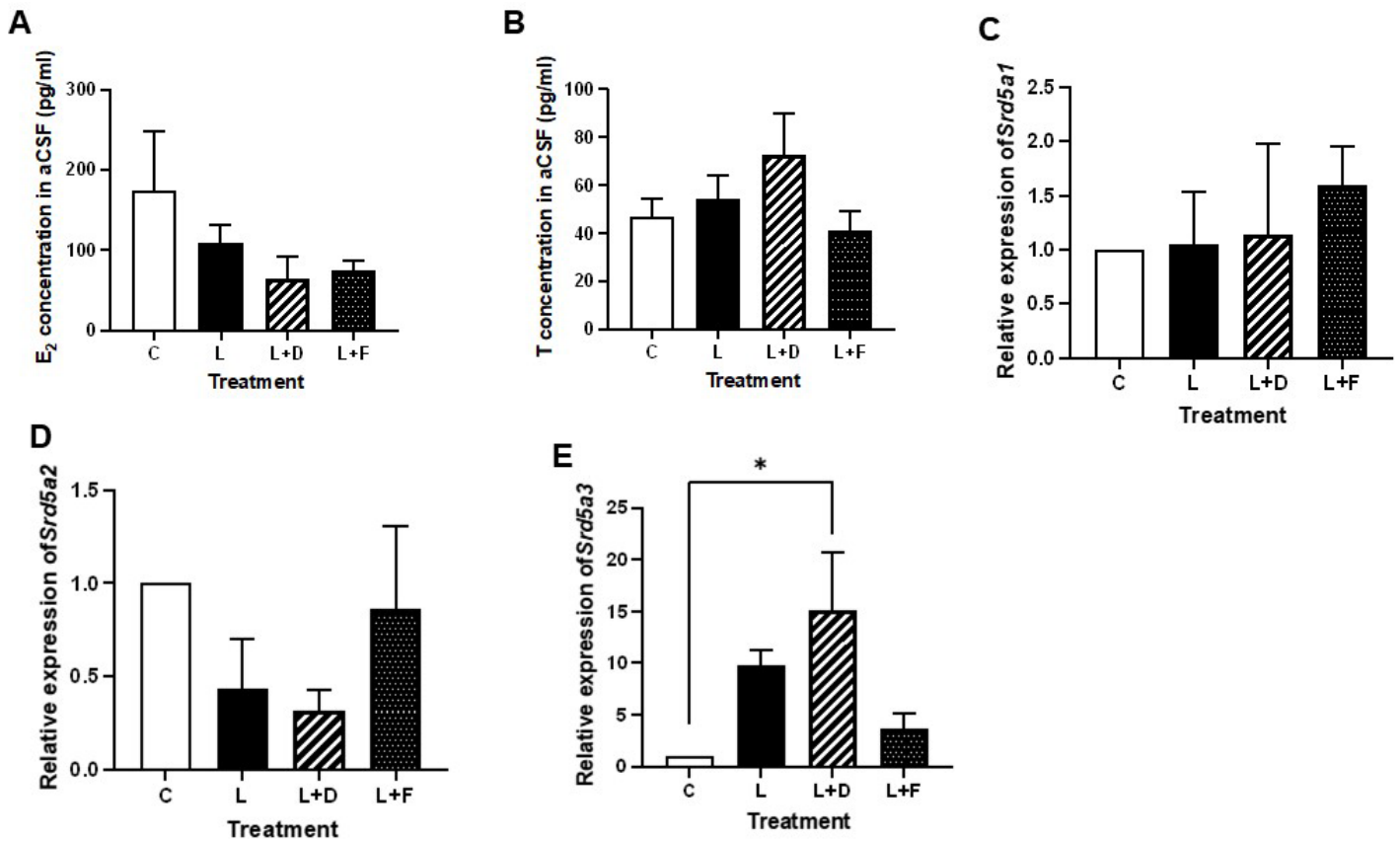


Figure 4.5. Effect of the inhibition of aromatase and 5 α -reductase on steroid hormone concentrations and enzyme expression in the adult female mouse ventromedial hypothalamus. Slices were incubated for 24 h with vehicle control (C), 10⁻⁸ M letrozole (L), with and without 10⁻⁸ M dutasteride (L + D) or 10⁻⁸ M finasteride (L + F). aCSF bathing ventromedial hypothalamus (VMH)-containing slices was used to measure neuroestrogen (**A**) and neurotestosterone (**B**). $n = 12$ slices per treatment group from a total of 9 animals. Punch dissections of the VMH from 3 animals were pooled into one, such that $n = 3$ from a total of 12 animals, which were used to measure gene expression. Expression levels, relative to the housekeeping gene (*Actb*) are shown for *Srd5a1* (**C**), *Srd5a2* (**D**), *Srd5a3* (**E**). For parametric datasets, differences were established by a one-way ANOVA with Bonferroni's multiple comparisons *post hoc*; nonparametric datasets were compared by a Kruskal-Wallis test with Dunn's multiple comparisons *post hoc*. * $P < 0.05$.

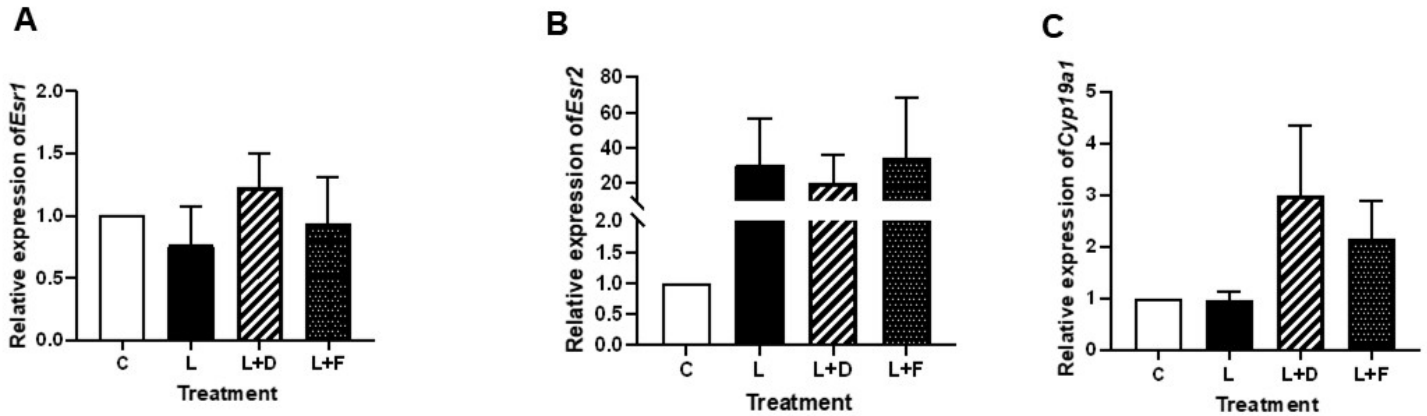


Figure 4.6. Effect of the inhibition of aromatase and 5 α -reductase on aromatase and ER expression in the adult female mouse ventromedial hypothalamus. Slices were incubated for 24 h with vehicle control (C), 10⁻⁸ M letrozole (L), with and without 10⁻⁸ M dutasteride (L + D) or 10⁻⁸ M finasteride (L + F). *n* = 12 slices per treatment group from a total of 9 animals. Punch dissections of the VMH from 3 animals were pooled into one, such that *n* = 3 from a total of 12 animals, which were used to measure gene expression. Expression levels, relative to the housekeeping gene (*Actb*) are shown for *Esr1* (A), *Esr2* (B), *Cyp19a1* (C). For parametric datasets, differences were established by a one-way ANOVA with Bonferroni's multiple comparisons *post hoc*; nonparametric datasets were compared by a Kruskal-Wallis test with Dunn's multiple comparisons *post hoc*.

Expression of other steroidogenic enzymes in the VMH is shown in **Supp. Fig. S4.2**. There was no significant effect of treatment on the expression of *Stard1* (**Supp. Fig. S.42A**), *Hsd3b1* (**Supp. Fig. S4.2C**), or *Hsd17b1* (**Supp. Fig. S4.2D**). *Cyp11a1* expression was increased with letrozole + dutasteride treatment relative to vehicle control ($P = 0.0334$) (**Supp. Fig. S4.2B**).

4.3.3 3β -diol reinstates neurosteroid production that is blocked by letrozole and dutasteride in the mPOA

In a third experiment, we investigated the effect of 3β -diol on neurosteroid concentrations and enzyme expression alone and in the presence of aromatase and 5α -reductase inhibitors (**Fig. 4.7 - 4.10**). As dutasteride inhibits all 3 isoforms of 5α -reductase (Titus et al., 2014), and was superior to finasteride in inhibiting E_2 production by the mPOA, we chose to use dutasteride as the 5α -reductase inhibitor for subsequent experiments.

mPOA: In agreement with the previous experiment, mPOA-containing slices treated with letrozole + dutasteride showed significantly less E_2 in aCSF compared with the slices treated with vehicle control ($P = 0.0165$) (**Fig. 4.7A**). 3β -diol had no significant effect on E_2 measured in mPOA-aCSF ($P > 0.9999$), but E_2 was significantly higher than that measured in mPOA-aCSF with letrozole + dutasteride treatment ($P = 0.0338$) (**Fig. 4.7A**). An unpaired Mann-Whitney U test also showed a significant increase in E_2 in mPOA-aCSF with 3β -diol + letrozole + dutasteride treatment when compared to letrozole + dutasteride alone ($P = 0.0287$) (**Fig. 4.7A**). For testosterone, there was a significant increase in mPOA-aCSF compared to control when treated with 3β -diol + letrozole + dutasteride ($P = 0.0111$) (**Fig. 4.7B**). This was also significantly greater than letrozole + dutasteride alone ($P = 0.0153$) (**Fig. 4.7B**). Expression of 5α -reductase isoforms was not significantly affected by treatment, though letrozole + dutasteride tended to increase expression of *Srd5a3* relative control ($P = 0.0545$) (**Fig. 4.7C-E**). *Esr1* and *Esr2* expression were also not affected by treatment (**Fig. 4.8A-B**). *Cyp19a1* expression was almost doubled with 3β -diol + letrozole + dutasteride treatment compared to letrozole + dutasteride or 3β -diol alone (3.030 ± 0.9725 vs L + D, 1.674 ± 0.2184 and vs 3β -diol, 1.547 ± 0.4776), but this did not reach statistical significance (**Fig. 4.8C**).

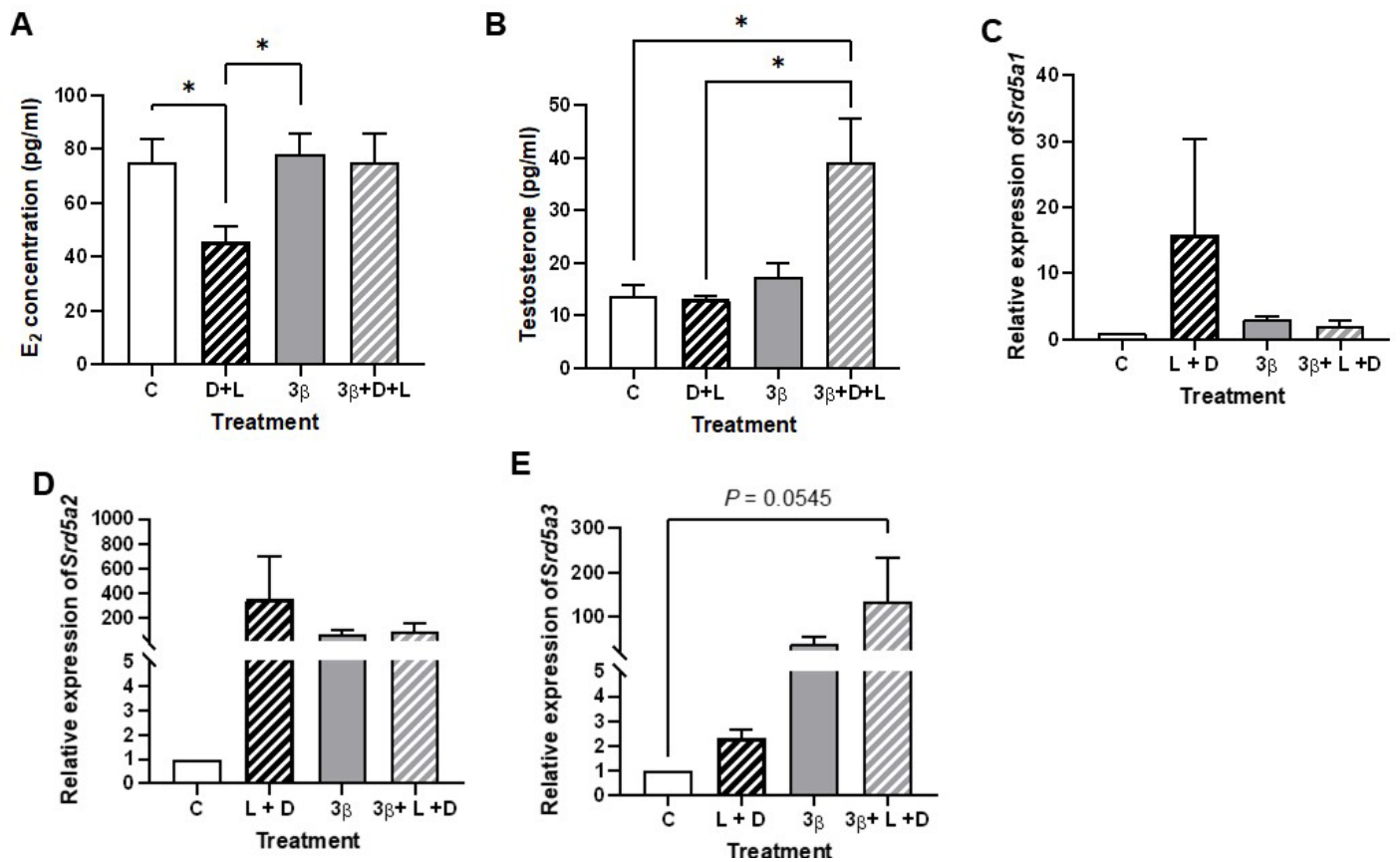


Figure 4.7. The effect of 3 β -diol on steroid hormone concentrations and enzyme expression in the adult female mouse mPOA. Slices were incubated for 24 h with vehicle control (C), 10⁻⁸ M letrozole with 10⁻⁸ M dutasteride (L + D), 10⁻⁸ M 3 β -diol (3 β), or a combination of all three treatments (3 β + L + D). aCSF bathing mPOA-containing slices was used to measure neuroestrogen (**A**) and neurotestosterone (**B**). $n = 15$ slices per treatment group from a total of 12 animals. Punch dissections of the mPOA from 4 animals were pooled into one, such that $n = 3$ from a total of 12 animals, which were used to measure gene expression. Expression levels, relative to the housekeeping gene (*Actb*) are shown for *Srd5a1* (**C**), *Srd5a2* (**D**), *Srd5a3* (**E**). For parametric datasets, differences were established by a one-way ANOVA with Bonferroni's multiple comparisons *post hoc*; nonparametric datasets were compared by a Kruskal-Wallis test with Dunn's multiple comparisons *post hoc*. * $P < 0.05$.

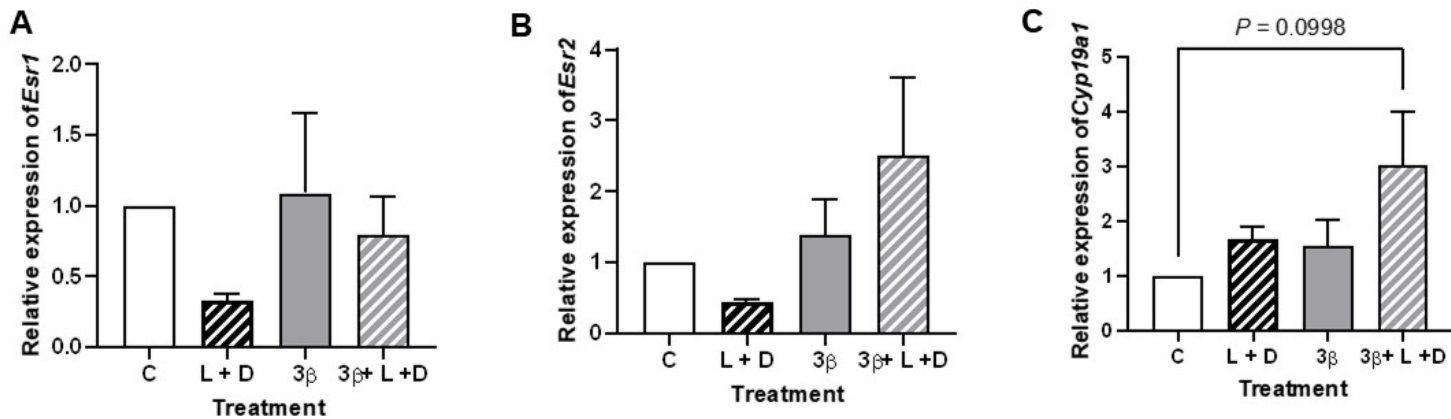


Figure 4.8. The effect of 3β-diol on aromatase and ER expression in the adult female mouse mPOA. Slices were incubated for 24 h with vehicle control (C), 10^{-8} M letrozole with 10^{-8} M dutasteride (L + D), 10^{-8} M 3β-diol (3β), or a combination of all three treatments (3β + L + D). $n = 15$ slices per treatment group from a total of 12 animals. Punch dissections of the mPOA from 4 animals were pooled into one, such that $n = 3$ from a total of 12 animals, which were used to measure gene expression. Expression levels, relative to the housekeeping gene (*Actb*) are shown for *Esr1* (A), *Esr2* (B), *Cyp19a1* (C). For parametric datasets, differences were established by a one-way ANOVA with Bonferroni's multiple comparisons *post hoc*; nonparametric datasets were compared by a Kruskal-Wallis test with Dunn's multiple comparisons *post hoc*.

The expression of other steroidogenic enzymes in the mPOA under this treatment protocol is shown in **Supp. Fig. S4.3**. There was no significant effect of treatment on *Stard1* expression (**Supp. Fig. S4.3A**), *Cyp11a1* expression (**Supp. Fig. S4.3B**), *Hsd3b1* expression (**Supp. Fig. S4.3C**) or *Hsd17b1* expression (**Supp. Fig. S4.3D**) in the mPOA.

VMH: In VMH-aCSF, there was no effect of treatment on E₂ concentrations (**Fig. 4.9A**), testosterone concentrations (**Fig. 4.9B**) or *Srd5a1* expression (**Fig 4.9C**). All treatments significantly reduced *Srd5a2* expression (C vs L+D, $P = 0.0008$; vs 3 β -diol, $P = 0.002$; vs 3 β -diol + letrozole + dutasteride, $P = 0.0008$ [**Fig. 4.9D**]) and *Srd5a3* expression ($P < 0.0001$ for all comparisons vs vehicle control [**Fig. 4.9E**]).

There was no effect of treatment on the expression of *Esr1*, *Esr2*, or *Cyp19a1* (**Fig. 4.10A-C**). Yet, 3 β -diol tended to increase expression of *Esr1* compared to vehicle control ($P = 0.0727$) (**Fig. 4.5F**). Expression of other steroidogenic enzymes is shown in **Supp. Fig. S4.4**. There was no significant effect of treatment on *Stard1* expression (**Supp. Fig. S4.4A**), *Cyp11a1* expression (**Supp. Fig. S4.4B**), or *Hsd3b1* expression (**Supp. Fig. S4.4C**) in the VMH. 3 β -diol tended to decrease *Hsd17b1* expression compared to vehicle control ($P = 0.0524$) (**Supp. Fig. S4.4D**).

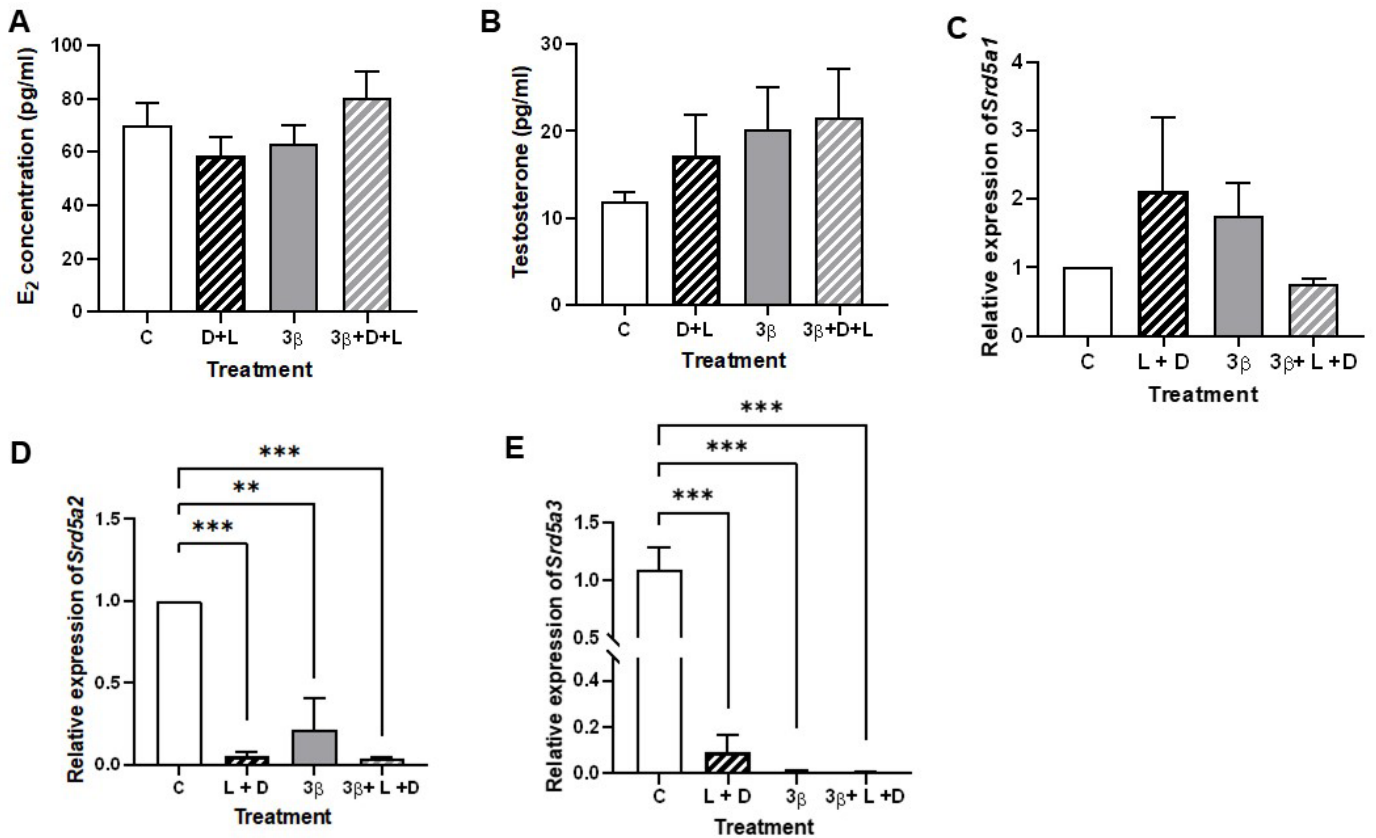


Figure 4.9. The effect of 3 β -diol on steroid hormone concentrations and enzyme expression in the adult female mouse VMH. Slices were incubated for 24 h with vehicle control (C), 10⁻⁸ M letrozole with 10⁻⁸ M dutasteride (L + D), 10⁻⁸ M 3 β -diol (3 β), or a combination of all three treatments (3 β + L + D). aCSF bathing VMH-containing slices was used to measure neuroestrogen (A) and neurotestosterone (B). $n = 12$ slices per treatment group from a total of 12 animals. Punch dissections of the VMH from 4 animals were pooled into one, such that $n = 3$ from a total of 12 animals, which were used to measure gene expression. Expression levels, relative to the housekeeping gene (*Actb*) are shown for *Srd5a1* (C), *Srd5a2* (D), *Srd5a3* (E). For parametric datasets, differences were established by a one-way ANOVA with Bonferroni's multiple comparisons *post hoc*; nonparametric datasets were compared by a Kruskal-Wallis test with Dunn's multiple comparisons *post hoc*. ** $P < 0.001$, *** $P < 0.0001$.

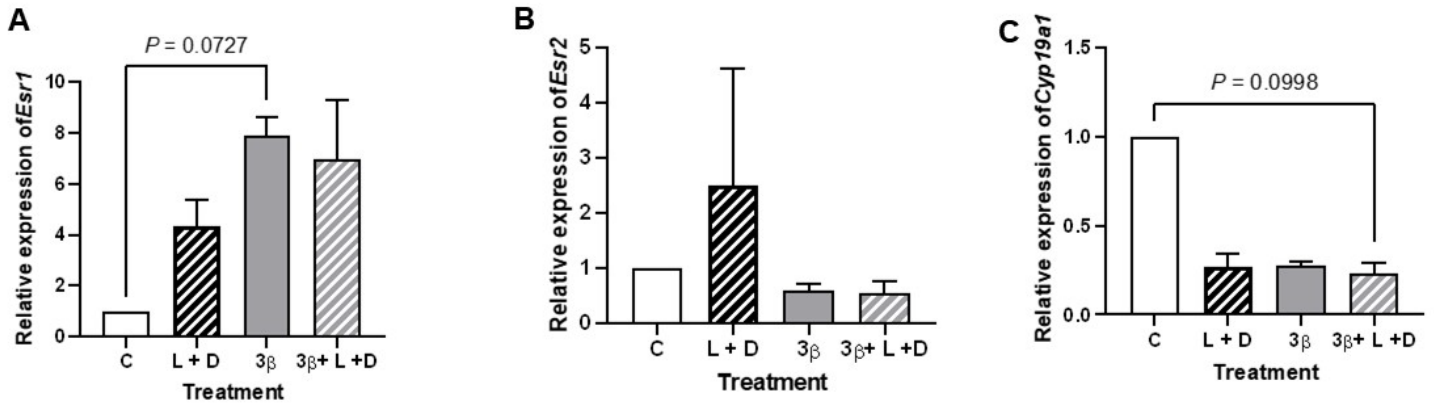


Figure 4.10. The effect of 3β-diol on aromatase and ER expression in the adult female mouse VMH. Slices were incubated for 24 h with vehicle control (C), 10⁻⁸ M letrozole with 10⁻⁸ M dutasteride (L + D), 10⁻⁸ M 3β-diol (3β), or a combination of all three treatments (3β + L + D). aCSF bathing VMH-containing slices was used to measure neuroestrogen (A) and neurotestosterone (B). *n* = 12 slices per treatment group from a total of 12 animals. Punch dissections of the VMH from 4 animals were pooled into one, such that *n* = 3 from a total of 12 animals, which were used to measure gene expression. Expression levels, relative to the housekeeping gene (*Actb*) are shown for *Srd5a1* (C), *Srd5a2* (D), *Srd5a3* (E). For parametric datasets, differences were established by a one-way ANOVA with Bonferroni's multiple comparisons *post hoc*; nonparametric datasets were compared by a Kruskal-Wallis test with Dunn's multiple comparisons *post hoc*. ** *P* < 0.001, *** *P* < 0.0001.

4.3.4 The induction of E₂ synthesis by 3β-diol may be ligand specific

To understand the involvement, if any, of ERs in neurosteroid production, slices were incubated in the presence of ER-specific agonists (PPT for ERα and DPN for ERβ) and an ER antagonist (ICI 182,780) for 24 h.

mPOA: mPOA-aCSF showed no significant effect of ICI treatment when compared to control, but a significant reduction in E₂ with ICI + PPT treatment ($P = 0.0391$) (**Fig. 4.11A**). This concentration of E₂ was also significantly less than that measured with ICI alone ($P = 0.025$) (**Fig. 4.11A**). Testosterone in mPOA-aCSF was significantly decreased by ICI when compared to control ($P = 0.0013$) (**Fig. 4.11B**). ICI treatment tended to reduce testosterone concentration in mPOA-aCSF when compared to PPT ($P = 0.0582$) and DPN ($P = 0.0746$) (**Fig. 4.11B**). There was no significant difference between ICI and ICI + PPT or ICI + DPN (**Fig. 4.11B**). ER mRNA expression was not significantly different between vehicle control and any other treatment group, but significantly increased with ICI + DPN treatment compared to ICI alone (*Esr1*, $P = 0.0419$; *Esr2*, $P = 0.0333$) (**Fig. 4.12A-B**). For *Cyp19a1*, expression tended to decrease with ICI treatment compared to vehicle control ($P = 0.0604$) (**Fig. 4.12C**).

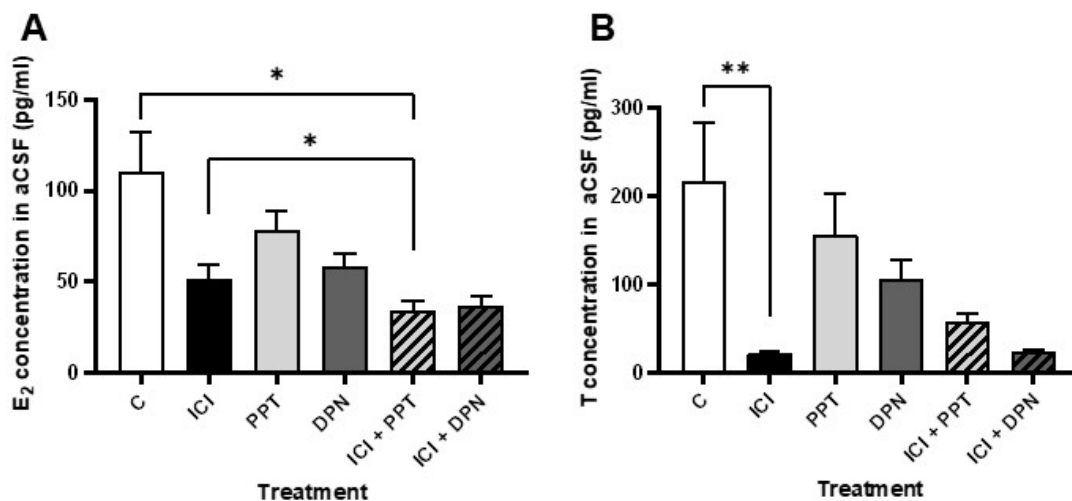


Figure 4.11. Effect of oestrogen receptor modulators on steroid hormone concentration in the adult female mouse mPOA. Slices were incubated for 24 h with vehicle control (C), 10⁻⁸ M ICI 182,780 (ICI), 10⁻⁹ M PPT, 10⁻⁹ M DPN, or a combination (ICI + PPT, ICI + DPN). aCSF bathing mPOA-containing slices was used to measure neuroestrogen (**A**) and neurotestosterone (**B**). $n = 26$ slices per treatment group from a total of 32 animals. For parametric datasets, differences were established by a one-way ANOVA with Bonferroni's multiple comparisons *post hoc*; nonparametric datasets were compared by a Kruskal-Wallis test with Dunn's multiple comparisons *post hoc*. * $P < 0.05$, ** $P < 0.01$.

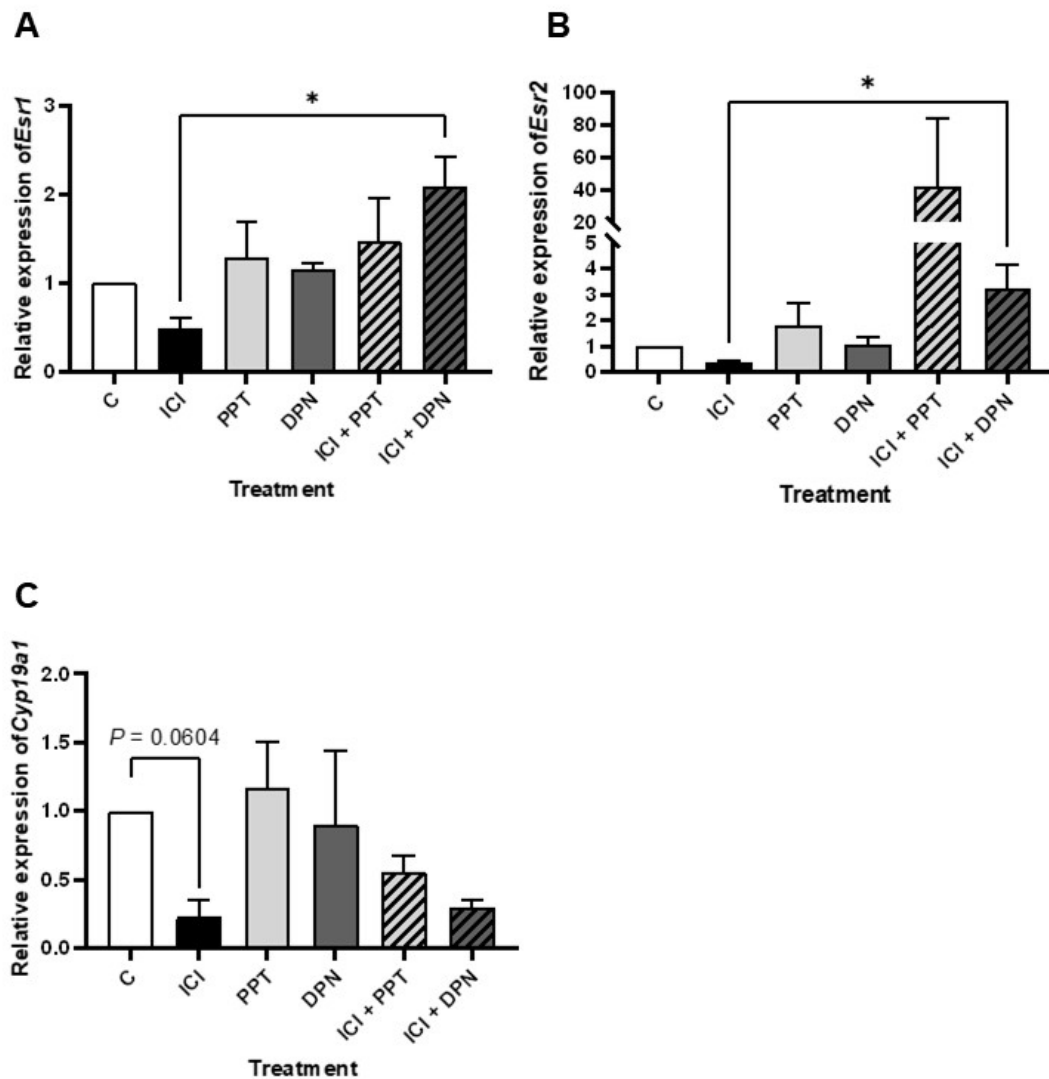


Figure 4.12. Effect of oestrogen receptor modulators on oestrogen receptor expression and *Cyp19a1* expression in the adult female mouse mPOA. Slices were incubated for 24 h with vehicle control (C), 10^{-8} M ICI 182,780 (ICI), 10^{-9} M PPT, 10^{-9} M DPN, or a combination (ICI + PPT, ICI + DPN). $n = 26$ slices per treatment group from a total of 32 animals. Punch dissections of the mPOA from 4 animals were pooled into one, such that $n = 3$ from a total of 12 animals, which were used to measure gene expression. Expression levels, relative to the housekeeping gene (*Actb*) are shown for *Esr1* (A), *Esr2* (B), and *Cyp19a1* (C). For parametric datasets, differences were established by a one-way ANOVA with Bonferroni's multiple comparisons *post hoc*; nonparametric datasets were compared by a Kruskal-Wallis test with Dunn's multiple comparisons *post hoc*. * $P < 0.05$.

Expression of other steroidogenic enzymes in the mPOA is shown in **Supp. Fig. S4.5**. ICI treatment decreased expression of *Cyp11a1* compared to PPT treatment ($P = 0.0127$) (**Supp. Fig. S4.5B**), and *Hsd17b1* compared to DPN treatment ($P = 0.0193$) (**Supp. Fig. S4.5D**). ICI also showed a tendency to decrease *Stard1* expression when compared with vehicle control ($P = 0.0604$) (**Supp. Fig. S4.5A**). PPT increased *Hsd3b1* expression compared to vehicle control ($P = 0.0345$) (**Supp. Fig. S4.5C**). There was no effect of any treatment on the expression of 5 α -reductase isoforms II or III (**Supp. Fig. S4.5F-G**), but expression of *Srd5a1* was increased with ICI treatment ($P = 0.0070$) and treatment with ICI + DPN ($P = 0.0470$) (**Supp. Fig. S4.5E**).

VMH: In VMH-aCSF, there was a significant interaction between E₂ concentration and treatment ($H(5) = 13.25$, $P = 0.0211$), but there were no pairwise differences found by Dunn's multiple comparisons test (**Fig. 4.13A**). However, there was a tendency for ICI + DPN to reduce E₂ in VMH-aCSF when compared to control ($P = 0.0691$) (**Fig. 4.13A**). There was no effect of treatment on testosterone concentrations measured in VMH-aCSF ($P = 0.1778$) (**Fig. 4.13B**). In line with the absence of treatment-related changes in neurosteroids, there was no effect of treatment on *Cyp19a1* expression in the VMH (**Fig. 4.14C**). ER expression levels were also not affected by treatment (**Fig. 4.14A-B**).

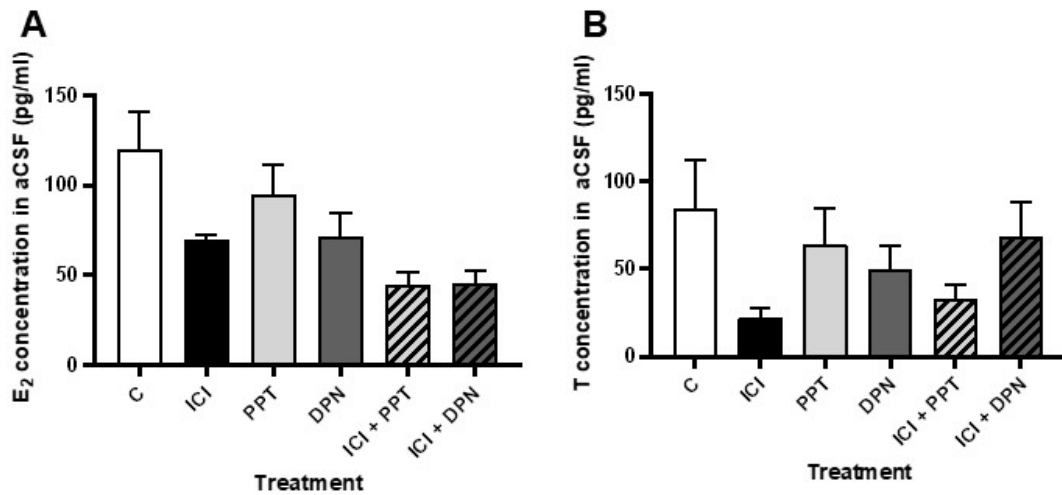


Figure 4.13. Effect of oestrogen receptor modulators on steroid hormone concentration in the adult female mouse VMH. Slices were incubated for 24 h with vehicle control (C), 10^{-8} M ICI 182,780 (ICI), 10^{-9} M PPT, 10^{-9} M DPN, or a combination (ICI + PPT, ICI + DPN). aCSF bathing VMH-containing slices was used to measure neuroestrogen (**A**) and neurotestosterone (**B**). $n = 18$ slices per treatment group from a total of 32 animals. For parametric datasets, differences were established by a one-way ANOVA with Bonferroni's multiple comparisons *post hoc*; nonparametric datasets were compared by a Kruskal-Wallis test with Dunn's multiple comparisons *post hoc*.

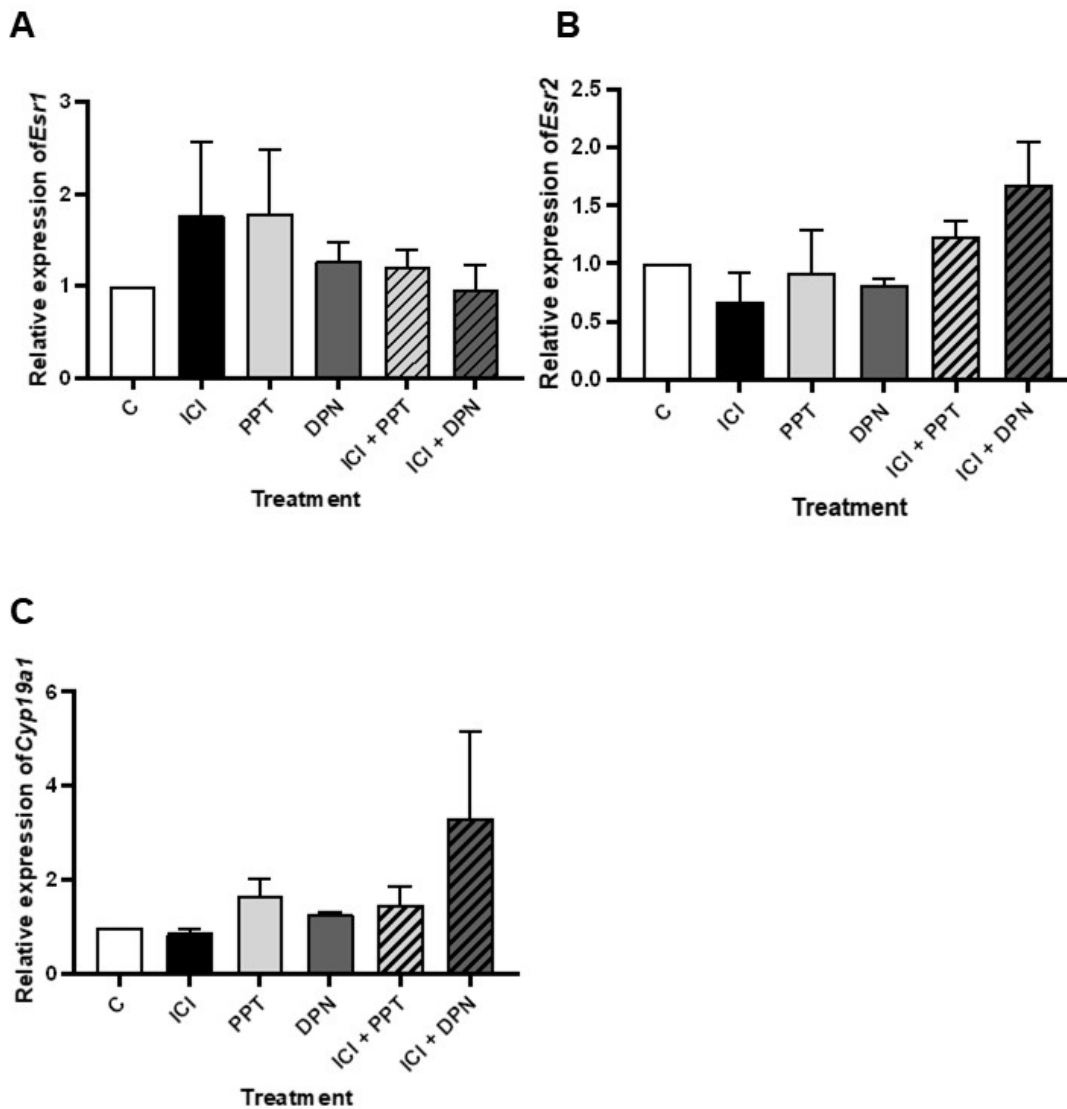


Figure 4.14. Effect of oestrogen receptor modulators on oestrogen receptor expression and *Cyp19a1* expression in the adult female mouse VMH. Slices were incubated for 24 h with vehicle control (C), 10^{-8} M ICI 182,780 (ICI), 10^{-9} M PPT, 10^{-9} M DPN, or a combination (ICI + PPT, ICI + DPN). $n = 18$ slices per treatment group from a total of 32 animals. Punch dissections of the mPOA from 4 animals were pooled into one, such that $n = 3$ from a total of 12 animals, which were used to measure gene expression. Expression levels, relative to the housekeeping gene (*Actb*) are shown for *Esr1* (A), *Esr2* (B), and *Cyp19a1* (C). For parametric datasets, differences were established by a one-way ANOVA with Bonferroni's multiple comparisons *post hoc*; nonparametric datasets were compared by a Kruskal-Wallis test with Dunn's multiple comparisons *post hoc*.

Supp. Fig. S4.6 shows the expression levels of other steroidogenic enzymes in the VMH under ER modulator treatments. *Stard1* (**Supp. Fig. S4.6A**), *Hsd3b1* (**Supp. Fig. S4.6C**), *Hsd17b1* (**Supp. Fig. S4.6D**), *Srd5a1* (**Supp. Fig. S4.6E**), and *Srd5a3* (**Supp. Fig. S4.6G**) were unaffected by treatment. *Cyp11a1* expression was increased with ICI + DPN compared to control ($P = 0.0314$), though there was no difference compared to ICI alone (**Supp. Fig. S4.6B**). ICI + DPN had the opposite effect on *Srd5a2*, significantly decreasing expression compared to vehicle control (**Supp. Fig. S4.6F**).

4.3.5 Ovariectomy does not seem to impede neurosteroid production

To understand the dependence of neurosteroids on gonadal hormones, steroids were measured from brain hemispheres of intact, OVX, long-term OVX (OVX-L), and OVX mice treated with EB, after C18 extraction (**Fig. 4.15**). There was no interaction between gonadal status and E_2 concentration in the mPOA ($P = 0.5578$) (**Fig. 4.15A**). A significant interaction was found in the VMH ($H(3) = 8.453$, $P = 0.0183$), but pairwise comparisons found no significant difference in E_2 between groups (**Fig. 4.15B**). Testosterone concentrations in the mPOA of OVX mice of any condition were not significantly different to intact mice, but long-term ovariectomy increased testosterone concentrations compared to OVX mice ($P = 0.0248$) (**Fig. 4.15C**). There was no effect on gonadal condition on testosterone concentrations in the VMH (**Fig. 4.15D**).

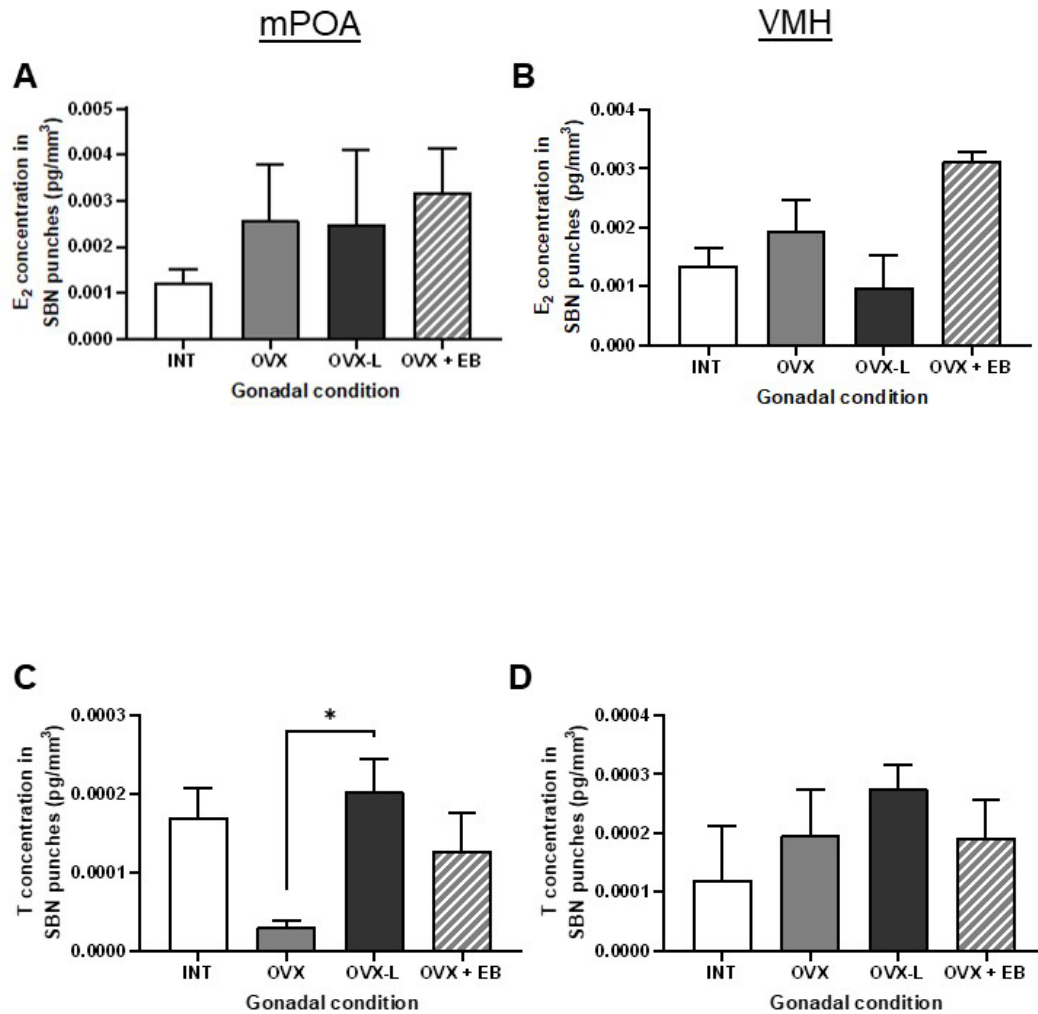


Figure 4.15. Effect of ovariectomy on E₂ and testosterone production in punch dissected medial preoptic area and ventromedial hypothalamus from the adult female mouse. Punch dissections from one hemisphere of the medial preoptic are (mPOA, left column) and ventromedial hypothalamus (VMH, right column) were taken from mice that were intact (INT), short-term ovariectomised (OVX), long-term ovariectomised (OVX-L), or short-term ovariectomised and treated with E₂ benzoate (OVX + EB). OVX animals were OVX one week prior to sacrifice whereas OVX-L animals were OVX seven weeks prior to sacrifice. $n = 4$ animals per treatment group, with the exception of INT, where $n = 3$. Punch dissections were used to measure neuroestrogen (A-B) and neurotestosterone (C-D). For parametric datasets, differences were established by a one-way ANOVA with Bonferroni's multiple comparisons *post hoc*; nonparametric datasets were compared by a Kruskal-Wallis test with Dunn's multiple comparisons *post hoc*. * $P < 0.05$.

The effect of OVX on steroidogenic enzyme expression is shown in **Fig. 4.16** and **4.17**. *Stard1* expression was increased in OVX mice compared to mice in the OVX + EB group ($P = 0.0210$), though neither group was significantly different to intact mice (**Fig. 4.16A**). OVX-L mice had significantly increased expression of *Cyp11a1* compared to intact, OVX and OVX + EB mice ($P < 0.0001$ for all comparisons) (**Fig. 4.16B**). *Hsd3b1* expression was significantly increased in OVX-L mice compared to OVX ($P = 0.0034$) and OVX + EB mice ($P = 0.0189$) (**Fig. 4.16C**). There was no effect of gonadal condition on the expression of *Hsd17b1* (**Fig. 4.16D**). The intact group showed higher expression of *Cyp19a1* compared to all other groups (vs OVX, $P = 0.0011$; vs OVX-L, $P = 0.0037$; vs OVX + EB, $P = 0.0007$) (**Fig. 4.17A**). OVX-L and OVX + EB mice had lower expression levels of *Esr1* compared to intact ($P = 0.0146$ and 0.0146 , respectively) and OVX mice ($P = 0.0221$ and 0.0382 , respectively) (**Fig. 4.17B**). OVX-L and OVX + EB mice had lower expression levels of *Esr1* compared to intact ($P = 0.0002$ and 0.0142 , respectively) and OVX mice ($P < 0.0001$ and $= 0.0004$, respectively), however, OVX + EB mice expressed greater levels of *Esr2* compared to OVX-L mice ($P = 0.007$) (**Fig. 4.17C**).

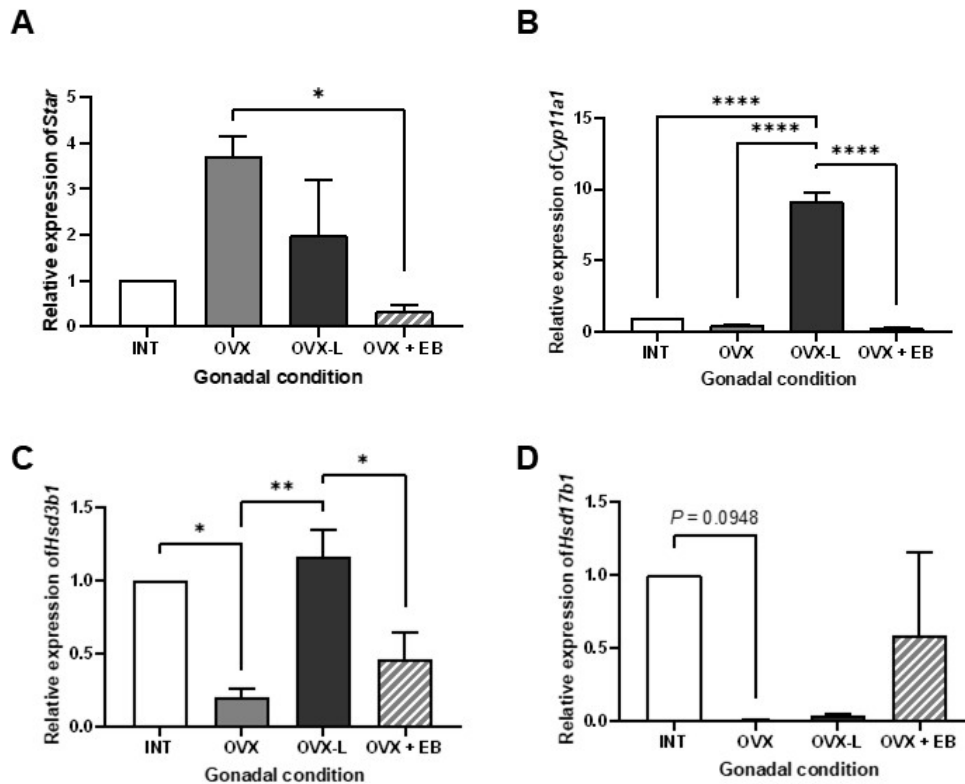


Figure 4.16. Effect of ovariectomy on steroidogenic enzyme expression in the adult female mouse hypothalamus. Hypothalami were excised from hemispheres of mice that were intact (INT), short-term ovariectomised (OVX), long-term ovariectomised (OVX-L), or short-term ovariectomised and treated with oestradiol benzoate (OVX + EB) and used to measure gene expression. Expression levels, relative to the housekeeping gene (*Actb*) are shown for *Stard1* (A), *Cyp11a1* (B), *Hsd3b1* (C), *Hsd17b1* (D). For parametric datasets, differences were established by a one-way ANOVA with Bonferroni's multiple comparisons *post hoc*; nonparametric datasets were compared by a Kruskal-Wallis test with Dunn's multiple comparisons *post hoc*. * $P < 0.05$, ** $P < 0.01$, **** $P < 0.0001$.

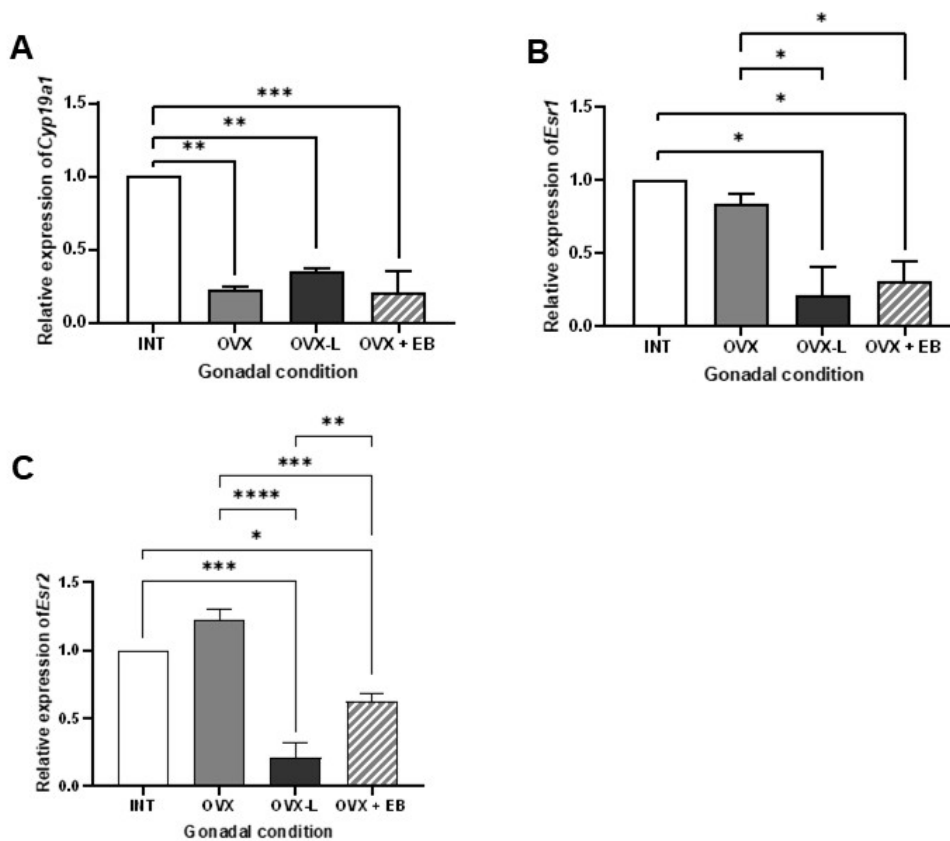


Figure 4.17. Effect of ovariectomy on oestrogen receptor expression and steroidogenic enzyme expression in the adult female mouse hypothalamus.

Hypothalami were excised from hemispheres of mice that were intact (INT), short-term ovariectomised (OVX), long-term ovariectomised (OVX-L), or short-term ovariectomised and treated with oestradiol benzoate (OVX + EB) and used to measure gene expression. Expression levels, relative to the housekeeping gene (*Actb*) are shown for *Cyp19a1* (A), *Esr1* (B), and *Esr2* (C). For parametric datasets, differences were established by a one-way ANOVA with Bonferroni's multiple comparisons *post hoc*; nonparametric datasets were compared by a Kruskal-Wallis test with Dunn's multiple comparisons *post hoc*. * $P < 0.05$, ** $P < 0.001$, *** $P < 0.001$, **** $P < 0.0001$.

Steroidogenic enzymes relevant to the 3β -diol pathway are shown in **Supp. Fig. S4.7**. *Srd5a1* expression was significantly decreased in OBX + EB mice compared to OVX-L ($P = 0.0059$) and OVX mice ($P = 0.0456$) (**Supp. Fig. S4.7A**). However, both OVX and OVX-L groups expressed significantly less *Srd5a2* compared to intact mice ($P = 0.0227$) (**Supp. Fig. S4.7B**). *Srd5a3* was not detected in OVX + EB mice (**Supp. Fig. S4.7C**).

4.4 Discussion

We have previously developed a protocol that allowed us to measure steroid production by *ex vivo* mouse brain slices (Chapter 3). In the present study, we utilised our established protocols to understand the regulation of neurosteroid synthesis by hypothalamic nuclei that contribute to social behaviours in the female mouse. The mPOA and VMH are nuclei integral to female reproductive and social behaviour (Spiteri et al., 2012, Correa et al., 2015), express ERs (Mitra et al., 2003, Moëne et al., 2019) and show aromatase activity (Roselli et al., 1984, Roselli, 1995). We hypothesised that, if true *de novo* synthesis was taking place within these brain regions, this could be inhibited with the aromatase inhibitor letrozole. This has been demonstrated in the rodent hippocampus. In mixed sex hippocampal slice cultures, E₂ release into the culture medium is decreased with the addition of letrozole (Kretz et al., 2004a). Likewise, letrozole reduces E₂ measured in culture medium of a rat glioma cell line (Dave et al., 2015). We failed to observe these effects with letrozole in hypothalamic slice culture but uncovered a novel regulatory mechanism for neuroestrogen synthesis in the female mouse hypothalamus.

4.4.1 The 3 β -diol pathway in the mPOA

Aside from E₂, testosterone can be metabolised to DHT by 5 α -reductase enzymes (Celotti et al., 1997). DHT is typically considered the most potent androgen since it cannot be aromatised to E₂-like metabolites and binds directly to the androgen receptor (Marchetti and Barth, 2013). DHT is effective at reinstating the decreased aromatase immunoreactivity in the BNST of castrated adrenalectomised male rats and is more effective at doing so than either testosterone or E₂ (Zhao et al., 2007). In primary amygdala cell cultures, DHT significantly increases aromatase expression specifically in cultures from female mice, yet this occurs through an ER β -dependent mechanism (Cisternas et al., 2015, Cisternas et al., 2017). For example, in primary amygdala cultures, treatment with DHT increases aromatase expression, but not in the presence of the specific ER β antagonist 4-[2-phenyl-5,7-bis(trifluoromethyl)pyrazolo[1,5-a]pyrimidin-3-yl]phenol (PHTPP) (Cisternas et al., 2017). Several reports have indicated that the actions of DHT may be caused by its metabolites, specifically 3 β -diol (Lund et al., 2004, Lund et al., 2006), and reviewed in Handa et al. (2011). 3 β -diol does not bind the androgen receptor, but preferentially binds ER β (Kuiper et al., 1998) which induces transcription of E₂-responsive genes through a canonical oestrogen response element (ERE) similar to E₂ (Pak et al., 2005).

Furthermore, 3 β -diol mimics the effect of DHT on aromatase expression in primary amygdala culture (Cisternas et al., 2017).

We hypothesised that a mechanism involving 3 β -diol may have prevented us from observing a decrease in E₂ following treatment with the aromatase inhibitor, letrozole, in the mPOA. Letrozole, a competitive inhibitor of aromatase (Brueggemeier et al., 2005), did not change concentration during slice incubation, therefore limiting testosterone to its own actions, or pushing its conversion to DHT and subsequent metabolism to 3 β -diol. If 3 β -diol resulted in more aromatase expression, this might relieve inhibition by letrozole (demonstrated in **Fig. 4.18**). Therefore, we supposed that if the female brain was truly synthesising E₂, its production would be diminished in the presence of inhibitors targeting both aromatase and 5 α -reductase. We used two different 5 α -reductase inhibitors: dutasteride, which inhibits all three isoforms of 5 α -reductase (types 1, 2 > type 3) and finasteride, which inhibits types 2 and 3 with a similar potency (Titus et al., 2014, Yamana et al., 2010). We found that letrozole and dutasteride significantly reduced E₂ concentration in mPOA-aCSF, and both 5 α -reductase inhibitors administered together with letrozole significantly reduced aromatase expression in the mPOA compared to letrozole alone. The efficiency of dutasteride over finasteride in reducing neuroestrogen synthesis could be due to the moderate expression of *Srd5a2* in the hypothalamus (Castelli et al., 2013). The results of this experiment strongly suggested that the activation of the 3 β -diol pathway counteracted the anticipated decrease in E₂ associated with letrozole treatment. It also substantiates the ability of the brain slices in our culture system to synthesise neurosteroids and provides the first empirical evidence that the female mouse mPOA synthesises neuroestrogen.

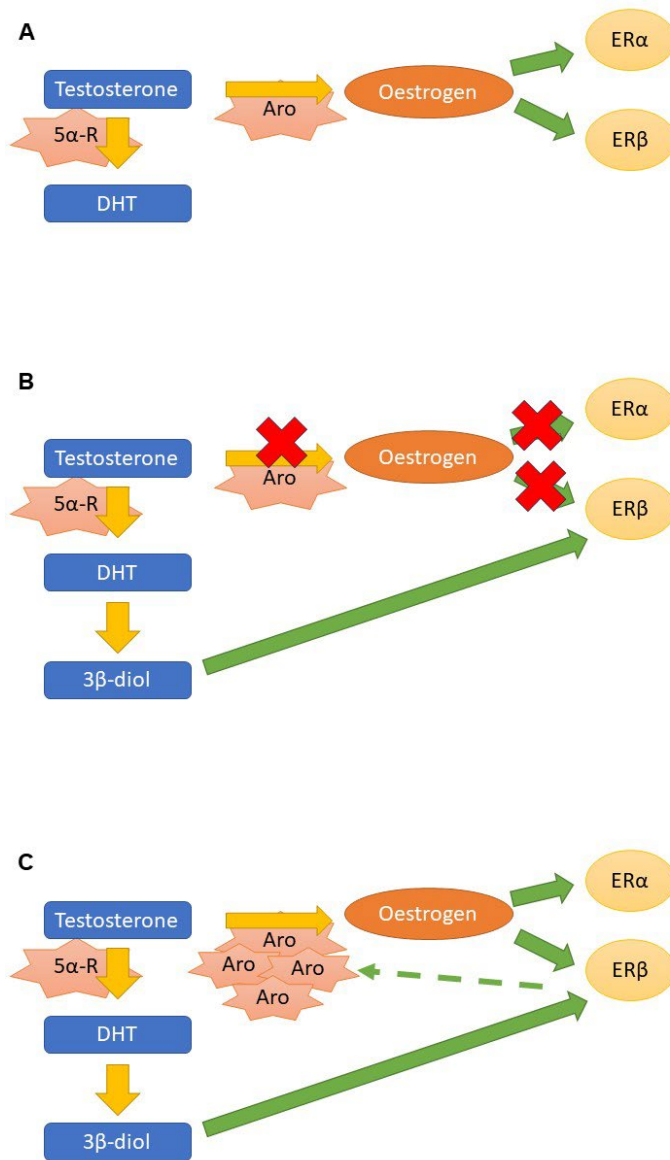


Figure 4.18. The mechanism of the 3β-diol pathway in *ex vivo* slice culture. Under normal physiological conditions, testosterone is converted to E₂ by aromatase (aro) and DHT by 5α-reductase enzymes (5α-R) (**A**). E₂ can bind to its cognate receptors. When the aromatization pathway is blocked by letrozole, there is a build-up of testosterone. Testosterone can either exert actions as is or it can be converted to DHT. As DHT concentration rises, it is metabolized to 5α-androstane 3β, 17β diol (3β-diol). 3β-diol is a natural ligand for ERβ (**B**). 3β-diol acts on ERβ to increase aromatase expression. Since the initial concentration of letrozole has not changed, the inhibition is relieved (**C**).

Effect on neuroestrogen synthesis: To strengthen our findings, we investigated neurosteroid synthesis and enzyme expression after administration of 3 β -diol, either alone or in combination with letrozole and dutasteride. By inhibiting the conversion of testosterone to E₂ and DHT whilst supplementing with 3 β -diol, we aimed to determine whether 3 β -diol could rescue neuroestrogen synthesis. We found that neuroestrogen concentrations in mPOA-aCSF were significantly increased with 3 β -diol and showed a tendency for increase when 3 β -diol was given with letrozole and dutasteride compared to letrozole and dutasteride treatment alone. The effects of dutasteride are not solely related to the inhibition of the conversion of testosterone to DHT; dutasteride has been shown to upregulate the enzymes that degrade DHT and its metabolites (Schmidt et al., 2004). Therefore, using all 3 treatments – letrozole, dutasteride, and 3 β -diol – at once could have limited the effectiveness of 3 β -diol. Interestingly, neither treatment involving 3 β -diol resulted in a significant increase in neuroestrogen concentrations compared to vehicle control. These observations suggest the presence of a possible ceiling effect on neuroestrogen synthesis in the female mouse mPOA where high concentrations are already present under control conditions. This is also believed to occur in the songbird caudomedial nidopallium (NCM) (Pawlish and Ramage-Healey, 2015), a region with high aromatase activity and neuroestrogen synthesis (Jalabert et al., 2022). It also suggests that not only is aromatase constitutively expressed in the brain (Cornil, 2018), but it is also constitutively active.

Effect on ER expression: The inhibitors used in these experiments clearly act directly on enzymes rather than acting on hormone receptors (Brueggemeier et al., 2005, Yamana et al., 2010). However, 3 β -diol is also a potent modulator of ER β expression in the rat prostate (Oliveira et al., 2007), and E₂ and DHT increase ER β mRNA expression in amygdala cultures (Cisternas et al., 2017). We were interested to see if the inhibition of 3 β -diol synthesis impacted ER expression. There appeared to be a positive effect of finasteride on ER α and ER β expression in the mPOA. In human prostatic tissue specimens, which predominantly express the type 2 5 α -reductase isozyme (Steers, 2001), gene methylation of *SRD5A2* increased the protein levels of phosphorylated ER α (Wang et al., 2017). Since finasteride inhibits the type 2 isozyme to a greater extent than dutasteride (Yamana et al., 2010), it is possible that the decreased activity of *Srd5a2* drove ER expression in the mPOA. 3 β -diol itself had no effect on ER expression in either the mPOA or the VMH, though in the prostate, 3 β -diol increased ER β protein (Oliveira et al., 2007). The possibility of a tissue-specific effect of 3 β -diol has not been explored.

Effect on steroidogenic enzyme expression: Clearly, the actions of the 3β -diol pathway work to increase neuroestrogen production in the mPOA. Whether this is through increased *de novo* synthesis, or redirection of existing precursors to the aromatisation pathway, is unclear. To explore if increased *de novo* synthesis is occurring, we examined various steroidogenic enzymes using RT-qPCR. Letrozole and dutasteride, 3β -diol, and all three treatments in combination had variable effects on the expression of steroidogenic enzymes. In the mPOA, we found no significant difference in expression levels of *Stard1*, *Cyp11a1*, *Hsd3b1*, or *Hsd17b1* with letrozole treatment. Yet, expression of these enzymes is decreased in the ovary of rats treated with letrozole (Ortega et al., 2013). However, with the addition of dutasteride, we found increased expression of *Stard1*, suggesting that *de novo* synthesis is upregulated when steroid synthesis is blocked at the level of testosterone. Furthermore, we found a tendency for letrozole + dutasteride to increase the expression of *Hsd17b1*, supporting our earlier findings that letrozole in combination with dutasteride increased neuroestrogen synthesis in the mPOA. 3β -diol alone tended not to increase *Stard1* expression, though expression showed a tendency to increase with letrozole and dutasteride alone or in combination with 3β -diol. This underscores the hypothesis that *de novo* synthesis in the mPOA is upregulated when androgens cannot be metabolised to oestrogenic compounds. It also suggests that at least some androgenic precursors are made *de novo*, and do not originate from the periphery, in the female mouse.

4.4.2 Regional specificity of the 3β -diol pathway

The 3β -diol pathway demonstrated region-specific effects within the hypothalamus. Although letrozole did not result in a significant alteration of 24 h E_2 concentrations when compared to the baseline (0 h), the levels of E_2 in VMH-aCSF were not significantly reduced with letrozole alone or in combination with 5α -reductase inhibitors in comparison to treatment with vehicle control. Consistently, there was no significant impact of 3β -diol on E_2 concentrations in VMH-aCSF or aromatase expression in the VMH. A possible explanation for this is the greater expression of ER α (Mitra et al., 2003), along with a relative lack of ER β expression in the VMH compared to the mPOA (Zuloaga et al., 2014). It has previously been noted that a number of aromatase-positive cells in the male and female mouse mPOA coexpress ER β , but not ER α (Stanic et al., 2014), which positions ER β perfectly to increase aromatase expression upon activation by 3β -diol. The amygdala, which expresses ER β in abundance (Shughrue and Merchenthaler, 2001), is currently the only other documented brain region exhibiting the 3β -diol pathway (Cisternas et al., 2015, Cisternas et al., 2017). Interestingly, we found that 3β -diol treatment tended to increase

the expression of ER α in the VMH; however, this tendency was dampened when 3 β -diol was given in combination with letrozole and dutasteride. As an ER β agonist (Kuiper et al., 1998), it is unclear why 3 β -diol has this effect on ER α in the VMH, and to our knowledge, this is the first report of such an observation. Notably, 3 β -diol had no effect on ER β expression in the VMH.

Like the mPOA, treatments had a variable effect on steroidogenic enzyme expression in the VMH. Interestingly, 3 β -diol decreased expression of *Hsd17b1*, supporting the idea that the 3 β -diol pathway does not increase neuroestrogen synthesis in the VMH. Furthermore, treatments involving 3 β -diol tended to decrease expression of *Stard1*, *Cyp11a1*, and *Hsd3b1*, suggesting that the VMH is not as active in neurosteroid synthesis as other hypothalamic regions, such as the mPOA. Indeed, aromatase expression is lower in the VMH than the mPOA (Stanic et al., 2014), suggesting a limited ability of the VMH to produce neuroestrogen. Therefore, modulation of steroidogenic enzymes by inhibition or activation of the 3 β -diol pathway is nuclei-specific.

4.4.3 Functional significance of 3 β -diol in the mPOA

What is the functional significance of the 3 β -diol pathway? 3 β -diol was initially discovered in the prostate, where it was proposed to function as the predominant ligand of ERs (Weihua et al., 2002). The aromatase gene contains both EREs and androgen response elements (Harada et al., 1993), suggesting regulation through a synergy of nuclear hormone receptors. In amygdala cultures, the effect of 3 β -diol on aromatase expression is dependent upon the sex chromosome complement, only taking place in female cultures (Cisternas et al., 2017, Cisternas et al., 2015). Preliminary data from our lab supports the idea that this is a sexually dimorphic pathway, as letrozole and dutasteride are ineffective at inhibiting neuroestrogen production and *Cyp19a1* expression in male hypothalamic slices (data not shown). Sex dimorphisms may occur at the level of 3 β -diol degradation as well as 3 β -diol production. 3 β -diol production is irreversible, and the effects of 3 β -diol are terminated by its conversion to inactive 6 α - or 7 α -triols by the *Cyp7b1* enzyme (Sundin et al., 1987).

Brain aromatase activity does not seem to vary across the oestrous cycle (Roselli et al., 1984), so the 3 β -diol pathway may be important for maintaining neuroestrogen concentrations when peripheral levels fall. Stress is known to suppress the hypothalamic-pituitary-ovarian axis (Whirledge and Cidlowski, 2013), yet acute stress has been shown to enhance hypothalamic aromatase activity in quail (Dickens et al.,

2013) and neuroestrogen concentrations in OVX rats (Liu et al., 2011). In the paraventricular nucleus of the hypothalamus (PVN), 3 β -diol increases oxytocin expression via ER β (Hiroi et al., 2013), inhibiting the activity of the hypothalamic-pituitary-adrenal axis (Neumann et al., 2000) and counteracting stress. It is known that ER β decreases anxiety-like behaviour in rodents (Imwalle et al., 2005, Hughes et al., 2008), and the mPOA, which expresses considerable amounts of ER β (Mitra et al., 2003), has been implicated in anxiolytic behaviours (Zhang et al., 2021). Taken together, the importance of 3 β -diol signalling in the mPOA is contextual and may be important to alleviate stress.

4.4.4 Effect of ER modulators

Neurosteroid synthesis: To investigate the contribution of ERs α and β to neuroestrogen synthesis and steroidogenic enzyme expression in the hypothalamus, we incubated slices containing the mPOA or VMH with ER modulators. As with the 3 β -diol experiments, the VMH proved less labile to regulation compared to the mPOA. Still, in both the mPOA and VMH, we found no significant effect of the ER α agonist PPT on neurosteroid concentration in aCSF or aromatase expression in tissue punches. Despite 3 β -diol increasing aromatase expression presumably through ER β , there was no effect of the ER β agonist DPN on neuroestrogen concentrations or aromatase expression in neither the mPOA nor the VMH. This discrepancy may be due to ligand-dependent effects on ER-mediated gene transcription and/or signalling cascades. ERs are ligand-regulated transcription factors that form dimers upon ligand binding (Tamrazi et al., 2002). Homo- and heterodimers can have differing kinetic stability (Tamrazi et al., 2002), and can have different transcriptional and physiological effects. For example, ER α/α homodimers promote, while ER β/β homodimers inhibit, E₂-dependent growth of mammary epithelial cells (Song et al., 2022), a process linked to the induction of aromatase (Díaz-Cruz et al., 2011). It is possible for ER α/β heterodimers to form with select compounds (Coriano et al., 2018), though the functional effects of the heterodimer are not well understood. It is possible that E₂ or DPN stimulates the formation of a particular type of dimer, whereas 3 β -diol stimulates the formation of another, giving rise to different transcriptional and functional effects on aromatase.

The ER antagonist ICI given alone tended to decrease aromatase expression in the mPOA, and when administered in combination with PPT, decreased neuroestrogen concentration in mPOA-aCSF. There are two potential reasons for this: first, ERs may be necessary for maintaining neuroestrogen synthesis, and their inhibition decreases

it. Although ICI is an ER antagonist, it is an agonist of the membrane-limited ER, G protein-coupled oestrogen receptor (GPER) 1 (Filardo et al., 2002). Thus, the second potential reason is that GPER1 antagonises the effect of ER-mediated neuroestrogen synthesis. One of the reasons neurosteroid synthesis is believed to occur is to allow discrete regions of the brain to rapidly reach the higher concentrations of E₂ required for membrane-initiated E₂ signalling (Prossnitz and Barton, 2014). Hence, this could be negative feedback by membrane ERs such as GPER1 to dampen non-genomic signalling by decreasing the amount of neuroestrogen produced. This may also be a neuroprotective effect, since too much E₂ has been shown to drive GABA-mediated excitotoxicity and widespread cell death in the neonatal rat brain (Nuñez et al., 2003).

Effect on ER modulators on ER expression: Whilst PPT and DPN had no effect on the expression of their respective target receptors in the hypothalamus, DPN administered with ICI significantly increased ER α expression solely in the mPOA. In PC-3 prostate cancer cells, DPN was shown to increase ER α mRNA but not ER β mRNA, suggesting a crosstalk between ERs to regulate expression of each other (Pisolato et al., 2016). On the other hand, ICI has been shown to upregulate ER α expression in the liver of teleost fish (Pinto et al., 2006). This action is surprising, since ICI is a selective ER degrader, effectively removing ER α from the cell (Wardell et al., 2011). This suggests that ER α protein levels may influence ER α mRNA expression and needs to be further explored.

Effect on ER modulators on steroidogenic enzyme expression: The effect of ER modulators on steroidogenic enzyme expression was mixed. In the mPOA, PPT increased the expression of *Hsd3b1*; this has been shown previously in the rat hypothalamus (Soma et al., 2005). The ER-mediated expression in *Hsd3b1* is prevented by ICI (Nenadov et al., 2018). Similarly, we found a tendency for lower expression in the mPOA with treatment paradigms involving ICI, which may account for the tendency for decreased neuroestrogen synthesis with ICI treatment. However, ICI was found to increase the expression of *Srd5a1* in the mPOA, though the significance of this is unknown. In the VMH, ICI combined with DPN was the only treatment that induced changes in mRNA of steroidogenic enzymes. ICI administered with DPN increased *Cyp11a1* expression and decreased *Srd5a2* expression. Again, the VMH was much less labile than the mPOA.

4.4.5 Gonadal status does not affect neurosteroidogenesis in the female mouse hypothalamus

Despite the documented expression of steroidogenic enzymes in the brain (King et al., 2002, Kohchi et al., 1998, Stanic et al., 2014), and the ability of the brain to synthesise neuroestrogen (Kretz et al., 2004a, Schlinger et al., 2014), the question of why this is important in the female, where E₂ is readily available from the ovaries, remains (Cornil, 2018). To answer this question, it is necessary to understand how neurosteroidogenesis is regulated in the absence of the ovaries.

Effect on neuroestrogen synthesis and steroidogenic enzyme expression: In punch dissections of the mPOA and VMH, we found no difference in neuroestrogen concentrations between gonadally intact, short- or long-term OVX mice, or OVX mice treated with EB 72 and 48 h prior to sacrifice. In a similar vein, hypothalamic aromatase activity is not significantly different between OVX and cycling rats at any stage of their oestrous cycle, although mRNA expression was not measured (Roselli et al., 1984). Despite the lack of observed effect on neuroestrogen concentrations, EB administration to OVX mice resulted in decreased *Cyp19a1* expression. We also found a decrease in *Stard1* and *Cyp11a1* expression in OVX mice supplemented with EB, though it is not clear why we did not detect a corresponding decrease in neuroestrogen concentration in hypothalamic tissue punches. Though it could be argued that EB was stored in the brain prior to sacrifice, this is unlikely as steroid hormones cannot easily be stored due to their lipophilic properties (Holst et al., 2004). This requires further exploration.

Previous literature has indicated that peripheral E₂ is necessary for neuroestrogen synthesis (Nelson et al., 2016, Prange-Kiel et al., 2013), yet in OVX rats treated with EB, mPOA aromatase mRNA expression was not significantly different to OVX rats treated with vehicle (Tabatadze et al., 2014b). This suggests that aromatase mRNA is not the target for increased neuroestrogens in the presence of circulating E₂.

Though long-term OVX did not change neuroestrogen concentrations, it resulted in an increase in neurotestosterone solely in the mPOA and increased hypothalamic *Hsd3b1* expression. To our knowledge, alterations in androgen production in the female brain as a result of OVX have not been reported. OVX leads to a gradual increase in extragonadal E₂ synthesis; the main contributing tissues being the liver and subcutaneous white adipose tissue (Zhao et al., 2005). Whether this occurs in the brain has not been properly investigated. However, our data suggests that the

increased levels of *Stard1*, *Cyp11a1*, and *Hsd3b1* in long-term OVX mice give the brain the capacity to synthesise steroids *de novo*.

Effect on ER expression: Recently, it was found that residual ERE-dependent transcription takes place in the hippocampus in the short-term following OVX, but not in the long-term (Baumgartner et al., 2019). We found no decrease in neuroestrogen or steroidogenic enzyme expression with long-term OVX, though we did find decreased hypothalamic ER expression. In the hippocampus and prefrontal cortex of middle-aged rats, ER expression declines after extended deprivation of ovarian hormones (Bohacek and Daniel, 2009). Thus, the decrease in ERE-dependent transcription in OVX rodents is likely caused by decreased receptor expression, as opposed to decreased neuroestrogen synthesis.

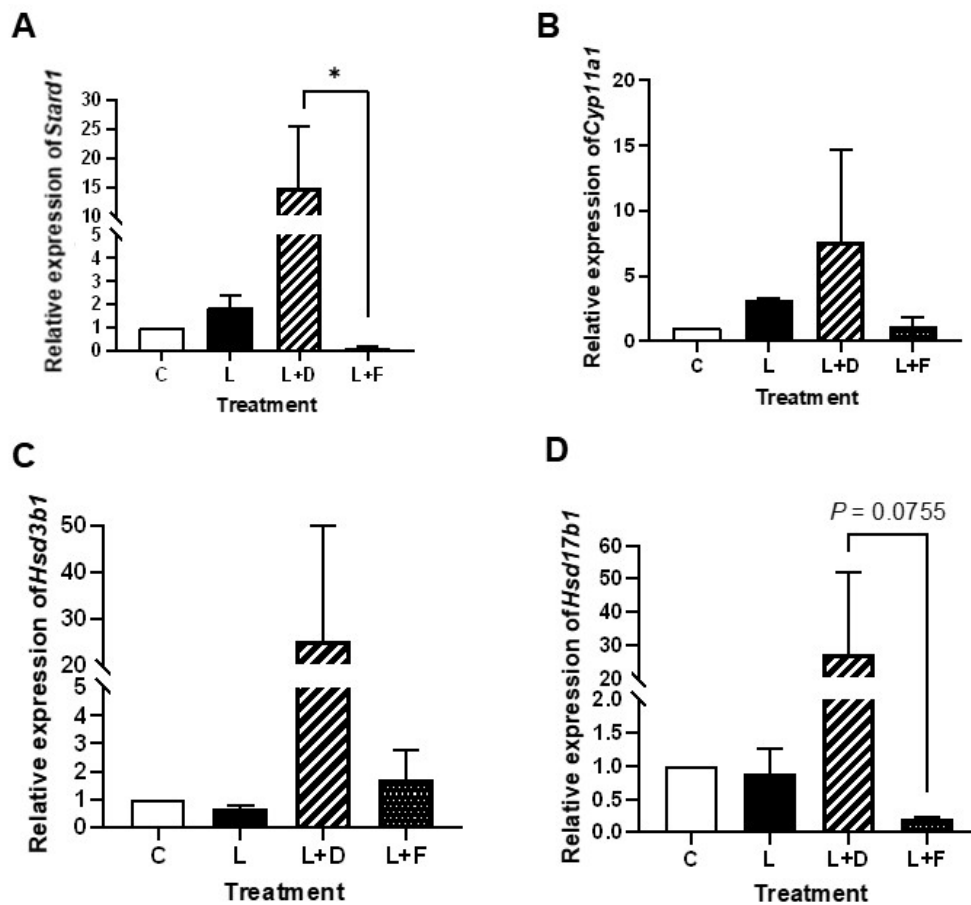
At present, it is difficult to conclude whether ovarian E₂ is necessary for neuroestrogen production, though our data shows E₂ can still be measured in the brain after OVX, regardless of duration of OVX. Previous studies from our lab have demonstrated the presence of E₂ in *ex vivo* brain slices (Chapter 3), which suggests that neurosteroidogenesis in the hypothalamus is *independent* of gonadal status in the female mouse. This is difficult to compare with other studies in the literature since there appears to be regional differences in the dependence on gonadal hormones. In rats, castration reduced aromatase activity in the POA but not in the amygdala (Roselli et al., 1984), and it has since been suggested that brain aromatase is gonad-sensitive in the hypothalamus but gonad-insensitive in the limbic system (Shay et al., 2018, Roselli et al., 1985b).

We found no difference in ER expression or neuroestrogen or neurotestosterone concentrations in the OVX group that was supplemented with EB in either the mPOA or VMH. Differences in hormonal priming regimens may contribute to differing results. High dosages of EB administered 72 and 48 h prior to sacrifice, as in the present study and in Tabatadze et al., (2014) produce supraphysiological levels of E₂ shortly after injection, which are metabolised to the physiological range within 24 h (Woolley and McEwen, 1993). Other studies have prolonged exposure to ovarian hormones following OVX using E₂ implants, resulting in region-specific alterations in ER expression that were reported in the hippocampus and prefrontal cortex (Bohacek and Daniel, 2009). EB supplementation also produces a dose-dependent increase in brain E₂ concentrations in OVX rats (Li and Gibbs, 2019), suggesting species level differences. There are also no comparable studies that have investigated both neurosteroid concentrations in conjunction with steroidogenic enzyme expression.

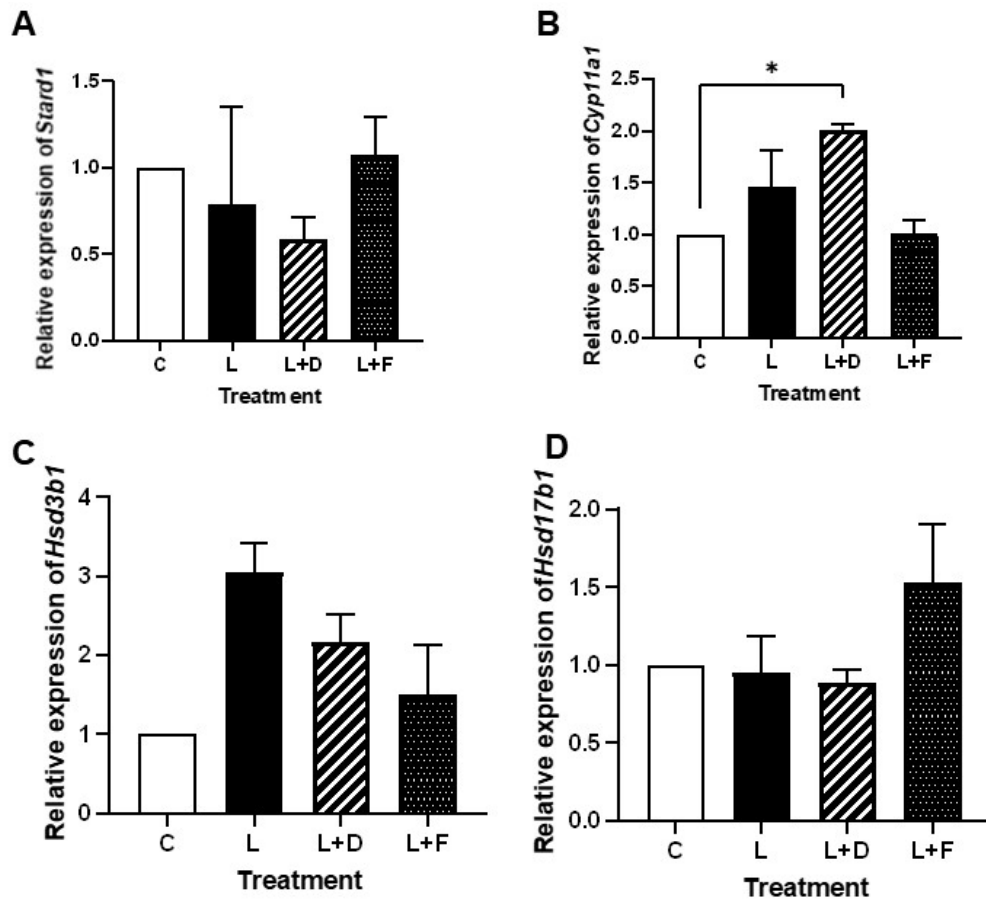
4.5 Summary

We have illustrated the presence of a novel pathway regulating neuroestrogen synthesis in the female mouse hypothalamus that is region-specific and possibly context dependent. Further experimentation is required to establish the functional significance of this pathway in the female mouse hypothalamus. We suspect that the 3 β -diol pathway initiates ligand-specific effects via ER β since we did not observe similar outcomes with the ER β -specific agonist DPN. It is possible that dosage lies at the heart of the inability to effectively inhibit E₂ production in the current system, which is restricted due to crossreactivity with letrozole. However, previous studies have shown effective reductions in E₂ synthesis in hippocampal slice cultures incubated with as little as 10⁻⁹ M letrozole (Kretz et al., 2004a). Neuroestrogen synthesis in the female mouse hypothalamus may be further regulated by ERs and ovarian steroids, though the intricacies of all these regulatory mechanisms demands further investigation. In light of previous findings that 3 β -diol exerts an anxiolytic effect in the male mouse (Lund et al., 2004), it is interesting to speculate that inhibition of 3 β -diol production produces an anxiogenic effect in the female. The behavioural significance of 3 β -diol pathway regulating neuroestrogen synthesis in the female mouse warrants further investigation.

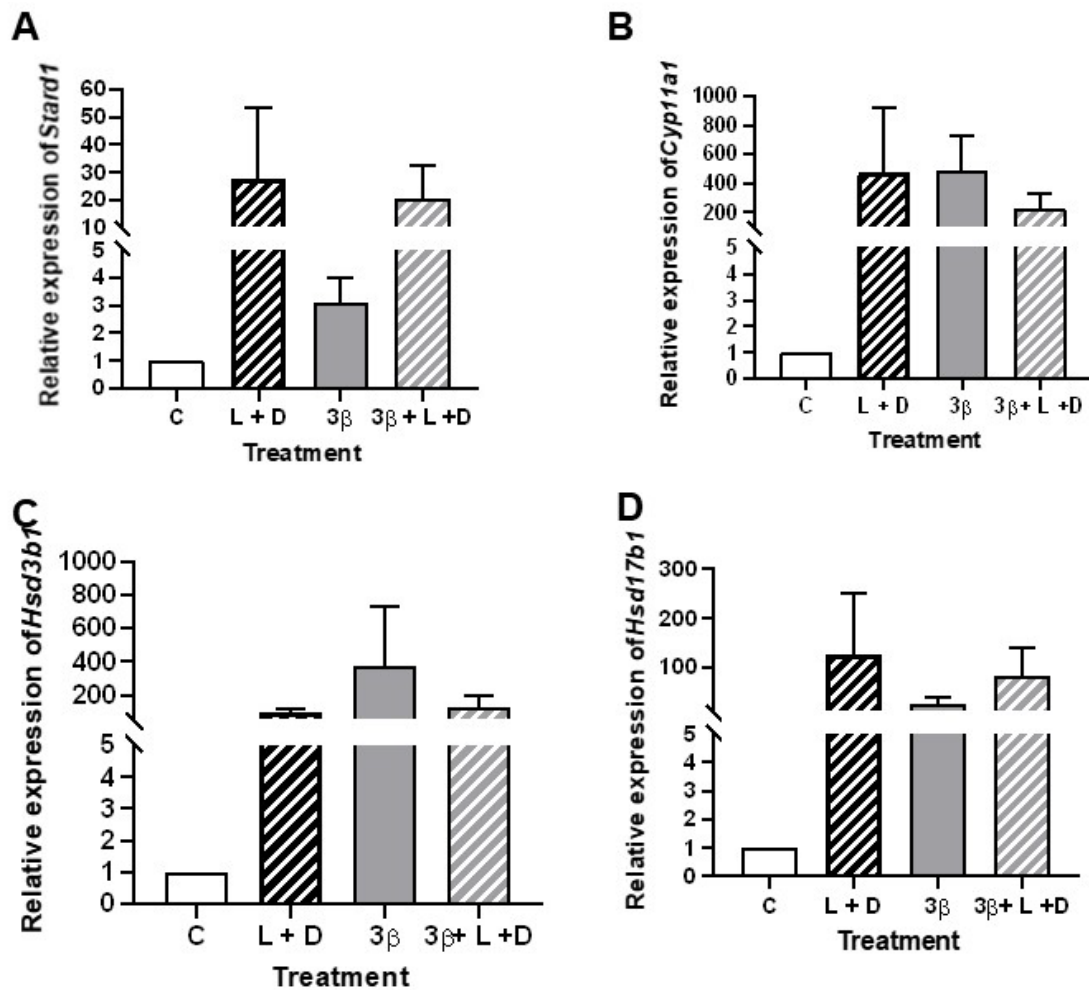
4.6 Supplementary information



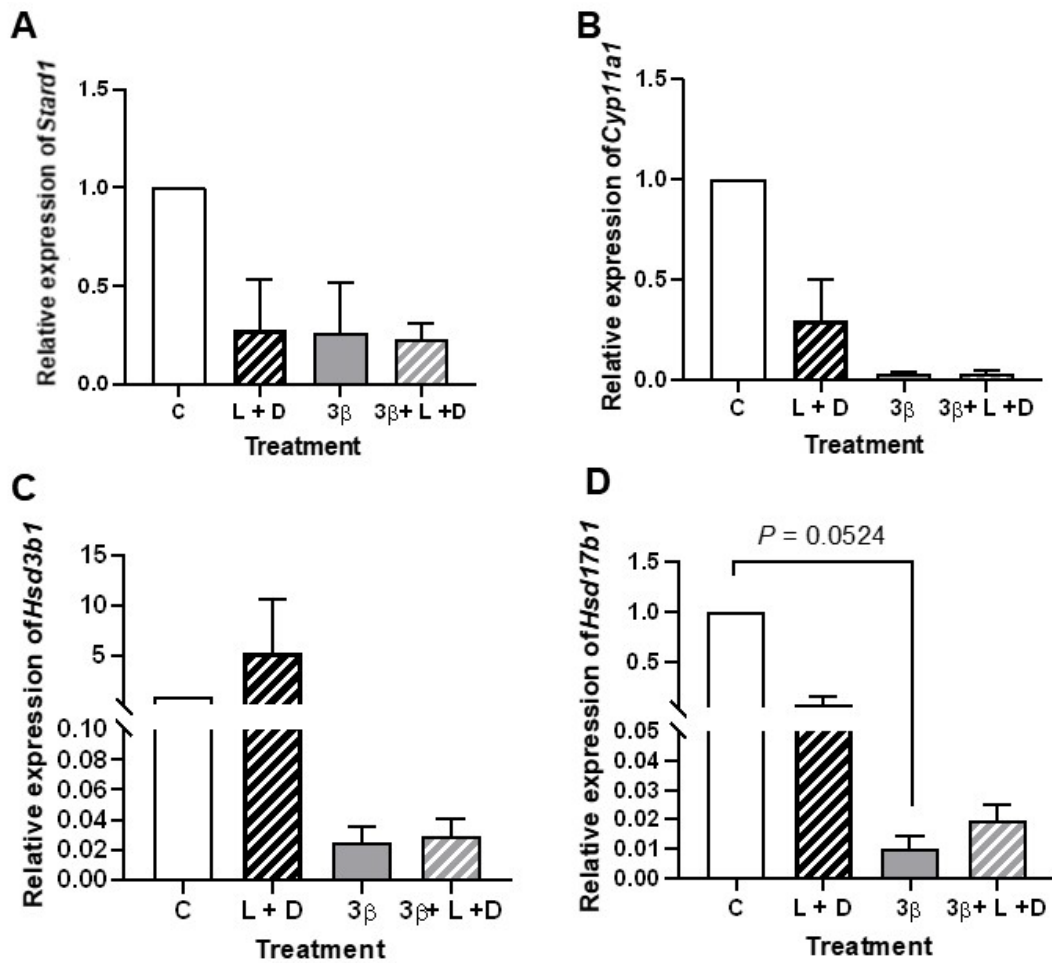
Supplementary Figure S4.1. Effect of the inhibition of aromatase and 5 α -reductase on steroid enzyme expression in the adult female mouse medial preoptic area. Slices were incubated for 24 h with vehicle control (C), 10⁻⁸ M letrozole (L), with and without 10⁻⁸ M dutasteride (L + D) or 10⁻⁸ M finasteride (L + F). Punch dissections of the medial preoptic area (mPOA) from 4 animals were pooled into one, such that $n = 3$ from a total of 12 animals, which were used to measure gene expression. Expression levels, relative to the housekeeping gene (*Actb*) are shown for *Stard1* (A), *Cyp11a1* (B), *Hsd3b1* (C), and *Hsd17b1* (D). For parametric datasets, differences were established by a one-way ANOVA with Bonferroni's multiple comparisons *post hoc*; nonparametric datasets were compared by a Kruskal-Wallis test with Dunn's multiple comparisons *post hoc*. * $P < 0.05$.



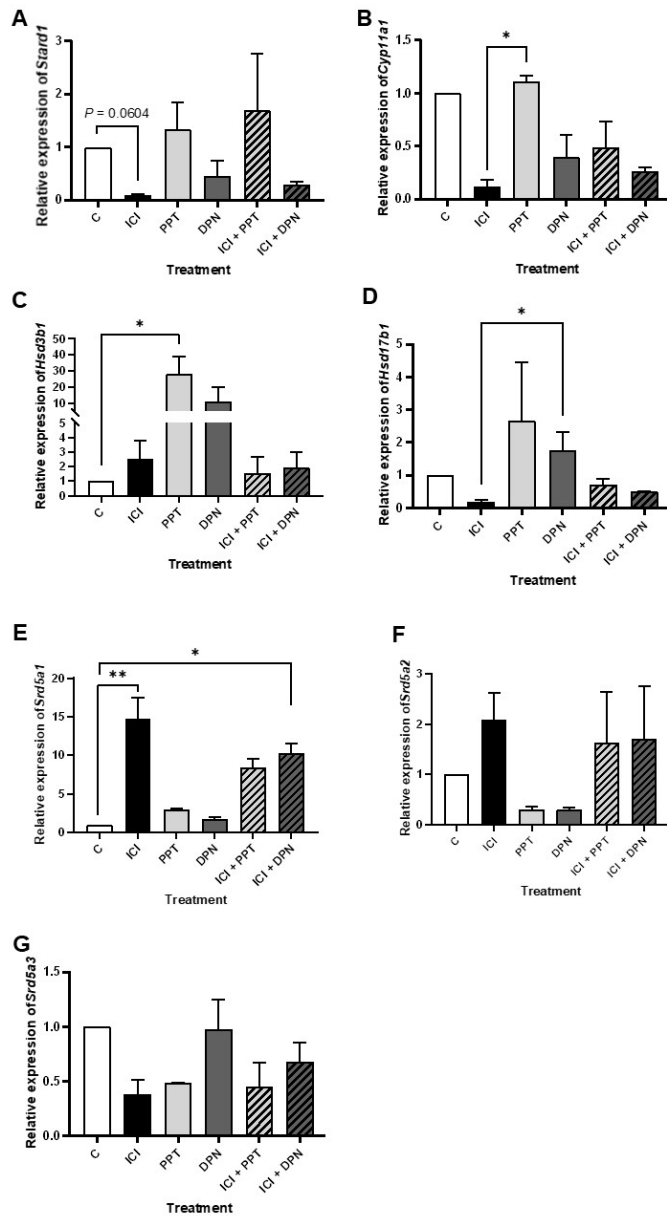
Supplementary Figure S4.2. Effect of the inhibition of aromatase and 5 α -reductase on steroid enzyme expression in the adult female mouse ventromedial hypothalamus. Slices were incubated for 24 h with vehicle control (C), 10^{-8} M letrozole (L), with and without 10^{-8} M dutasteride (L + D) or 10^{-8} M finasteride (L + F). Punch dissections of the ventromedial hypothalamus (VMH) from 4 animals were pooled into one, such that $n = 3$ from a total of 12 animals, which were used to measure gene expression. Expression levels, relative to the housekeeping gene (*Actb*) are shown for *Stard1* (A), *Cyp11a1* (B), *Hsd3b1* (C), and *Hsd17b1* (D). For parametric datasets, differences were established by a one-way ANOVA with Bonferroni's multiple comparisons *post hoc*; nonparametric datasets were compared by a Kruskal-Wallis test with Dunn's multiple comparisons *post hoc*.



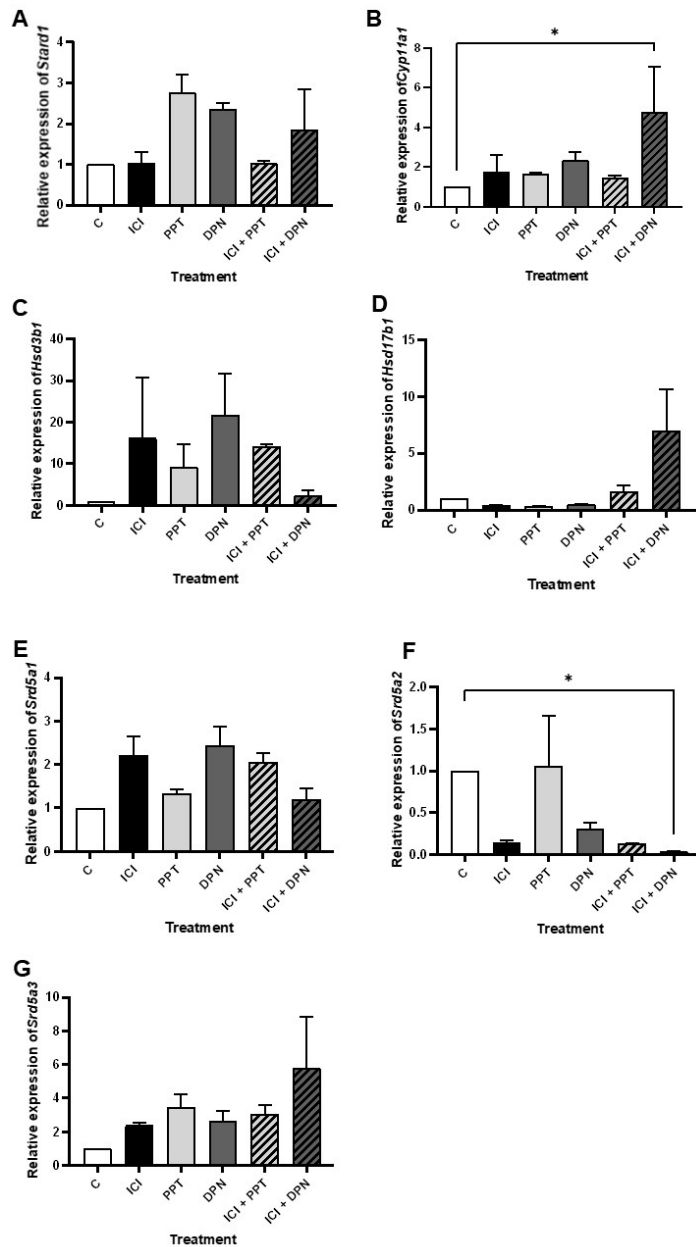
Supplementary Figure S4.3. The effect of 3 β -diol on steroid enzyme expression in the adult female mouse mPOA. Slices were incubated for 24 h with vehicle control (C), 10⁻⁸ M letrozole with 10⁻⁸ M dutasteride (L + D), 10⁻⁸ M 3 β -diol (3 β), or a combination of all three treatments (3 β + L + D). Punch dissections of the mPOA from 4 animals were pooled into one, such that $n = 3$ from a total of 12 animals, which were used to measure gene expression. Expression levels, relative to the housekeeping gene (*Actb*) are shown for *Stard1* (A), *Cyp11a1* (B), *Hsd3b1* (C), and *Hsd17b1* (D). For parametric datasets, differences were established by a one-way ANOVA with Bonferroni's multiple comparisons *post hoc*; nonparametric datasets were compared by a Kruskal-Wallis test with Dunn's multiple comparisons *post hoc*.



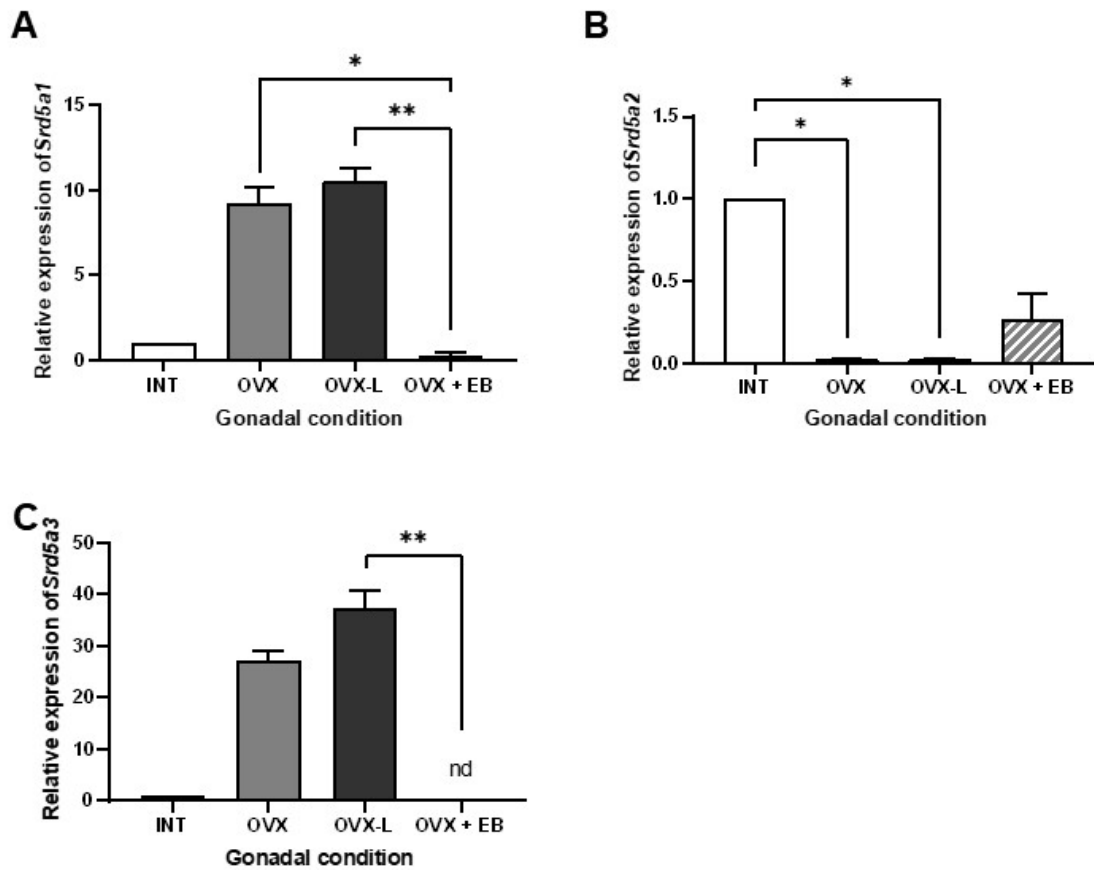
Supplementary Figure S4.4. The effect of 3 β -diol on steroid enzyme expression in the adult female mouse VMH. Slices were incubated for 24 h with vehicle control (C), 10⁻⁸ M letrozole with 10⁻⁸ M dutasteride (L + D), 10⁻⁸ M 3 β -diol (3 β), or a combination of all three treatments (3 β + L + D). Punch dissections of the VMH from 4 animals were pooled into one, such that *n* = 3 from a total of 12 animals, which were used to measure gene expression. Expression levels, relative to the housekeeping gene (*Actb*) are shown for *Stard1* (A), *Cyp11a1* (B), *Hsd3b1* (C), and *Hsd17b1* (D). For parametric datasets, differences were established by a one-way ANOVA with Bonferroni's multiple comparisons *post hoc*; nonparametric datasets were compared by a Kruskal-Wallis test with Dunn's multiple comparisons *post hoc*.



Supplementary Figure S4.5. Effect of oestrogen receptor modulators on steroid enzyme expression in the adult female mouse mPOA. Slices were incubated for 24 h with vehicle control (C), 10^{-8} M ICI 182,780 (ICI), 10^{-9} M PPT, 10^{-9} M DPN, or a combination (ICI + PPT, ICI + DPN). Punch dissections of the mPOA from 4 animals were pooled into one, such that $n = 3$ from a total of 12 animals, which were used to measure gene expression. Expression levels, relative to the housekeeping gene (*Actb*) are shown for *Stard1* (A), *Cyp11a1* (B), *Hsd3b1* (C), *Hsd17b1* (D), *Srd5a1* (E), *Srd5a2* (F), and *Srd5a3* (G). For parametric datasets, differences were established by a one-way ANOVA with Bonferroni's multiple comparisons *post hoc*; nonparametric datasets were compared by a Kruskal-Wallis test with Dunn's multiple comparisons *post hoc*. ** $P < 0.01$, *** $P < 0.001$, vs C. \$\$\$ $P < 0.001$, \$\$\$\$ $P < 0.0001$, vs ICI.



Supplementary Figure S4.6. Effect of oestrogen receptor modulators on steroid enzyme expression in the adult female mouse VMH. Slices were incubated for 24 h with vehicle control (C), 10^{-8} M ICI 182,780 (ICI), 10^{-9} M PPT, 10^{-9} M DPN, or a combination (ICI + PPT, ICI + DPN). Punch dissections of the VMH from 4 animals were pooled into one, such that $n = 3$ from a total of 12 animals, which were used to measure gene expression. Expression levels, relative to the housekeeping gene (*Actb*) are shown for *Stard1* (A), *Cyp11a1* (B), *Hsd3b1* (C), *Hsd17b1* (D), *Srd5a1* (E), *Srd5a2* (F), and *Srd5a3* (G). For parametric datasets, differences were established by a one-way ANOVA with Bonferroni's multiple comparisons *post hoc*; nonparametric datasets were compared by a Kruskal-Wallis test with Dunn's multiple comparisons *post hoc*. * $P < 0.05$.



Supplementary Figure S4.7. Effect of ovariectomy on the expression of steroidogenic enzymes related to the 3β -diol pathway in the adult female mouse hypothalamus. Hypothalami were excised from hemispheres of mice that were intact (INT), short-term ovariectomised (OVX), long-term ovariectomised (OVX-L), or short-term ovariectomised and treated with oestradiol benzoate (OVX + EB) and used to measure gene expression. Expression levels, relative to the housekeeping gene (*Actb*) are shown for *Srd5a1* (A), *Srd5a2* (B), and *Srd5a3* (C). For parametric datasets, differences were established by a one-way ANOVA with Bonferroni's multiple comparisons *post hoc*; nonparametric datasets were compared by a Kruskal-Wallis test with Dunn's multiple comparisons *post hoc*. * $P < 0.05$, ** $P < 0.01$.

Chapter 5

Behavioural and Neuroarchitectural Relevance of Neuroestrogens and 3 β -diol in the Adult Female Mouse

5.1 Introduction

The social behaviour network (SBN) is a bidirectional and reciprocally connected network consisting of six key brain nuclei: the medial amygdala (meA) and bed nucleus of stria terminalis (BNST), lateral septum (LS), medial preoptic area (mPOA), anterior hypothalamus (AH), and the ventromedial hypothalamus (VMH) (Newman, 1999). Among these, four nodes are located in the hypothalamus (Goodson, 2005), a key region underlying innate social behaviours such as reproductive behaviour (Pfaff and Sakuma, 1979, Micevych and Meisel, 2017) and parental behaviour (Fang et al., 2018). The SBN is profoundly regulated by oestrogens, specifically 17 β -oestradiol (E₂) (Newman, 1999, Wood and Newman, 1995). Emerging evidence suggests that E₂ exerts profound effects on brain regions involved in emotional regulation in both murine models and humans. A reduction in E₂ can increase anxiety (Berent-Spillson et al., 2017, Krężel et al., 2001), an adaptive response characterised by a state of apprehension associated with heightened arousal and vigilance (Craske and Stein, 2016). Emotional regulation is controlled by the limbic system, which consists of several nuclei in the cerebral cortex, the amygdala, hippocampus, and hypothalamus (Rajagopalan et al., 2017). Recently, the mPOA has been shown to be important in the induction of anxiety in rodents. Optogenetic stimulation of glutamatergic neurones in the mPOA of female mice enhances anxious behaviours by reducing time spent in the centre of the open field test (OFT) and reducing time spent in the open arms of the elevated plus maze (EPM) (Zhang et al., 2021). Conversely, optogenetic stimulation of GABAergic neurones in the mPOA of female mice alleviated anxious behaviours (Zhang et al., 2021). Anxiety may also be antagonistically mediated by oestrogen receptor (ER) subtypes. Subcutaneous injection of the ER β agonist diarylpropionitrile (DPN) significantly increased the number of open arm entries and time spent in the open arms in the EPM (Lund et al., 2005). The ER α -selective agonist propylpyrazoletriol (PPT) significantly increased defecations and time spent grooming (Lund et al., 2005); under high stress, mice are more likely to display short, rapid, and erratic bouts of grooming that do not follow a particular pattern (Denmark et al., 2010). Female rats given an infusion in the mPOA with a small hairpin RNA against ER α spend more time in the light compartment in the light-dark test (Spiteri et al., 2012). Together, this implies ER α promotes anxiogenic behavioural effects while ER β promotes anxiolytic effects.

The contribution of neuroestrogens to anxiety remains poorly understood. In forebrain-specific aromatase knockout (ArKO) mice (which includes loss of aromatase in the hypothalamus), levels of anxiety in the OFT are similar to FLOX controls of the same

sex and gonadal status (Lu et al., 2019). However, in fear conditioning tests, mice with forebrain knockout of aromatase showed a significant decrease in contextual, but not cued, fear memory compared to FLOX controls of the same sex and gonadal status (Lu et al., 2019). This is believed to be dependent on the hippocampus, a key limbic region, which showed reduced long-term potentiation (LTP) amplitude in forebrain-specific ArKO mice (Lu et al., 2019). Reduced LTP amplitude is a reflection of impaired synaptic plasticity, which is impaired in the hippocampus of mice that have experienced early life stress (Wang et al., 2020) or anxiety caused by noise-induced hearing loss (Pak et al., 2022). To our knowledge, the specific contribution of neuroestrogens in the mPOA to anxiety remains unexplored.

We have previously shown the existence of a novel pathway of regulation of neuroestrogen synthesis that occurs specifically in the mPOA (Chapter 4). We found that neuroestrogen production by hypothalamic brain slices corresponding to the mPOA was only suppressed by treatment with the 5 α -reductase inhibitor dutasteride and the aromatase inhibitor letrozole; not letrozole alone. We hypothesised that letrozole treatment diverted testosterone metabolism to the non-aromatisable androgen dihydrotestosterone (DHT), which was subsequently metabolised to the ER β agonist 3 β -diol. 3 β -diol acted on ER β to increase aromatase expression, relieving competitive inhibition imposed by letrozole and restoring neuroestrogen synthesis in the mPOA. This mechanism has been described only in primary amygdala cell cultures where it shows sexual dimorphism, existing only in cultures from female rats (Cisternas et al., 2017). Preliminary data from our lab suggests the mPOA also shows the sex dimorphism (data not shown), but the physiological and functional significance of this pathway in neuroestrogen regulation in the mPOA is yet to be elucidated. 3 β -diol is thought to be an anxiolytic agent, though this has only been tested in male rats (Handa et al., 2009). Bilateral cannulation of the paraventricular nucleus (PVN), a key hypothalamic node controlling anxiety and arousal (Wu and Zetter, 2022), and delivery of 3 β -diol significantly reduces plasma corticosterone in response to restraint stress in male rats (Lund et al., 2006). Similar results are also achieved with delivery of DHT and DPN. Additionally, these compounds decrease *c-fos* mRNA expression in the PVN following restraint stress, whilst delivery of PPT significantly increases restraint-induced *c-fos* mRNA expression (Lund et al., 2006)

The mechanisms which govern the response to stressful events include neuromorphological changes, such as plasticity in dendrites and dendritic spines (Gorman and Docherty, 2010). These events have been shown to be regulated by E₂ (Woolley and McEwen, 1992, Frankfurt et al., 1990), implicating spine density as a

mechanism by which E₂ controls anxiety-like behaviours. The hypothalamus is one of the key sites for neural plasticity (Wei et al., 2021), yet few studies have investigated the plastic changes associated with E₂ in the hypothalamus. In the arcuate nucleus of the hypothalamus (ARC), a region necessary for the induction of lordosis behaviour in female rodents, E₂ treatment increases spine density in 4 h (Christensen et al., 2011). Subsequently, over time, spine density remains stable, while the existing spines undergo maturation (Christensen et al., 2011). Initially, spines appear as long, thin filipodia that are motile and transient. As they mature, they transition into stable mushroom-shaped spines characterised by larger postsynaptic densities, more AMPA receptor content, and a larger presynapse (Kasai et al., 2003). In the VMH, E₂ treatment increases spine density (Frankfurt et al., 1990), but this effect is differential across the VMH and across individual dendrites. For example, in the dorsal VMH, E₂ has no effect on spine density, whilst in the ventrolateral VMH, E₂ increases spine density on short, but not long, primary dendrites (Calizo and Flanagan-Cato, 2000), on neurones that do not express ER α . To our knowledge, how E₂, or lack of, affects neuroarchitecture in the mPOA has not been investigated.

In this study, we investigated the ability of androgenic metabolites to influence behaviours that denote anxiety and exploration in female mice using subcutaneous injection with inhibitors of this metabolite, 3 β -diol. We hypothesised that animals treated with the aromatase inhibitor letrozole would not show anxious behaviour, as we have previously shown that it is ineffective in reducing E₂ in *ex vivo* hypothalamic brain slices. We also hypothesised that animals treated with dutasteride and letrozole would show greater levels of anxiety due to blockade of neuroestrogen synthesis. Following behavioural analyses, we used Golgi staining to investigate the neuroarchitectural changes in the mPOA that may underlie anxiety in female mice.

5.2 Methods

5.2.1 Animals

Mice were randomly assigned to one of four treatment groups (letrozole + dutasteride, L + D, $n = 6$; letrozole + vehicle, L, $n = 8$; 2x vehicle control + ovariectomy, OVX, $n = 6$; 2x vehicle control + intact, C, $n = 7$) and group-housed accordingly as described in section 2.1 for animals kept at the University of Tsukuba. Mice were OVX as described in section 2.2.1. Animals were weighed before receiving intraperitoneal (i.p.) injections (see section 2.2.3) to ensure appropriate dosages were delivered.

Behavioural tests (open field test, OFT; elevated plus maze, EPM; light-dark transition test, LDT; social investigation test, SIT; see section 2.3) were carried out according to the timeline shown in **Fig. 5.1**. The order of testing in behavioural tests was counterbalanced between different treatment groups.

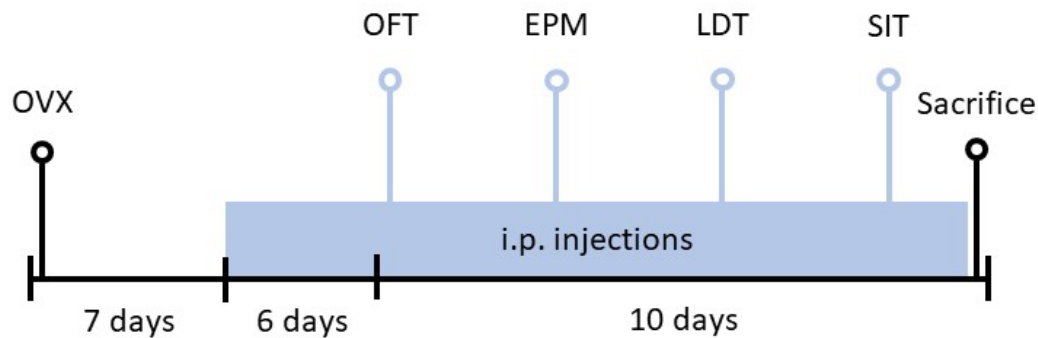


Figure 5.1. Experimental timeline. Mice were sorted into treatment groups and relevant mice were ovariectomised (OVX) 1 week before injections began. Intraperitoneal (i.p.) injections were administered during the light phase at the same time each day. Mice were weighed daily just before receiving their injection to ensure correct dosing of vehicle, letrozole, and/or dutasteride. Mice received injections for 6 days before behavioural testing began. All tests were conducted 48 h apart, with the exception of the light-dark test (LDT), which took place 72 h after the elevated plus maze (EPM) due to a weekend. Mice from different treatment groups were counterbalanced with respect to the order of testing in each of the behavioural tests. Animals were sacrificed on the 17th day following the first injection and did not receive an injection on this day. Animals were sacrificed at the same times as they previously received injections. OFT, open field test. SIT, social investigation test.

5.2.2 Samples for Golgi staining and hormone measurements

Following sacrifice, mice were transcardially perfused (see section 2.4) using the fixative provided in the sliceGolgi Kit (Bioenno Tech 003760). Trunk blood was collected and plasma was prepared as described in section 2.6. Brains were cut into hemispheres using a razor blade. One hemisphere was used for Golgi staining (see section 2.13). The hypothalamus of the second hemisphere was excised and

hormones extracted by solid phase extraction (see section 2.10). Hormones in brain tissue and plasma were measured by ELISAs as described in section 2.11.

5.2.3 Statistical analysis

Statistical analysis and presentation of results is as described in section 2.15.

5.3 Results

5.3.1 Treatment can cross the blood brain barrier to alter hypothalamic E₂ concentration

The concentrations and route of the inhibitors used have previously been shown to cross the blood brain barrier (Litim et al., 2017, Chaiton et al., 2019). Though treatments were administered by i.p. injection, there was no difference in plasma E₂ concentration between groups (**Fig. 5.2A**). Animals administered letrozole or letrozole and dutasteride had over double the amount of testosterone in plasma compared to controls (L, 15.87 ± 6.11 pg/ml, L + D, 15.12 ± 8.93 pg/ml vs C, 7.17 ± 6.53 pg/ml), though statistical analysis revealed no differences between groups (**Fig 5.2C**). In excised hypothalami, for which hormones were extracted, letrozole-treated mice tended towards having significantly greater E₂ concentrations than any other treatment group (L vs C, $P = 0.05$, vs OVX, $P = 0.05$) (**Fig. 5.2B**). A non-parametric Mann-Whitney U test between L and L + D revealed a significantly greater concentration of E₂ in the hypothalamus of L-treated mice ($P = 0.0286$). This solidifies our previous findings [from Chapter 4] that letrozole increases neuroestrogen concentration in the mPOA, and strongly suggests that treatments were able to cross the blood brain barrier. There were no significant differences in hypothalamic testosterone concentrations between groups (**Fig. 5.2D**). A two-way ANOVA found a significant effect of tissue on E₂ and testosterone concentrations, with all groups having significantly more of each hormone in the hypothalamus than the plasma (E₂, $P < 0.0001$, testosterone, $P = 0.0247$) (**Supp. Fig. S5.1**). Bonferroni's multiple comparisons revealed that the difference in E₂ between the hypothalamus and plasma was evident in all groups (**Supp. Fig. S5.1A**). There was also a significant effect of treatment ($P = 0.0196$) and the interaction between treatment and tissue ($P = 0.0260$) on the concentration of E₂ (**Supp. Fig. S5.1A**), though the same was not observed for testosterone (**Supp Fig. S5.1B**).

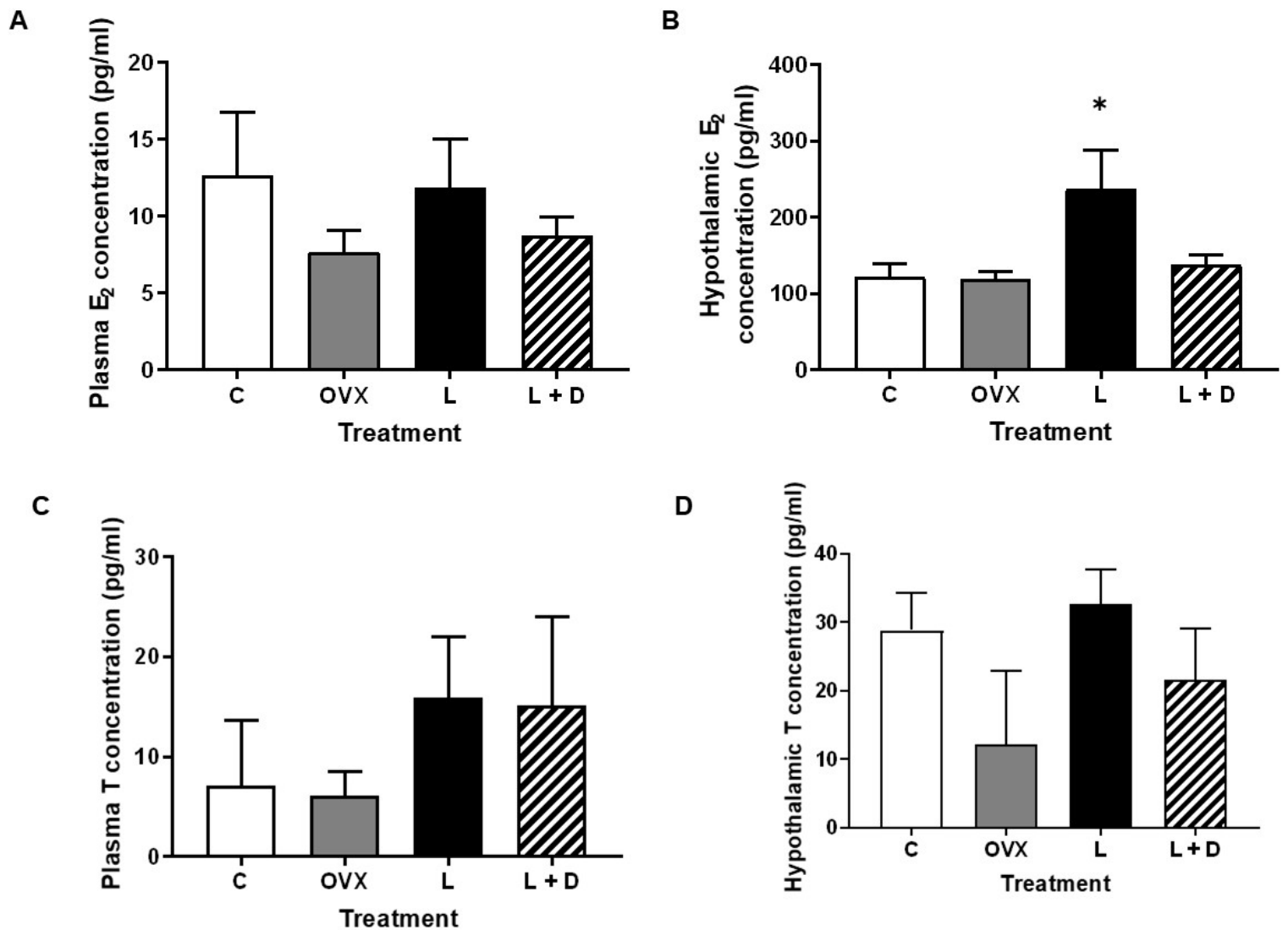


Figure 5.2. Hormone concentrations in plasma and hypothalamic extractions from adult female mice treated with steroidogenic enzyme inhibitors. Hormones were measured in plasma (**A, C**) and excised hypothalami of one hemisphere (**B, D**) for E₂ (**A-B**) and testosterone (**C-D**) from a subset of intact (C), ovariectomised (OVX), letrozole-treated (L), and letrozole + dutasteride-treated (L + D) mice following behavioural testing and sacrifice. For **A** and **C**, $n = 3$ for C and L + D; $n = 4$ for OVX, and $n = 5$ for L. For **B** and **D**, $n = 4$ for all treatment groups. All data are presented as mean \pm SEM. Differences were established by a one-way ANOVA with Bonferroni's multiple comparisons test *post hoc* or Kruskal-Wallis test with Dunn's multiple comparisons test *post hoc*, or by a Mann-Whitney U test. * $P < 0.05$ compared to all other treatment groups.

5.3.2 Systemically blocking the 3 β -diol pathway does not affect anxious behaviours in the adult female mouse

Open field test: In the OFT, the total ambulatory distance, duration, and moving speed were not significantly different between treatment groups, showing that treatment did not affect locomotor activity (**Fig. 5.3A-C**). Mice treated with letrozole + dutasteride spent significantly less time in the centre of the arena compared to mice treated with vehicle control ($P = 0.0334$) and tended to spend less time in the centre compared to mice treated with letrozole ($P = 0.0504$). There was no difference in the time spent in the centre of the arena between mice treated with letrozole + dutasteride and OVX mice ($P = 0.1127$) (**Fig. 5.3D**).

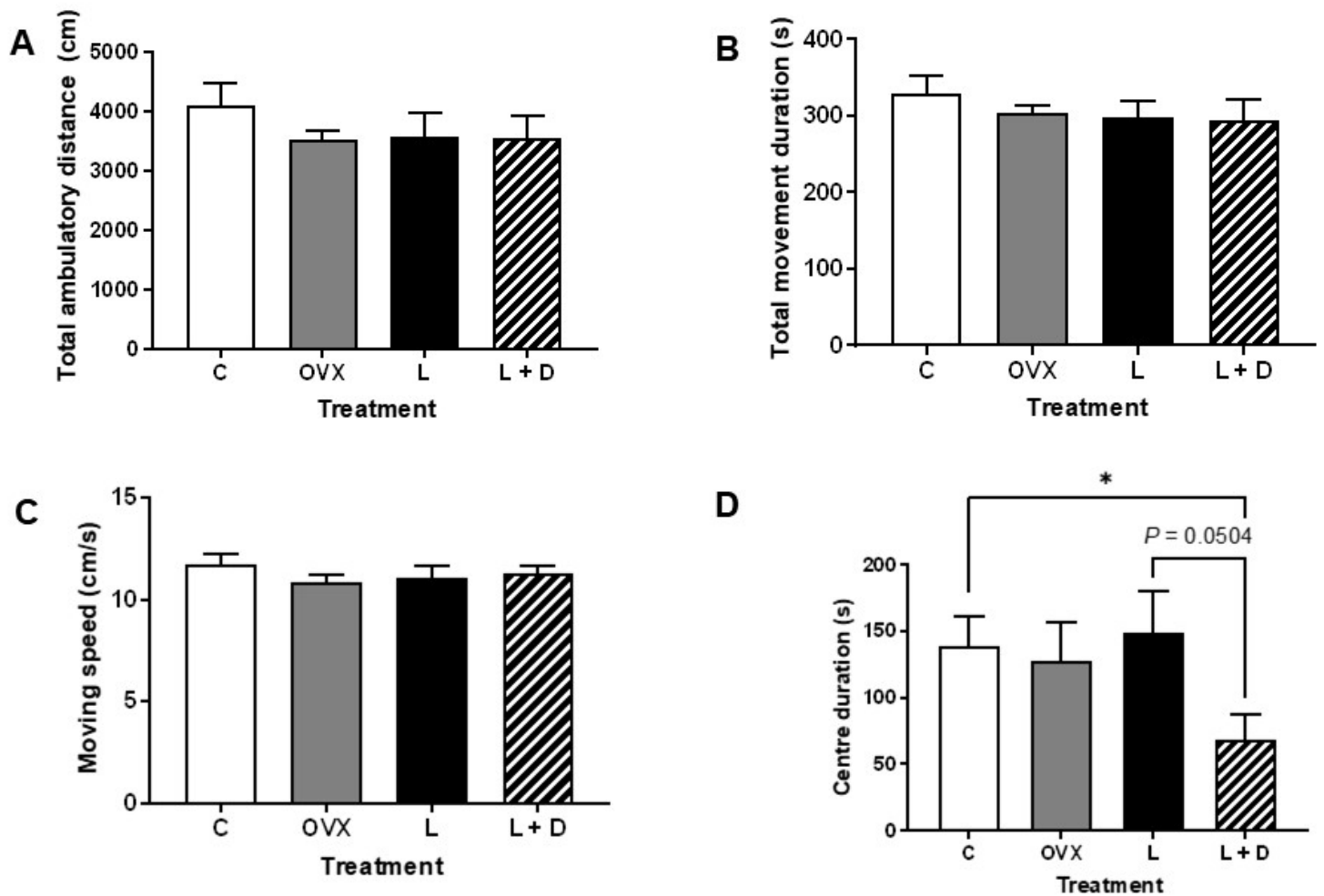


Figure 5.3. Open field test. Mice were assessed for the following behaviours: distance travelled (A), duration of movement (B), moving speed (C), and the duration of time spent in the centre of the open field arena (D). For intact mice (C), $n = 8$; ovariectomised mice (OVX), $n = 6$; letrozole-treated mice (L) $n = 8$; letrozole + dutasteride-treated mice (L + D), $n = 7$. All data are presented as mean + SEM. Parametric datasets (C, D) were analysed by a one-way ANOVA with Bonferroni's multiple comparisons *post hoc*. Nonparametric datasets (A, B) were analysed by a Kruskal-Wallis test with Dunn's multiple comparisons *post hoc*. Statistical differences in panel D were established by a student's unpaired t-test between groups.

Elevated plus maze: Treatment did not affect total ambulatory distance or movement duration in the EPM (Fig. 5.4A-B). Time spent in the open arms was variable between treatment groups (Fig. 5.4C), but mice treated with letrozole + dutasteride showed a tendency to spend more time in the closed arms compared to letrozole-treated mice ($P = 0.0893$) (Fig. 5.4D). Letrozole-treated mice showed

significantly more open arm entries than OVX mice ($P = 0.0468$), but there were no further differences between groups (**Fig. 5.5A**). Numerically, letrozole-treated mice showed a shorter latency to enter the open arms (84.38 ± 51.18 sec, vs C, 262.50 ± 100.80 sec; OVX, 224.50 ± 119.60 sec; L + D, 286.60 ± 112.20 sec) compared to other groups, though this did not reach statistical significance (**Fig. 5.5B**). Time spent in the centre square, the cross-section between all four arms, was not different between treatment groups, though letrozole + dutasteride mice spent numerically less time in this portion of the maze (71.43 ± 27.05 sec vs C, 99.25 ± 33.04 sec; OVX, 184.10 ± 75.42 sec; L, 169.8 ± 49.11 sec), presumably due to a greater amount of time in the closed arms (**Fig. 5.5C**). The amount of time spent immobile was not different between treatment groups (**Fig. 5.5D**).

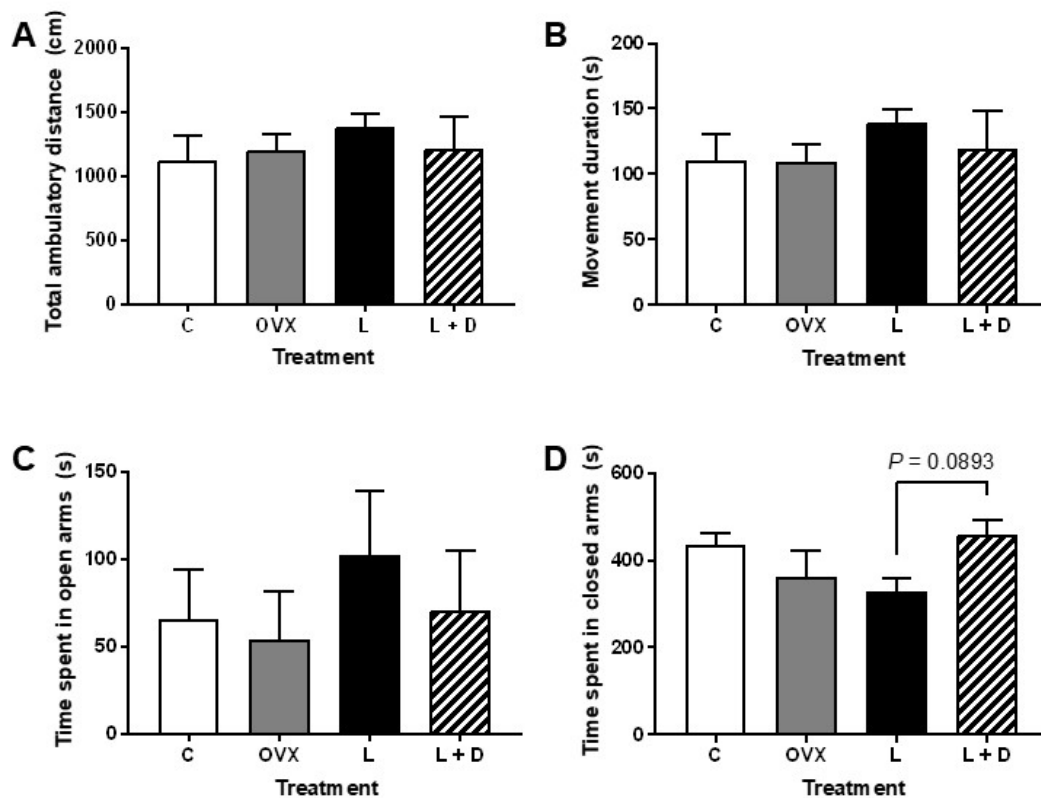


Figure 5.4. Elevated plus maze (i). Mice were assessed for the following behaviours: distance travelled (**A**), duration of movement (**B**), time spent in the open arms (**C**), time spent in the closed arms (**D**). For intact mice (C), $n = 8$; ovariectomised mice (OVX), $n = 6$; letrozole-treated mice (L), $n = 8$; letrozole + dutasteride-treated mice (L + D), $n = 7$. All data are presented as mean \pm SEM. Parametric datasets (**A**, **B**) were analysed by a one-way ANOVA with Bonferroni's multiple comparisons *post hoc*. Nonparametric datasets (**C**, **D**) were analysed by a Kruskal-Wallis test with Dunn's multiple comparisons *post hoc*.

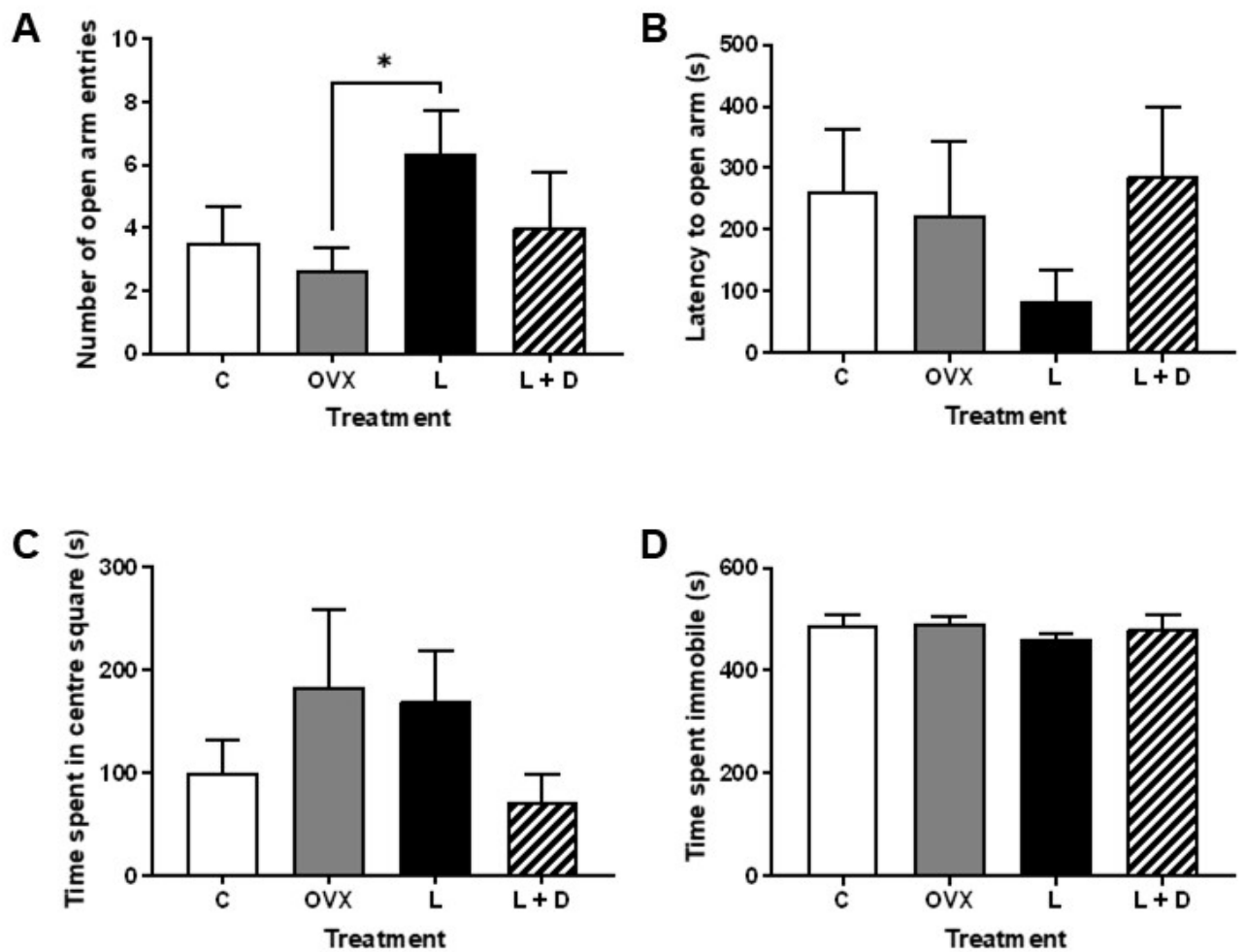


Figure 5.5. Elevated plus maze (ii). Mice were assessed for the following behaviours: the number of entries to the open arms (**A**), the latency to enter the open arms (**B**), time spent in the centre square (**C**), and time spent immobile (**D**). For intact mice (C), $n = 8$; ovariectomised mice (OVX), $n = 6$; letrozole-treated mice (L), $n = 8$; letrozole + dutasteride-treated mice (L + D), $n = 7$. All data are presented as mean + SEM. Parametric datasets (**A**, **C**, **D**) were analysed by a one-way ANOVA with Bonferroni's multiple comparisons *post hoc*. Nonparametric datasets (**B**) were analysed by a Kruskal-Wallis test with Dunn's multiple comparisons *post hoc*. * $P < 0.05$.

Light-dark test: Letrozole-treated mice travelled a greater distance in the light ($P = 0.0236$) and spent more time in the light ($P = 0.0423$) compared to OVX mice (**Fig. 5.6A-B**). Letrozole-treated mice tended to travel a greater distance in the light than mice treated with letrozole + dutasteride ($P = 0.0709$) (**Fig. 5.6A**) and spent

significantly more time in the light ($P = 0.0202$) (**Fig. 5.6B**). There was no effect of treatment on distance travelled or time spent in the dark compartment (**Fig. 5.6C-D**). Letrozole-treated mice showed numerically more transitions into the light compartment compared to mice that were OVX or treated with letrozole + dutasteride (median value 26 vs OVX, 15; L + D, 11) (**Fig. 5.6E**); the comparison between letrozole-treated mice and mice treated with letrozole + dutasteride was statistically significant ($P = 0.0462$). There was no statistical difference between groups in latency to enter the light (**Fig. 5.6F**).

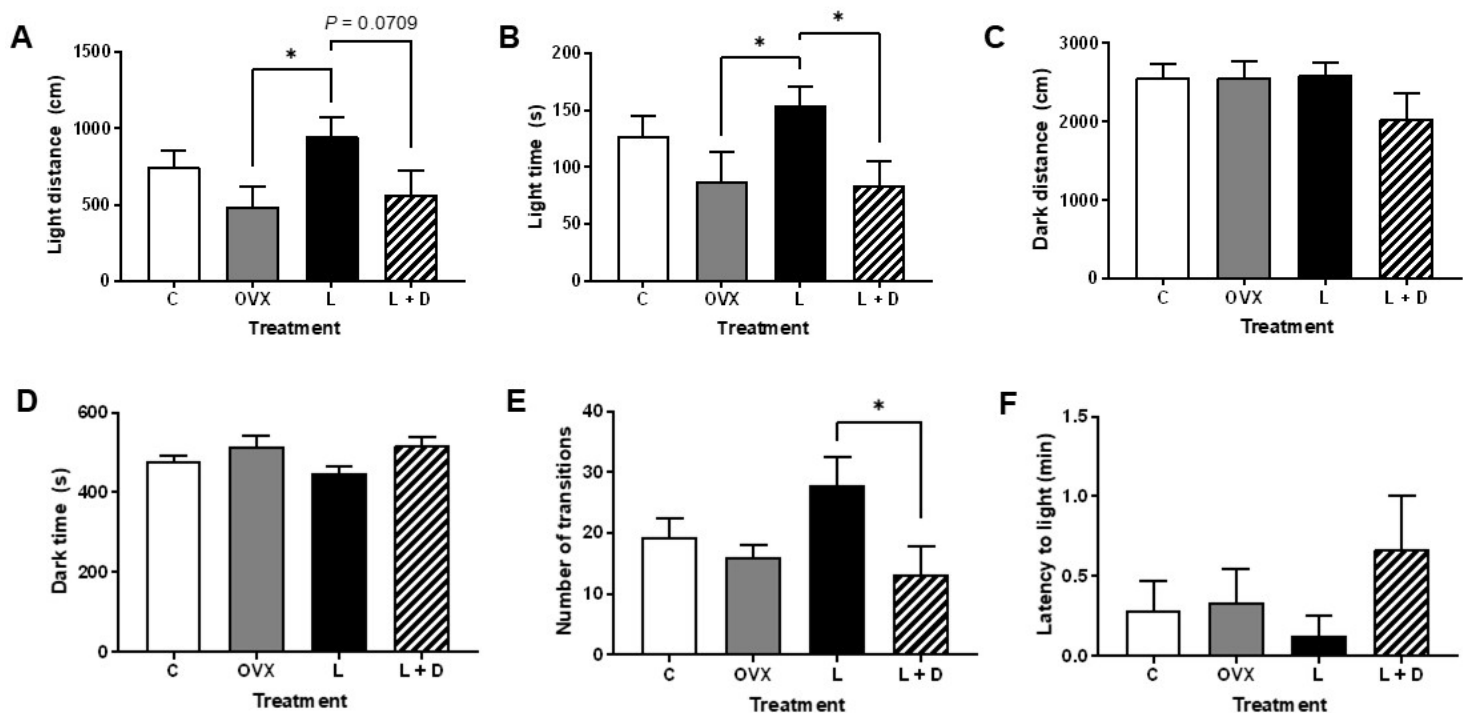


Figure 5.6. Light-dark test. Mice were assessed for the following behaviours: distance travelled in the light compartment (**A**), time spent in the light compartment (**B**), distance travelled in the dark compartment (**C**), time spent in the dark compartment (**D**), the number of transitions from the dark compartment into the light (**E**), and the latency to enter the light compartment (**F**). For intact mice (C), $n = 7$; ovariectomised mice (OVX), $n = 6$; letrozole-treated mice (L), $n = 8$; letrozole + dutasteride-treated mice (L + D), $n = 6$. All data are presented as mean + SEM. Parametric datasets (**A**, **B**, **C**, **D**) were analysed by a one-way ANOVA with Bonferroni's multiple comparisons *post hoc*. Nonparametric datasets (**E**, **F**) were analysed by a Kruskal-Wallis test with Dunn's multiple comparisons *post hoc*. Statistical significance in panels **A**, **B**, and **E** was obtained by student's unpaired t test between groups. * $P < 0.05$.

Social investigation test: Total ambulatory distance, average speed across the whole arena, and total time spent immobile were not significantly different between the treatment groups (**Fig. 5.7A-C**). Treatment also did not affect the counts of contact with the SI cone (**Fig. 5.7D**). OVX mice spent a greater amount of time in contact with SI cone, indicative of more social investigation (**Fig 5.7E**). This was significantly greater than the time observed for all other groups (OVX vs C, $P = 0.0336$, vs L, $P = 0.0454$, vs L + D, $P = 0.0512$).

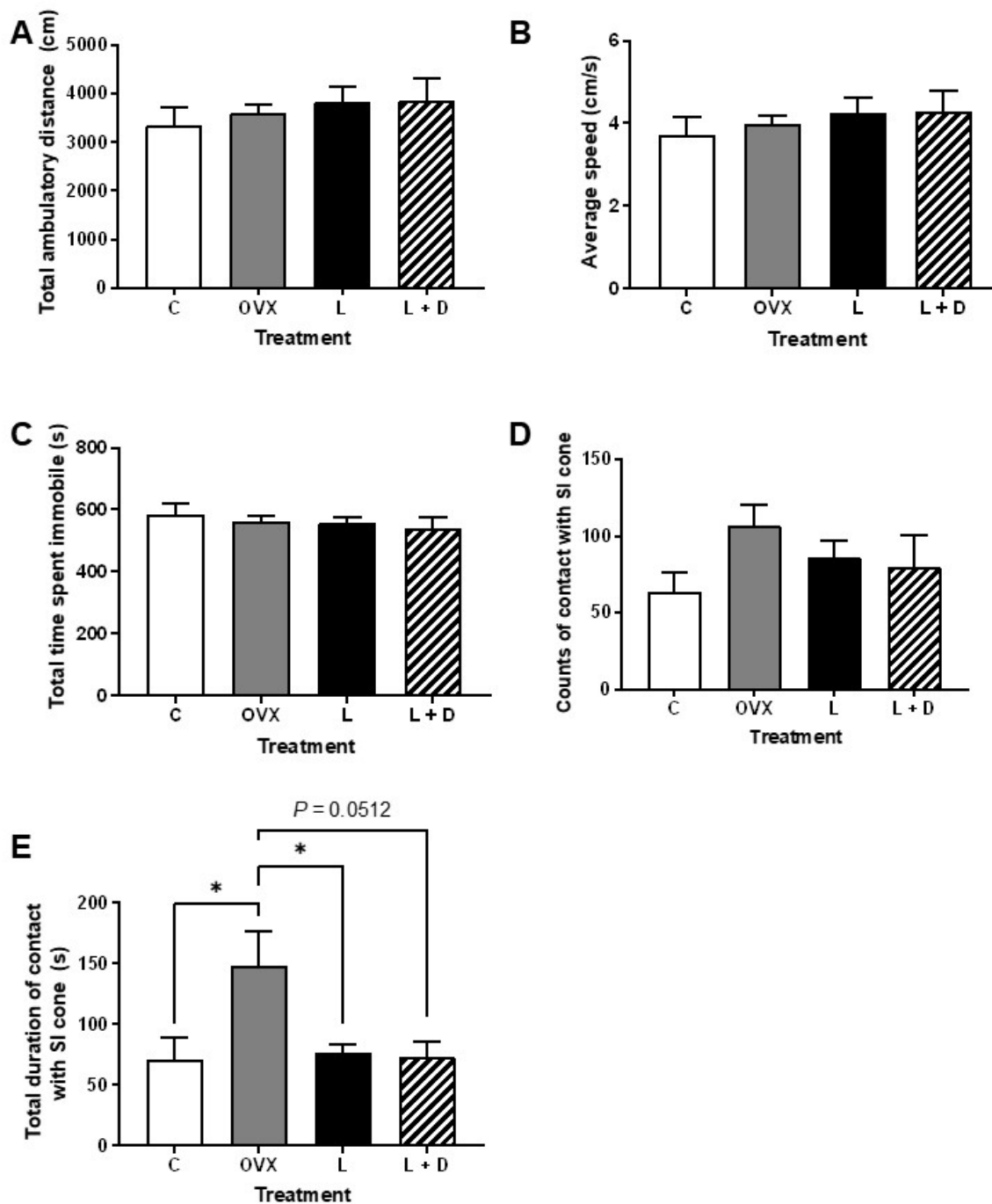


Figure 5.7. Social investigation test. Mice were assessed for the following behaviours: distance travelled (**A**), average movement speed (**B**), time spent immobile (**C**), counts of contact with the SI cone, inferred as the number of social interactions (**D**), and the total duration of contact with the SI cone, inferred as the total duration of social interactions (**E**). For intact mice (C), $n = 7$; ovariectomised mice (OVX), $n = 6$; letrozole-treated mice (L), $n = 8$; letrozole + dutasteride-treated mice (L + D), $n = 6$. All data are presented as mean + SEM. Data were analysed by a one-way ANOVA with Bonferroni's multiple comparisons *post hoc*. * $P < 0.05$.

To ensure that behaviours were not a result of environmental novelty, the 5 min preceding the SIT with the empty cone were analysed against the first 5 min of the test with the stimulus mouse (**Supp. Fig. S5.2**). Two-way ANOVAs revealed that the presence of the stimulus mouse had a significant effect on total ambulatory distance ($P < 0.0001$, **Supp. Fig. S5.2A**), average speed across the whole arena ($P < 0.0001$, **Supp. Fig. S5.2B**), and time spent immobile ($P < 0.0001$, **Supp. Fig. S5.2C**), and Bonferroni's multiple comparisons *post hoc* revealed that this was evident in all treatment groups. The counts of interaction with the SI cone were not significantly affected by the presence of the stimulus mouse (**Supp. Fig. S5.2D**), though the duration of contact with the SI cone was significantly affected ($P = 0.0007$, **Supp. Fig. S5.2E**). Bonferroni's multiple comparisons revealed that this difference was only in the OVX group, where duration of contact with the SI cone was significantly increased with the presence of the stimulus mouse ($P = 0.0011$).

5.3.3 Systemically blocking the 3β -diol pathway causes significant changes in neuroarchitecture

On the day following behavioural testing, mice were sacrificed, and brains were used for Golgi staining. There were no differences in soma size between treatment groups (**Fig. 5.8A**), nor the average number of primary dendrites per neurone (**Fig. 5.8B**). However, we observed that letrozole + dutasteride-treated mice had significantly fewer secondary dendrites and tertiary dendrites compared to intact mice treated with vehicle control or letrozole (secondary dendrites, L + D vs C, $P < 0.0001$, vs L, $P = 0.0003$; tertiary dendrites, L + D vs C, $P < 0.0001$, vs L, $P < 0.0001$) (**Fig. 5.8B**). OVX mice had fewer secondary dendrites compared to letrozole-treated mice ($P = 0.0348$) and more tertiary dendrites than letrozole + dutasteride-treated mice ($P < 0.0001$) (**Fig. 5.8B**). There was no effect of treatment on the average number of quaternary dendrites per neurone. Treatment showed a significant effect on average dendrite lengths, specifically the lengths of secondary, tertiary, and quaternary dendrites (**Fig. 5.9A**). The length of secondary dendrites in OVX mice was significantly less than that of intact mice ($P = 0.0064$) and mice treated with letrozole ($P = 0.0397$). In mice treated with letrozole + dutasteride, the lengths of secondary dendrites were significantly less than intact vehicle control ($P = 0.0036$) and mice treated with letrozole ($P = 0.0247$). Tertiary dendrites in letrozole + dutasteride-treated mice were significantly shorter than in intact controls and mice treated with letrozole (L + D vs C, $P = 0.0002$, vs L, $P < 0.0001$), as were higher order dendrites (L + D vs L, $P = 0.0120$, vs OVX, $P = 0.0146$). Dendritic arbourisation was significantly affected by treatment (**Fig. 5.9B**). The average total number of branch points per neurone was significantly less in the letrozole +

dutasteride treatment group ($P < 0.0001$ for all comparisons). When we investigated the average number of branch points for individual order of dendrites, we found that branch points on secondary dendrites were significantly decreased in letrozole + dutasteride-treated mice compared to all other treatment groups (L + D vs C, $P = 0.0032$, vs OVX, $P = 0.0151$, vs L, $P = 0.0007$), with no differences between remaining treatment groups (**Fig. 5.9B**). Letrozole + dutasteride-treated mice also had fewer primary dendrites than vehicle control-treated mice ($P = 0.0177$, **Fig. 5.9B**). Representative images of neuroarchitecture are shown in **Supp. Fig. S5.3**.

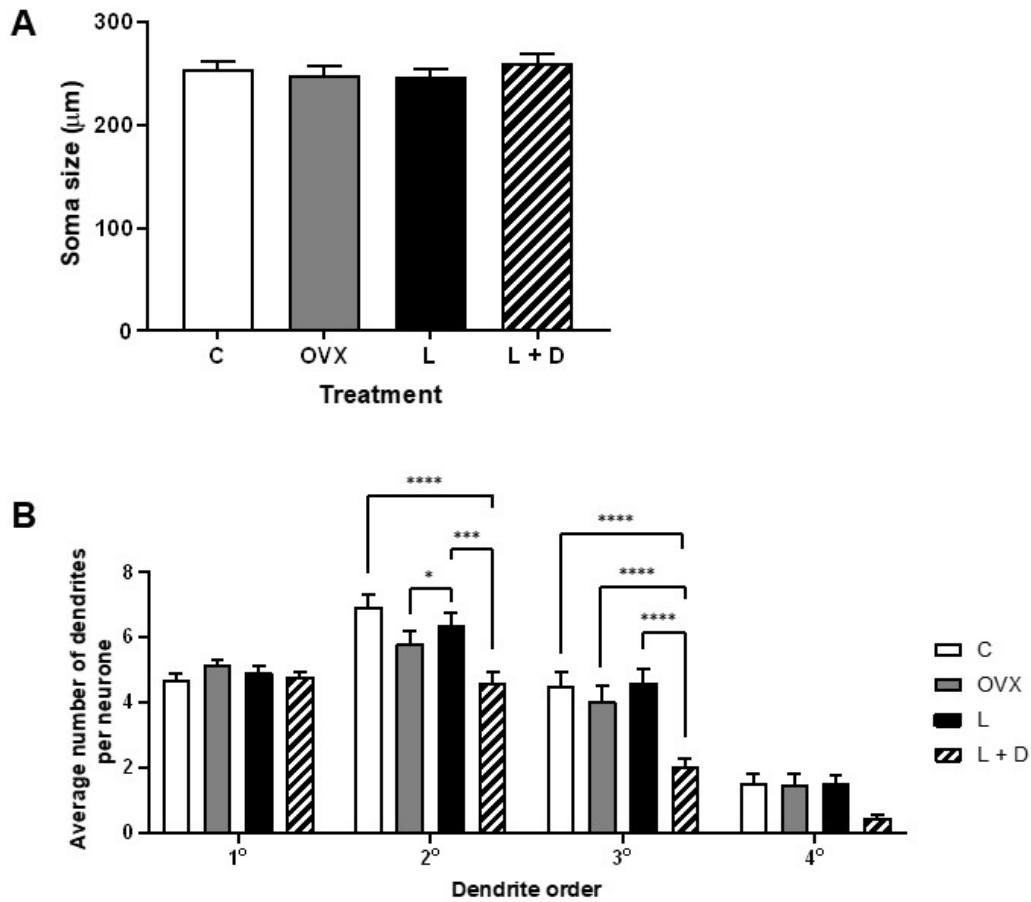


Figure 5.8. Neuroarchitectural analysis (i). Neurones were imaged at 20X magnification for neuroarchitectural analysis, in which soma size (**A**) and average number of dendrites per neurone (**B**) were measured. For panel **B**, dendrites were separated into primary (originating from the neurone), secondary (originating from a primary dendrite), tertiary (originating from a secondary dendrite), and quaternary (also referred to as higher order, originating from a tertiary dendrite) dendrites. $n = 60$ neurones per treatment group except OVX, where $n = 61$. In **C**, not all neurones had secondary, tertiary, or quaternary dendrites; the number of neurones harbouring each class of dendrite is shown above each bar. All data are presented as mean + SEM. Data were analysed by a Kruskal-Wallis test with Dunn's multiple comparisons *post hoc* (A) or by a two-way ANOVA with Bonferroni's multiple comparisons *post hoc* (B). * $P < 0.05$, ** $P < 0.01$, *** $P < 0.001$, **** $P < 0.0001$.

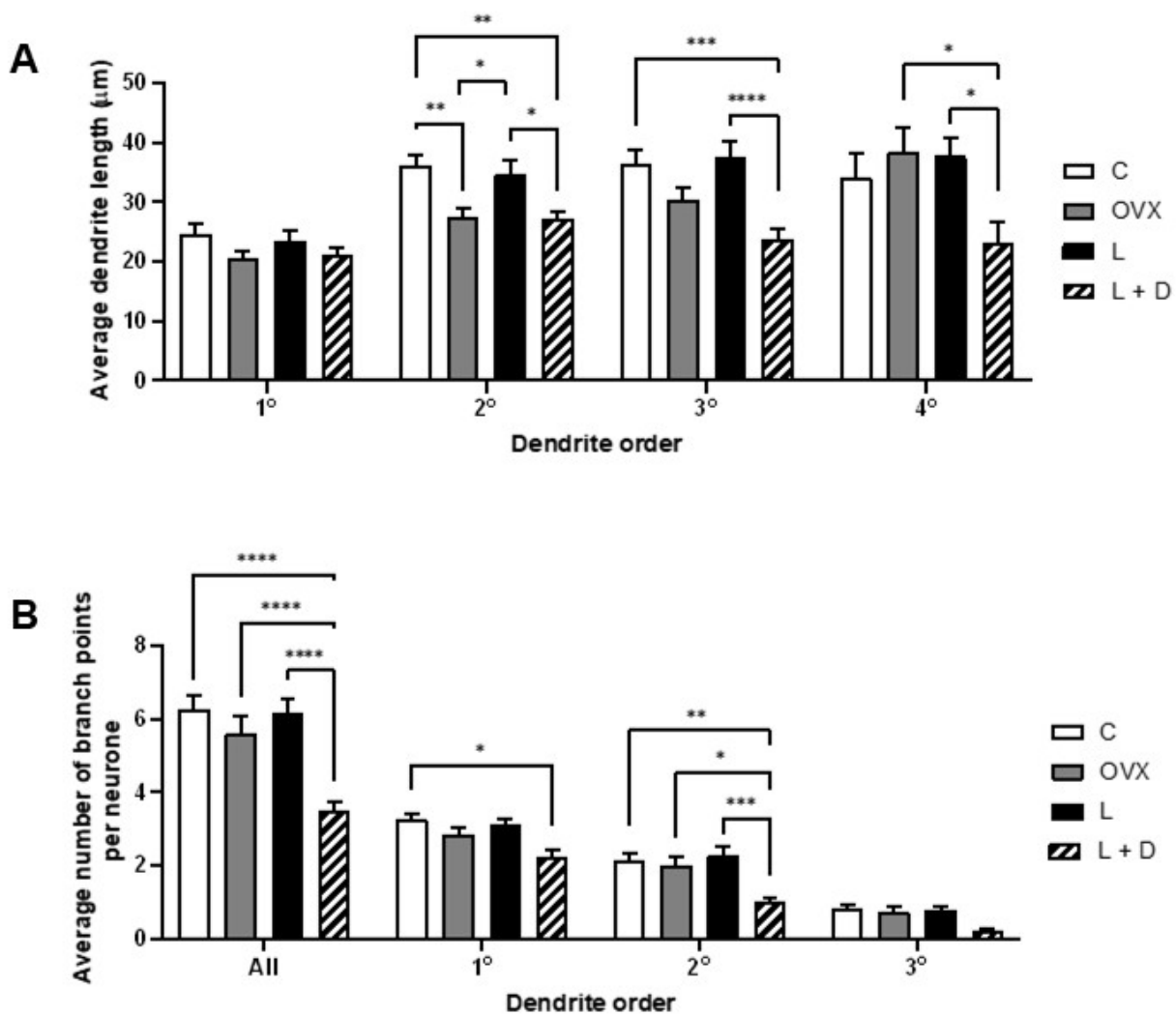


Figure 5.9. Neuroarchitectural analysis (ii). Neurones were imaged at 20X magnification for neuroarchitectural analysis, in which average dendrite length (**A**), and average number of branch points per neurone (dendritic arbourisation, **B**) were measured. Dendrites were separated into primary (originating from the neurone), secondary (originating from a primary dendrite), tertiary (originating from a secondary dendrite), and quaternary (also referred to as higher order, originating from a tertiary dendrite) dendrites. $n = 60$ neurones per treatment group except OVX, where $n = 61$. In **C**, not all neurones had secondary, tertiary, or quaternary dendrites; the number of neurones harbouring each class of dendrite is shown above each bar. All data are presented as mean \pm SEM. Data were analysed by a Kruskal-Wallis test with Dunn's multiple comparisons *post hoc* (A) or by a two-way ANOVA with Bonferroni's multiple comparisons *post hoc* (B-D). * $P < 0.05$, ** $P < 0.01$, *** $P < 0.001$, **** $P < 0.0001$.

Spine density, measured as the number of protrusions per μm , was significantly affected by all treatments compared to intact mice treated with vehicle control (C vs OVX, $P < 0.0001$, vs L, $P = 0.0119$, vs L + D, $P = 0.0021$) (**Fig. 5.10A**). OVX mice had the lowest spine density of all treatment groups, showing significantly less spines than letrozole- and letrozole + dutasteride-treated mice ($P = 0.0013$ and $P = 0.0076$, respectively) (**Fig. 5.10A**). Representative images of spine density are shown in **Supp. Figs. S5.4-7**. Spine maturation was variable between spine type and treatment group. The most immature spine types, filopodial and long thin, and the most mature spine type, branched, were not affected by treatment (**Fig. 5.10B**). OVX mice had fewer thin, stubby, and mushroom spines compared to mice treated with vehicle control ($P < 0.0001$, $P < 0.0001$, and $P = 0.0018$, respectively). For thin spines, we observed that mice treated with letrozole + dutasteride had significantly more spines than OVX mice ($P = 0.0003$), but letrozole + dutasteride-treated mice were no different to mice treated with vehicle control. Letrozole-treated mice had fewer thin spines than mice in the vehicle control group ($P = 0.006$), but there was no difference between letrozole-treated mice and OVX or letrozole + dutasteride-treated mice (**Fig. 5.10B**). For stubby spines, we found significantly less in letrozole- and letrozole + dutasteride-treated mice compared to intact mice treated with vehicle control ($P = 0.0127$ and $P = 0.0043$, respectively); mice treated with letrozole or letrozole + dutasteride were no different to each other (**Fig. 5.10B**). Letrozole-treated mice had significantly more mushroom spines than OVX mice ($P = 0.0227$) (**Fig. 5.10B**). There were no further differences in mushroom spines between groups aside from those already mentioned.

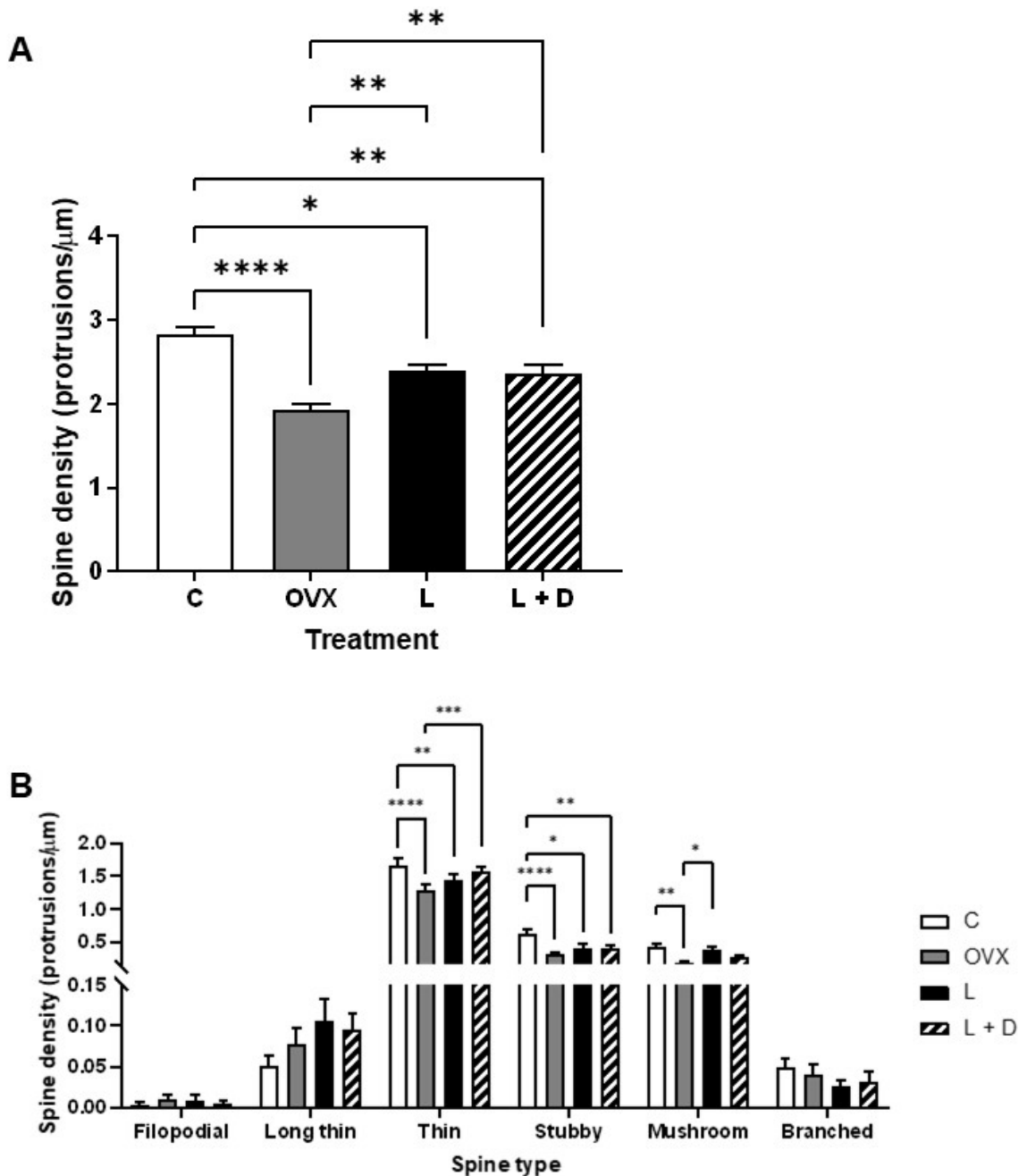


Figure 5.10. Dendritic spine analysis. Neurones were imaged at 100X magnification for dendritic spine analysis. Spine density (**A**) was measured along primary dendrites. Spines were further categorised into their morphology (**B**), defined by Risher et al. (2014). Filopodial spines are defined by a length of $>2 \mu\text{m}$, long thin spines defined by a length of $<2 \mu\text{m}$, and thin spines are defined by a length of $<1 \mu\text{m}$. Stubby spines have a length:width ratio <1 . Mushroom spines have a width $>0.6 \mu\text{m}$. Branched spines are those with two heads. $n = 40$ dendrites per treatment group. All data are presented as mean \pm SEM. Data were analysed by a Kruskal-Wallis test with Dunn's multiple comparisons *post hoc* (A) or by a two-way ANOVA with Bonferroni's multiple comparisons *post hoc* (B). * $P < 0.05$, ** $P < 0.01$, *** $P < 0.001$, **** $P < 0.0001$.

5.4 Discussion

In our previous studies, we uncovered a novel mechanism where 3 β -diol regulates neuroestrogen synthesis in the mPOA of the female mouse. Our primary aim was to explore the functional significance of this mechanism in both behaviour and the underlying neural circuitry of the mPOA. Hence, we investigated the neuromorphological and behavioural consequences of inhibiting 3 β -diol synthesis in the female mouse. To assess behaviour, we employed tests based on the animals' innate aversion to non-social cues i.e., open, and brightly lit areas and novel male conspecifics. Despite administering i.p. injections that were designed to decrease E₂ synthesis, we observed no significant differences in plasma E₂ levels between groups. However, intact controls and mice treated with letrozole exhibited a tendency toward higher plasma E₂ concentrations compared to mice that were OVX or treated with letrozole + dutasteride. Notably, the hypothalamic concentration of E₂ was significantly greater in mice treated with letrozole than in any other group. We believe this is the first report of such a finding. Whilst other studies have observed behavioural effects with comparable concentrations of letrozole (Renczes et al., 2020, Chaiton et al., 2019), they did not report on the plasma or brain concentrations of E₂. However, it was reported that i.p. administration of letrozole at 1 mg/kg significantly increased plasma testosterone (Renczes et al., 2020). Though our results showed that mice treated with letrozole had over double the amount of testosterone in plasma compared to controls, this was not significantly different due to the variability between animals. Nevertheless, our findings reinforce our previous observations [Chapter 4] that neuroestrogen production persists even in the presence of an aromatase inhibitor, likely attributable to the production of 3 β -diol.

5.4.1 *The influence of ovarian hormones on behaviours that denote anxiety*

Ovarian hormones are important in regulating anxious and depressive behaviours (Ramos-Ortolaza et al., 2017, Hiroi and Neumaier, 2006, Krężel et al., 2001). However, studies have shown variable results of loss of oestrogen by OVX in behavioural tests used to measure anxiety (Rodríguez-Landa, 2022). The hormonal consequences of OVX are believed to be anxiogenic, yet we found no effect of OVX on anxious behaviours in the OFT. This is consistent with other studies that have found no effect of OVX on anxiety-denoting behaviours in the OFT when compared to sham-operated intact (de Chaves et al., 2009, Bronstein and Hirsch, 1974) or hormonally-primed OVX controls (Hiroi and Neumaier, 2006).

We observed a small effect of OVX on anxious behaviours in the EPM, specifically in the number of entries to the open arms. A similar study that used intact and OVX rats found that time spent in the open arms and the number of open arm entries was significantly less in OVX rats (Puga-Olguín et al., 2019). Contrasting studies have found that time spent in the open arms and the number of open arm entries were no different between OVX mice treated with sesame oil and OVX mice primed with E₂ benzoate (EB) (Galeeva and Tuohimaa, 2001), though it is arguable that administration with EB alone does not supplement the hormonal milieu that is lost with OVX (Wise and Ratner, 1980). However, the results from Galeeva and Tuohimaa (2001) are consistent with our own, suggesting that factors besides E₂ exposure could influence anxiety of OVX mice in the EPM. In the LDT, we observed a tendency for OVX mice to travel less distance in the light. This is not due to decreased locomotor activity, since dark distances were no different between treatment groups and we saw no differences in total ambulatory distance in any of the other behavioural tests between treatment groups.

It has recently been suggested that the age at which OVX is performed can alter behavioural phenotypes (Woodward et al., 2023). Prepubertal OVX increases time spent in the light compartment of the LDT in Siberian hamsters (Kyne et al., 2019). OVX aged rats (18 months old) spent less time in the open arms of the EPM with fewer open arm entries compared to sham-operated controls, whereas there was no difference in these same parameters in adult (6 months old) sham and OVX rats (de Chaves et al., 2009). Since the mice in the current study were OVX in early adulthood (12 weeks old), this may explain why we observed little difference in anxiety between treatment groups.

The SIT was developed to examine the social investigative behaviours of mice in their home territory toward unfamiliar stimulus mice as a measure of social anxiety (Tomihara et al., 2009). The SIT exposes mice to visual, auditory, and olfactory cues but prevents direct physical contact, thereby allowing the investigator to assess social behaviours without the influence of stress caused by physical conflict with an intruder mouse (Tsuda and Ogawa, 2012). All groups showed decreased ambulation and increased immobile time upon the introduction of the stimulus mouse, suggesting the behaviours were not due to the effects of a novel environment. The moving distance in the SIT is believed to be a measure of the animals' anxiety level in social situations, such that a greater distance corresponds to less anxiety (Tomihara et al., 2009), though we observed no difference between treatment groups in this metric. Interestingly, the cumulative duration of social interaction was increased in OVX mice,

indicating less social anxiety. To our knowledge, this is the first time that this has been reported despite the OVX mice in our study exhibiting similar social investigation times to OVX mice in a previous comparable study (Tsuda and Ogawa, 2012).

It has been reported that anxious behaviours become more apparent over time post-OVX (Rodríguez-Landa, 2022). In macaques, social behaviours (which included physical contact by way of grooming, social play, and touch) were decreased with long-term OVX, though the effects of short-term OVX were not investigated (Coleman et al., 2011). Behaviours that denote anxiety and the response to anxiolytic agents are increased in rats that were OVX 12 weeks prior to testing as opposed to rats OVX 3 weeks prior to testing (Picazo et al., 2006). The mice in the current study had been OVX only for a total of 3 weeks at the end of behavioural testing, which may offer a reason for less anxiety in the OFT, EPM, and LDT, though it does not account for the decrease anxiety in the SIT. This may be explained by the fact that the regulation of anxiety is context-dependent (Haller et al., 2004, Diab et al., 2020).

5.4.2 3β -diol and anxiety

The properties of E_2 in anxiety are mediated by $ER\alpha$ and $ER\beta$, which respectively produce predominantly anxiogenic and anxiolytic behavioural responses (Lund et al., 2005). Mice deficient in $ER\beta$ show increased anxiety (Krężel et al., 2001, Tomihara et al., 2009) and agonism of the receptor with subcutaneous injections of WAY-200070 in intact mice produces an anxiolytic and antidepressant effect in the four-plate test for anxiety and tail suspension test (Hughes et al., 2008). The androgen metabolite 3β -diol, which has a strong affinity for $ER\beta$, is also anxiolytic and significantly reduces plasma corticosterone during restraint stress when delivered bilaterally in the PVN (Lund et al., 2006). Due to the unavailability of 3β -diol at the time of this study (COVID and Brexit restrictions), we inhibited the synthesis of 3β -diol and E_2 using letrozole and dutasteride, a 5α -reductase inhibitor, which we have shown to be effective previously in Chapter 4. We also treated mice with letrozole alone, since we have previously shown that neuroestrogen production in the mPOA continues with the addition of an aromatase inhibitor (Chapter 4). We observed increased hypothalamic concentrations of E_2 with letrozole treatment, and behavioural data suggested anxiolytic response to letrozole in the EPM as mice tended to spend less time in the closed arms and exhibited significantly more entries to the open arms. Together, this suggests that letrozole at a concentration of 1 mg/kg is ineffective at blocking E_2 synthesis in the hypothalamus *in vivo*, and this could cause less anxiety in behavioural tests. In line with this, it was found that 1 mg/kg letrozole treatment in

intact, sham-operated rats had no effect on anxious behaviours in the OFT or EPM (Renczes et al., 2020). Furthermore, consistent with our data, other studies have described only a mild effect of letrozole in increasing the latency to enter the centre of the OFT compared to vehicle-treated mice, and no differences in anxiety were observed in the LDT or in depressive behaviour in the forced swim test (Meng et al., 2011).

Administration of letrozole pushes the conversion of testosterone to DHT and subsequently 3β -diol which could maintain state anxiety. Therefore, we hypothesised that blocking this conversion using dutasteride in addition to letrozole would be anxiogenic. This hypothesis was supported by the observation of decreased time spent in the centre of the OFT, a tendency to spend more time in the closed arms of the EPM, decreased time spent and distance travelled in the light compartment of the LDT and fewer transitions in the LDT in mice that were treated with letrozole and dutasteride. Interestingly we observed no anxiogenic effect of this treatment in the SIT. It was previously shown that subcutaneous injections of 1 mg/kg 3β -diol increased the amount of time spent in the centre of the OFT, time spent in the open arms in the EPM, and time spent in the light compartment of the LDT in male wildtype mice, but not in ER β knockout male mice (Frye et al., 2008). To our knowledge, the physiological levels of 3β -diol have not been measured in the mouse, but in humans, men have greater circulating levels of 3β -diol which are associated with lower scores of depression than in women (Tanabe et al., 2021). The lack of significant behavioural findings in the current study compared to previous studies (Pak et al., 2005, Frye et al., 2008, Lund et al., 2006) could be due to the intrinsically lower levels of 3β -diol in the female. Alternatively, the treatments used in the current study may not have completely inhibited the production of 3β -diol, though this cannot be confirmed without an assay to measure this metabolite. Furthermore, previous studies using male rodents may have used supraphysiological levels of 3β -diol, leading to an exaggerated anxiolytic response.

5.4.3 The mPOA is implicated in behaviours that denote anxiety

Anxiety-related neuronal inputs are integrated at the level of the paraventricular nucleus of the hypothalamus (PVN) (Wu and Zetter, 2022, Liu et al., 2022). The PVN contains exclusively ER β (Suzuki and Handa, 2005) which, upon activation, increases oxytocin synthesis and directly modulates the hypothalamic-pituitary-adrenal axis to decrease anxiety (Acevedo-Rodriguez et al., 2015). Recently, the mPOA was found to reduce anxiety via neurones that provide GABAergic input to the PVN (Zhang et al.,

2021). This is likely mediated by ER β since it colocalises with parvalbumin, the GABAergic-associated calcium-binding protein (Blurton-Jones and Tuszynski, 2002). In studies demonstrating the anxiolytic properties of 3 β -diol, it is feasible that some of the molecular effects occur within the mPOA, where binding ER β leads to increased GABAergic input to the PVN. This hypothesis requires further investigation.

Considering the mPOA's involvement in anxiety and our discovery of the 3 β -diol pathway regulating neuroestrogen synthesis in this region, we investigated how treatment influenced dendritic and synaptic plasticity in the mPOA.

5.4.4 Neuroarchitectural changes associated with blockade of steroid hormones

E₂-regulated spinogenesis has been well documented in multiple brain areas (Kato et al., 2013, Mukai et al., 2007, Sheppard et al., 2019). Furthermore, these neuroarchitectural changes underlie changes in learning, memory, and behaviour (Lu et al., 2019, Phan et al., 2015, Christensen et al., 2011). CA1 pyramidal neurones in the hippocampus display rapid and reversible plastic changes in spine and synapse densities across the oestrous cycle (Woolley and McEwen, 1992, Woolley and McEwen, 1993). Similarly, spine density in the rat ventromedial hypothalamus (VMH) varies across the oestrous cycle, peaking in proestrous (Frankfurt et al., 1990). In the arcuate nucleus of the hypothalamus (ARC), E₂ rapidly increases spine density, a change required for sexual receptivity in the female rat (Christensen et al., 2011).

The mPOA is critically involved in female sexual behaviour, maternal behaviour, and anxiety, all of which are modulated by E₂ (Sano et al., 2013, Bridges, 2015, Zhang et al., 2021). Given the plastic nature of the neural correlates for these behaviours, we investigated the effects of OVX and the inhibition of 3 β -diol on neuronal morphology in the mPOA. We observed a reduction in the number of dendrites per neurone, dendritic arbourisation, and spine density following OVX. Previous research has yielded mixed insights into the effects of OVX on neuronal morphology. While studies have shown that OVX has no effect on dendritic arbourisation in the nucleus accumbens (Quiñones et al., 2009) or the CA3 layer of the hippocampus (Mendell et al., 2017), other investigations align with our findings, reporting that OVX leads to a reduction in spine density, though this was measured in the hippocampus (Wallace et al., 2006, Gould et al., 1990). A loss of roughly 25% of spine and synapse density in the apical dendrites of CA1 neurones and diminished social recognition memory is associated with OVX (Woolley and McEwen, 1993, Wallace et al., 2006), which is reversed by treatment with E₂ (Woolley and McEwen, 1993). We observed a similar outcome for mice treated with letrozole + dutasteride, a treatment regime which we have previously shown decreases

neuroestrogen in *ex vivo* hypothalamic slices containing the mPOA (Chapter 4). Interestingly, we observed no difference between intact control mice and mice treated with letrozole in the length, number, or arbourisation of dendrites. This may be attributed to the high concentrations of hypothalamic E₂, though spine density is decreased. This could be due to consistently lower concentrations of neuroestrogen in the mPOA in the letrozole treated group as compared to control (Chapter 4). We found that mice that were OVX or treated with letrozole + dutasteride had significantly less thin, stubby, and mushroom spines compared to intact controls, and tended to have more immature long thin spines. This supports previous studies in the ARC, where maturation of spines depends on E₂ and is associated with the phosphorylation and deactivation of cofilin, an actin depolymerising factor (Christensen et al., 2011). We also observed that letrozole-treated mice had less thin and stubby spines compared to intact controls.

The physiological significance of the disparity in dendritic arbourisation and spine density in letrozole-treated mice remains unclear. The discrepancy may stem from the distinct functional roles of dendritic vs spine plasticity in neuronal communication and information processing. Dendritic length and arbourisation primarily determines the complexity of a neurone's receptive field and its ability to integrate incoming signals from multiple sources, which allow it to perform intricate computational tasks (Bird and Cuntz, 2019). On the other hand, dendritic spine density reflects the potential for synaptic connectivity and excitatory/inhibitory signal transmission, affecting the overall strength and efficacy of neuronal communication (Risher et al., 2014). It is also unclear why we observed such profound differences in dendrite and spine morphology with a relative lack of behavioural differences between treatment groups. Neurological changes occur 1-2 weeks post-OVX (Velázquez-Zamora et al., 2012) whereas behavioural changes may not occur until 3 weeks post-OVX (Picazo et al., 2006). It is possible that, with an extended period of treatment, the mice in the current study may have exhibited phenotypes in the tests that denote anxiety.

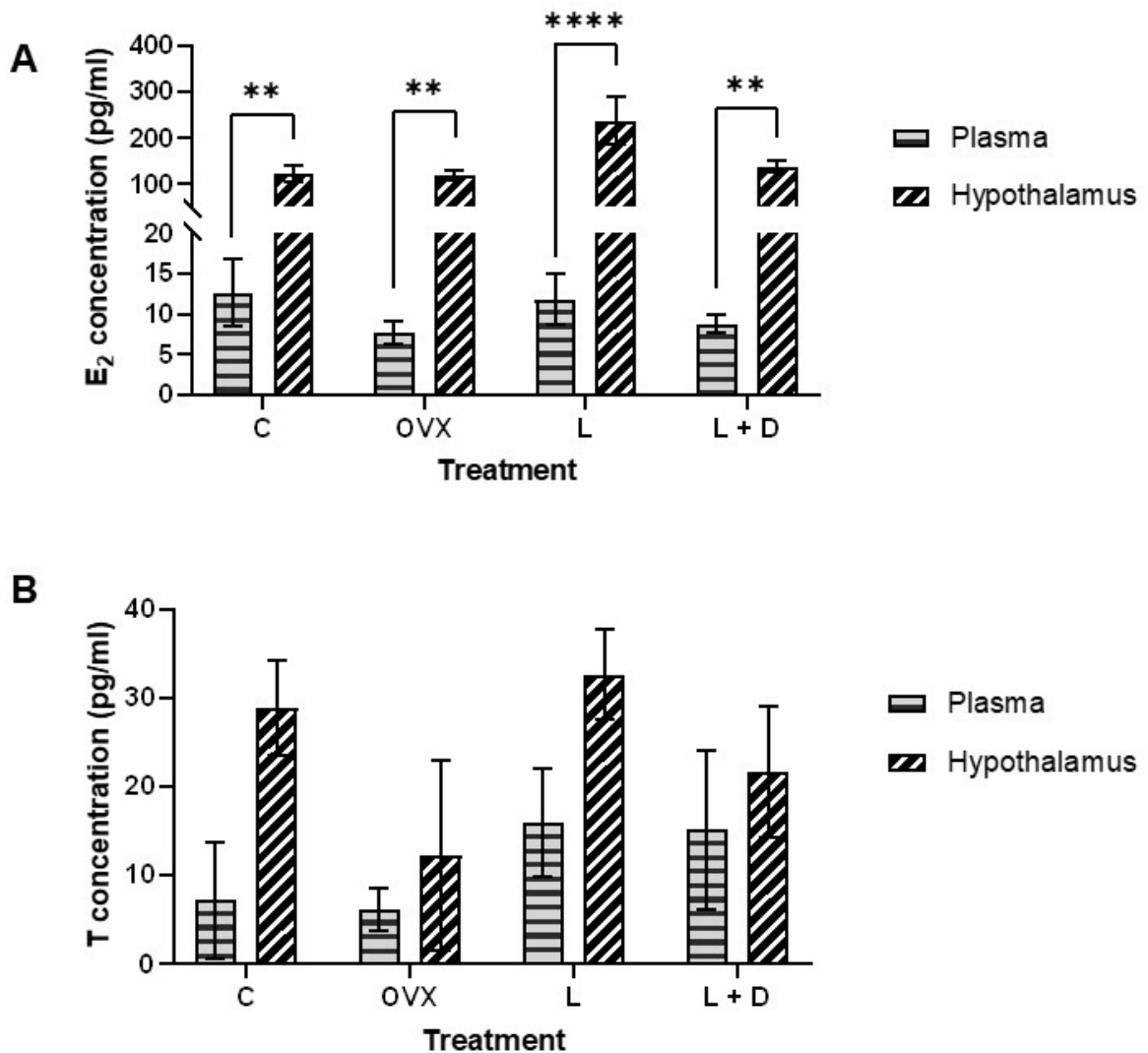
Our combined data suggest that a complete gonadal hormonal milieu is crucial for the maintenance of a complex neuronal network and inhibiting both E₂ and 3β-diol synthesis using letrozole + dutasteride mimics the effects of OVX in the mouse mPOA. Notably, the impact of OVX and letrozole + dutasteride on dendrite length, number, and branching seems to vary across different orders of dendrites. This spatial specificity is not uncommon; in the ventrolateral VMH, E₂ influences spine density specifically on long dendrites (Calizo and Flanagan-Cato, 2000). Clearly, there is an intricate and complex nature of E₂ signalling that shapes neural circuitry, which may relate to an

anxiolytic effect (Gorman and Docherty, 2010). One theory for the aetiology of mood disorders such as anxiety involves a decrease in neurotrophic factors and a consequent reduction in hippocampal neurogenesis (Kempermann et al., 2008). However, these disorders are dependent on multiple areas of the brain that are not believed to exhibit neurogenesis in adulthood (Gorman and Docherty, 2010, Ming and Song, 2011). It has been proposed that remodelling of dendritic arbours and spines in anxiety is a neuroprotective mechanism that prevents the excessive stimulation and subsequent apoptosis of neurones (Gorman and Docherty, 2010), and this may take place in the mPOA.

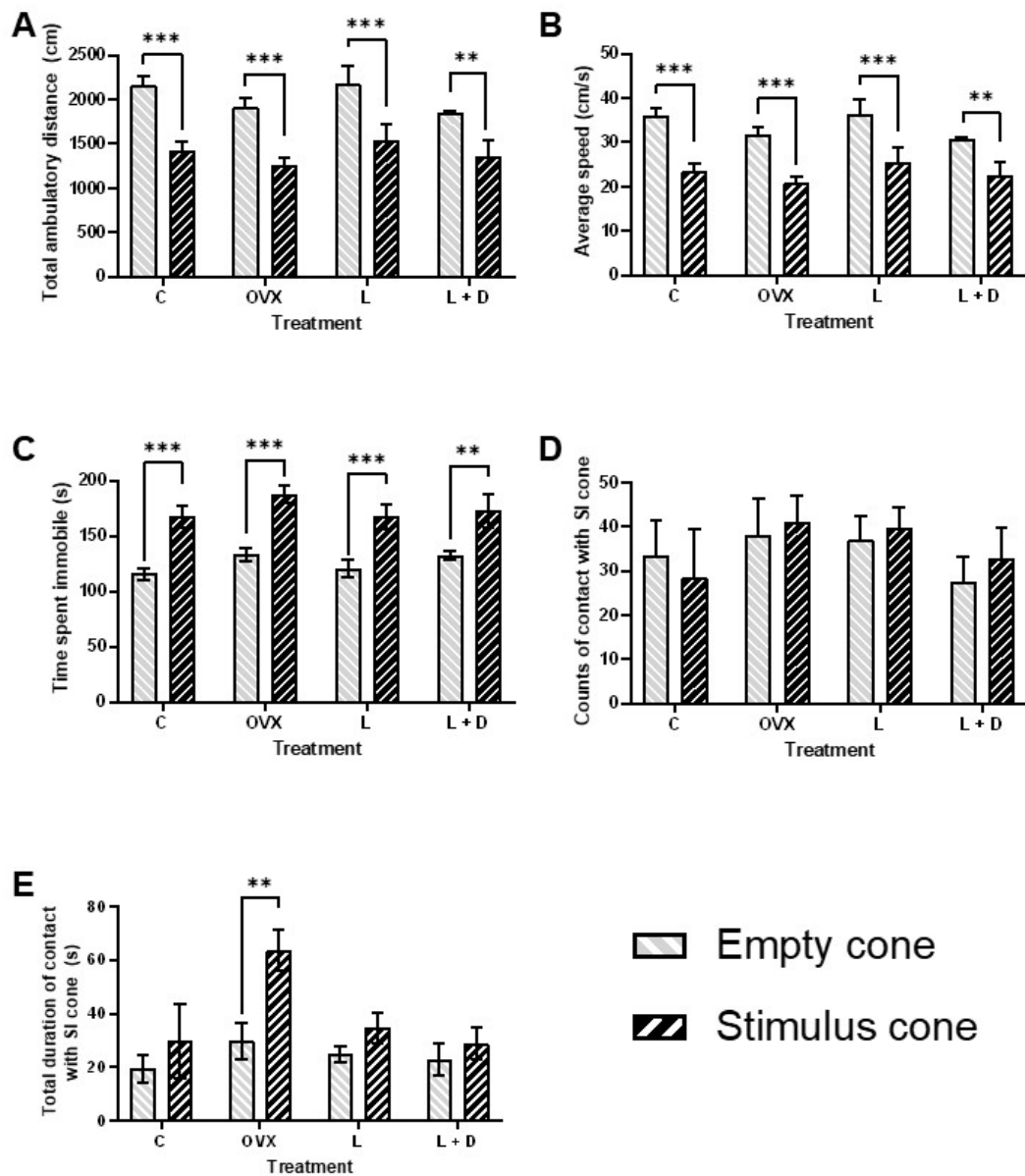
5.5 Summary

3β -diol is implicated in anxiolysis, and our recent findings have revealed its synthesis and activity in the female mouse mPOA. We observed significant neuroarchitectural changes in the mPOA following OVX, and this effect was replicated in mice that were treated with an aromatase inhibitor and unable to produce 3β -diol. The literature offers varying perspectives regarding the specific ER responsible for modulating dendritic and spine plasticity. For instance, in hippocampal glutamatergic neurones, the ER α agonist PPT led to an increase in spine density, while the ER β agonist DPN had no such effect, implicating ER α as the primary ER in hippocampal spinogenesis (Mukai et al., 2007). Conversely, in cortical neurones, the ER β -specific agonist WAY-200070 resulted in increased spine density and an accumulation of postsynaptic density protein (PSD)-95 in membrane regions (Srivastava et al., 2010). In the mPOA, 3β diol and E_2 could maintain spine density and remodeling via ER β and ER α though this remains to be investigated. For a more comprehensive understanding of the functions of 3β -diol, future studies should explore its direct administration to specific brain regions of interest. Our study is the first to show an effect of 3β -diol on morphology in an important nucleus of the social behaviour network in females.

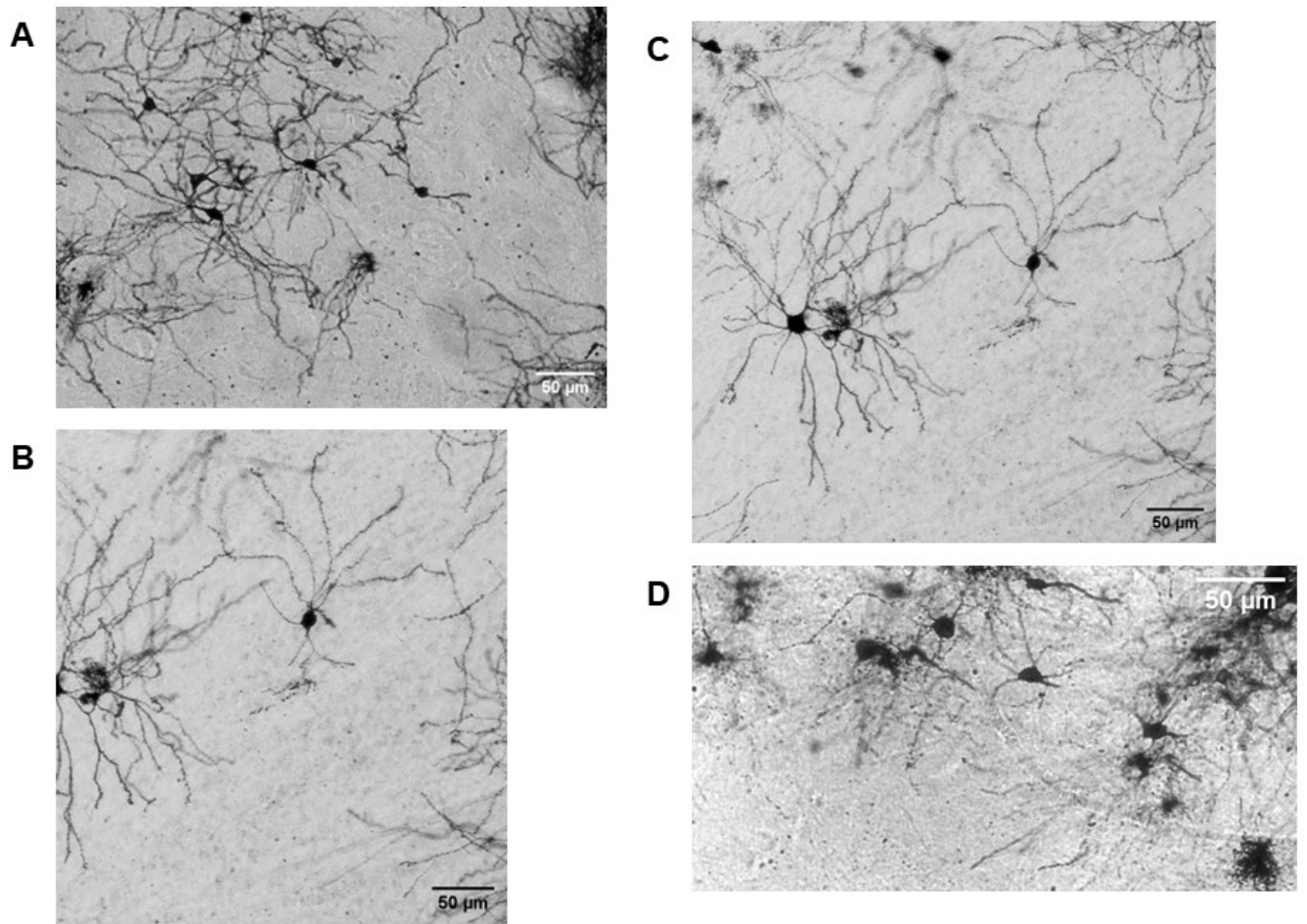
5.6 Supplementary information



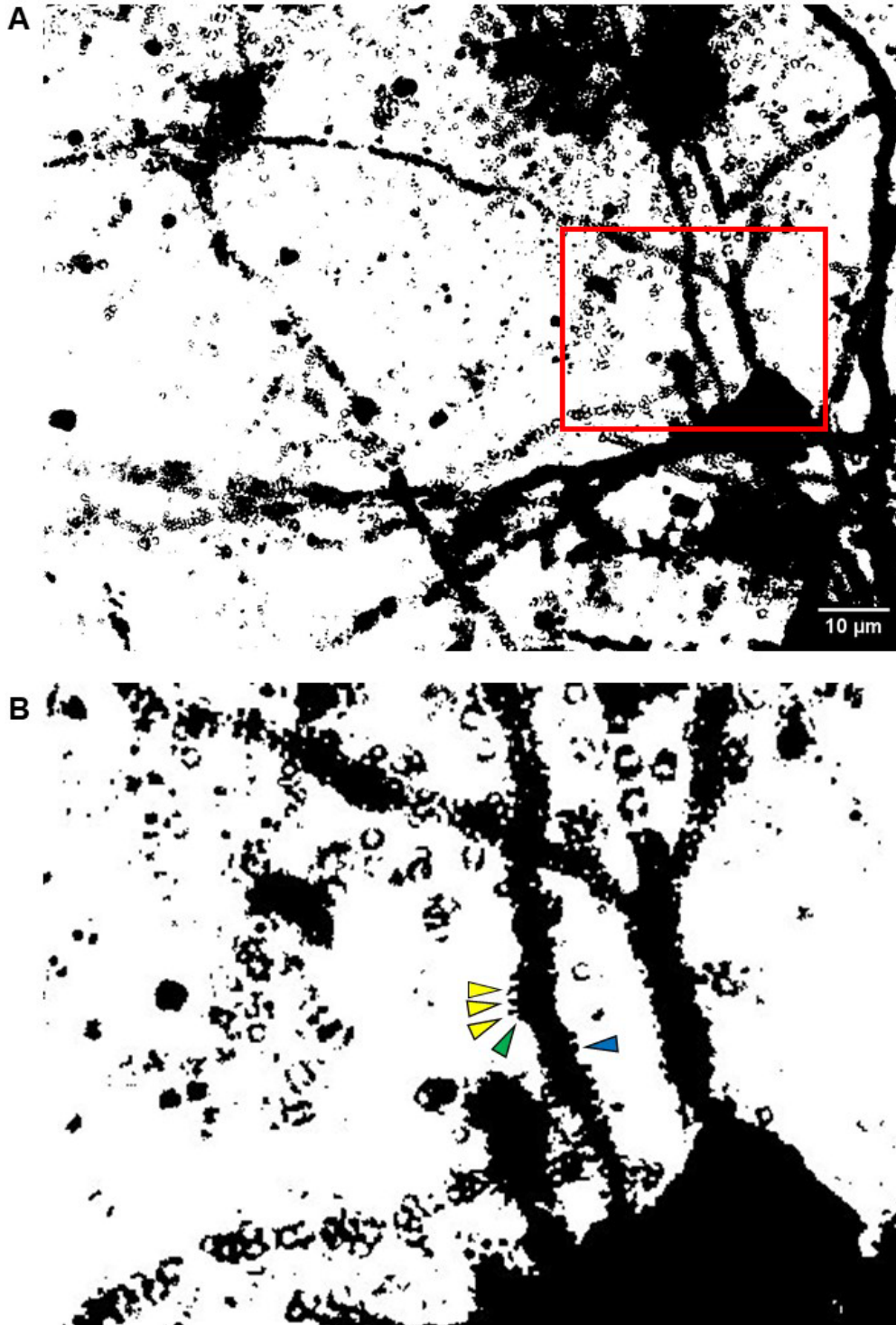
Supplementary Figure S5.1. Hormone concentrations in plasma vs hypothalamic extractions. E₂ (A) and testosterone (B) were measured in plasma (grey horizontally lined bars) and excised hypothalami from one hemisphere (white hashed bars) from a subset of intact (C), ovariectomised (OVX), letrozole-treated (L), and letrozole + dutasteride-treated (L+D) mice following behavioural testing and sacrifice. For plasma, $n = 3$ for C and L + D; $n = 4$ for OVX, and $n = 5$ for L. For excised hypothalami, $n = 4$ for all groups. All data are presented as mean \pm SEM. Differences were established by a two-way ANOVA with Bonferroni's multiple comparisons test *post hoc*, or by a Mann-Whitney U test. ** $P < 0.01$, **** $P < 0.0001$.



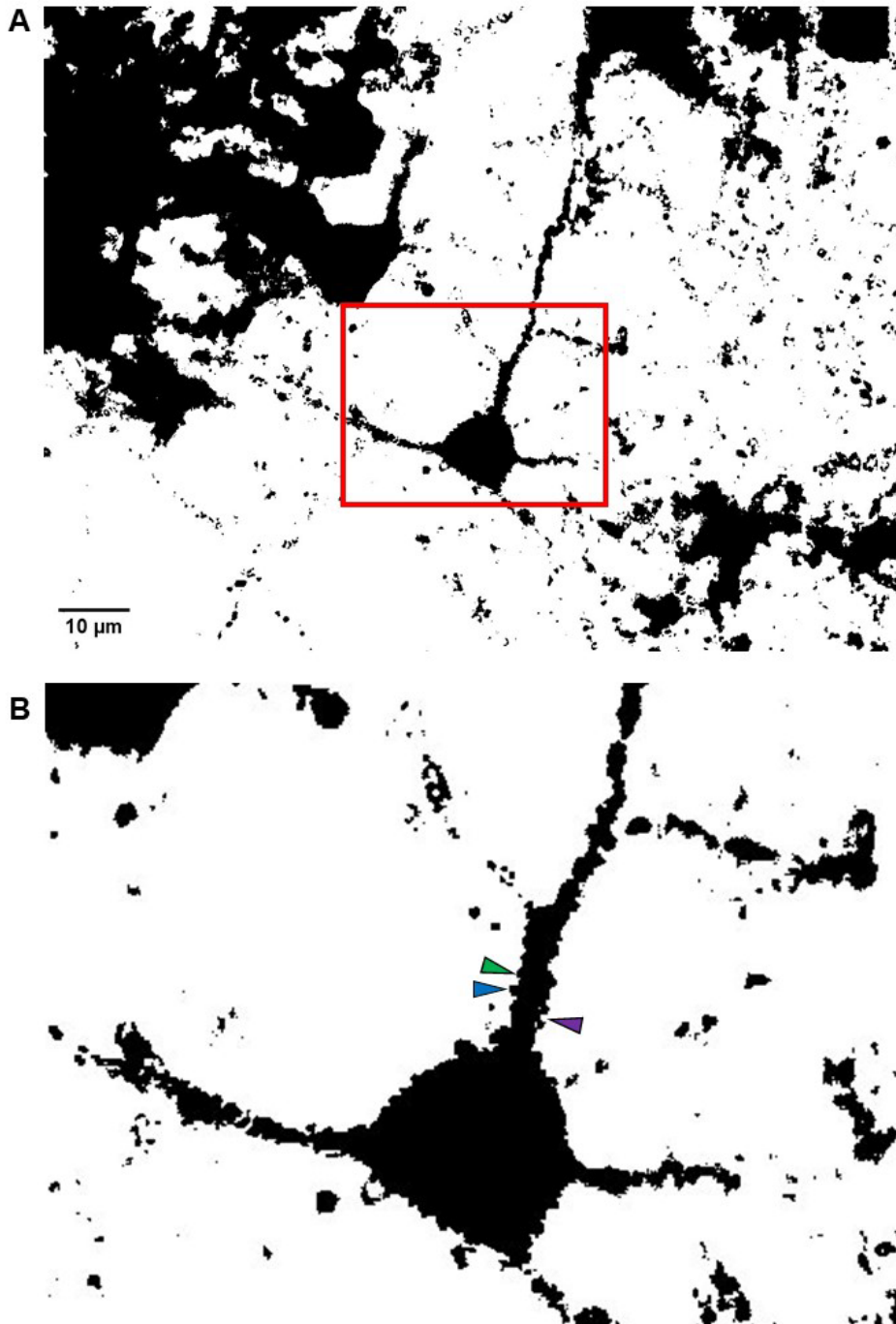
Supplementary Figure S5.2. Social investigation test empty cone data. During the 5 min with the empty cone before the test began and during the first 5 min of the test, mice were assessed for the following behaviours: distance travelled (**A**), average movement speed (**B**), time spent immobile (**C**), counts of contact with the SI cone, inferred as the number of social interactions (**D**), and the total duration of contact with the SI cone, inferred as the total duration of social interactions (**E**). For intact mice (C), $n = 7$; ovariectomised mice (OVX), $n = 6$; letrozole-treated mice (L), $n = 8$; letrozole + dutasteride-treated mice (L + D), $n = 6$. All data are presented as mean \pm SEM. Data were analysed by a two-way ANOVA with Bonferroni's multiple comparisons *post hoc*. ** $P < 0.01$, *** $P < 0.001$.



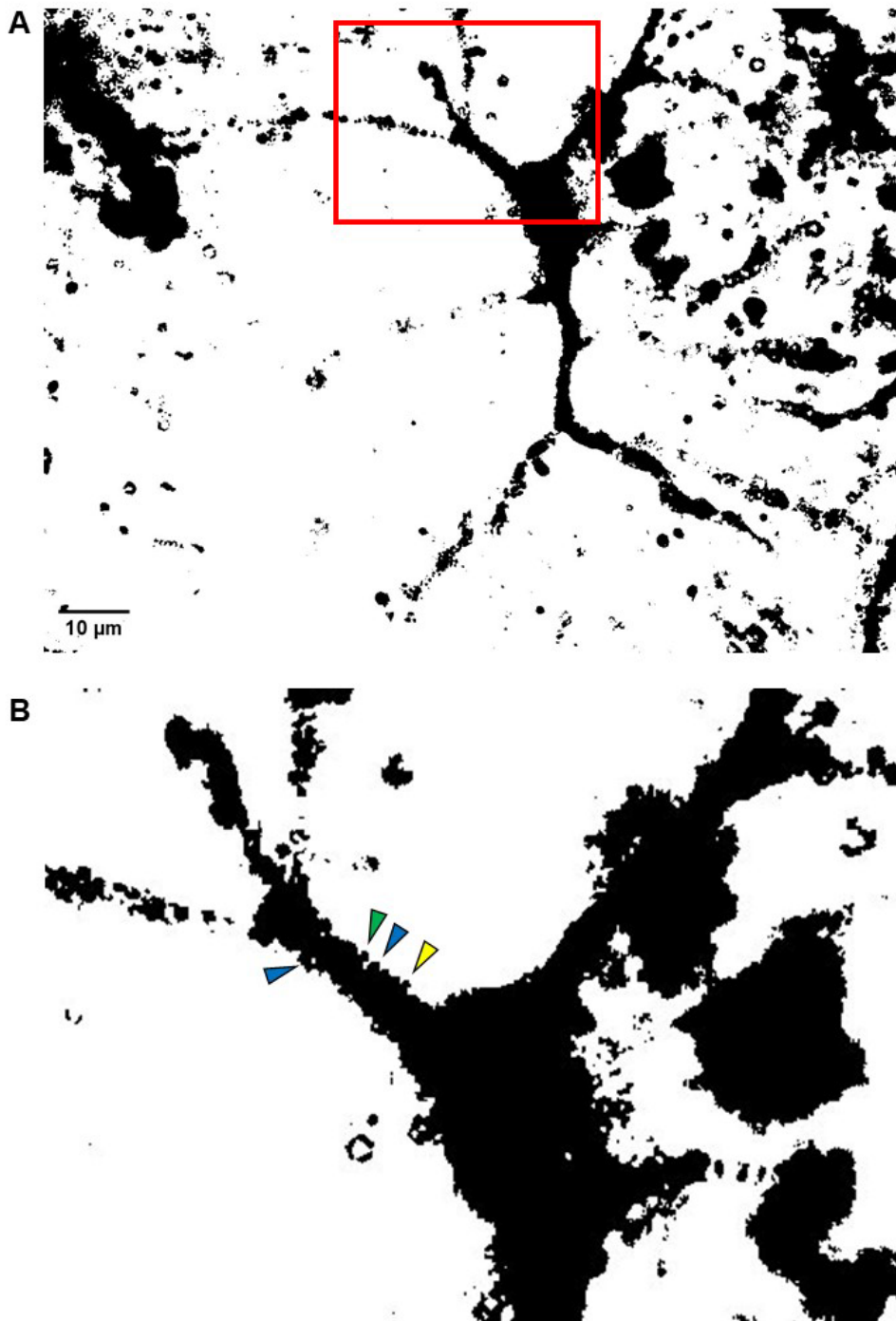
Supplementary Figure S5.3. Representative 20X images of neuroarchitecture in the medial preoptic area of adult female mice treated with steroidogenic enzyme inhibitors. Representative images of neuroarchitecture in intact female mice treated with vehicle control (**A**), OVX mice treated with vehicle control (**B**), intact mice treated with letrozole (**C**), and intact mice treated with letrozole and dutasteride (**D**).



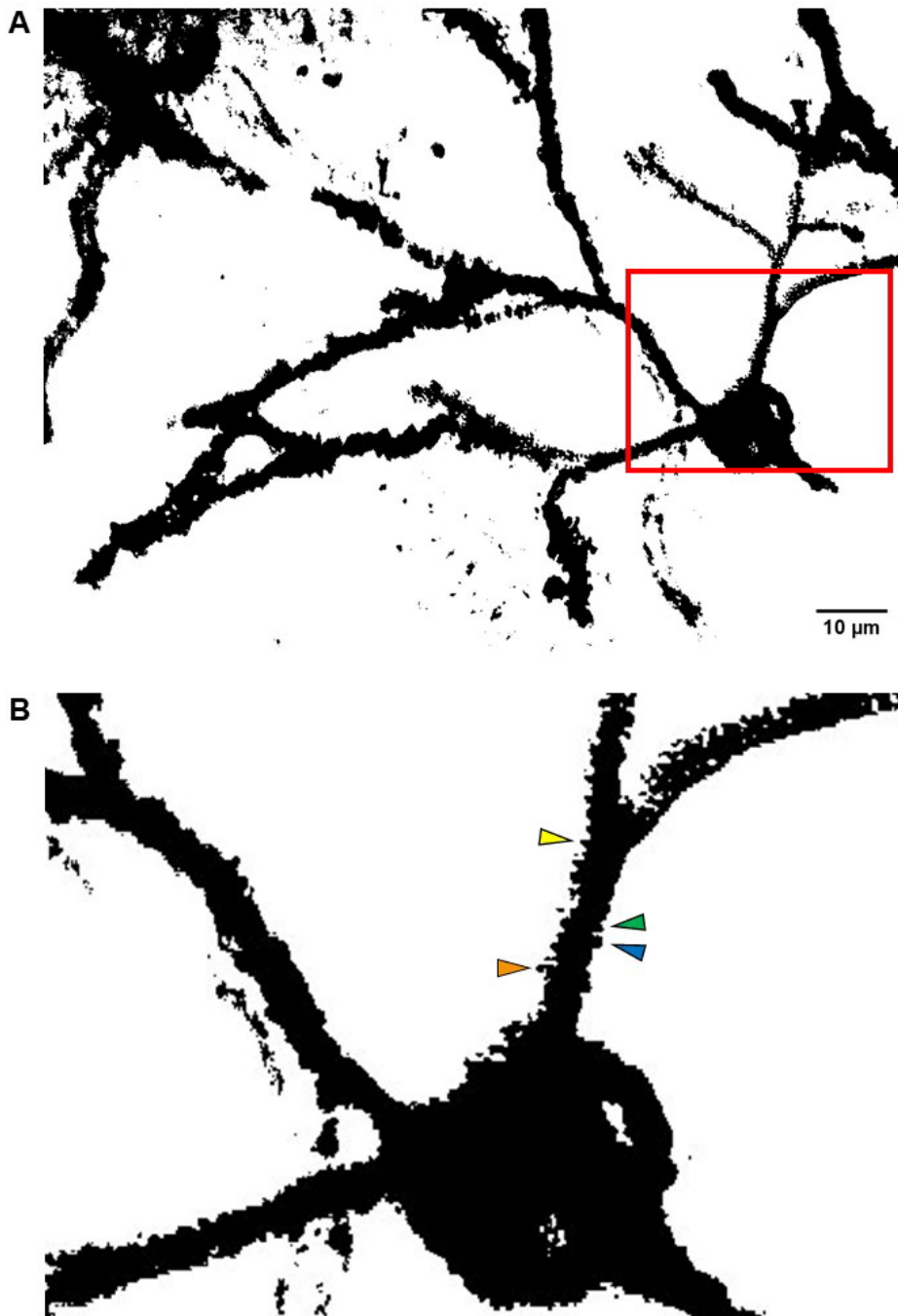
Supplementary Figure S5.4. Representative 100X image of spine density of a neurone in the medial preoptic area in vehicle-treated intact female mice. A representative 100X image of spine density (A). The red square shows a region that is magnified in (B) to show spines. Thin spines (length $<1 \mu\text{m}$) are indicated by yellow arrows, a stubby spine (length:width ratio <1) is indicated by the green arrow, and a mushroom spine (width $>0.6 \mu\text{m}$) is indicated by the blue arrow.



Supplementary Figure S5.5. Representative 100X image of spine density of a neurone in the medial preoptic area in vehicle-treated ovariectomised mice. A representative 100X image of spine density (A). The red square shows a region that is zoomed in in (B) to show spines. A stubby spine (length:width ratio <1) is indicated by the green arrow, a mushroom spine (width $>0.6 \mu\text{m}$) is indicated by the blue arrow, and a branched spine (two heads) is indicated by the purple arrow.



Supplementary Figure S5.6. Representative 100X image of spine density of a neurone in the medial preoptic area in letrozole-treated intact female mice. A representative 100X image of spine density (A). The red square shows a region that is zoomed in in (B) to show spines. A thin spine (length $<1 \mu\text{m}$) is indicated by a yellow arrow, a stubby spine (length:width ratio <1) is indicated by the green arrow, and mushroom spines (width $>0.6 \mu\text{m}$) are indicated by the blue arrow.



Supplementary Figure S5.7. Representative 100X image of spine density of a neurone in the medial preoptic area in letrozole- and dutasteride-treated intact female mice. A representative 100X image of spine density (**A**). The red square shows a region that is zoomed in in (**B**) to show spines. A long thin spine (length $<2\ \mu\text{m}$) is indicated by the orange arrow, a thin spine (length $<1\ \mu\text{m}$) is indicated by a yellow arrow, a stubby spine (length:width ratio <1) is indicated by the green arrow, and a mushroom spine (width $>0.6\ \mu\text{m}$) is indicated by the blue arrow.

Chapter 6

Behavioural Significance of Neuroestrogens Originating from the Hypothalamus: Observations from A Novel Conditional and Site-Specific Aromatase Knockout Mouse (*Aro^{fl/fl}*)

6.1 Introduction

The neurobehavioural effects of steroid hormones, particularly the physiologically relevant oestrogen 17 β -oestradiol (E₂), have garnered significant attention in recent years (Micevych and Christensen, 2012, Renczes et al., 2020, Remage-Healey et al., 2008, Serendynski et al., 2013, Cornil et al., 2013). At the core of E₂ synthesis lies the aromatase enzyme, encoded by the *Cyp19a1* gene, which is responsible for the conversion of C-19 androgens to C-18 oestrogens (Brueggemeier et al., 2001). Enzymatic activity is present mainly in the gonads, but also in extra-gonadal locations including the brain, adipose tissue, and bone (Nelson and Bulun, 2001). In the brain, aromatase is highest in the amygdala, hippocampus, hypothalamus, and cortex (Stanic et al., 2014). Neurones in these regions constitutively express aromatase (Lu et al., 2019, Duncan and Saldanha, 2020) and can produce neuroestrogen (i.e., E₂ derived from neuronal sources) in synergy with other cell types that produce the essential precursors required for the synthesis of E₂ (Zwain and Yen, 1999). This aids neurotransmission, synaptic plasticity, cognitive function, neuroinflammation, and neuroprotection (Brann et al., 2022). Aromatase expression is also induced in astrocytes in response to cerebral ischemia, implicating E₂ as a protective factor against hypoxia-related stress (Wang et al., 2023). Thus, aromatase and E₂ are essential for the proper development, regulation, and function of neural processes.

The social behaviour network (SBN) is a connective neural construct consisting of six bidirectional nodes spanning the hypothalamus, amygdala, and hippocampus (Newman, 1999, Goodson, 2005). Collectively, these nodes facilitate sex-typical behaviours (Newman, 1999). The role of each node was initially elucidated by lesions that resulted in deficits in social behaviours (Goodson, 2005). Further neuroendocrine studies have shown that these regions possess oestrogen receptors (ERs) and express aromatase (Goodson, 2005, Stanic et al., 2014). Both male and female mice have been shown to coexpress ERs with aromatase in cells of the bed nucleus of stria terminalis (BNST), medial amygdala (meA), and medial preoptic area (mPOA) (Stanic et al., 2014, Tsuruo et al., 1995), which underpins the importance of steroid hormones, particularly E₂, in the choreography of neuroendocrine responses that lend themselves to a myriad of behaviours.

Previous research has utilised genetic and pharmaceutical approaches to disentangle the complex hormonal mechanisms driving neurobehavioural responses to aromatase activity and E₂ deficiency. Pharmaceutical approaches have included the use of

specific ER agonists (Seredynski et al., 2015, Mazzucco et al., 2008) and antagonists (Gardener and Clark, 2001), and aromatase inhibitors (Olvera-Hernández et al., 2015, Bonsall et al., 1992). However, these methods are typically not as robust as they can result in incomplete suppression of enzyme or receptor activity, off-target effects (Catalano et al., 2014), or interactions with other biological processes that render the inhibition ineffective, as we have highlighted with letrozole and the induction of the 3 β -diol pathway (Chapters 4 & 5). Whole-body aromatase knockout (ArKO) mice have been generated which provide a more comprehensive assessment of the role of E₂ in brain development (Bakker et al., 2002) and male reproductive function (Honda et al., 1998). Whole-body ArKO mice show severe impairments in sexually dimorphic behaviours, particularly sexual behaviour (Honda et al., 1998) (Bakker et al., 2002) and aggressive behaviour (Toda et al., 2001). These mice also show an obese phenotype (Jones et al., 2000) and impaired olfaction (Bakker et al., 2002). Whole-body ArKO models, however, prevent E₂ production in both gonadal and extragonadal tissues and its secretion into the circulation, forbidding the investigation of tissue-specific effects of aromatase. A brain-specific aromatase knockout model was generated recently, which demonstrated the requirement of brain aromatase in normal male sexual behaviour and the regulation of serum testosterone concentrations (Brooks et al., 2020b). Brain-ArKO mice showed a sexual behaviour profile between that of wildtype (WT) controls and whole-body ArKO mice, suggesting neurosteroids contribute to the normal expression of sexual behaviour in the male mouse (Brooks et al., 2020b). However, a whole-brain KO does not facilitate the differentiation of aromatase significance in specific brain regions. A forebrain-specific ArKO (fbn-ArKO) model was generated by Lu et al., (2019), which demonstrated a critical role for neuroestrogen in regulating synaptic plasticity and cognitive function in both the male and female forebrain. A resounding caveat to all of these ArKO models is the ambiguity in whether the observed phenotype is due to the organisational or the activational effects of E₂ (McCarthy et al., 2009), and/or whether the phenotype is due to lack of aromatase function in a specific area.

We have utilised a unique aromatase-flox (*Aro^{fl/fl}*) mouse model to knockout aromatase expression in male mice using an AAV targeted at the mPOA. The mPOA is intricately intertwined with the regulation of sex-typical behaviours, encompassing aggression (Albert et al., 1986), parenting (Tsuneoka et al., 2013), sexual behaviour (Dominguez and Hull, 2005), and anxiety (Zhang et al., 2021). Its central position within the neural circuitry of the SBN and rest of the brain enables it to integrate hormonal signals with environmental cues, thereby facilitating a coordinated orchestration of behaviours. In

using this model, we have been able to demonstrate for the first time the activational importance of aromatase and E₂ in the hypothalamus, as brain development proceeded in the presence of functional aromatase and archetypal E₂ production.

Though our primary interest was to use female mice in this thesis, only male mice were available at the time of experimentation. Notably, this discrepancy is not due to any genetic or fertility anomalies. Originally, the experiments in this chapter were meant to be undertaken by a different researcher; however, persistent travel restrictions during the COVID-19 pandemic prevent their execution. In an conscientious effort to avoid wastage of animal life and adhere to the principles of the 3Rs, the mice were housed until JD could travel to Japan, and the experiments were conducted as supplementary to those originally proposed for the thesis. Due to the interim period between breeding and experimentation, the mice utilised by JD were significantly aged. In a second run of the experiment (see section 6.2 below), younger male Aro^{fl/fl} mice were used. Data from each run were analysed both separately and collectively by JD to confirm that there was no effect of age on the observed behaviours. We would like to emphasise that, since the phenotype of Aro^{fl/fl} mice with knockdown specifically in hypothalamic areas is unknown, the use of male mice in this thesis does not diminish the originality or significance of the findings.

6.2 Methods

Experiments in this chapter were designed by JD and conducted in two separate runs by JD and Kongkidakorn Thaweepanyaporn (KT) at the University of Tsukuba, Japan. In run one, JD performed stereotaxic surgeries and behavioural tests on 13 mice (control group, n = 3; knockdown group, n = 10). In run two, KT performed stereotaxic surgeries and behavioural tests on 15 mice (control group, n = 4; knockdown group, n = 10). All data were pooled and analysed by JD at the University of Reading, UK.

6.2.1 Animals and behavioural tests

Aro^{fl/fl} mice were generated and genotyped as described in section 2.1.1; animals were housed at the University of Tsukuba as described in section 2.1. Aromatase knockout by stereotaxic injection was performed as described in section 2.2.4 and mice recovered in running wheel cages (see section 2.3.5). The behavioural testing timeline is shown in **Fig. 6.1**. Sexual behaviour testing was carried out as described in section 2.3.6; aggressive behaviour experiments were carried out as described in section

2.3.7; the light-dark transition test (LDT) was carried out as described in section 2.3.3. For sexual behaviour tests, stimulus ICR/Jcl female mice were ovariectomised (OVX) and hormonally primed as described in sections 2.2.1 and 2.2.2. For experiments measuring aggressive behaviour, stimulus ICR/Jcl male mice underwent olfactory bulbectomy (OBX) as described in section 2.2.5.

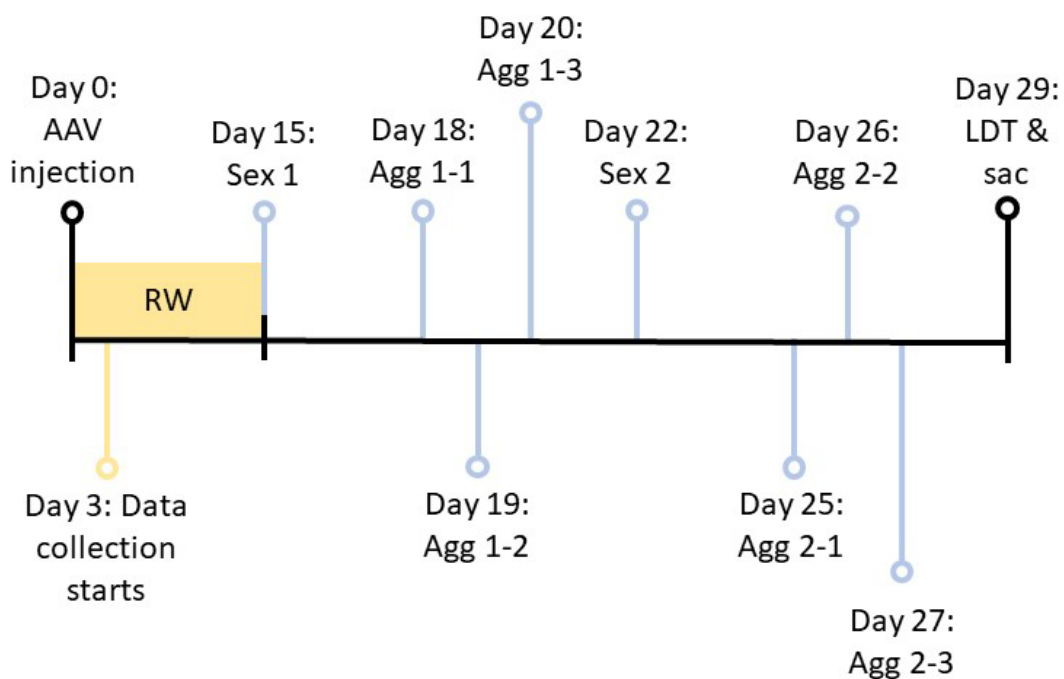


Figure 6.1. Experimental timeline. Following stereotaxic injections, mice were individually housed in running wheel cages (RW). Data collection started on day 3 to allow mice to recover from surgery and acclimate to their new home cage. On day 15, mice remained individually housed but the running wheel was removed. On this day, the first sexual behaviour test took place (Sex 1). Aggressive behaviour tests were carried out over three consecutive days following sexual behaviour tests (Agg 1-1 – 1-3). 48 h later, the second sexual behaviour test took place (Sex 2), followed by a second round of three consecutive aggressive behaviour tests (Agg 2-1 – 2-3). On the 29th day, mice were tested in the light-dark test (LDT) before being sacrificed by perfusion-fixation.

After the completion of all behavioural tests, mice were killed by perfusion fixation and the injection site was confirmed by immunocytochemistry (see section 2.4). The collection of brains and storage in sucrose was completed by JD at the University of Tsukuba. Due to time constraints, immunocytochemistry was carried out by collaborators at the University of Tsukuba after JD's departure. Stained sections were shipped to the UK and JD analysed the site of injection at the University of Reading. Trunk blood was collected at time of death and plasma was prepared as described in section 2.6.

6.2.2 Hormone measurements

Steroids in plasma were concentrated by solid phase extraction (section 2.10) and measured using a competitive ELISA for 17 β -oestradiol (section 2.11.1).

6.2.3 Statistical analysis

Statistical analysis and data presentation as described in section 2.15.

6.3 Results

6.3.1 Confirmation of injection site

The injection site was confirmed by immunocytochemistry for GFP. Whilst all mice had received Cre or GFP injections in the mPOA (with some overspill into the BNST), a subset of mice had been injected in both the mPOA and surrounding hypothalamo-limbic regions, particularly the paraventricular nucleus (PVN) but also in the hippocampus (**Table 6.1**). One animal (H0563) was most likely injected in the third ventricle, resulting in GFP detection in the mPOA, BNST, VMH, hippocampus, and meA. At the time of experimentation, the site of injection was unknown, but this subset of mice (including H0563) displayed a profound difference in their physiological phenotype. Upon confirmation of the site of injection, mice that received Cre injection in the mPOA/BNST (hypo-ArKO) were analysed separately to the subset that received Cre injection in the mPOA and surrounding hypothalamo-limbic regions (hypo-lim-ArKO).

Table 6.1. Location of Cre injection sites. The cre-GFP vector was detected by immunocytochemistry as detailed in Methods. DAB-positive cells were visualised at 5X (Zeiss Axioskop) across coronal sections of animals perfused in experiment run 1 (JD). Animals injected with the cre vector were separated on the basis of body weight gain during the experiment. mPOA: medial preoptic area; BNST: bed nucleus of stria terminalis; LS: lateral septum; hip: hippocampus; PVN: paraventricular nucleus; VMH: ventromedial hypothalamus; meA: medial amygdala; 3V: third ventricle.

Animal ID	Phenotype	Genotype	Location of DAB-positive cells
H0573	Normal BW	C	mPOA: +++; BNST: ++; possible 3V
H0585	Normal BW	hypo-ArKO	mPOA: ++++; BNST: ++; meA: +
H0590	Normal BW	hypo-ArKO	mPOA: ++++; BNST: ++
H0565	Normal BW	hypo-ArKO	mPOA: ++++; BNST: ++
H0598	Normal BW	hypo-ArKO	mPOA: ++++; BNST: +
H0572	Normal BW	hypo-ArKO	mPOA: +++; BNST: +++; hip: +
H0584	Obese	hypo-lim-ArKO	mPOA: +++; BNST: +++; hip: +; PVN: +
H0564	Obese	hypo-lim-ArKO	mPOA: +++; BNST: +++; hip: +++; PVN: ++
H0563	Obese	hypo-lim-ArKO	mPOA: +++; BNST: +++; VMH: ++; hip: +; PVN: +; meA: +

6.3.2 Site-specific ArKO does not affect plasma E₂ concentrations

Plasma E₂ was measured in mice at the time of death. All groups of mice showed a comparable concentration of plasma E₂ (**Fig 6.2**).

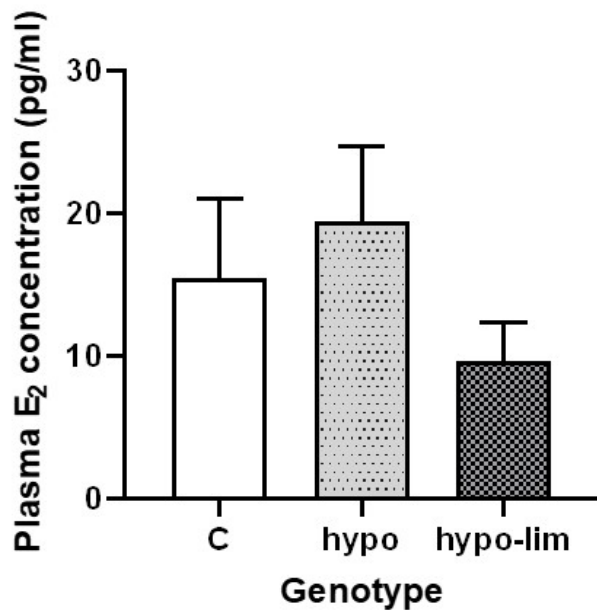


Figure 6.2. Plasma E₂ concentrations. Plasma E₂ concentrations are shown for a subset of control (C, $n = 3$), hypo-ArKO (mPOA, $n = 5$), and hypo-lim-ArKO (mPOA-lim-ArKO $n = 4$) mice. All data are presented as mean \pm SEM. Comparisons were made a one-way ANOVA with Bonferroni's multiple comparisons *post hoc*.

6.3.3 Running wheel activity is significantly decreased by site-specific ArKO without affecting bodyweight in hypo-ArKO

In the running wheel, both hypo-ArKO and hypo-lim-ArKO mice showed significantly fewer mean daily revolutions compared to controls (C vs hypo-ArKO, $P = 0.0107$; vs hypo-lim-ArKO, $P = 0.0030$) (**Fig. 6.4A**). Mean hourly revolutions revealed that this was due to differences in activity during the dark phase (**Fig. 6.4B**). Despite this, only hypo-lim-ArKO mice gained a significant amount of weight during the study. Notably, the increase in weight exceeded not only the weight gain observed in control mice ($P < 0.0001$) but also that of hypo-ArKO mice ($P < 0.0001$) (**Fig. 6.4C**). The divergence in weight gain was observed from the second week of study (**Fig. 6.4D**).

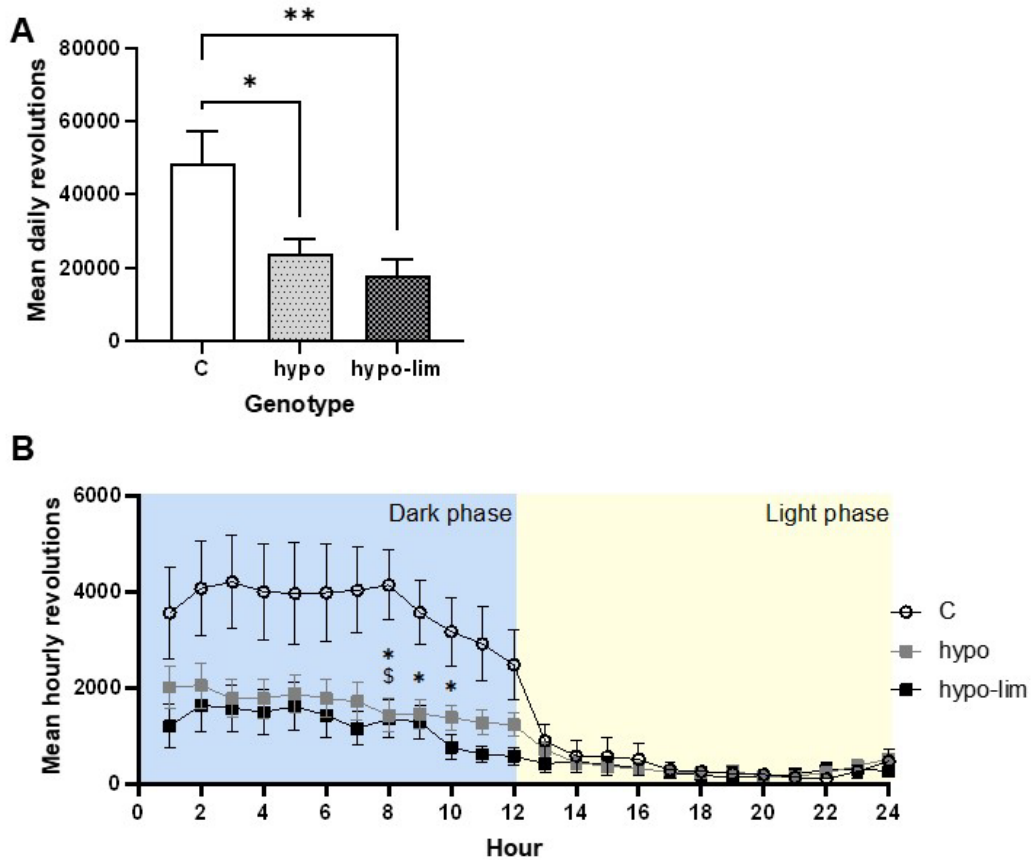


Figure 6.3. Running wheel activity. Mean daily revolutions (**A**), presented as mean + SEM, and mean hourly revolutions (**B**), presented as mean \pm SEM, for control (C, $n = 7$), hypo-ArKO (hypo, $n = 14$), and hypo-lim-ArKO (hypo-lim, $n = 10$) mice housed in running wheel cages. For **A**, differences were established by means of a one-way ANOVA with Bonferroni's multiple comparisons *post hoc*. For **B**, differences were established by a two-way ANOVA with Bonferroni's multiple comparisons test *post hoc*. * denotes a difference between hypo-lim-ArKO and control and \$ denotes a difference between hypo-ArKO and control. * $P < 0.05$, ** $P < 0.01$.

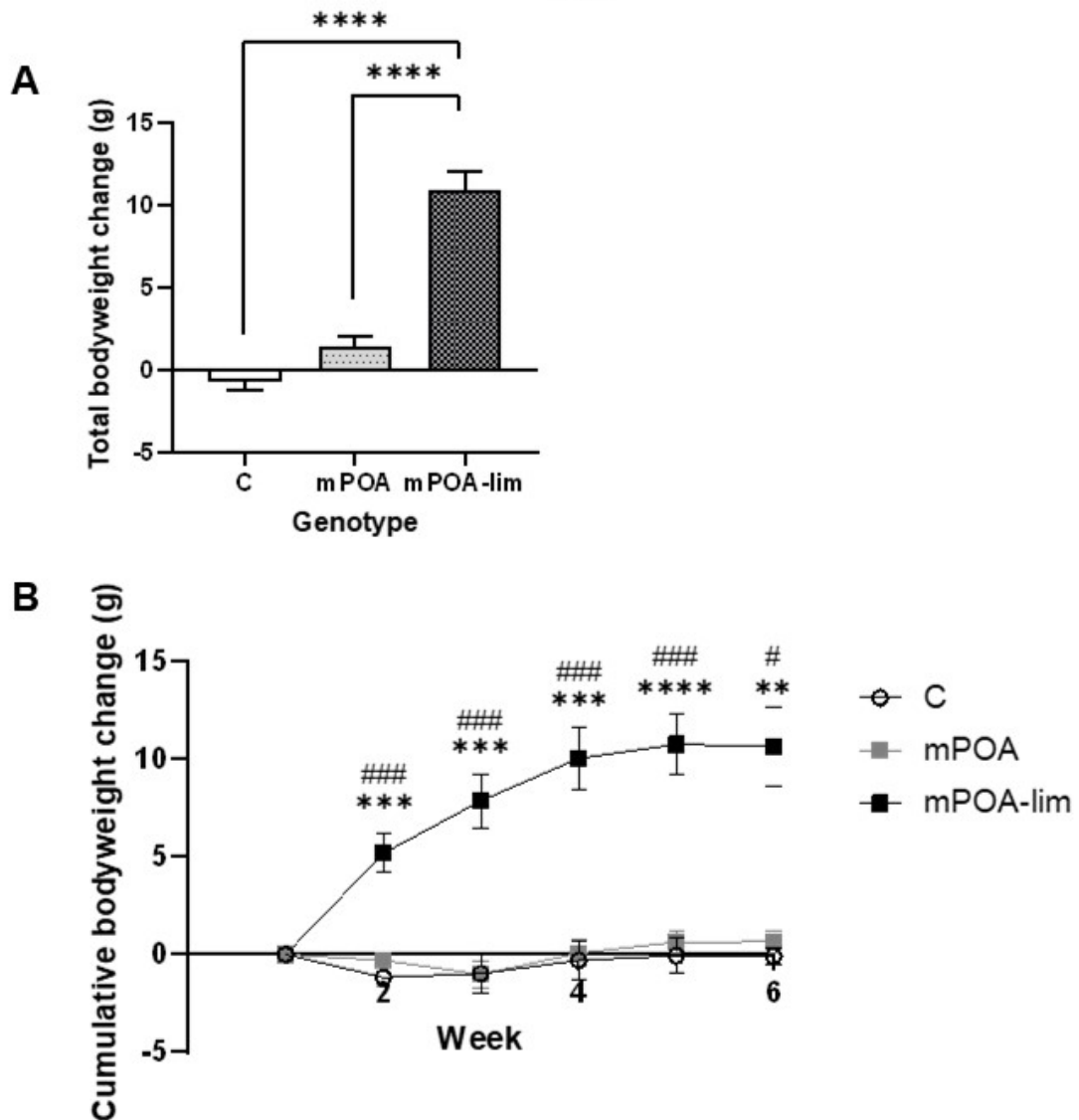


Figure 6.4. Body weight. Total bodyweight change (**A**) and cumulative bodyweight change (**B**) for control (C, $n = 7$), hypo-ArKO (hypo, $n = 14$), and hypo-lim-ArKO (hypo-lim, $n = 10$) mice housed in running wheel cages. For **A**, the average total bodyweight change was calculated by subtracting the final body weight from the initial body weight for each animal in the group. Data are presented as mean + SEM. For **B**, bodyweight was measured every week over the course of the study for each mouse to obtain the average cumulative change in bodyweight. Data are presented as mean \pm SEM. For **A**, differences were established by means of a one-way ANOVA with Bonferroni's multiple comparisons *post hoc*. For **B**, differences were established by a two-way ANOVA with Bonferroni's multiple comparisons test *post hoc*. * denotes a difference between hypo-lim-ArKO and control and # denotes a difference between hypo-lim-ArKO and hypo-ArKO. * or #, $P < 0.05$; ** or ##, $P < 0.01$; *** or ###, $P < 0.001$; **** $P < 0.0001$.

6.3.4 Site-specific ArKO in the mPOA/BNST alone or in conjunction with adjacent limbic regions does not affect sex or aggressive behaviour

hypo-ArKO and hypo-lim-ArKO mice showed equivalent levels of sexual behaviour as the control group (**Fig. 6.5**). There were no statistical differences between control, hypo-ArKO, or hypo-lim-ArKO groups in the number of attempted mounts (**Fig. 6.5A**), the latency to the first mount attempt (**Fig. 6.5B**), or the cumulative duration of following the female (**Fig. 6.5C**). In test 1 and test 2 respectively, only 3 and 2 male mice successfully mounted a female, 0 and 2 male mice showed any intromissions (**Supp. Fig. S6.1**) and no male mouse ejaculated (data not shown). During sexual behaviour, some ArKO mice were observed actively avoiding the female, who was hormonally primed to be sexually proceptive. Therefore, in addition to traditional measurements of sexual behaviour, we also analysed when the male rejected the female's advances and/or actively avoided the female. We observed significantly more of this avoidance behaviour in hypo-lim-ArKO mice compared to controls ($P = 0.0466$) (**Fig. 6.5D**).

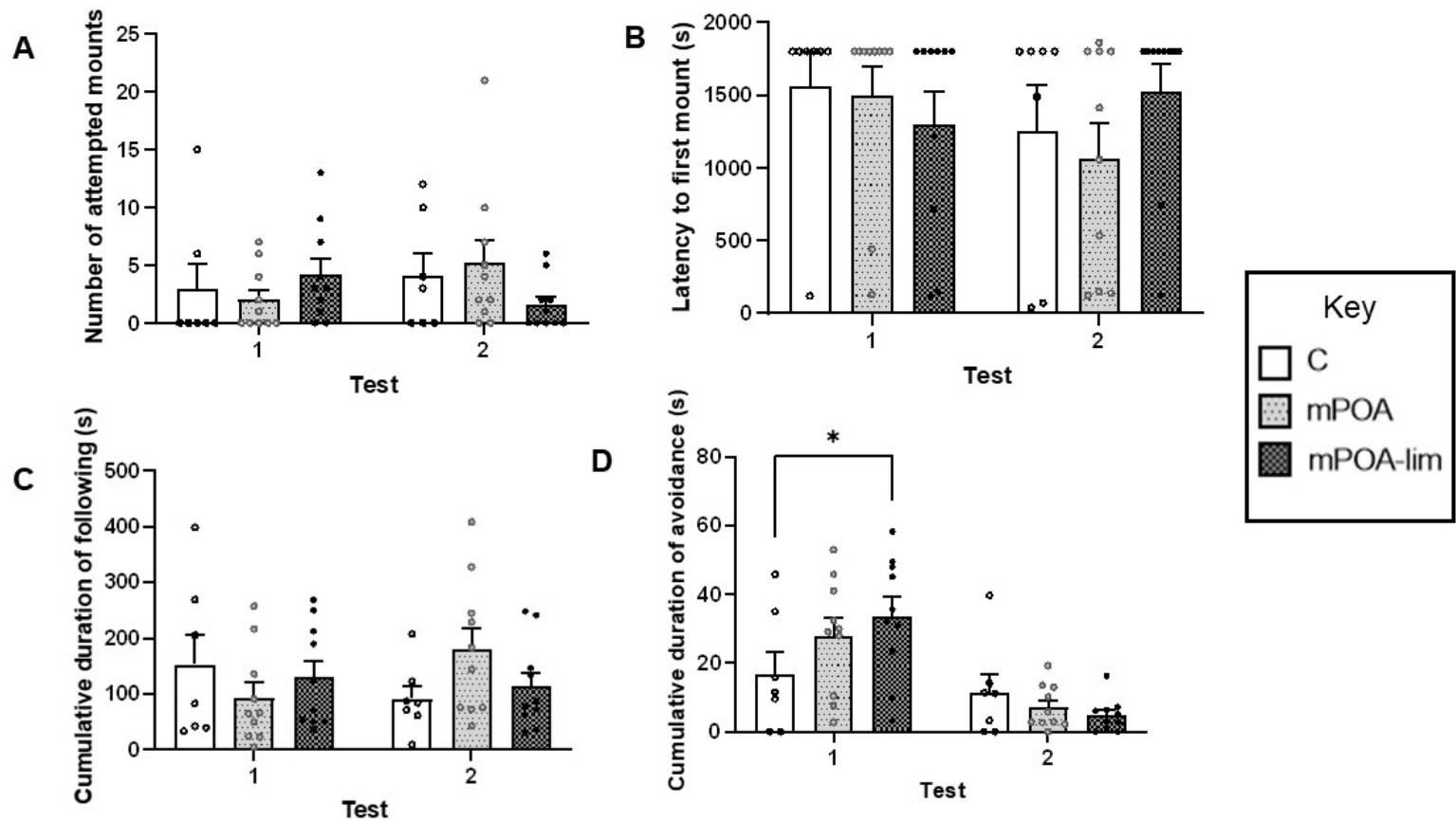


Figure 6.5. Sexual behaviour. The number of attempted mounts (**A**), latency to first mount, whether successful or unsuccessful (**B**), and the cumulative duration of time spent following the female (**C**) were analysed in control (C, $n = 7$), hypo-ArKO (hypo, $n = 14$), and hypo-lim-ArKO (hypo-lim, $n = 10$) mice. Some mice were observed actively avoiding the sexually proceptive female. The cumulative time of this behaviour is shown in **D**. All data are presented as mean + SEM. Data were analysed by means of a two-way ANOVA with Bonferroni's multiple comparisons *post hoc*. * $P < 0.05$.

Similar aggression levels were shown between groups in the resident-intruder test (**Fig. 6.6-6.7**). A two-way ANOVA revealed no differences between groups, tests or the interaction between groups and tests in the number of aggressive bouts (**Fig. 6.6A**), cumulative duration of aggressive bouts (**Fig. 6.6B**), latency to aggressive behaviour (**Fig. 6.7A**), or the number of instances of tail rattling (**Fig. 6.7C**). When mice encounter and approach a conspecific, they engage in sniffing as an investigative behaviour (Arakawa et al., 2011). We observed no difference in sniffing behaviour between groups in the first week of tests (**Fig. 6.7B**). In test 3 of the second week, hypo-lim-ArKO mice sniffed significantly less than controls ($P = 0.0190$) (**Fig. 6.7B**).

During this same test, we also observed a tendency for hypo-ArKO mice to sniff less than controls ($P = 0.0630$) (Fig. 6.7B).

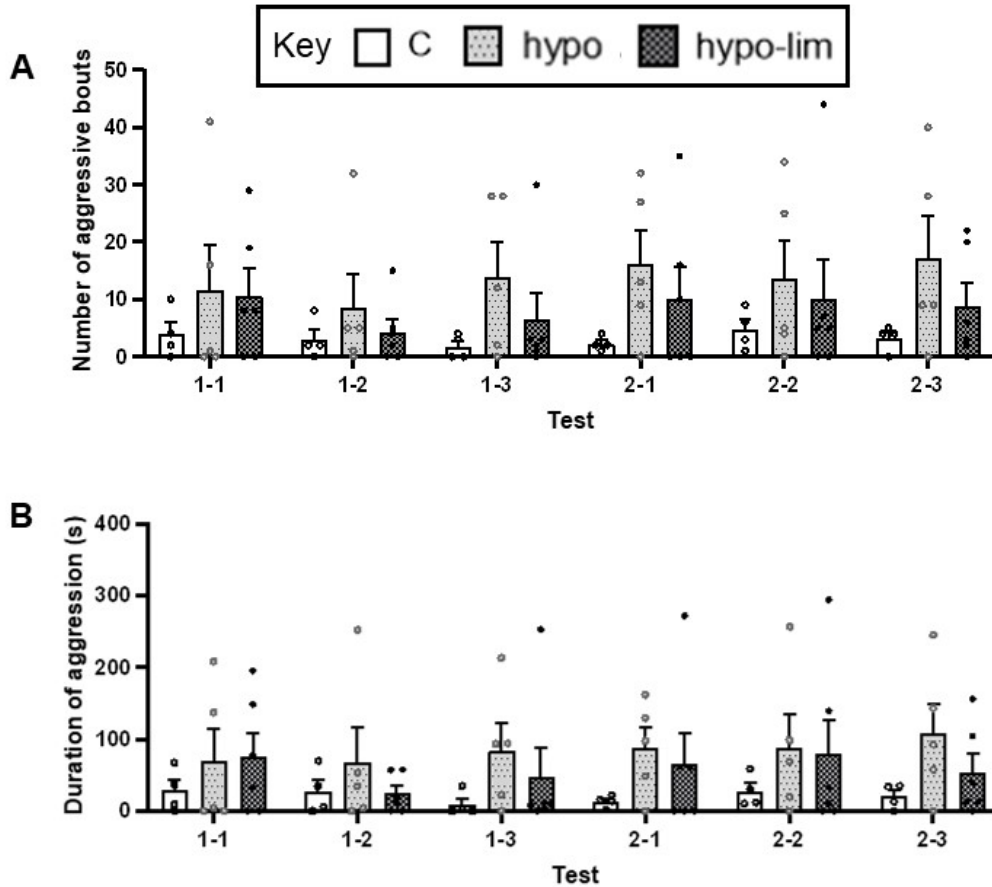


Figure 6.6. Aggressive bouts. The number of aggressive bouts (A) and cumulative duration of aggressive bouts (B), latency to aggression (C), duration of sniffing the intruder (D), and number of tail rattling bouts (E) were analysed in control (C, $n = 7$), hypo-ArKO (hypo, $n = 14$), and hypo-lim-ArKO (hypo-lim, $n = 10$) mice. All data are presented as mean \pm SEM. Data were analysed by means of a two-way ANOVA with Bonferroni's multiple comparisons *post hoc*. * $P < 0.05$.

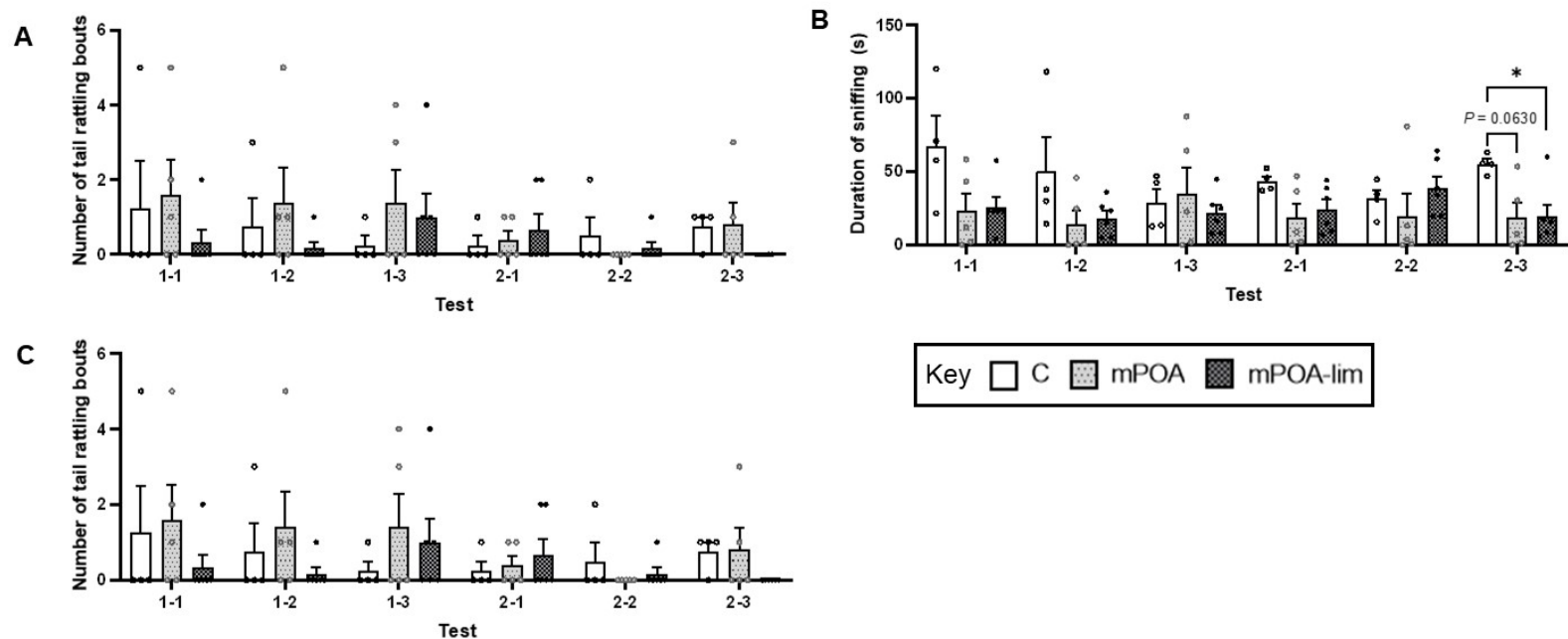


Figure 6.7. Aggressive behaviours. The latency to aggression (**A**), duration of sniffing the intruder (**B**), and number of tail rattling bouts (**C**) were analysed in control (C, $n = 7$), hypo-ArKO (hypo, $n = 14$), and hypo-lim-ArKO (hypo-lim, $n = 10$) mice. All data are presented as mean + SEM. Data were analysed by means of a two-way ANOVA with Bonferroni's multiple comparisons *post hoc*. * $P < 0.05$.

6.3.5 hypo-lim-ArKO increases anxiety in the light-dark test

In the LDT, there was no difference between groups in the distance travelled in the light (**Fig. 6.8A**) or dark compartments (**Fig. 6.8C**). However, compared to controls, hypo-lim-ArKO mice spent significantly less time in the light ($P = 0.0256$) (**Fig. 6.8B**) and significantly more time in the dark ($P = 0.0447$) (**Fig. 6.8D**). On average, hypo-lim-ArKO mice transitioned between the light and dark portions of the box 10 times, compared to 19 times in both control and hypo-ArKO groups. Yet, there was no statistical difference between the groups in the number of transitions (**Fig. 6.9A**). There was also no difference between groups in the latency to enter the light compartment (**Fig. 6.9B**) or the number of defecations and urinations in either the light or dark compartments (**Fig. 6.9C-D**).

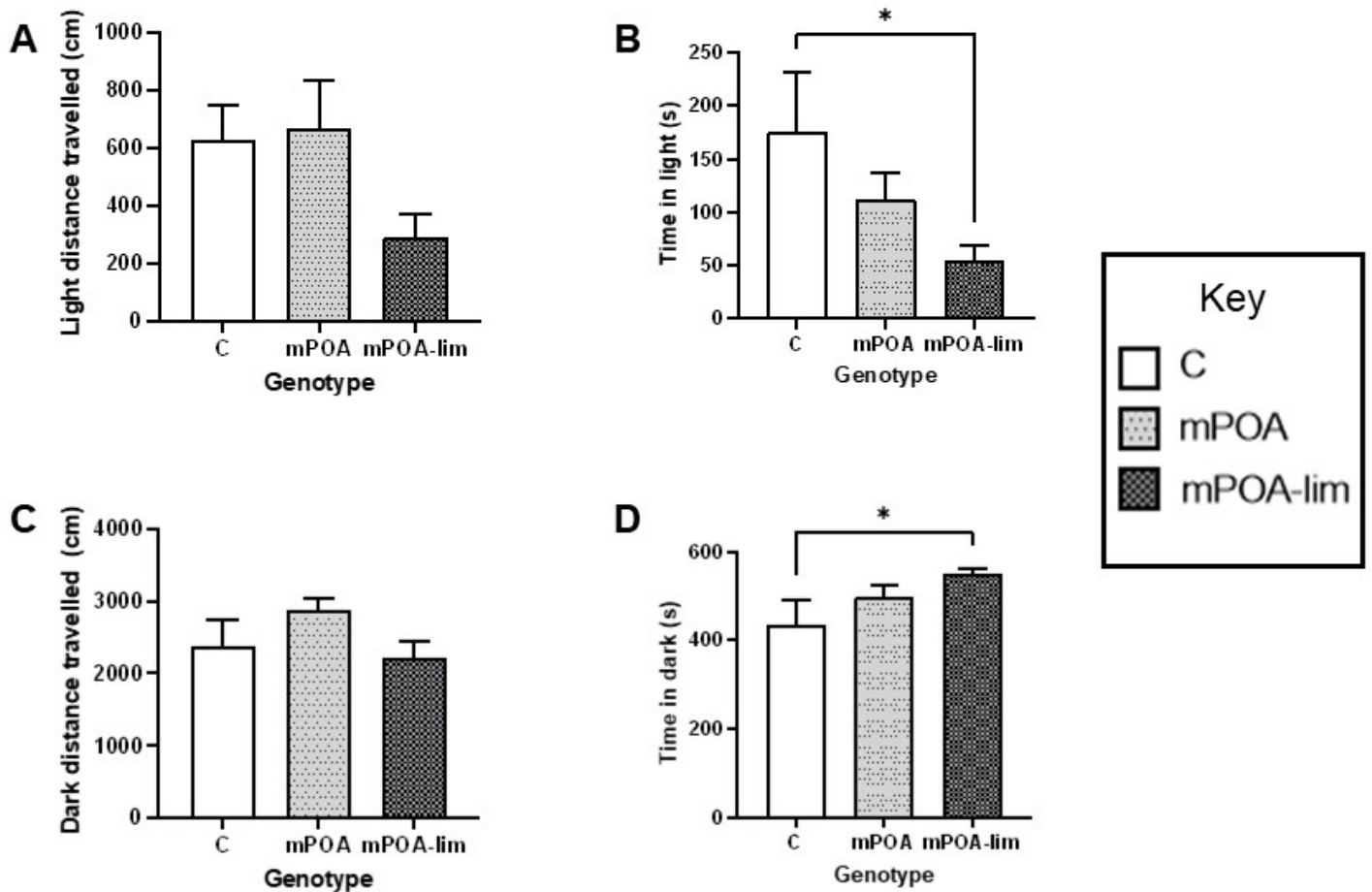


Figure 6.8. Light-dark test (i). The distance travelled in the light (A) and dark (C) and the time spent in the light (B) and dark (D) were analysed in control (C, $n = 7$), hypo-ArKO (hypo, $n = 14$), and hypo-lim-ArKO (hypo-lim, $n = 10$) mice. All data are presented as mean + SEM. Parametric datasets were analysed by a one-way ANOVA with Bonferroni's multiple comparisons test *post hoc*; nonparametric datasets were analysed by a Kruskal-Wallis test with Dunn's multiple comparisons test *post hoc*. * $P < 0.05$.

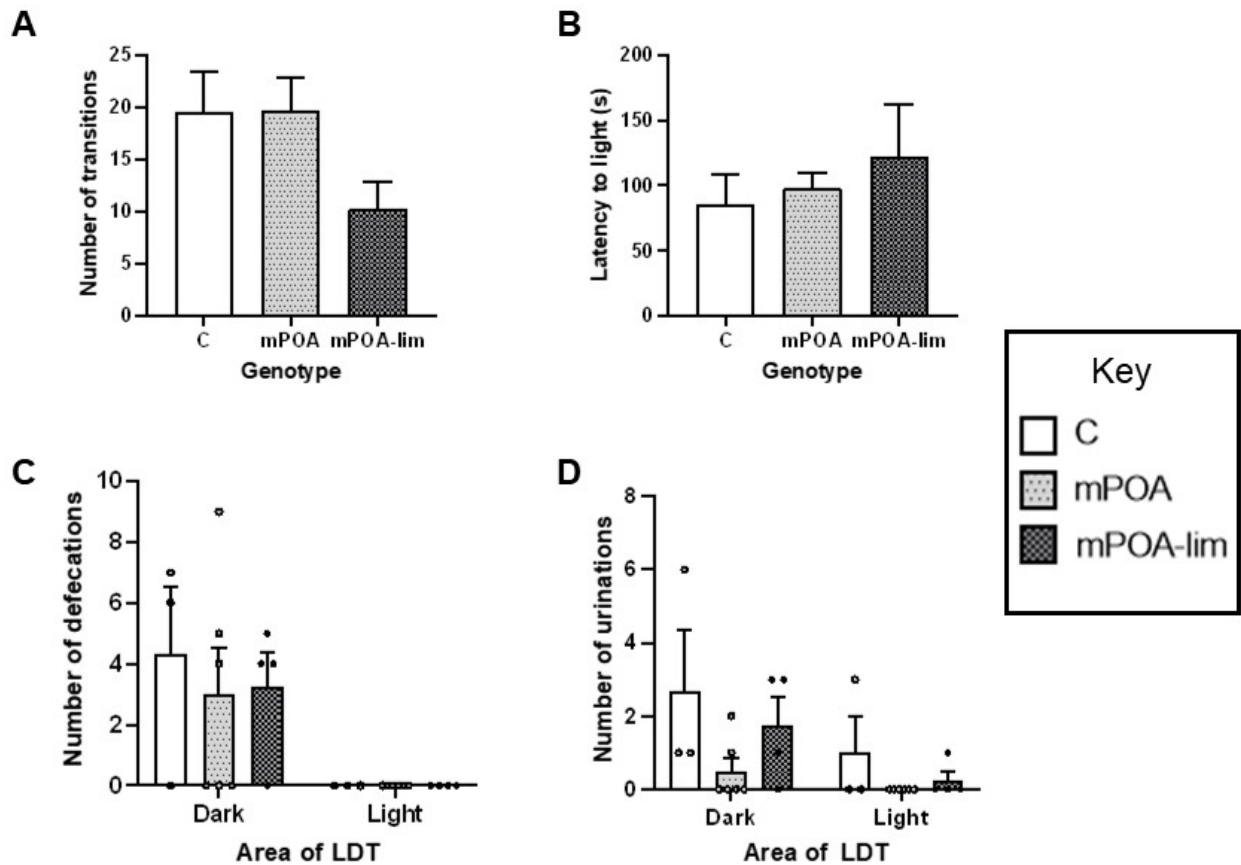


Figure 6.9. Light-dark test (ii). The number of transitions between the light and dark (A), and the latency to enter the light (B), the number of defecations (C), and the number of urinations (D) were analysed in control (C, $n = 7$), hypo-ArKO (hypo, $n = 14$), and hypo-lim-ArKO (hypo-lim, $n = 10$) mice. All data are presented as mean + SEM. Parametric datasets were analysed by a one-way ANOVA with Bonferroni's multiple comparisons test *post hoc*; nonparametric datasets were analysed by a Kruskal-Wallis test with Dunn's multiple comparisons test *post hoc*.

6.4 Discussion

In the present study, we utilised a unique ArKO mouse model to understand the importance of neuroestrogen synthesis in the regulation of social behaviours in the mouse. Due to the unavailability of female *Aro^{fl/fl}* mice at the time of study, the behavioural phenotype was characterised in the male mouse. We set out to knockout aromatase in the mPOA of experimental mice, given its central role in sexual (Dominguez and Hull, 2005), aggressive (Nelson and Trainor, 2007), and recently documented anxious behaviours (Zhang et al., 2021). We had also previously

identified this node as one of the predominant neurosteroidogenic sites of the SBN (Chapters 3 & 4). However, due to the intricate anatomical structure of the brain and limitations in precision during the AAV injection procedure, it was determined that the injection overspilled slightly into the BNST, and some mice were injected in both the mPOA and adjacent limbic regions, including the PVN and hippocampus. Although this deviated from our initial intent, we wish to emphasise that this unanticipated outcome does not diminish the value of the data we have collected.

It is essential to note that, currently, there are no available conditional *and* region-specific aromatase knockout mouse models. To date, the ArKO mouse most valuable for understanding the activational roles of neuroestrogens is the forebrain-specific conditional ArKO mouse (fbn-ArKO) (Lu et al., 2019). In a Cre/loxP recombination system, mice express *Cre* under the control of the *CaMKII α* promoter, which is expressed in excitatory neurones of the forebrain by postnatal days 18-23 (Tsien et al., 1996). Male and female mice of this genotype showed deficits in forebrain spine and synaptic density, impaired hippocampal-dependent spatial reference memory, recognition memory, and contextual fear memory, but had normal locomotor function and anxiety levels (sex and aggressive behaviours were not explored) (Lu et al., 2019). As the largest region of the brain, the forebrain contains the entire cerebrum and several structures contained within it, including the hypothalamus and the limbic system (Ackerman, 1992). Thus, the spatial specificity of the fbn-ArKO mouse is somewhat poor. Aromatase is not only expressed in cell bodies but also in fibres that connect several regions of the brain (Stanic et al., 2014), suggesting that neuroestrogens are synthesised and passed between areas as part of a steroidogenic circuit. Furthermore, the induction of *Cre* expression and aromatase knockout during the pubertal period could have overlapping organisational consequences on brain development and behaviours. Puberty is a major developmental window, as pubertal hormones acting in the hippocampus increase expression of GABA_A receptors (Keating et al., 2019), modulate synaptic plasticity (Meyer et al., 1978), and regulate cell survival and differentiation (Schulz and Sisk, 2016). Targeted knockdown of ER α in the meA of pubertal male mice reduces neurone numbers (Sano et al., 2013) and prepubertal gonadectomy in males reduces aromatase activity in adulthood (Roselli and Klosterman, 1998b). Our model, which permits the specific knockout of aromatase in designated brain regions, offers the advantage of selective aromatase knockout in adulthood whilst preserving the organisational effects of both neuroestrogens and gonadal E₂.

6.4.1 *Physiological characteristics and voluntary running wheel activity*

The mice used in this study were gonadally intact and showed similar levels of E₂ in blood plasma, showing that knockout of aromatase in the mPOA/BNST (hypo-ArKO) or hypothalamo-limbic regions (hypo-lim-ArKO) does not impact peripheral E₂ production.

We found that both groups of ArKO mice showed significantly decreased running wheel activity compared to controls. The modulation of running wheel activity by E₂ has been well established through the use of gonadectomised male and female rats, which show decreased running activity that is increased by E₂ treatment (Roy and Wade, 1975, Gentry and Wade, 1976, Ahdieh and Wade, 1982). Lesion (King, 1979) and preoptic E₂ implant studies (Fahrbach et al., 1985) have demonstrated that the mPOA is the primary brain site responsible for this behavioural effect, and ERKO studies have shown that ER α is the primary ER mediating running wheel activity (Ogawa et al., 2003). In whole-body ArKO mice, running wheel activity is significantly decreased compared to WT controls (Watai et al., 2007). However, this model does not allow for the distinction between central and peripheral aromatase. Ours is the first study to demonstrate that neuroestrogens from the mPOA/BNST are critical mediators of running wheel activity in the male mouse. Knocking out aromatase either in the mPOA/BNST or hypothalamo-limbic areas led to a significant decrease in average daily revolutions, seen especially during the dark phase. These effects were observed despite intact gonads and plasma E₂ levels equivalent to those observed in control mice.

Despite both ArKO groups showing significantly reduced running wheel activity, only the hypo-lim-ArKO mice showed a significant gain in body weight. Similarly, whole-body ArKO mice display increased adiposity (Jones et al., 2000), though it has not been clear if or how brain aromatase may contribute. The obese phenotype of hypo-lim-ArKO mice in our study suggests that aromatase within limbic areas exerts a regulatory control over body weight. The role of the hippocampus in regulating food intake and body weight has been explored previously (Davidson et al., 2007). Hippocampal lesion studies have been shown to interfere with controls of food intake regulation, such as interoceptive energy state signals, appetitive behaviours that lead to food, and feeding duration (Davidson et al., 2005). How hippocampal E₂ contributes to the regulation of feeding and body weight has not been investigated, though in male rats fed a high-fat diet there is an acute increase in hippocampal ER α mRNA expression (Scudiero and Verdame, 2017), suggesting a link between E₂, the

hippocampus, and food intake exists. The PVN is a critical hypothalamo-limbic region at the centre of the neurocircuitry regulating food intake (Yousefvand and Hamidi, 2020), and the contribution of E₂ to this has been well-researched. Within the PVN, oxytocinergic neurones signal to decrease food intake (Liu et al., 2021), and E₂ administration to OVX female rats further enhances the anorexigenic effects of oxytocin (Liu et al., 2020). E₂ exerts a strong homeostatic influence over feeding behaviours, producing anorectic effects by decreasing either meal size or meal frequency (Rivera and Stincic, 2018). The anorectic effects of E₂ are believed to be due to action in the PVN which decreases the release of neuropeptide-Y, a potent orexigenic signal (Bonavera et al., 1994). Since we did not measure food intake in our study, it is not possible to conclude whether increased body weight was caused by increased feeding related to a lack of functional aromatase within the limbic region. It is unlikely that the increased body weight in hypo-lim-ArKO mice was due to reduced activity, as running wheel activity was significantly reduced in both knockout groups and the bodyweight of hypo-ArKO mice did not significantly change. Other studies have found that subcutaneous letrozole implants in female rats led to increased body weight although food intake and total energy expenditure remained unchanged (Skarra et al., 2017). Thus, food intake, activity, and body weight are not always mutually exclusive. This finding illustrates the potential for a new avenue of research investigating neuroestrogens within hypothalamo-limbic regions and their role in regulating body weight and feeding behaviours.

6.4.2 Sexual behaviour

Sex and aggression are modulated by E₂, and the mPOA has been identified as a key node in the modulation of both behaviours (Dominguez and Hull, 2005, Nelson and Trainor, 2007), though the contribution of neuroestrogens remains unclear. We hypothesised that a lack of functional aromatase in the mPOA would diminish sexual behaviour rather than abolish it completely, given the availability of gonadal hormones. Indeed, androgens are capable of mediating at least some behavioural effects, demonstrated by the partial restoration of sexual behaviour in castrated brain ArKO mice treated with testosterone (Brooks et al., 2020b).

In fact, we observed no alteration in sexual behaviour with ArKO in either the mPOA/BNST or hypothalamo-limbic regions. E₂ signalling is critical for the display of sexual behaviours in the male rodent and previous research has demonstrated that ERKO $\alpha\beta$ completely abolishes sexual behaviour in the male mouse (Ogawa et al., 2000). ERKO β has no effect on male sexual behaviour (Ogawa et al., 1999),

implicating ER α as the predominant ER contributing to male sexual behaviours. Region-specific knockout of ER α in the mPOA or VMH of gonadally intact male mice results in impaired mounting and intromission in compared to WT controls (Sano et al., 2013). Considering this evidence together with our own, it appears that, whilst E₂ signalling within the mPOA in particular is critical for male sexual behaviour, neuroestrogen synthesis within the mPOA or hypothalamo-limbic regions is not required for sexual behaviour in the male mouse.

In the present study, no mice exhibited ejaculation in any sexual behaviour test. Thus, we could not determine whether hypothalamo-limbic neuroestrogens contribute to erectile function. Nevertheless, our data does suggest that neuroestrogens from either the mPOA/BNST or hypothalamo-limbic regions are not required for the consummatory aspects of male sexual behaviour such as mounting or appetitive behaviours such as genital sniffing or following of the female. To fully understand neuroestrogen-mediated regulation of male sexual behaviour, it is necessary to examine appetitive aspects such as odour preference for oestrous females, which is known to be impaired in ERKO α mice (Wersinger and Rissman, 2001).

During sexual behaviour tests, we observed that some ArKO mice spent a notable amount of time actively avoiding the receptive female. When we quantified this during behavioural analysis, we found that avoidance behaviour (characterised by the male moving away from the female and/or rejecting her advances) was increased in mPOA-lim-ArKO mice. To our knowledge, avoidance behaviour is not commonly reported in male rodent sexual behaviour testing. The limbic system integrates and relays threat- and stress-related signals to modulate defensive behaviours, which could include freezing, moving away, or hiding from the perceived threat (Kirouac, 2021b). As far as we know, a role for E₂ in the modulation of these behaviours has not been described, although it has formerly been noted that freezing behaviour is increased in OVX rats compared to sham-operated female rats (Gupta et al., 2001). Since we did not observe a significant level of avoidance in mice with ArKO in the mPOA/BNST, it is likely that neuroestrogens synthesised within the limbic system modulate avoidance behaviour, which may be linked to the increased levels of anxiety observed in hypo-lim-ArKO mice, as described below.

6.4.3 Aggressive behaviour

There were no alterations in aggressive behaviour with ArKO in the mPOA/BNST or in hypothalamo-limbic regions. E₂ has a well-established role in the organisation and activation of aggressive behaviour, with several studies showing that

neonatal castration (Peters et al., 1972), ERKO α (Ogawa et al., 1997), and ArKO (Matsumoto et al., 2003) leads to impaired intermale aggression in rodents, although ERKO β mice are more aggressive than WT mice in resident intruder tests (Ogawa et al., 1999). There is limited evidence for the involvement of the mPOA in the regulation of male aggressive behaviour in rodents. It has been reported that the number of ER α -positive cells in the mPOA is not correlated with aggression levels in male mice (Trainor et al., 2006). In line with this, ERKO α in the mPOA had no effect on aggressive behaviours in male mice (Sano et al., 2013). However, ER α -positive cells from the mPOA project to other aggression loci, such as the ventrolateral part of the VMH (VMHvl), and increase fighting in male mice upon their activation (Wei et al., 2023). Although one mouse in the hypo-lim-ArKO group was hit in the VMH, all measured parameters were comparable to other mice in the hypo-lim-ArKO group. Knockout of ER α within the VMH was shown to reduce intermale aggression in the mouse (Sano et al., 2013) which suggests that ER α signalling in the VMH is important for aggressive behaviour in the mouse, but neuroestrogen synthesis in the VMH may not be.

The BNST has been suggested to interact with the mPOA to process sex-specific odour cues (Been and Petrulis, 2011) which could regulate sex and aggressive behaviour. A positive correlation between ER α immunopositive cells in the anteroventral BNST and aggression level has been reported in male mice (Trainor et al., 2006), although aromatase activity in the BNST has been shown to be negatively correlated with aggression (Trainor et al., 2004). Our data suggests that neuroestrogens originating from the mPOA/BNST do not contribute to aggression, and regulation by these areas may depend more heavily on other hormones such as vasopressin (Bester-Meredith and Marler, 2001, Irvin et al., 1990).

In male Japanese quail, neuroestrogen within the POA has a bimodal effect on bird aggression, such that low concentrations increase aggression compared to vehicle, but high concentrations inhibit the frequency of aggressive behaviours (Ubuka et al., 2014). Aromatase activity in the POA is increased by gonadotropin inhibitory hormone (GnIH), a hypothalamic peptide secreted by the PVN, which activates aromatase through dephosphorylation (Ubuka et al., 2014). Suppression of GnIH, achieved by the consumption of a large amount of soya bean, has been shown to reduce aromatase activity and increase aggression in male mice (Abdel-Aleem et al., 2019). Given the dependence of aggressive behaviours on POA-derived neuroestrogen in the quail, it is not clear why ArKO in areas that included the mPOA had no effect on aggressive behaviour in our study, though it could be due to species differences. Other potential reasons include the possibility that aggression is dependent upon neuroestrogen

synthesis in other brain areas. One neurosteroidogenic aggression locus is the meA, where genetic ablation of aromatase-positive cells did not affect the attack frequency but resulted in a greater latency to initiate aggression (Unger et al., 2015). Additionally, it is not clear whether aggressive behaviour was maintained by the presence of testicular hormones, since all mice in our study were gonadally intact. Indeed, the study by Unger et al. (2015), in which mice were tested intact, would suggest that at least some level of aggression was maintained by steroids synthesised from the periphery or from other regions of the brain, suggesting that neuroestrogens play only a small part in male aggressive behaviours. Finally - though perhaps the least likely with no available evidence – the brain may have compensatory mechanisms to offset the lack of aromatase activity within the mPOA and limbic regions to maintain normal aggressive behaviour. We have previously shown an androgen-driven mechanism by which the female brain can continue to synthesise neuroestrogens even in the presence of letrozole (Chapter 4). Whether such mechanisms exist elsewhere in the male brain, and whether they can be induced by region-specific ArKO to maintain wildtype levels of aggression, requires further investigation.

The limbic system has been implicated in mediating reactive aggression, which is evoked by threat, provocation, or frustration (Chang and Gean, 2019). In using OBX stimulus mice, we were able to investigate aggressive behaviours in mice that were not influenced by defeat or provocation (Ogawa et al., 2000, Sano et al., 2013). Though hypo-lim-ArKO mice did not show any change in aggression compared to controls, our experimental setup did not allow us to investigate reactive aggression. This may be addressed in future studies by exposing experimental mice to acute stress before the resident-intruder paradigm with an OBX intruder mouse.

A potential reason underlying the lack of differences in sex and aggressive behaviours in hypo-ArKO and hypo-lim-ArKO mice could be the age at which the mice were tested. The mice used in this study ranged from 10-37 weeks old and may have been too aged to display normal sociosexual behaviours.

6.4.4 Anxiety

The mPOA is typically investigated in the context of reproductive and aggressive behaviours and has only recently been considered as part of the anxiety circuit. The role of the mPOA in anxiety is complex as it has been found to have antagonistic effects via GABAergic neurones, which mediate anxiolytic effects, and glutamatergic neurones, which mediate anxiogenic effects (Zhang et al., 2021). E₂ signalling via ER α in the mPOA is believed to be anxiogenic, since female mice treated

with a shNA against ER α in the mPOA spent more time in the light compartment of the LDT and more time in the centre of the open field test (OFT), indicative of less anxiety (Spiteri et al., 2012). Yet, we found that hypo-ArKO mice did not show any significant alterations in anxiety levels compared to controls.

E₂ also has anxiolytic effects, which are mediated through ER β (Lund et al., 2005). The hippocampus and PVN are some of the few areas to express ER β in greater quantities than ER α (Shughrue et al., 1997), and it is well accepted that the PVN and limbic regions are the predominant brain areas involved in anxiety (Kirouac, 2021b). However, the role of neuroestrogens synthesised within or around the PVN and limbic region has not been investigated. Interestingly, we observed significantly increased anxiety in hypo-lim-ArKO mice, suggesting that neuroestrogens synthesized within the limbic region have an anxiolytic effect.

A range of studies have shown that reducing E₂ levels by way of OVX (Puga-Olguín et al., 2019), castration (McDermott et al., 2012), or pharmacological aromatase inhibition (Meng et al., 2011) results in increased anxiety. In contrast, whole-body ArKO male and female mice did not differ from WT mice in anxiety levels in the OFT or elevated plus maze (EPM) (Dalla et al., 2004, Dalla et al., 2005), although it is difficult to interpret the contributions of neuroestrogens in these models. In the fbn-ArKO mouse, males showed similar levels of anxiety to WT mice in the OFT (Lu et al., 2019). It is not clear why ArKO in a generalised brain area did not affect anxiety whereas the targeted KO in our study did, though a possible contributing factor is the timing of gene disruption. In the fbn-ArKO mouse, Cre recombinase was expressed between postnatal days 18-23 (Lu et al., 2019). Although these mice developed with archetypal E₂ concentrations in the postnatal period, the disruption of aromatase during puberty may have led to unintended consequences on development. Puberty is a critical developmental phase characterized by numerous processes that ultimately have effects on adult behaviour (Dovey and Vasudevan, 2020). For example, prepubertal gonadectomy of male rats had an anxiolytic effect on behaviours in the OFT and EPM in adulthood (Renczes et al., 2020). Meanwhile, gonadectomy of adult male rats is associated with increased anxiety (McDermott et al., 2012). Therefore, the timing of aromatase disruption is likely to have a profound impact on behaviours. In our study, the conditional knockout was performed at 10-37 weeks of age, meaning that mice developed with normal E₂ levels and aromatase function postnatally and throughout puberty, offering a more accurate depiction of the activational properties of E₂ in anxious behaviour.

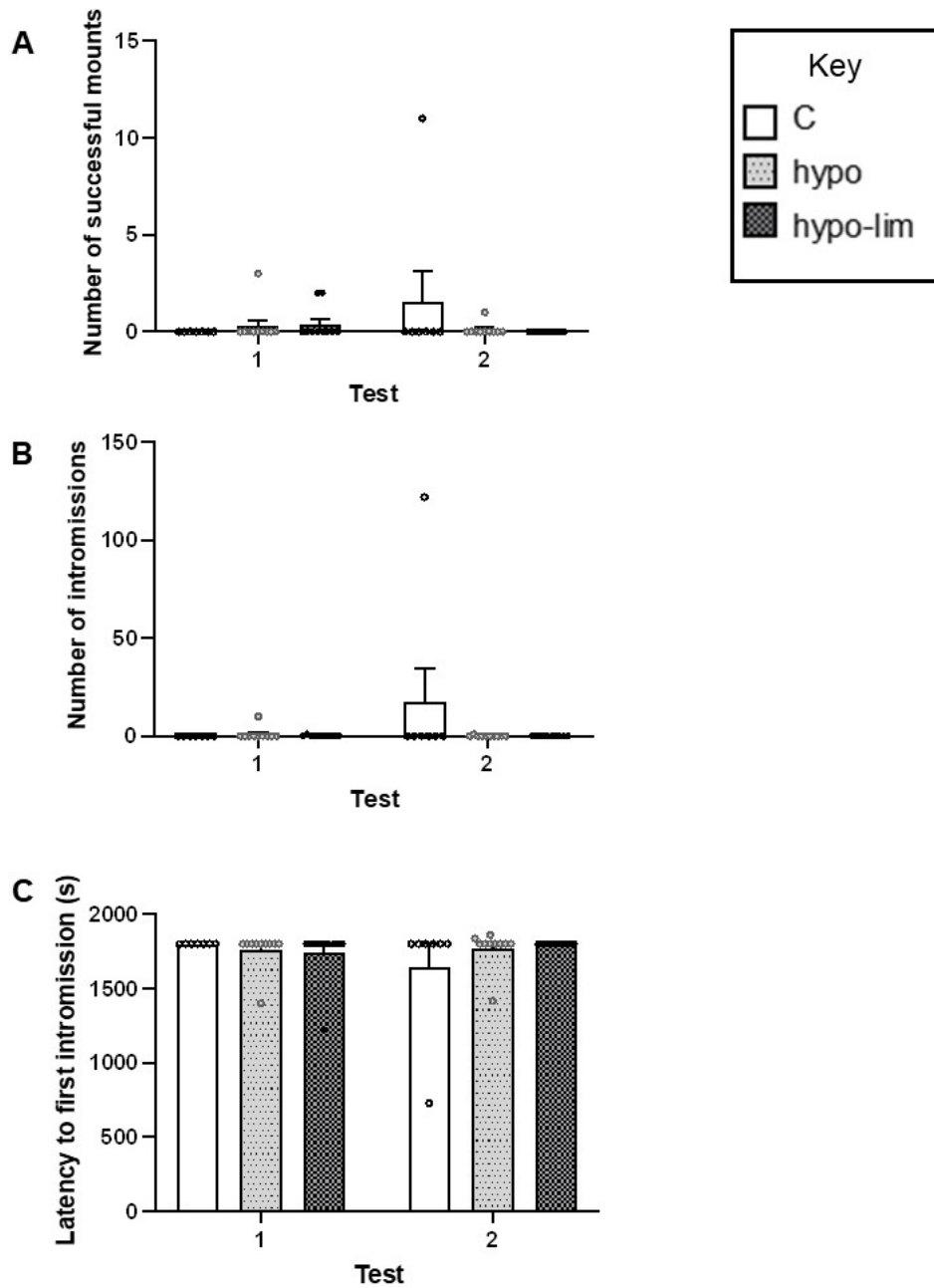
We have previously shown the existence of a novel regulatory pathway that exists within the female mouse mPOA (Chapter 4). In this pathway, blockade of aromatase by the aromatase inhibitor letrozole is bypassed, as testosterone is instead converted to DHT, which is metabolised to 3 β -diol. 3 β -diol is an endogenous agonist of ER β , though which it signals to increase aromatase expression (Chapters 4 & 5, Cisternas et al., 2017). The current research suggests that this mechanism exists in female, but not male, amygdala cultures (Cisternas et al., 2017), and preliminary data from our laboratory suggests that this sex dimorphism is also present in the mPOA (data not shown). Whilst this pathway may not be induced in the male mPOA by the administration of letrozole, the production of 3 β -diol is still possible given the fact that the enzymes responsible for its synthesis, 5 α -reductase and 3 β -HSD, are expressed in the male mouse hypothalamus (Chapter 3, Karolczak et al., 1998). The effects of 3 β -diol have been studied mainly by RJ Handa and colleagues, who have shown that 3 β -diol implants in the PVN significantly reduce plasma corticosterone in response to restraint stress (Lund et al., 2006). These effects are thought to be mediated by ER β , which induces oxytocin production in the PVN (Kudwa et al., 2014, Blume et al., 2008). Whilst this shows the site of 3 β -diol action, the site of its synthesis has not been elucidated. In microdissected PVN from male rats, 5 α -reductase mRNA was expressed, indicating that the PVN can produce DHT, but 3 β -HSD was not expressed (Lund et al., 2006). 3 β -HSD is required for the conversion of DHT to 3 β -diol. Theoretically, all of the mice in our study retained the capacity to synthesise 3 β -diol in the mPOA, which may have a paracrine action in the PVN and/or limbic regions. Yet, we observed a notable divergence in anxiety levels, with hypo-ArKO mice displaying no significant change compared to controls, whilst hypo-lim-ArKO mice exhibited heightened anxiety. This enigma raises a fundamental question: could the anxiolytic effect of 3 β -diol be a product of a dynamic collaboration with neuroestrogens? To begin to explore this question, a dedicated assay for the measurement of 3 β -diol becomes an indispensable tool.

6.5 Summary

In this study, we have utilised a conditional ArKO mouse model that has allowed us to selectively knockout aromatase expression in specific brain regions. In contrast to previous studies utilising whole-body ArKO mice, we did not observe any alterations in sex or aggressive behaviour of mice lacking functional aromatase in either the mPOA/BNST or adjacent limbic regions. Though this could be a product of the age of

the mice used in the study, it may also be a reflection of the predominant role of gonadal steroids in modulating these behaviours. Interestingly, our study revealed an increase in anxiety in mice lacking functional aromatase in the mPOA/BNST and limbic regions, but not in those with ArKO limited to the mPOA/BNST. This discrepancy suggests the involvement of neuroestrogens originating from limbic regions in the modulation of anxiety in adult male mice. This observation not only expands the horizons of potential research avenues but underscores the significance of this mouse model in unravelling the neurosteroidogenic networks within the brain and their contributions to sociosexual behaviours.

6.6 Supplementary information



Supplementary Figure S6.1. Sexual behaviour. The number of successful mounts (**A**), number of intromissions (**B**), and the latency to first intromission (**C**) were analysed in control (C, $n = 7$), hypo-ARKO (hypo, $n = 14$), and hypo-lim-ARKO (hypo-lim, $n = 10$) mice. All data are presented as mean \pm SEM. Data were analysed by means of a two-way ANOVA with Bonferroni's multiple comparisons *post hoc*.

Chapter 7
General Discussion

The aim of this thesis was to investigate neuroestrogen production and regulation of neuroestrogen production in the nuclei of the SBN and hypothalamic nodes related to social behaviours in the female mouse. We also investigated the functional relevance of neurosteroid production in the female and male hypothalamus. To achieve this, we developed a novel method, incorporating modifications of incubation techniques (Loryan et al, 2013) and sensitive in-house ELISAs to measure neurosteroid levels in aCSF and brain tissue. This approach enabled a comprehensive examination of sex differences in neurosteroid synthesis and enzyme expression, contributing to a greater understanding on the mechanisms underlying neuroendocrine regulation and social behaviours.

Our findings revealed significant differences in neurosteroid synthesis and regulation within the female brain and between the sexes. Notably, this is the first research to directly measure neurosteroid concentrations with direct comparisons between intact, non-hormone-primed male and female mice. Furthermore, our research uncovered previously unexplored regional differences in neurosteroid synthesis regulation in female mice. This regulation has previously been described in amygdala primary cell culture (Cisternas et al, 2017), and has never before been demonstrated to exist in *ex vivo* brain slices or *in vivo*. By measuring hormones in *ex vivo* slices from intact non-hormone-primed females and observing the behavioural consequences of neurosteroid synthesis, we have contributed to mitigating the prevalent sex bias in biomedical research. This endeavour enriches our understanding of female neuroendocrine function and fosters a more accurate portrayal of physiological processes.

Beyond their contributions to basic science, these discoveries highlight potential avenues for the development of pharmacological interventions targeting neurosteroid pathways. Such interventions could offer new treatment modalities to address unmet clinical needs and improve patient outcomes in diseases that are characterised by dysregulation of neurosteroids, such as mental disorders and menopausal medicine. Of particular interest is the behavioural relevance of neuroestrogen depletion in the context of anxiety, especially given that this had a much greater effect in female mice than in male. This warrants further investigation as it suggests that the region-dependence of neurosteroid synthesis may also be sexually dimorphic, offering the potential for the development of personalised medicines and/or interventions for anxiety.

Additionally, our exploration of the effects of neuroestrogen depletion on dendritic spine morphology provides a critical insight into the mechanisms underlying neuronal

plasticity. These insights have profound implications for understanding neurodevelopmental and neuropsychiatric disorders that may be associated with either altered neuronal architecture and/or dysregulated E₂.

7.1 Limitations

Whilst our research has provided valuable knowledge to the field, there are some limitations that should be discussed. Such limitations may be addressed through future work.

Measuring hormone production in *ex vivo* brain slices allowed us to expose brain slices to different treatments to elucidate how hormone production is regulated in the SBN. However, the brain slices contained several other adjacent regions that were not part of the SBN but may have contributed to the concentration of hormones measured in aCSF. A more precise way to measure hormones in individual SBN nuclei would have been to punch out these regions following brain slicing; the punches could then be incubated in aCSF. However, given the small size of the punches, it would have been difficult to retrieve them for use in downstream RT-qPCR experiments. Therefore, we would have had to use double the animals to have enough samples for all experiments. This would not satisfy the 3Rs, and thus was not pursued.

The brain slice incubation method we developed has demonstrated its utility in investigating neuroestrogen production and related pathways. To further enhance the capacity of this method, one potential refinement could involve the incorporation of radiolabelled steroid precursors. Tracking the conversion of precursors to downstream neuroestrogens in real time would allow for a more dynamic assessment of enzymatic reactions and their modulation under various conditions. Furthermore, this could enable the quantification of enzyme kinetics and how this may be differentially regulated throughout the brain and between sexes.

Our approach for measuring neurosteroids involved competitive in-house ELISA assays that were previously developed by Prof. P. Knight at the University of Reading. These highly sensitive assays were useful for our understanding of neuroestrogen synthesis but limited us with regards to which hormones we could measure. For example, it would have been particularly useful to measure 3 β -diol concentrations during brain slice incubation and treatment of mice with letrozole and dutasteride. Additionally, assessing corticosterone levels in mice undergoing these treatments would have been particularly beneficial for understanding how these treatments may

affect anxiety. Future studies could utilise other techniques such as LC-MS/MS to gather a library of hormonal information. This could even be achieved with the samples currently in our possession from the experiments detailed in this thesis.

To understand the specific roles of 3β -diol in behaviours, injecting with 3β -diol rather than the inhibitors of its synthesis would have been preferable. However, due to the challenges posed by COVID and Brexit, as well as the limited access to 3β -diol in Japan where the studies took place, we opted to block 3β -diol synthesis instead. Additionally, future studies could investigate the importance of this pathway in other female behaviours such as reproduction and maternal behaviour, in which the mPOA plays a pivotal role (Micevych and Meisel, 2017, Fang et al., 2018). Studies from primary amygdala cell cultures have suggested that the regulation of aromatase expression by 3β -diol is sexually dimorphic, occurring in female cultures but not male (Cisternas et al., 2017). Preliminary data from our lab suggests that this is also the case in the hypothalamus, though the functional significance of this is not known. To begin to understand this, it would be beneficial to perform parallel behavioural experiments with 3

The *Aro^{fl/fl}* mouse model promises to be a valuable asset for future studies aiming to understand the regional contributions of aromatase and neuroestrogens to brain function and behaviour. Whilst we did not observe any effects of hypothalamo-limbic ArKO in sexual or aggressive behaviour, future studies could include a group of castrated *Aro^{fl/fl}* mice, to understand if behavioural persistence is due to gonadal hormones. Other studies using the *Aro^{fl/fl}* mouse should investigate the effect of knockout in other behaviourally relevant areas, such as the VMH and meA. Knocking out aromatase expression from a series of regions in one mouse could help to further understand the circuitry of neuroestrogens. This could help to identify the discrete regions responsible for neuroestrogen synthesis, explore autocrine and paracrine signalling between regions of synthesis and target regions, and determine the specific behavioural outcomes associated with each region of synthesis. Additionally, these studies could be carried out in parallel with female mice to explore sex differences in the regulation of behaviours by neuroestrogens.

7.2 Concluding statement

E_2 is involved in numerous physiological processes in the central nervous system. The brain possesses the necessary enzymatic machinery to synthesise E_2 *de novo* from either cholesterol or precursors available from the periphery, termed

neuroestrogens. However, the regulation of neuroestrogen synthesis within specific brain nuclei underlying social behaviours has not previously been explored. The findings of this thesis are shown in **Fig. 7.1**. We have used a novel brain slice incubation method to demonstrate that neuroestrogens are produced by the social behaviour network and synthesis is differentially regulated between nuclei. In doing this, we have discovered a novel pathway of regulation that exists within the female mouse mPOA. Using *in vivo* experiments, we have been able to understand how this regulatory mechanism contributes to behaviours in the female mouse. Finally, using a novel conditional ArKO model, we were able to knockout aromatase expression within the hypothalamo-limbic regions to characterise, for the first time, the behavioural phenotype of mice that are unable to produce neuroestrogens in the hypothalamus.

Figure 7.1. Findings of this thesis. A novel pathway exists in the female mouse mPOA in which aromatase expression is increased by 3β -diol acting on ER β . Blocking 3β -diol production leads to decreased connectivity of the brain, as dendrites are shorter in length, show less arbourisation, and have fewer dendritic spines. Blockade of 3β -diol tended to increase anxiety, specifically in the EPM. The changes in neural connectivity may underlie these behavioural changes. In the male mouse, knockout of

aromatase expression in the hypothalamo-limbic region leads to increased anxiety in the LDT and increased avoidance of sexually receptive females in sexual behaviour tests.

Appendix

Appendix Table S1. List of specific reagents for each experiment.

Material	Experiment series	Supplier	Product ID/code/cat #
0.5 M EDTA	Hormone immunoassay	Fisher Scientific	10306983
1 M hydrochloric acid	General lab usage	Scientific Laboratory Supplies	CHE2164
17 β -oestradiol	Hormone immunoassay	Sigma-Aldrich	50-28-2
5alpha-androstane-3beta,17beta-diol	Treatments	Sigma-Aldrich	NMID635
6-CMO-Estradiol-HP	Hormone immunoassay	Fitzgerald Industries	65-IE16
Aromatase antibody	Immunohistochemistry	Novus Biologicals	NB-100-1596
Bovine serum albumin	Immunohistochemistry	Sigma-Aldrich	9048-46-8
Calcium chloride dihydrate	Brain slice preparation	ThermoFisher Scientific	11964171
Citric acid anhydrous	Hormone immunoassay	Scientific Laboratory Supplies	77-92-9
Diarylpropionitrile (DPN)	Treatments	MedChemExpress	1428-67-7
Dimethyl sulfoxide	Treatments	ThermoFisher Scientific	J66650.AK
Di-sodium hydrogen orthophosphate anhydrous	Hormone immunoassay	Scientific Laboratory Supplies	7558-79-4
Dutasteride	Treatments	Fisher Scientific	164656-23-9
Ethanol	General lab usage	Fisher Scientific	10680993
Finasteride	Treatments	Fisher Scientific	98319-26-7
Fluoromount-G™ Mounting Medium, with DAPI	Immunohistochemistry	Invitrogen™, ThermoFisher Scientific	00-4959-52

Gelatin	Solid phase extraction/hormone immunoassay	Fisher Scientific	G7-500
Glucose	Brain slice preparation	Fisher Scientific	10335850
Glycine	Immunohistochemistry	Fisher Scientific	50-40-6
Goat anti-Rabbit IgG (H+L) Cross-Adsorbed Secondary Antibody, Alexa Fluor™ 568	Immunohistochemistry	Invitrogen™, ThermoFisher Scientific	A-11011
Greiner ELISA plate flat bottomed high binding	Hormone immunoassay	Scientific Laboratory Supplies	G655061
HEPES	Brain slice preparation	Sigma-Aldrich	H3375-5KG
High-Capacity cDNA Reverse Transcription Kit	RT-qPCR	Applied Biosystems™, ThermoFisher Scientific	4268814
Hydrogen peroxide solution, 30%	Hormone immunoassay	Scientific Laboratory Supplies	31642-1L
ICI 182,780	Treatments	MedChemExpress	129453-61-8
Kinesis TELOS SPE Column, C18	Solid phase extraction	Scientific Laboratory Supplies	CH5586
L-ascorbic acid	Brain slice preparation	ThermoFisher Scientific	11946881
Letrozole	Treatments	Fisher Scientific	16461716
Magnesium chloride hexahydrate	Brain slice preparation	Fisher Scientific	10647032
Magnesium sulfate	Brain slice preparation	ThermoFisher Scientific	11397658
Methanol (HPLC)	Solid phase extraction	Fisher Scientific	67-56-1
MicroAmp™ fast optical 96-well reaction plate	RT-qPCR	Applied Biosystems™, ThermoFisher Scientific	4346907

Nuclease free water	RT-qPCR	Scientific Laboratory Supplies	3098SIG
OCT	Immunohistochemistry	Fisher Scientific	23-730-571
OPD (o-phenylenediamine dihydrochloride)	Hormone immunoassay	ThermoFisher Scientific	34005
PBS tablets	General lab usage	Scientific Laboratory Supplies	P4417-50TAB
Potassium chloride	Brain slice preparation	ThermoFisher Scientific	10236350
Potassium hydrogen phosphate	Brain slice preparation	ThermoFisher Scientific	11493714
PowerSYBR Green PCR Master Mix	RT-qPCR	Fitzgerald Industries	10219284
Primers	RT-qPCR	Integrated DNA Technologies	Various
ProClin™ 300	Hormone immunoassay	Sigma-Aldrich	48912-U
Propyl pyrazole triol (PPT)	Treatments	MedChemExpress	263717-53-9
Rabbit polyclonal to aromatase	Immunohistochemistry	Novus Biotechne	NBP2-48998
RNA/ater™ Stabilization Solution	RT-qPCR	Invitrogen™, ThermoFisher Scientific	AM7021
RnaseZAP	RT-qPCR	Scientific Laboratory Supplies	R2020-250ML
RNeasy® Plus Mini Kit	RT-qPCR	Qiagen	74134
sliceGolgi kit	Golgi staining	Bioenno Lifesciences	003760
Sodium bicarbonate	Brain slice preparation	ThermoFisher Scientific	10082840
Sodium carbonate	Hormone immunoassay	ThermoFisher Scientific	11307886

Sodium chloride	Brain slice preparation	ThermoFisher Scientific	10092740
Sodium citrate dihydrate	Immunohistochemistry	Scientific Laboratory Supplies	W302600-1KG-K
Sodium dihydrogen orthophosphate dihydrate	Brain slice preparation	Fisher Scientific	10723621
Sucrose	Brain slice preparation	Fisher Scientific	57-50-1
SuperBlock™ Blocking Buffer	Immunohistochemistry	ThermoFisher Scientific	37515
Testosterone	Hormone immunoassay	Sigma	T6147
Testosterone-3-CMO-HP	Hormone immunoassay	Fitzgerald Industries	65-IT07
Triton X-100	Immunohistochemistry	ThermoFisher Scientific	A16046.AP
Trypan blue solution, 0.4%	Brain slice preparation	Gibco™, ThermoFisher Scientific	11538886
Tween-20	Hormone immunoassay	Scientific Laboratory Supplies	P1379-250ML
Tween-80	Treatments	Scientific Laboratory Supplies	P1754-25ML
Xylene	Golgi staining	Fisher Scientific	10467270
pENN.AAV.hSyn.HI.eGFP-Cre.WPRE.SV40	<i>Aro^{fl/fl}</i>	Addgene	Addgene_105540
pAAV-hSyn-EGFP	<i>Aro^{fl/fl}</i>	Addgene	Addgene_50465

Bibliography

- ABDEL-ALEEM, G. A., SHAFIK, N. M., EL-MAGD, M. A. & MOHAMED, D. A. 2019. Soya bean rich diet is associated with adult male rat aggressive behavior: relation to RF amide-related peptide 3-aromatase-neuroestrogen pathway in the brain. *Metab Brain Dis*, **34**, 1103.
- ABDELGADIR, S. E., RESKO, J. A., OJEDA, S. R., LEPHART, E. D., MCPHAUL, M. J. & ROSELLI, C. E. 1994. Androgens regulate aromatase cytochrome P450 messenger ribonucleic acid in rat brain. *Endocrinology*, **135**, 395.
- ACEVEDO-RODRIGUEZ, A., MANI, S. K. & HANDA, R. J. 2015. Oxytocin and estrogen receptor β in the brain: an overview. *Front Endocrinol (Lausanne)*, **6**, 160.
- ACKERMAN, S. 1992. Major Structures and Functions of the Brain. Discovering the Brain. Washington (DC): National Academies Press (US).
- AGÍS-BALBOA, R. C., PINNA, G., ZHUBI, A., MALOKU, E., VELDIC, M., COSTA, E. & GUIDOTTI, A. 2006. Characterization of brain neurons that express enzymes mediating neurosteroid biosynthesis. *PNAS*, **103**, 14602.
- AHDIEH, H. B. & WADE, G. N. 1982. Effects of hysterectomy on sexual receptivity, food intake, running wheel activity, and hypothalamic estrogen and progesterin receptors in rats. *J Comp Physiol Psychol*, **96**, 886.
- AHMED, E. I., ZEHR, J. L., SCHULZ, K. M., LORENZ, B. H., DONCARLOS, L. L. & SISK, C. L. 2008. Pubertal hormones modulate the addition of new cells to sexually dimorphic brain regions. *Nat Neurosci*, **11**, 995.
- AKAMA, K. T., THOMPSON, L. I., MILNER, T. A. & MCEWEN, B. S. 2013. Post-synaptic Density-95 (PSD-95) Binding Capacity of G-protein-coupled Receptor 30 (GPR30), an Estrogen Receptor That Can Be Identified in Hippocampal Dendritic Spines. *J Biol Chem*, **288**, 6438.
- ALBERT, D. J., WALSH, M. L., GORZALKA, B. B., MENDELSON, S. & ZALYS, C. 1986. Intermale social aggression: suppression by medial preoptic area lesions. *Physiol Behav*, **38**, 169.
- ANCHAN, D., GAFUR, A., SANO, K., OGAWA, S. & VASUDEVAN, N. 2014. Activation of the GPR30 receptor promotes lordosis in female mice. *Neuroendocrinology*, **100**, 71.

- ANDO, T., NISHIYAMA, T., TAKIZAWA, I., ISHIZAKI, F., MIYASHIRO, Y., TAKEDA, K., HARA, N. & TOMITA, Y. 2016. Dihydrotestosterone synthesis pathways from inactive androgen 5 α -androstane-3 β ,17 β -diol in prostate cancer cells: Inhibition of intratumoural 3 β -hydroxysteroid dehydrogenase activities by abiraterone. *Sci Rep*, **6**, 32198.
- ARAI, Y. & GORSKI, R. A. 1968. Critical exposure time for androgenization of the developing hypothalamus in the female rat. *Endocrinology*, **82**, 1010.
- ARAKAWA, H., CRUZ, S. & DEAK, T. 2011. From models to mechanisms: odorant communication as a key determinant of social behavior in rodents during illness-associated states. *Neurosci Biobehav Rev*, **35**, 1916.
- BABAYAN, A. H. & KRAMÁR, E. A. 2013. Rapid Effects of Oestrogen on Synaptic Plasticity: Interactions with Actin and its Signaling Proteins. *J Neuroendocrinol*, **25**, 1163.
- BAILEY, D. J., MA, C., SOMA, K. K. & SALDANHA, C. J. 2013. Inhibition of hippocampal aromatization impairs spatial memory performance in a male songbird. *Endocrinology*, **154**, 4707.
- BAKKER, J., HONDA, S.-I., HARADA, N. & BALTHAZART, J. 2002. The Aromatase Knock-Out Mouse Provides New Evidence That Estradiol Is Required during Development in the Female for the Expression of Sociosexual Behaviors in Adulthood. *J Neurosci*, **22**, 9104.
- BALTHAZART, J. & BALL, G. F. 1998. New insights into the regulation and function of brain estrogen synthase (aromatase). *Trends Neurosci*, **21**, 243.
- BALTHAZART, J., DUPIEREUX, V., ASTE, N., VIGLIETTI-PANZICA, C., BARRESE, M. & PANZICA, G. C. 1994. Afferent and efferent connections of the sexually dimorphic medial preoptic nucleus of the male quail revealed by in vitro transport of Dil. *Cell Tissue Res*, **276**, 455.
- BANKS, W. A. 2012. Brain Meets Body: The Blood-Brain Barrier as an Endocrine Interface. *Endocrinology*, **153**, 4111.
- BARFIELD, R. J. & CHEN, J. J. 1977. Activation of Estrous Behavior in Ovariectomized Rats by Intracerebral Implants of Estradiol Benzoate. *Endocrinology*, **101**, 1716.

- BARSON, J. R., MACK, N. R. & GAO, W.-J. 2020. The Paraventricular Nucleus of the Thalamus Is an Important Node in the Emotional Processing Network. *Front Behav Neurosci*, **14**, 598469.
- BAUM, M. J. & VREEBURG, J. T. 1973. Copulation in castrated male rats following combined treatment with estradiol and dihydrotestosterone. *Science*, **182**, 283.
- BAUMGARTNER, N. E., GRISSOM, E. M., POLLARD, K. J., MCQUILLEN, S. M. & DANIEL, J. M. 2019. Neuroestrogen-Dependent Transcriptional Activity in the Brains of ERE-Luciferase Reporter Mice following Short- and Long-Term Ovariectomy. *eNeuro*, **6**, ENEURO.0275-19.
- BEACH, F. A. 1976. Sexual attractivity, proceptivity, and receptivity in female mammals. *Horm Behav*, **7**, 105.
- BECK, S. G. & HANDA, R. J. 2004. Dehydroepiandrosterone (DHEA): A Misunderstood Adrenal Hormone and Spine-Tingling Neurosteroid? *Endocrinology*, **145**, 1039.
- BEEN, L. E. & PETRULIS, A. 2011. Chemosensory and hormone information are relayed directly between the medial amygdala, posterior bed nucleus of the stria terminalis, and medial preoptic area in male Syrian hamsters. *Horm Behav*, **59**, 536.
- BENNESCH, M. A. & PICARD, D. 2015. Minireview: Tipping the Balance: Ligand-Independent Activation of Steroid Receptors. *Mol Endocrinol*, **29**, 349.
- BERENT-SPILLSON, A., MARSH, C., PERSAD, C., RANDOLPH, J., ZUBIETA, J.-K. & SMITH, Y. 2017. Metabolic and hormone influences on emotion processing during menopause. *Psychoneuroendocrinology*, **76**, 218.
- BERMOND, B. 1982. Effects of medial preoptic hypothalamus anterior lesions on three kinds of behavior in the rat: Intermale aggressive, male-sexual, and mouse-killing behavior. *Aggress Behav*, **8**, 335.
- BESTER-MEREDITH, J. K. & MARLER, C. A. 2001. Vasopressin and aggression in cross-fostered California mice (*Peromyscus californicus*) and white-footed mice (*Peromyscus leucopus*). *Horm Behav*, **40**, 51.
- BHARADWAJ, P., MCINNIS, C., MADDEN, A. M. K., BONTHUIS, P. J., ZUP, S., RISSMAN, E. F. & PARK, J. H. 2013. Increased Dendritic Spine Density and Tau Expression Are Associated with Individual Differences in Steroidal Regulation of Male Sexual Behavior. *PLoS ONE*, **8**, e69672.

- BIRD, A. D. & CUNTZ, H. 2019. Dissecting Sholl Analysis into Its Functional Components. *Cell Rep*, **27**, 3081.
- BLAUSTEIN, J. D., LEHMAN, M. N., TURCOTTE, J. C. & GREENE, G. 1992. Estrogen receptors in dendrites and axon terminals in the guinea pig hypothalamus. *Endocrinology*, **131**, 281.
- BLUME, A., BOSCH, O. J., MIKLOS, S., TORNER, L., WALES, L., WALDHERR, M. & NEUMANN, I. D. 2008. Oxytocin reduces anxiety via ERK1/2 activation: local effect within the rat hypothalamic paraventricular nucleus. *Eur J Neurosci*, **27**, 1947.
- BLURTON-JONES, M. & TUSZYNSKI, M. H. 2002. Estrogen receptor-beta colocalizes extensively with parvalbumin-labeled inhibitory neurons in the cortex, amygdala, basal forebrain, and hippocampal formation of intact and ovariectomized adult rats. *J Comp Neurol*, **452**, 276.
- BOHACEK, J. & DANIEL, J. M. 2009. The ability of oestradiol administration to regulate protein levels of oestrogen receptor alpha in the hippocampus and prefrontal cortex of middle-aged rats is altered following long-term ovarian hormone deprivation. *J Neuroendocrinol*, **21**, 640.
- BONAVERA, J. J., DUBE, M. G., KALRA, P. S. & KALRA, S. P. 1994. Anorectic effects of estrogen may be mediated by decreased neuropeptide-Y release in the hypothalamic paraventricular nucleus. *Endocrinology*, **134**, 2367.
- BONSALL, R. W., CLANCY, A. N. & MICHAEL, R. P. 1992. Effects of the nonsteroidal aromatase inhibitor, Fadrozole, on sexual behavior in male rats. *Horm Behav*, **26**, 240.
- BORROW, A. P. & HANDA, R. J. 2017. Estrogen Receptors Modulation of Anxiety-Like Behavior. *Vitam Horm*, **103**, 27.
- BOURQUE, M., MORISSETTE, M. & DI PAOLO, T. 2015. Neuroprotection in Parkinsonian-treated mice via estrogen receptor α activation requires G protein-coupled estrogen receptor 1. *Neuropharmacology*, **95**, 343.
- BRAILOIU, E., DUN, S. L., BRAILOIU, G. C., MIZUO, K., SKLAR, L. A., OPREA, T. I., PROSSNITZ, E. R. & DUN, N. J. 2007. Distribution and characterization of estrogen receptor G protein-coupled receptor 30 in the rat central nervous system. *J Endocrinol*, **193**, 311.

- BRANN, D. W., DHANDAPANI, K., WAKADE, C., MAHESH, V. B. & KHAN, M. M. 2007. Neurotrophic and Neuroprotective Actions of Estrogen: Basic Mechanisms and Clinical Implications. *Steroids*, **72**, 381.
- BRANN, D. W., LU, Y., WANG, J., ZHANG, Q., THAKKAR, R., SAREDDY, G. R., PRATAP, U. P., TEKMAL, R. R. & VADLAMUDI, R. K. 2022. Brain-derived estrogen and neural function. *Neurosci Biobehav Rev*, **132**, 793.
- BRIDGES, R. S. 2015. Neuroendocrine regulation of maternal behavior. *Frontiers in Neuroendocrinology*, **36**, 178.
- BROCK, O., BAUM, M. J. & BAKKER, J. 2011. The Development of Female Sexual Behavior Requires Prepubertal Estradiol. *J Neurosci*, **31**, 5574.
- BROCK, O., DE MEES, C. & BAKKER, J. 2015. Hypothalamic Expression of Oestrogen Receptor α and Androgen Receptor is Sex-, Age- and Region-Dependent in Mice. *Journal of Neuroendocrinology*, **27**, 264.
- BRONSTEIN, P. M. & HIRSCH, S. M. 1974. Reactivity in the rat: Ovariectomy fails to affect open-field behaviors. *B Psychonomic Soc*, **3**, 257.
- BROOKS, D. C., COON V, J. S., ERCAN, C. M., XU, X., DONG, H., LEVINE, J. E., BULUN, S. E. & ZHAO, H. 2020a. Brain Aromatase and the Regulation of Sexual Activity in Male Mice. *Endocrinology*, **161**, 137.
- BROWN, G. R., KULBARSH, K. D., SPENCER, K. A. & DUVAL, C. 2015. Peri-pubertal exposure to testicular hormones organizes response to novel environments and social behaviour in adult male rats. *Horm Behav*, **73**, 135.
- BRUEGGEMEIER, R. W., HACKETT, J. C. & DIAZ-CRUZ, E. S. 2005. Aromatase Inhibitors in the Treatment of Breast Cancer. *Endocr Rev*, **26**, 331.
- BRUEGGEMEIER, R. W., RICHARDS, J. A., JOOMPRAUTRA, S., BHAT, A. S. & WHETSTONE, J. L. 2001. Molecular pharmacology of aromatase and its regulation by endogenous and exogenous agents. *J Steroid Biochem Mol Biol*, **79**, 75.
- BUSKILA, Y., BREEN, P. P., TAPSON, J., VAN SCHAİK, A., BARTON, M. & MORLEY, J. W. 2014. Extending the viability of acute brain slices. *Sci Rep*, **4**, 5309.
- BYERS, S. L., WILES, M. V., DUNN, S. L. & TAFT, R. A. 2012. Mouse Estrous Cycle Identification Tool and Images. *PLoS ONE*, **7**, e35538.

- CALIZO, L. H. & FLANAGAN-CATO, L. M. 2000. Estrogen Selectively Regulates Spine Density within the Dendritic Arbor of Rat Ventromedial Hypothalamic Neurons. *J Neurosci*, **20**, 1589.
- CALLARD, G. V., KRUGER, A. & BETKA, M. 1995. The goldfish as a model for studying neuroestrogen synthesis, localization, and action in the brain and visual system. *Environ Health Perspect*, **103**, 51.
- CALLARD, G. V. & TCHOUDAKOVA, A. 1997. Evolutionary and functional significance of two CYP19 genes differentially expressed in brain and ovary of goldfish. *J Steroid Biochem Mol Biol*, **61**, 387.
- CAO, J. & PATISAUL, H. B. 2011. Sexually dimorphic expression of hypothalamic estrogen receptors α and β and kiss1 in neonatal male and female rats. *J Comp Neurol*, **519**, 2954.
- CARRIER, N., SALAND, S. K., DUCLOT, F., HE, H., MERCER, R. & KABBAJ, M. 2015. The Anxiolytic and Antidepressant-like Effects of Testosterone and Estrogen in Gonadectomized Male Rats. *Biol Psychiatry*, **78**, 259.
- CARUSO, D., PESARESI, M., ABBIATI, F., CALABRESE, D., GIATTI, S., GARCIS-SEGURA, L. M. & MELCANGI, R. C. 2013. Comparison of plasma and cerebrospinal fluid levels of neuroactive steroids with their brain, spinal cord and peripheral nerve levels in male and female rats. *Psychoneuroendocrinology*, **38**, 2278.
- CASTELLI, M. P., CASTI, A., CASU, A., FRAU, R., BORTOLATO, M., SPIGA, S. & ENNAS, M. G. 2013. Regional distribution of 5 α -reductase type 2 in the adult rat brain: An immunohistochemical analysis. *Psychoneuroendocrinology*, **38**, 281.
- CATALANO, S., GIORDANO, C., PANZA, S., CHEMI, F., BONOFILIO, D., LANZINO, M., RIZZA, P., ROMEO, F., FUQUA, S. A., MAGGIOLINI, M., ANDO, S. & BARONE, I. 2014. Tamoxifen through GPER upregulates aromatase expression: a novel mechanism sustaining tamoxifen-resistant breast cancer cell growth. *Breast Cancer Res Treat*, **146**, 273.
- CELOTTI, F., NEGRI-CESI, P. & POLETTI, A. 1997. Steroid metabolism in the mammalian brain: 5 α -reduction and aromatization. *Brain Res Bull*, **44**, 365.
- CHABAN, V. V., LAKHTER, A. J. & MICEVYCH, P. 2004. A Membrane Estrogen Receptor Mediates Intracellular Calcium Release in Astrocytes. *Endocrinology*, **145**, 3788.

- CHAITON, J. A., WONG, S. J. & GALEA, L. A. 2019. Chronic aromatase inhibition increases ventral hippocampal neurogenesis in middle-aged female mice. *Psychoneuroendocrinology*, **106**, 111.
- CHAKRABORTY, M. & BURMEISTER, S. S. 2015. Effects of estradiol on neural responses to social signals in female túngara frogs. *J Exp Biol*, **218**, 3671.
- CHAKRABORTY, T. R., RAJENDREN, G. & GORE, A. C. 2005. Expression of estrogen receptor {alpha} in the anteroventral periventricular nucleus of hypogonadal mice. *Exp Biol Med (Maywood)*, **230**, 49.
- CHAMPLIN, A. K., DORR, D. L. & GATES, A. H. 1973. Determining the Stage of the Estrous Cycle in the Mouse by the Appearance of the Vagina. *Biol Reprod*, **8**, 491.
- CHAN, H. J., PETROSSIAN, K. & CHEN, S. 2016. Structural and functional characterization of aromatase, estrogen receptor, and their genes in endocrine-responsive and –resistant breast cancer cells. *J Steroid Biochem Mol Biol*, **161**, 73.
- CHANG, C.-H. & GEAN, P.-W. 2019. The Ventral Hippocampus Controls Stress-Provoked Impulsive Aggression through the Ventromedial Hypothalamus in Post-Weaning Social Isolation Mice. *Cell Rep*, **28**, 1195.
- CHARKOUDIAN, N., HART, E. C. J., BARNES, J. N. & JOYNER, M. J. 2017. Autonomic control of body temperature and blood pressure: influences of female sex hormones. *Clin Auton Res*, **27**, 149.
- CHARLIER, T. D., CORNIL, C. A., BALL, G. F. & BALTHAZART, J. 2010a. Diversity of mechanisms involved in aromatase regulation and estrogen action in the brain. *Biochim Biophys Acta*, **1800**, 1094.
- CHARLIER, T. D., CORNIL, C. A. & BALTHAZART, J. 2013. Rapid Modulation of Aromatase Activity in the Vertebrate Brain. *J Exp Neurosci*, **7**, 31.
- CHARLIER, T. D., PO, K. W. L., NEWMAN, A. E. M., SHAH, A. H., SALDANHA, C. J. & SOMA, K. K. 2010b. 17 β -Estradiol levels in male zebra finch brain: Combining Palkovits punch and an ultrasensitive radioimmunoassay. *Gen Comp Endocrinol*, **167**, 18.
- CHEN, C.-Y., LOPES-RAMOS, C., KUIJER, M. L., PAULSON, J. N., SONAWANE, A. R., FAGNY, M., PLATIG, J., GLASS, K., QUACKENBUSH, J. & DEMEO, D. L. 2016. Sexual dimorphism in gene expression and regulatory networks across human tissues. *bioRxiv*, **082289**.

- CHEN, P., LI, B. & OU-YANG, L. 2022. Role of estrogen receptors in health and disease. *Front Endocrinol (Lausanne)*, **13**, 839005.
- CHEN, Y., DUBÉ, C. M., RICE, C. J. & BARAM, T. Z. 2008. Rapid Loss of Dendritic Spines after Stress Involves Derangement of Spine Dynamics by Corticotropin-Releasing Hormone. *J Neurosci*, **28**, 2903.
- CHIANG, E. F., YAN, Y. L., GUIGUEN, Y., POSTLETHWAIT, J. & BC, C. 2001. Two Cyp19 (P450 aromatase) genes on duplicated zebrafish chromosomes are expressed in ovary or brain. *Mol Biol Evol*, **18**, 542.
- CHRISTENSEN, A., DEWING, P. & MICEVYCH, P. 2011. Membrane-Initiated Estradiol Signaling Induces Spinogenesis Required for Female Sexual Receptivity. *J Neurosci*, **31**, 17583.
- CHRISTENSEN, L. W. & CLEMENS, L. G. 1974. Intrahypothalamic Implants of Testosterone or Estradiol and Resumption of Masculine Sexual Behavior in Long-term Castrated Male Rats *Endocrinology*, **95**, 984.
- CISTERNAS, C. D., CABRERA ZAPATA, L. E., AREVALO, M. A., GARCIA-SEGURA, L. M. & CAMBIASSO, M. J. 2017. Regulation of aromatase expression in the anterior amygdala of the developing mouse brain depends on ERbeta and sex chromosome complement. *Sci Rep*, **7**, 5320.
- CISTERNAS, C. D., TOME, K., CAEIRO, X. E., DADAM, F. M., GARCIA-SEGURA, L. M. & CAMBIASSO, M. J. 2015. Sex chromosome complement determines sex differences in aromatase expression and regulation in the stria terminalis and anterior amygdala of the developing mouse brain. *Mol Cell Endocrinol*, **414**, 99.
- COLEMAN, K., ROBERTSON, N. D. & BETHEA, C. L. 2011. Long-term ovariectomy alters social and anxious behaviors in semi-free ranging Japanese macaques. *Behav Brain Res*, **225**, 317.
- CORBIN, C. J., GRAHAM-LORENCE, S., MCPHAUL, M., MASON, J. I., MENDELSON, C. R. & SIMPSON, E. R. 1988. Isolation of a full-length cDNA insert encoding human aromatase system cytochrome P-450 and its expression in nonsteroidogenic cells. *PNAS*, **85**, 8948.
- CORIANO, C. G., LIU, F., SIEVERS, C. K., LIANG, M., WANG, Y., LIM, Y., YU, M. & XU, W. 2018. A Computational-Based Approach to Identify Estrogen Receptor $\alpha\beta$ Heterodimer Selective Ligands. *Mol Pharmacol*, **93**, 197.

- CORNIL, C. A. 2018. On the role of brain aromatase in females: why are estrogens produced locally when they are available systemically? *J Comp Physiol*, **204**, 31.
- CORNIL, C. A., BALL, G. F. & BALTHAZART, J. 2006. Functional significance of the rapid regulation of brain estrogens: Where do the estrogens come from? *Brain Res*, **1126**, 2.
- CORNIL, C. A., SEREDYNSKI, A. L., DE BOURNONVILLE, C., DICKENS, M. J., CHARLIER, T. D., BALL, G. F. & BALTHAZART, J. 2013. Rapid Control of Reproductive Behaviour by Locally Synthesised Oestrogens: Focus on Aromatase. *J Neuroendocrinol*, **25**, 1070.
- CORREA, S. M., NEWSTROM, D. W., WARNE, J. P., FLANDIN, P., CHEUNG, C. C., LIN-MOORE, A. T., PIERCE, A. A., XU, A. W., RUBENSTEIN, J. L. & INGRAHAM, H. A. 2015. An Estrogen-Responsive Module in the Ventromedial Hypothalamus Selectively Drives Sex-Specific Activity in Females. *Cell Rep*, **10**, 62.
- CRASKE, M. G. & STEIN, M. B. 2016. Anxiety. *Lancet*, **388**, 3048.
- CRESPO-CASTRILLO, A. & AREVALO, M.-A. 2020. Microglial and Astrocytic Function in Physiological and Pathological Conditions: Estrogenic Modulation. *Int J Mol Sci*, **21**, 3219.
- CRIDER, A. & PILLAI, A. 2017. Estrogen Signaling as a Therapeutic Target in Neurodevelopmental Disorders. *J Pharmacol Exp Ther*, **360**, 48.
- CROSS, E. & ROSELLI, C. E. 1999. 17beta-estradiol rapidly facilitates chemoinvestigation and mounting in castrated male rats. *Am J Physiol*, **276**, 1346.
- CUMMINGS, J. A. & BECKER, J. B. 2012. Quantitative assessment of female sexual motivation in the rat: Hormonal control of motivation. *J Neurosci Methods*, **204**, 227.
- CURLIK II, D. M., DIFEO, G. & SHORS, T. J. 2014. Preparing for adulthood: thousands upon thousands of new cells are born in the hippocampus during puberty, and most survive with effortful learning. *Front Neurosci*, **8**, 70.
- DALLA, C., ANTONIOU, K., PAPADOPOULOU-DAIFOTI, Z., BALTHAZART, J. & BAKKER, J. 2004. Oestrogen-deficient female aromatase knockout (ArKO) mice exhibit 'depressive-like' symptomatology. *Eur J Neurosci*, **20**, 217.
- DALLA, C., ANTONIOU, K., PAPADOPOULOU-DAIFOTI, Z., BALTHAZART, J. & BAKKER, J. 2005. Male aromatase-knockout mice exhibit normal levels of activity, anxiety and "depressive-like" symptomatology. *Behav Brain Res*, **163**, 186.

- DAVE, N., CHOW, L. M. L., GUDELSKY, G. A., LASANCE, K., QI, X. & DESAI, P. B. 2015. Preclinical Pharmacological Evaluation of Letrozole as a Novel Treatment for Gliomas. *Mol Cancer Ther*, **14**, 857.
- DAVIDSON, T. L., KANOSKI, S. E., SCHIER, L. A., CLEGG, D. J. & BENOIT, S. C. 2007. A potential role for the hippocampus in energy intake and body weight regulation. *Curr Opin Pharmacol*, **7**, 613.
- DAVIDSON, T. L., KANOSKI, S. E., WALLS, E. K. & JARRARD, L. E. 2005. Memory inhibition and energy regulation. *Physiol Behav*, **86**, 731.
- DAVIS, E. C., POPPER, P. & GORSKI, R. A. 1996. The role of apoptosis in sexual differentiation of the rat sexually dimorphic nucleus of the preoptic area. *Brain Res*, **734**, 10.
- DAVIS, P. G., MCEWEN, B. S. & PFAFF, D. W. 1979. Localized Behavioral Effects of Tritiated Estradiol Implants in the Ventromedial Hypothalamus of Female Rats. *Endocrinology*, **104**, 898.
- DE CHAVES, G., MORETTI, M., CASTRO, A. A., DAGOSTIN, W., DA SILVA, G. G., BOECK, C. R., QUEVEDO, J. & GAVIOLI, E. C. 2009. Effects of long-term ovariectomy on anxiety and despair in rats. *Physiol Behav*, **97**, 420.
- DE JONGE, F. H., MUNTJEWERFF, J. W., LOUWERSE, A. L. & VAN DE POLL, N. E. 1988. Sexual behavior and sexual orientation of the female rat after hormonal treatment during various stages of development. *Horm Behav*, **22**, 100.
- DENENBERG, V. H., GAULIN-KREMER, E., GANDELMAN, R. & ZARROW, M. X. 1973. The development of standard stimulus animals for mouse (*Mus musculus*) aggression testing by means of olfactory bulbectomy. *Anim Behav*, **21**, 590.
- DENMARK, A., TIEN, D., WONG, K., CHUNG, A., CACHAT, J., GOODSPEED, J., GRIMES, C., ELEGANTE, M., SUCIU, C., ELKHAYAT, S., BARTELS, B., JACKSON, A., ROSENBERG, M., MIN CHUNG, K., BADANI, H., KADRI, F., ROY, S., TAN, J., GAIKWAD, S., STEWART, A., ZAPOLSKY, I., GILDER, T. & KALUEFF, A. V. 2010. The effects of chronic social defeat stress on mouse self-grooming behavior and its patterning. *Behav Brain Res*, **208**, 553.
- DI MAURO, M., TOZZI, A., CALABRESI, P., PETTOROSSO, V. E. & GRASSI, S. 2015. Neo-synthesis of estrogenic or androgenic neurosteroids determine whether long-term potentiation or depression is induced in hippocampus of male rat. *Front Cell Neurosci*, **9**, 376.

- DI, S., MALCHER-LOPES, R., MARCHESELLI, L., BAZAN, N. G. & TASKER, J. G. 2005. Rapid glucocorticoid-mediated endocannabinoid release and opposing regulation of glutamate and gamma-aminobutyric acid inputs to hypothalamic magnocellular neurons. *Endocrinology*, **146**, 4292.
- DIAB, A., QI, J., SHAHIN, I., MILLIGAN, C. & FAWCETT, J. P. 2020. NCK1 Regulates Amygdala Activity to Control Context-dependent Stress Responses and Anxiety in Male Mice. *Neuroscience*, **448**, 107.
- DÍAZ-CRUZ, E. S., SUGIMOTO, Y., GALLICANO, G. I., BRUEGGEMEIER, R. W. & FURTH, P. A. 2011. Comparison of increased aromatase versus ER α in the generation of mammary hyperplasia and cancer. *Cancer Res*, **71**, 5477.
- DICKENS, M. J., CORNIL, C. A. & BALTHAZART, J. 2013. Neurochemical control of rapid stress-induced changes in brain aromatase activity. *J Neuroendocrinol*, **25**, 329.
- DO REGO, J. L., SEONG, J. Y., BUREL, D., LEPRINCE, J., LUU-THE, V., TSUTSUI, K., TONON, M., -C., PELLETIER, G. & VAUDRY, H. 2009. Neurosteroid biosynthesis: enzymatic pathways and neuroendocrine regulation by neurotransmitters and neuropeptides. *Front Neuroendocrinol*, **30**, 259.
- DOMÍNGUEZ-ORDÓÑEZ, R., GARCÍA-JUÁREZ, M., LIMA-HERNÁNDEZ, F. J., GÓMORA-ARRATI, P., DOMÍNGUEZ-SALAZAR, E., LUNA-HERNÁNDEZ, A., HOFFMAN, K. L., BLAUSTEIN, J. D., ETGEN, A. M. & GONZÁLEZ-FLORES, O. 2019. Protein kinase inhibitors infused intraventricularly or into the ventromedial hypothalamus block short latency facilitation of lordosis by oestradiol. *J Neuroendocrinol*, **31**, e12809.
- DOMINGUEZ, J. M. & HULL, E. M. 2005. Dopamine, the medial preoptic area, and male sexual behavior. *Physiol Behav*, **86**, 356.
- DOMINGUEZ, R. & MICEVYCH, P. 2010. Estradiol Rapidly Regulates Membrane Estrogen Receptor α Levels in Hypothalamic Neurons. *J Neurosci*, **30**, 12589.
- DOMONKOS, E., HODOSY, J., OSTATNÍKOVÁ, D. & CELEC, P. 2018. On the Role of Testosterone in Anxiety-Like Behavior Across Life in Experimental Rodents. *Front Endocrinol (Lausanne)*, **9**, 441.
- DONG, X., LI, S. & KIROUAC, G. J. 2017. Collateralization of projections from the paraventricular nucleus of the thalamus to the nucleus accumbens, bed nucleus of the stria terminalis, and central nucleus of the amygdala. *Brain Struct Funct*, **222**, 3927.

- DOVEY, J. L. & VASUDEVAN, N. 2020. Does GPER1 Play a Role in Sexual Dimorphism? *Front Endocrinol (Lausanne)*, **11**, 595895.
- DULCE MADEIRA, M., FERREIRA-SILVA, L. S. & PAULA-BARBOSA, M. M. 2001. Influence of sex and estrus cycle on the sexual dimorphisms of the hypothalamic ventromedial nucleus: Stereological evaluation and golgi study. *J Comp Neurol*, **432**, 329.
- DUNCAN, K. A. & SALDANHA, C. J. 2020. Central aromatization: A dramatic and responsive defense against threat and trauma to the vertebrate brain. *Front Neuroendocrinol*, **56**, 100816.
- EMANUELSSON, I., ALMOKHTAR, M., WIKVALL, K., GRÖNBLADH, A., NYLANDER, E., SVENSSON, A.-L., FEX SVENNINGSSEN, Å. & NORLIN, M. 2018. Expression and regulation of CYP17A1 and 3 β -hydroxysteroid dehydrogenase in cells of the nervous system: Potential effects of vitamin D on brain steroidogenesis. *Neurochem Int*, **113**, 46.
- EVANS, N. J., BAYLISS, A. L., REALE, V. & EVANS, P. D. 2016. Characterisation of Signalling by the Endogenous GPER1 (GPR30) Receptor in an Embryonic Mouse Hippocampal Cell Line (mHippoE-18). *PLoS One*, **11**, e0152138.
- EVERITT, B. J. & STACEY, P. 1987. Studies of instrumental behavior with sexual reinforcement in male rats (*Rattus norvegicus*): II. Effects of preoptic area lesions, castration, and testosterone. *J Comp Psychol*, **101**, 407.
- FAHRBACH, S. E., MEISEL, R. L. & PFAFF, D. W. 1985. Preoptic implants of estradiol increase wheel running but not the open field activity of female rats. *Physiol Behav*, **35**, 985992.
- FALKNER, A. L., GROSENICK, L., DAVIDSON, T. J., DEISSEROTH, K. & LIN, D. 2016. Hypothalamic control of male aggression-seeking behavior. *Nat Neurosci*, **19**, 596.
- FANG, Y.-Y., YAMAGUCHI, T., SONG, S. C., TRITSCH, N. X. & LIN, D. 2018. A Hypothalamic Midbrain Pathway Essential for Driving Maternal Behaviors. *Neuron*, **98**, 192.
- FESTER, L., ZHOU, L., BUTOW, A., HUBER, C., VON LOSSOW, R., PRANGE-KIEL, J., JARRY, H. & RUNE, G. M. 2009. Cholesterol-promoted synaptogenesis requires the conversion of cholesterol to estradiol in the hippocampus. *Hippocampus*, **19**, 692.

- FIGTREE, G. A., MCDONALD, D., WATKINS, H. & CHANNON, K. M. 2003. Truncated Estrogen Receptor α 46-kDa Isoform in Human Endothelial Cells. *Circulation*, **107**, 120.
- FILARDO, E. J., QUINN, J. A., FRACKELTON JR, A. R. & BLAND, K. I. 2002. Estrogen Action Via the G Protein-Coupled Receptor, GPR30: Stimulation of Adenylyl Cyclase and cAMP-Mediated Attenuation of the Epidermal Growth Factor Receptor-to-MAPK Signaling Axis. *Mol Endocrinol*, **16**, 70.
- FLANAGAN-CATO, L. M. 2011. Sex differences in the neural circuit that mediates female sexual receptivity. *Front Neuroendocrinol*, **32**, 124.
- FOWLER, C. D., LIU, Y. & WANG, Z. 2008. Estrogen and adult neurogenesis in the amygdala and hypothalamus. *Brain Res Rev*, **57**, 342.
- FOY, M. R., XU, J., XIE, X., BRINTON, R. D., THOMPSON, R. F. & BERGER, T. W. 1999. 17 β -estradiol enhances NMDA receptor-mediated EPSPs and long-term potentiation. *J Neurophysiol*, **81**, 925.
- FRANKFURT, M., GOULD, E., WOOLLEY, C. S. & MCEWEN, B. S. 1990. Gonadal steroids modify dendritic spine density in ventromedial hypothalamic neurons: a Golgi study in the adult rat. *Neuroendocrinology*, **51**, 530.
- FRICK, K. M. & KIM, J. 2018. Mechanisms underlying the rapid effects of estradiol and progesterone on hippocampal memory consolidation in female rodents. *Horm Behav*, **104**, 100.
- FRYE, C., KOONCE, C., EDINGER, K., OSBORNE, D. & WALF, A. 2008. Androgens with activity at estrogen receptor beta have anxiolytic and cognitive-enhancing effects in male rats and mice. *Horm Behav*, **54**, 726.
- FRYE, C. A., PETRALIA, S. M. & RHODES, M. E. 2000. Estrous cycle and sex differences in performance on anxiety tasks coincide with increases in hippocampal progesterone and 3 α ,5 α -THP. *Pharmacol Biochem Behav*, **67**, 587.
- FRYE, C. A. & SELIGA, A. M. 2001. Testosterone increases analgesia, anxiolysis, and cognitive performance of male rats. *Cogn affect Behav Neurosci*, **1**, 371.
- FUENTES, N. & SILVEYRA, P. 2019. Estrogen receptor signaling mechanisms. *Adv Protein Chem Struct Biol*, **116**, 135.
- FURUKAWA, A., MIYATAKE, A., OHNISHI, T. & ICHIKAWA, Y. 2002. Steroidogenic Acute Regulatory Protein (StAR) Transcripts Constitutively Expressed in the Adult Rat

Central Nervous System: Colocalization of StAR, Cytochrome P-450SCC (CYP XIA1), and 3 β -Hydroxysteroid Dehydrogenase in the Rat Brain. *J Neurochem*, **71**, 2231.

GALEEVA, A. & TUOHIMAA, P. 2001. Analysis of mouse plus-maze behavior modulated by ovarian steroids. *Behav Brain Res*, **119**, 41.

GARDENER, H. E. & CLARK, A. S. 2001. Systemic ICI 182,780 alters the display of sexual behaviors in the female rat. *Horm Behav*, **39**, 121.

GENTRY, R. T. & WADE, G. N. 1976. Sex differences in sensitivity of food intake, body weight, and running-wheel activity to ovarian steroids in rats. *J Comp Physiol Psychol*, **90**, 747.

GERALL, A. A., DUNLAP, J. L. & HENDRICKS, S. E. 1973. Effect of ovarian secretions on female behavioral potentiality in the rat. *J Comp Physiol Psychol*, **82**, 449.

GIATTI, S., DIVICCARO, S., GARCIA-SEGURA, L. M. & MELCANGI, R. C. 2019. Sex differences in the brain expression of steroidogenic molecules under basal conditions and after gonadectomy. *J Neuroendocrinol*, **31**, e12736.

GOEL, N. & BALE, T. L. 2008. Organizational and Activational Effects of Testosterone on Masculinization of Female Physiological and Behavioral Stress Responses. *Endocrinology*, **149**, 6399.

GOLDEN, S. A., JIN, M. & SHAHAM, Y. 2019. Animal Models of (or for) Aggression Reward, Addiction, and Relapse: Behavior and Circuits. *J Neurosci*, **39**, 3996.

GOLOVINE, K., SCHWERIN, M. & VANSELOW, J. 2003. Three different promoters control expression of the aromatase cytochrome p450 gene (*cyp19*) in mouse gonads and brain. *Biol Reprod*, **68**, 978.

GOODSON, J. L. 2005. The vertebrate social behavior network: Evolutionary themes and variations. *Horm Behav*, **48**, 11.

GORMAN, J. M. & DOCHERTY, J. P. 2010. A Hypothesized Role for Dendritic Remodeling in the Etiology of Mood and Anxiety Disorders. *J Neuropsychiatry Clin Neurosci*, **22**, 256.

GORSKI, R. A., HARLAN, R. E., JACOBSON, C. D., SHRYNE, J. E. & SOUTHAM, A. M. 1980. Evidence for the existence of a sexually dimorphic nucleus in the preoptic area of the rat. *J Comp Neurol*, **193**, 529.

- GOTTFRIED-BLACKMORE, A., SIERRA, A., JELLINCK, P. H., MCEWEN, B. S. & BULLOCH, K. 2008. Brain microglia express steroid-converting enzymes in the mouse. *J Steroid Biochem Mol Biol*, **109**, 96.
- GOULD, E., WOOLLEY, C., FRANKFURT, M. & MCEWEN, B. 1990. Gonadal steroids regulate dendritic spine density in hippocampal pyramidal cells in adulthood. *J Neurosci*, **10**, 1286.
- GREEN, S., WALTER, P., KUMAR, V., KRUST, A., BORNERT, J.-M., ARGOS, P. & CHAMBON, P. 1986. Human oestrogen receptor cDNA: sequence, expression and homology to v-erb-A. *Nature*, **320**, 134.
- GUENNOUN, R., FIDDES, R. J., GOUÉZOU, M., LOMBÈS, M. & BAULIEU, E. E. 1995. A key enzyme in the biosynthesis of neurosteroids, 3 beta-hydroxysteroid dehydrogenase/delta 5-delta 4-isomerase (3 beta-HSD), is expressed in rat brain. *Brain Res Mol Brain Res*, **30**, 287.
- GUPTA, R. R., SEN, S., DIEPENHORST, L. L., RUDICK, C. N. & MAREN, S. 2001. Estrogen modulates sexually dimorphic contextual fear conditioning and hippocampal long-term potentiation (LTP) in rats(1). *Brain Res*, **888**, 356.
- HADJIMARKOU, M. M. & VASUDEVAN, N. 2018. GPER1/GPR30 in the brain: Crosstalk with classical estrogen receptors and implications for behavior. *J Steroid Biochem Mol Biol*, **176**, 57.
- HALL, J. M., COUSE, J. F. & KORACH, K. S. 2001. The Multifaceted Mechanisms of Estradiol and Estrogen Receptor Signaling. *J Biol Chem*, **276**, 36869.
- HALLER, J., VARGA, B., LEDENT, C., BARNA, I. & FREUND, T. F. 2004. Context-dependent effects of CB1 cannabinoid gene disruption on anxiety-like and social behaviour in mice. *Eur J Neurosci*, **19**, 1906.
- HANDA, R. J., OGAWA, S., WANG, J. M. & HERBISON, A. E. 2012. Roles for Oestrogen Receptor β in Adult Brain Function. *J Neuroendocrinol*, **24**, 160.
- HANDA, R. J., SHARMA, D. & UHT, R. 2011. A role for the androgen metabolite, 5alpha androstane 3beta, 17beta diol (3beta-diol) in the regulation of the hypothalamo-pituitary-adrenal axis. *Front Endocrinol (Lausanne)*, **2**, 65.
- HANDA, R. J., WEISER, M. J. & ZULOAGA, D. G. 2009. A Role for the Androgen Metabolite, 5 α -Androstane-3 β ,17 β -Diol, in Modulating Oestrogen Receptor β -Mediated Regulation of Hormonal Stress Reactivity. *J Neuroendocrinol*, **21**, 351.

- HARADA, N., ABE-DOHMAE, S., LOEFFEN, R., FOIDART, A. & BALTHAZART, J. 1993. Synergism between androgens and estrogens in the induction of aromatase and its messenger RNA in the brain. *Brain Res*, **622**, 243.
- HART, D., NILGES, M., POLLARD, K., LYNN, T., PATSOS, O., SHIEL, C., CLARK, S. M. & VASUDEVAN, N. 2014. Activation of the G-protein coupled receptor 30 (GPR30) has different effects on anxiety in male and female mice. *Steroids*, **81**, 49.
- HART, S. A., SNYDER, M. A., SMEJKALOVA, T. & WOOLLEY, C. S. 2007. Estrogen Mobilizes a Subset of Estrogen Receptor- α -Immunoreactive Vesicles in Inhibitory Presynaptic Boutons in Hippocampal CA1. *J Neurosci*, **27**, 2102.
- HASHIKAWA, K., HASHIKAWA, Y., TREMBLAY, R., ZHANG, J., FENG, J. E., SABOL, A., PIPER, W. T., LEE, H., RUDY, B. & LIN, D. 2017. Esr1+ cells in the ventromedial hypothalamus control female aggression. *Nat Neurosci*, **20**, 1580.
- HAYASHI, T. & HARADA, N. 2014. Post-translational dual regulation of cytochrome P450 aromatase at the catalytic and protein levels by phosphorylation/dephosphorylation. *FEBS J*, **281**, 4830.
- HAZELL, G. G. J., YAO, S. T., ROPER, J. A., PROSSNITZ, E. R., O'CARROLL, A.-M. & LOLAIT, S. J. 2009. Localisation of GPR30, a novel G protein-coupled oestrogen receptor, suggests multiple functions in rodent brain and peripheral tissues. *J Endocrinol*, **202**, 223.
- HESS, R. A. 2003. Estrogen in the adult male reproductive tract: a review. *Reprod Biol Endocrinol*, **1**, 52.
- HIROI, R., LACAGNINA, A. F., HINDS, L. R., CARBONE, D. G., UHT, R. M. & HANDA, R. J. 2013. The Androgen Metabolite, 5 α -Androstane-3 β ,17 β -Diol (3 β -Diol), Activates the Oxytocin Promoter Through an Estrogen Receptor- β Pathway. *Endocrinology*, **154**, 1802.
- HIROI, R. & NEUMAIER, J. F. 2006. Differential effects of ovarian steroids on anxiety versus fear as measured by open field test and fear-potentiated startle. *Behav Brain Res*, **166**, 93.
- HOJO, Y., HATTORI, T. A., ENAMI, T., FURUKAWA, A., SUZUKI, K., ISHII, H. T., MUKAI, H., MORRISON, J. H., JANSSEN, W. G., KOMINAMI, S., HARADA, N., KIMOTO, T. & KAWATO, S. 2004b. Adult male rat hippocampus synthesizes estradiol from pregnenolone by cytochromes P45017 α and P450 aromatase localized in neurons. *Proc Natl Acad Sci USA*, **101**, 865.

- HOJO, Y., HIGO, S., ISHII, H., OOISHI, Y., MUKAI, H., MURAKAMI, G., KOMINAMI, T., KIMOTO, T., HONMA, S., POIRIER, D. & KAWATO, S. 2009. Comparison between Hippocampus-Synthesized and Circulation-Derived Sex Steroids in the Hippocampus. *Endocrinology*, **150**, 5106.
- HOJO, Y. & KAWATO, S. 2018. Neurosteroids in Adult Hippocampus of Male and Female Rodents: Biosynthesis and Actions of Sex Steroids. *Front Endocrinol (Lausanne)*, **23**, 183.
- HOLST, J. P., SOLDIN, O. P., GUO, T. & SOLDIN, S. J. 2004. Steroid hormones: relevance and measurement in the clinical laboratory. *Clin Lab Med*, **24**, 105.
- HONDA, S., HARADA, N., ITO, S., TAKAGI, Y. & MAEDA, S. 1998. Disruption of sexual behavior in male aromatase-deficient mice lacking exons 1 and 2 of the cyp19 gene. *Biochem Biophys Res Commun*, **252**, 445.
- HONG, Y., LI, H., YE, J., MIKI, Y., YUAN, Y.-C., SASANO, H., EVANS, D. B. & CHEN, S. 2009. Epitope Characterization of an Aromatase Monoclonal Antibody Suitable for the Assessment of Intratumoral Aromatase Activity. *PLoS One*, **4**, e8050.
- HORNSBY, A. K. E., BUNTWAL, L., CARISI, M. C., SANTOS, V. V., JOHNSTON, F., ROBERTS, L. D., SASSI, M., MEQUINION, M., STARK, R., REICHENBACH, A., LOCKIE, S. H., SIERVO, M., HOWELL, O., MORGAN, A. H., WELLS, T., ANDREWS, Z. B., BURN, D. J. & DAVIES, J. S. 2020. Unacylated-Ghrelin Impairs Hippocampal Neurogenesis and Memory in Mice and Is Altered in Parkinson's Dementia in Humans. *Cell Rep Med*, **1**, 100120.
- HU, M., RICHARD, J. E., MALIQUEO, M., KOKOSAR, M., FORNES, R., BENRICK, A., JANSSON, T., OHLSSON, C., WU, X., SKIBICKA, K. P. & STENER-VICTORIN, E. 2015. Maternal testosterone exposure increases anxiety-like behavior and impacts the limbic system in the offspring. *Proc Natl Acad Sci USA*, **112**, 14348.
- HUGHES, Z. A., LIU, F., PLATT, B. J., DWYER, J. M., PULICICCHIO, C. M., ZHANG, G., SCHECHTER, L. E., ROSENZWEIG-LIPSON, S. & DAY, M. 2008. WAY-200070, a selective agonist of estrogen receptor beta as a potential novel anxiolytic/antidepressant agent. *Neuropharmacology*, **54**, 1136.
- HULL, E. M. & DOMINGUEZ, J. M. 2007. Sexual behavior in male rodents. *Horm Behav*, **52**, 45.

- HUTCHISON, R. E., WOZNIAK, A. W. & HUTCHISON, J. B. 1992. Regulation of female brain aromatase activity during the reproductive cycle of the dove. *J Endocrinol*, **134**, 385.
- HUTSON, D. D., GURRALA, R., OGOLA, B. O., ZIMMERMAN, M. A., MOSTANY, R., SATOU, R. & LINDSEY, S. H. 2019. Estrogen receptor profiles across tissues from male and female *Rattus norvegicus*. *Biol Sex Differ*, **10**, 4.
- HUTTON, L. A., GU, G. & SIMERLY, R. B. 1998. Development of a Sexually Dimorphic Projection from the Bed Nuclei of the Stria Terminalis to the Anteroventral Periventricular Nucleus in the Rat. *J Neurosci*, **18**, 3003.
- HYDER, S. M., CHIAPPETTA, C. & STANCEL, G. M. 1999. Interaction of human estrogen receptors alpha and beta with the same naturally occurring estrogen response elements. *Biochem Pharmacol*, **57**, 597.
- IBANEZ, C., GUENNOUN, R., LIERE, P., EYCHENNE, B., PIANOS, A., EL-ETR, M., BAULIEU, E. E. & SCHUMACHER, M. 2003. Developmental expression of genes involved in neurosteroidogenesis: 3beta-hydroxysteroid dehydrogenase/delta5-delta4 isomerase in the rat brain. *Endocrinology*, **144**, 2902.
- IKEDA, Y., NAGAI, A., IKEDA, M.-A. & HAYASHI, S. 2003. Sexually Dimorphic and Estrogen-Dependent Expression of Estrogen Receptor β in the Ventromedial Hypothalamus during Rat Postnatal Development. *Endocrinology*, **144**, 5098.
- IMWALLE, D. B., GUSTAFSSON, J. Å. & RISSMAN, E. F. 2005. Lack of functional estrogen receptor beta influences anxiety behavior and serotonin content in female mice. *Physiol Behav*, **84**, 157.
- IRVIN, R. W., SZOT, P., DORSA, D. M., POTEHAL, M. & FERRIS, C. F. 1990. Vasopressin in the septal area of the golden hamster controls scent marking and grooming. *Physiol Behav*, **48**, 693.
- JACOBSON, C. D., TERKEL, J., GORSKI, R. A. & SAWYER, C. H. 1980. Effects of small medial preoptic area lesions on maternal behavior: retrieving and nest building in the rat. *Brain Res*, **194**, 471.
- JALABERT, C., SHOCK, M. A., MA, C., BOOTSMA, T. J., LIU, M. Q. & SOMA, K. K. 2022. Ultrasensitive Quantification of Multiple Estrogens in Songbird Blood and Microdissected Brain by LC-MS/MS. *eNeuro*, **9**, ENEURO.0037.

- JEAN, A., TROUILLET, A.-C., ANDRIANARIVELO, N. A., MHAOUTY-KODJA, S. & HARDIN-POUZET, H. 2017. Phospho-ERK and sex steroids in the mPOA: involvement in male mouse sexual behaviour. *J Endocrinol*, **233**, 257.
- JENNINGS, K. & DE LECEA, L. 2020. Neural and Hormonal Control of Sexual Behavior. *Endocrinology*, **161**, 150.
- JIA, B., GAO, Y., LI, M., SHI, J., PENG, Y., DU, X., KLOCKER, H., SAMPSON, N., SHEN, Y., LIU, M. & ZHANG, J. 2016. GPR30 Promotes Prostate Stromal Cell Activation via Suppression of ER α Expression and Its Downstream Signaling Pathway. *Endocrinology*, **157**, 3023.
- JIANG, T., WANG, R., YIN, W., ZHOU, Y., KONG, D., XU, S., GAO, P., YU, W., JIAO, Y. & WEN, D. 2019. Hypothalamic paraventricular nucleus neurons activated by estrogen GPER1 receptors promote anti-inflammation effects in the early stage of colitis. *Acta Biochim Biophys Sin (Shanghai)*, **51**: 1216.
- JONES, M. E. E., THORBURN, A. W., BRITT, K. L., HEWITT, K. N., WREFORD, N. G., PROIETTO, J., OZ, O. K., LEURY, B. J., ROBERTSON, K. M., YAO, S. & SIMPSON, E. R. 2000. Aromatase-deficient (ArKO) mice have a phenotype of increased adiposity. *Proc Natl Acad Sci*, **97**, 12735.
- KANAYA, M., HIGO, S. & OZAWA, H. 2019. Neurochemical Characterization of Neurons Expressing Estrogen Receptor β in the Hypothalamic Nuclei of Rats Using in Situ Hybridization and Immunofluorescence. *Int J Mol Sci*, **21**, 115.
- KARIGO, T., KENNEDY, A., YANG, B., LIU, M., TAI, D., WAHLE, I. A. & ANDERSON, D. J. 2021. Distinct hypothalamic control of same- and opposite-sex mounting behaviour in mice. *Nature*, **589**, 258.
- KAROLCZAK, M., KÜPPERS, E. & BEYER, C. 1998. Developmental expression and regulation of aromatase- and 5 α -reductase type I mRNA in the male and female mouse hypothalamus. *J Neuroendocrinol*, **10**, 267.
- KASAI, H., MATSUZAKI, M., NOGUCHI, J., YASUMATSU, N. & NAKAHARA, H. 2003. Structure-stability-function relationships of dendritic spines. *Trends Neurosci*, **26**, 360.
- KASTENBERGER, I., LUTSCH, C. & SCHWARZER, C. 2012. Activation of the G-protein-coupled receptor GPR30 induces anxiogenic effects in mice, similar to oestradiol. *Psychopharmacology*, **221**, 527.

- KATO, A., HOJO, Y., HIGO, S., KOMATSUZAKI, Y., MURAKAMI, G., YOSHINO, H., UEBAYASHI, M. & KAWATO, S. 2013. Female hippocampal estrogens have a significant correlation with cyclic fluctuation of hippocampal spines. *Front Neural Circuits*, **7**, 149.
- KAWATO, S., HOJO, Y. & KIMOTO, T. 2002. Histological and metabolism analysis of P450 expression in the brain. *Methods Enzymol*, **357**, 241.
- KEATING, N., ZEAKE, N. & SMITH, S. S. 2019. Pubertal hormones increase hippocampal expression of $\alpha 4\beta\delta$ GABAA receptors. *Neurosci Lett*, **701**, 65.
- KELLOGG, C. K. & LUNDIN, A. 1999. Brain androgen-inducible aromatase is critical for adolescent organization of environment-specific social interaction in male rats. *Horm Behav*, **35**, 155.
- KELLY, D. A., VARNUM, M. M., KRENTZEL, A. A., KRUG, S. & FORGER, N. G. 2013. Differential control of sex differences in estrogen receptor α in the bed nucleus of the stria terminalis and anteroventral periventricular nucleus. *Endocrinology*, **154**, 3836.
- KEMPERMANN, G., KREBS, J. & FABEL, K. 2008. The contribution of failing adult hippocampal neurogenesis to psychiatric disorders. *Curr Opin Psychiatry*, **21**, 290.
- KENEALY, B. P., KAPOOR, A., GUERRIERO, K. A., KEEN, K. L., GARCIA, J. P., KURIAN, J. R., ZIEGLER, T. E. & TERASAWA, E. 2013. Neuroestradiol in the Hypothalamus Contributes to the Regulation of Gonadotropin Releasing Hormone Release. *J Neurosci*, **33**, 19051.
- KENEALY, B. P., KEEN, K. L., GARCIA, J. P., KOHLENBERG, L. K. & TERASAWA, E. 2017. Obligatory role of hypothalamic neuroestradiol during the estrogen-induced LH surge in female ovariectomized rhesus monkeys. *Proc Natl Acad Sci*, **114**, 13804.
- KHBOUZ, B., DE BOURNONVILLE, C., COURT, L., TAZIAUX, M., CORONA, R., ARNAL, J. F., LENFANT, F. & CORNIL, C. A. 2020. Role for the membrane estrogen receptor alpha in the sexual differentiation of the brain. *Eur J Neurosci*, **52**, 2627.
- KIM, J., SCHALK, J. C., KOSS, W. A., GREMMINGER, R. L., TAXIER, L. R., GROSS, K. S. & FRICK, K. M. 2019. Dorsal Hippocampal Actin Polymerization Is Necessary for Activation of G-Protein-Coupled Estrogen Receptor (GPER) to Increase CA1 Dendritic Spine Density and Enhance Memory Consolidation. *J Neurosci*, **39**, 9598.
- KING, J. M. 1979. Effects of lesions of the amygdala, preoptic area, and hypothalamus on estradiol-induced activity in the female rat. *J Comp Physiol Psychol*, **93**, 360.

- KING, S. R., MANNA, P. R., ISHII, T., SYAPIN, P. J., GINSBERG, S. D., WILSON, K., WALSH, L. P., PARKER, K. L., STOCCO, D. M., SMITH, R. G. & LAMB, D. J. 2002. An Essential Component in Steroid Synthesis, the Steroidogenic Acute Regulatory Protein, Is Expressed in Discrete Regions of the Brain. *J Neurosci*, **22**, 10613.
- KIROUAC, G. J. 2021. The Paraventricular Nucleus of the Thalamus as an Integrating and Relay Node in the Brain Anxiety Network. *Front Behav Neurosci*, **15**, 627.
- KLINGE, C. M. 2001. Estrogen receptor interaction with estrogen response elements. *Nucleic Acids Res*, **29**, 2905.
- KOHCHI, C., UKENA, K. & TSUTSUI, K. 1998. Age- and region-specific expressions of the messenger RNAs encoding for steroidogenic enzymes p450scc, P450c17 and 3beta-HSD in the postnatal rat brain. *Brain Res*, **801**, 233.
- KONKLE, A. T. & MCCARTHY, M. M. 2011a. Developmental time course of estradiol, testosterone, and dihydrotestosterone levels in discrete regions of male and female rat brain. *Endocrinology*, **152**, 223.
- KONKLE, A. T. M. & BALTHAZART, J. 2011. Sex Differences in the Rapid Control of Aromatase Activity in the Quail Preoptic Area. *J Neuroendocrinol*, **23**, 424.
- KONKLE, A. T. M. & MCCARTHY, M. M. 2011b. Developmental Time Course of Estradiol, Testosterone, and Dihydrotestosterone Levels in Discrete Regions of Male and Female Rat Brain. *Endocrinology*, **152**, 223.
- KOOK, S.-Y., JEONG, H., KANG, M. J., PARK, R., SHIN, H. J., HAN, S.-H., SON, S. M., SONG, H., BAIK, S. H., MOON, M., YI, E. C., HWANG, D. & MOOK-JUNG, I. 2014. Crucial role of calbindin-D28k in the pathogenesis of Alzheimer's disease mouse model. *Cell Death Differ*, **21**, 1575.
- KOOLHAAS, J. M., COPPENS, C. M., DE BOER, S. F., BUWALDA, B., MEERLO, P. & TIMMERMANS, P. J. A. 2013. The Resident-intruder Paradigm: A Standardized Test for Aggression, Violence and Social Stress. *J Vis Exp*, **2013**: 4367.
- KOW, L. M., DEVIDZE, N., PATAKY, S., SHIBUYA, I. & PFAFF, D. W. 2006. Acute estradiol application increases inward and decreases outward whole-cell currents of neurons in rat hypothalamic ventromedial nucleus. *Brain Res*, **1116**, 1.
- KRAUSE, W. C. & INGRAHAM, H. A. 2017. Origins and Functions of the Ventrolateral VMH: A Complex Neuronal Cluster Orchestrating Sex Differences in Metabolism and Behavior. *Adv Exp Med Biol*, **1043**: 199.

- KRETZ, O., FESTER, L., WEHRENBURG, U., ZHOU, L., BRAUCKMANN, S., ZHAO, S., PRANGE-KIEL, J., NAUMANN, T., JARRY, H., FROTSCHER, M. & RUNE, G. M. 2004. Hippocampal synapses depend on hippocampal estrogen synthesis. *J Neurosci*, **24**, 5913.
- KRĘŻEL, W., DUPONT, S., KRUST, A., CHAMBON, P. & CHAPMAN, P. F. 2001. Increased anxiety and synaptic plasticity in estrogen receptor β -deficient mice. *Proc Natl Acad Sci*, **98**, 12278
- KUDWA, A. E., MCGIVERN, R. F. & HANDA, R. J. 2014. Estrogen receptor β and oxytocin interact to modulate anxiety-like behavior and neuroendocrine stress reactivity in adult male and female rats. *Physiol Behav*, **129**, 287.
- KUIPER, G. G., ENMARK, E., PELTO-HUIKKO, M., NILSSON, S. & GUSTAFSSON, J. A. 1996. Cloning of a novel receptor expressed in rat prostate and ovary. *Proc Natl Acad Sci*, **93**, 5925.
- KUIPER, G. G., LEMMEN, J. G., CARLSSON, B., CORTON, J. C., SAFE, S. H., VAN DER SAAG, P. T., VAN DER BURG, B. & GUSTAFSSON, J. Å. 1998. Interaction of estrogenic chemicals and phytoestrogens with estrogen receptor beta. *Endocrinology*, **139**, 4252.
- KUMAR, R., ZAKHAROV, M. N., KHAN, S. H., MIKI, R., JANG, H., TORALDO, G., SINGH, R., BHASIN, S. & JASUJA, R. 2011. The Dynamic Structure of the Estrogen Receptor. *J Amino Acids*, **2011**, 1.
- KUMAR, V., GREEN, S., STACK, G., BERRY, M., JIN, J. R. & CHAMBON, P. 1987. Functional domains of the human estrogen receptor. *Cell*, **51**, 941.
- KYNE, R. F., BARRETT, A. R., BROWN, L. M. & PAUL, M. J. 2019. Prepubertal ovarian inhibition of Light/Dark Box exploration and novel object investigation in juvenile Siberian hamsters. *Horm Behav*, **115**, 104559.
- LABRIE, F., LUU-THE, V., LIN, S. W., LABRIE, C., SIMARD, J., BRETON, R. & BÉLANGER, A. 1997. The key role of 17 β -hydroxysteroid dehydrogenases in sex steroid biology. *Steroids*, **62**, 148.
- LAI, Y.-J., YU, D., ZHANG, J. H. & CHEN, G.-J. 2017. Cooperation of Genomic and Rapid Nongenomic Actions of Estrogens in Synaptic Plasticity. *Mol Neurobiol*, **54**, 4113.

- LAREDO, S. A., VILLALON LANDEROS, R., DOOLEY, J. C., STEINMAN, M. Q., ORR, V., SILVA, A. L., CREAN, K. K., ROBLES, C. F. & TRAINOR, B. C. 2013. Nongenomic effects of estradiol on aggression under short day photoperiods. *Horm Behav*, **64**, 557.
- LAREDO, S. A., VILLALON LANDEROS, R. & TRAINOR, B. C. 2014. Rapid effects of estrogens on behavior: Environmental modulation and molecular mechanisms. *Front Neuroendocrinol*, **35**, 447.
- LAUBE, C., VAN DEN BOS, W. & FANDAKOVA, Y. 2020. The relationship between pubertal hormones and brain plasticity: Implications for cognitive training in adolescence. *Dev Cogn Neurosci*, **42**, 100753.
- LAUBER, M. E., SARASIN, A. & LICHTENSTEIGER, W. 1997. Transient sex differences of aromatase (CYP19) mRNA expression in the developing rat brain. *Neuroendocrinology*, **66**, 173.
- LEE, S. E., GREENOUGH, E. K., OANCEA, P., FONKEN, L. K. & GAUDET, A. D. 2022. Anxiety-like behaviors in mice unmasked: Revealing sex differences in anxiety using a novel light-heat conflict test. Cold Spring Harbor Laboratory. *bioRxiv*.
- LENZ, K. M., WRIGHT, C. L., MARTIN, R. C. & MCCARTHY, M. M. 2011. Prostaglandin E2 Regulates AMPA Receptor Phosphorylation and Promotes Membrane Insertion in Preoptic Area Neurons and Glia during Sexual Differentiation. *PLoS One*, **6**, e18500.
- LEVIN, E. R. 2009. Membrane oestrogen receptor α signalling to cell functions. *J Physiol*, **587**, 5019.
- LI, J. & GIBBS, R. B. 2019. Detection of estradiol in rat brain tissues: Contribution of local versus systemic production. *Psychoneuroendocrinology*, **102**, 84.
- LI, X., JOHANN, S., RUNE, G. M. & BENDER, R. A. 2021. Sex-specific Regulation of Spine Density and Synaptic Proteins by G-protein-coupled Estrogen Receptor (GPER)1 in Developing Hippocampus. *Neuroscience*, **472**, 35.
- LIN, D., BOYLE, M. P., DOLLAR, P., LEE, H., LEIN, E. S., PERONA, P. & ANDERSON, D. J. 2011. Functional identification of an aggression locus in the mouse hypothalamus. *Nature*, **470**, 221.
- LITIM, N., MORISSETTE, M., CARUSO, D., MELCANGI, R. C. & DI PAOLO, T. 2017. Effect of the 5 α -reductase enzyme inhibitor dutasteride in the brain of intact and parkinsonian mice. *J Steroid Biochem Mol Biol*, **174**, 242.

- LIU, C. M., DAVIS, E. A., SUAREZ, A. N., WOOD, R. I., NOBLE, E. E. & KANOSKI, S. E. 2020. Sex Differences and Estrous Influences on Oxytocin Control of Food Intake. *Neuroscience*, **447**, 63.
- LIU, C. M., SPAULDING, M. O., REA, J. J., NOBLE, E. E. & KANOSKI, S. E. 2021. Oxytocin and Food Intake Control: Neural, Behavioral, and Signaling Mechanisms. *Int J Mol Sci*, **22**, 10859.
- LIU, J., HU, P., QI, X. R., MENG, F. T., KALSBECK, A. & ZHOU, J. N. 2011. Acute restraint stress increases intrahypothalamic oestradiol concentrations in conjunction with increased hypothalamic oestrogen receptor β and aromatase mRNA expression in female rats. *J Neuroendocrinol*, **23**, 435.
- LIU, M., XING, F., BIAN, C., ZHAO, Y., ZHAO, J., LIU, Y. & ZHANG, J. 2019. Letrozole induces worse hippocampal synaptic and dendritic changes and spatial memory impairment than ovariectomy in adult female mice. *Neurosci Lett*, **706**, 61.
- LIU, Y.-C., SALAMONE, J. D. & SACHS, B. D. 1997. Lesions in Medial Preoptic Area and Bed Nucleus of Stria Terminalis: Differential Effects on Copulatory Behavior and Noncontact Erection in Male Rats. *J Neurosci*, **17**, 5245.
- LIU, Y. J., RAO, B., LI, S., ZHENG, N., WANG, J., BI, L. & XI, H. 2022. Distinct Hypothalamic Paraventricular Nucleus Inputs to the Cingulate Cortex and Paraventricular Thalamic Nucleus Modulate Anxiety and Arousal. *Front Pharmacol*, **13**, 814623.
- LIVAK, K. J. & SCHMITTGEN, T. D. 2001. Analysis of relative gene expression data using real-time quantitative PCR and the 2(-Delta Delta C(T)) Method. *Methods*, **25**, 402.
- LORYAN, I., FRIDÉN, M. & HAMMARLUND-UDENAES, M. 2013. The brain slice method for studying drug distribution in the CNS. *Fluids Barriers CNS*, **10**, 6.
- LOVEN, M. A., WOOD, J. R. & NARDULLI, A. M. 2001. Interaction of estrogen receptors alpha and beta with estrogen response elements. *Mol Cell Endocrinol*, **181**, 151.
- LU, Y., SAREDDY, G. R., WANG, J., WANG, R., LI, Y., DONG, Y., ZHANG, Q., LIU, J., O'CONNOR, J. C., XU, J., VADLAMUDI, R. K. & BRANN, D. W. 2019. Neuron-Derived Estrogen Regulates Synaptic Plasticity and Memory. *J Neurosci*, **39**, 2792.

- LUCHETTI, S., HUITINGA, I. & SWAAB, D. F. 2011. Neurosteroid and GABA-A receptor alterations in Alzheimer's disease, Parkinson's disease and multiple sclerosis. *Neuroscience*, **191**, 6.
- LUND, T. D., HINDS, L. R. & HANDA, R. J. 2006. The Androgen 5 α -Dihydrotestosterone and Its Metabolite 5 α -Androstan-3 β , 17 β -Diol Inhibit the Hypothalamo–Pituitary–Adrenal Response to Stress by Acting through Estrogen Receptor β -Expressing Neurons in the Hypothalamus. *J Neurosci*, **26**, 1448.
- LUND, T. D., MUNSON, D. J., HALDY, M. E. & HANDA, R. J. 2004. Dihydrotestosterone may inhibit hypothalamo–pituitary–adrenal activity by acting through estrogen receptor in the male mouse. *Neurosci Lett*, **365**, 43.
- LUND, T. D., ROVIS, T., CHUNG, W. C. J. & HANDA, R. J. 2005. Novel Actions of Estrogen Receptor- β on Anxiety-Related Behaviors. *Endocrinology*, **146**, 797.
- LUTTGE, W. G. 1976. Intracerebral implantation of the anti-estrogen CN-69, 725-27: Effects on female sexual. *Pharmacol Biochem Behav*, **4**, 685.
- MACLUSKY, N. J., NAFTOLIN, F. & GOLDMAN-RAKIC, P. S. 1986. Estrogen formation and binding in the cerebral cortex of the developing rhesus monkey. *Proc Natl Acad Sci*, **83**, 513.
- MARCHETTI, P. M. & BARTH, J. H. 2013. Clinical biochemistry of dihydrotestosterone. *Ann Clin Biochem*, **50**, 95.
- MATHEWS, D., DONOVAN, K. M., HOLLINGSWORTH, E. M., HUTSON, V. B. & OVERSTREET, C. T. 1983. Permanent deficits in lordosis behavior in female rats with lesions of the ventromedial nucleus of the hypothalamus. *Exp Neurol*, **79**, 714.
- MATSUMOTO, T., HONDA, S. & HARADA, N. 2003. Alteration in sex-specific behaviors in male mice lacking the aromatase gene. *Neuroendocrinology*, **77**, 416.
- MATSUNAGA, M., UKENA, K. & TSUTSUI, K. 2002. Androgen biosynthesis in the quail brain. *Brain Res*, **948**, 180.
- MAZZUCCO, C. A., WALKER, H. A., PAWLUSKI, J. L., LIEBLICH, S. E. & GALEA, L. A. M. 2008. ER α , but not ER β , mediates the expression of sexual behavior in the female rat. *Behav Brain Res*, **191**, 111.
- MCCARTHY, M. M. 2008. Estradiol and the Developing Brain. *Physiol Rev*, **88**, 91.
- MCCARTHY, M. M., SCHLENKER, E. H. & PFAFF, D. W. 1993. Enduring consequences of neonatal treatment with antisense oligodeoxynucleotides to estrogen

receptor messenger ribonucleic acid on sexual differentiation of rat brain.

Endocrinology, **133**, 433.

MCCARTHY, M. M., WRIGHT, C. L. & SCHWARZ, J. M. 2009. New tricks by an old dogma: Mechanisms of the Organizational / Activational Hypothesis of steroid-mediated sexual differentiation of brain and behavior. *Horm Behav*, **55**, 655.

MCDERMOTT, C. M., LIU, D. & SCHRADER, L. A. 2012. Role of gonadal hormones in anxiety and fear memory formation and inhibition in male mice. *Physiol Behav*, **105**, 1168.

MELCANGI, R. C., CELOTTI, F., CASTANO, P. & MARTINI, L. 1993. Differential localization of the 5 alpha-reductase and the 3 alpha-hydroxysteroid dehydrogenase in neuronal and glial cultures. *Endocrinology*, **132**, 1252.

MELLON, S. H. & DESCHEPPER, C. F. 1993. Neurosteroid biosynthesis: genes for adrenal steroidogenic enzymes are expressed in the brain. *Brain Res*, **629**, 283.

MENDELL, A. L., ATWI, S., BAILEY, C. D. C., MCCLOSKEY, D., SCHARFMAN, H. E. & MACLUSKY, N. J. 2017. Expansion of mossy fibers and CA3 apical dendritic length accompanies the fall in dendritic spine density after gonadectomy in male, but not female, rats. *Brain Struct Funct*, **222**, 587.

MENG, F. T., NI, R. J., ZHANG, Z., ZHAO, J., LIU, Y. J. & ZHOU, J. N. 2011. Inhibition of oestrogen biosynthesis induces mild anxiety in C57BL/6J ovariectomized female mice. *Neurosci Bull*, **27**, 241.

MERCHENTHALER, I., LANE, M. V., NUMAN, S. & DELLOVADE, T. L. 2004. Distribution of estrogen receptor α and β in the mouse central nervous system: In vivo autoradiographic and immunocytochemical analyses. *J Comp Neurol*, **473**, 270.

MEYER, G., FERRES-TORRES, R. & MAS, M. 1978. The effects of puberty and castration on hippocampal dendritic spines of mice. A Golgi study. *Brain Res*, **155**, 108.

MICEVYCH, P. & CHRISTENSEN, A. 2012. Membrane-initiated estradiol actions mediate structural plasticity and reproduction. *Front Neuroendocrinol*, **33**, 331.

MICEVYCH, P. & MEISEL, R. L. 2017. Integrating Neural Circuits Controlling Female Sexual Behavior. *Front Syst Neurosci*, **11**, 42.

MICEVYCH, P. & SINCHAK, K. 2011. The Neurosteroid Progesterone Underlies Estrogen Positive Feedback of the LH Surge. *Front Endocrinol (Lausanne)*, **2**, 90.

- MILLER, W. L. & BOSE, H. S. 2011. Early steps in steroidogenesis: intracellular cholesterol trafficking. *J Lipid Res*, **52**, 2111.
- MILNER, T. A., MCEWEN, B. S., HAYASHI, S., LI, C. J., REAGAN, L. P. & ALVES, S. E. 2001. Ultrastructural evidence that hippocampal alpha estrogen receptors are located at extranuclear sites. *J Comp Neurol*, **429**, 355.
- MING, G.-L. & SONG, H. 2011. Adult Neurogenesis in the Mammalian Brain: Significant Answers and Significant Questions. *Neuron*, **70**, 687.
- MITRA, S. W., HOSKIN, E., YUDKOVITZ, J., PEAR, L., WILKINSON, H. A., HAYASHI, S., PFAFF, D. W., OGAWA, S., ROHRER, S. P., SCHAEFFER, J. M., MCEWEN, B. S. & ALVES, S. E. 2003. Immunolocalization of estrogen receptor beta in the mouse brain: comparison with estrogen receptor alpha. *Endocrinology*, **144**, 2055.
- MIZIAK, B., CHROŚCIŃSKA-KRAWCZYK, M. & CZUCZWAR, S. J. 2020. Neurosteroids and Seizure Activity. *Front Endocrinol (Lausanne)*, **11**, 541802.
- MOËNE, O. L., STAVARACHE, M., OGAWA, S., MUSATOV, S. & ÁGMO, A. 2019. Estrogen receptors α and β in the central amygdala and the ventromedial nucleus of the hypothalamus: Sociosexual behaviors, fear and arousal in female rats during emotionally challenging events. *Behav Brain Res*, **367**, 128.
- MORGAN, M. A. & PFAFF, D. W. 2001. Effects of estrogen on activity and fear-related behaviors in mice. *Horm Behav*, **40**, 472.
- MORRELL, J. I. & PFAFF, D. W. 1978. A Neuroendocrine Approach to Brain Function: Localization of Sex Steroid Concentrating Cells in Vertebrate Brains. *Am Zool*, **18**, 447.
- MUKAI, H., TSURUGIZAWA, T., MURAKAMI, G., KOMINAMI, S., ISHII, H., OGIUE-IKEDA, M., TAKATA, N., TANABE, N., FURUKAWA, A., HOJO, Y., OOISHI, Y., MORRISON, J. H., JANSSEN, W. G., ROSE, J. A., CHAMBON, P., KATO, S., IZUMI, S., YAMAZAKI, T., KIMOTO, T. & KAWATO, S. 2007. Rapid modulation of long-term depression and spinogenesis via synaptic estrogen receptors in hippocampal principal neurons. *J Neurochem*, **100**, 950.
- MURAKAMI, G., HOJO, Y., KATO, A., KOMATSUZAKI, Y., HORIE, S., SOMA, M., KIM, J. & KAWATO, S. 2018. Rapid nongenomic modulation by neurosteroids of dendritic spines in the hippocampus: Androgen, oestrogen and corticosteroid. *J Neuroendocrinol*, **30**, e12561.

- MUSATOV, S., CHEN, W., PFAFF, D. W., KAPLITT, M. G. & OGAWA, S. 2006. RNAi-mediated silencing of estrogen receptor α in the ventromedial nucleus of hypothalamus abolishes female sexual behaviors. *Proc Natl Acad Sci*, **103**, 10456.
- MUSATOV, S., CHEN, W., PFAFF, D. W., MOBBS, C. V., YANG, X.-J., CLEGG, D. J., KAPLITT, M. G. & OGAWA, S. 2007. Silencing of estrogen receptor α in the ventromedial nucleus of hypothalamus leads to metabolic syndrome. *Proc Natl Acad Sci*, **104**, 2501.
- NAKAMURA, K. & MORRISON, S. F. 2008. A thermosensory pathway that controls body temperature. *Nat Neurosci*, **11**, 62.
- NARITA, K., MURATA, T. & MATSUOKA, S. 2016. The ventromedial hypothalamus oxytocin induces locomotor behavior regulated by estrogen. *Physiol Behav*, **164**, 107.
- NELSON, B. S., BLACK, K. L. & DANIEL, J. M. 2016. Circulating Estradiol Regulates Brain-Derived Estradiol via Actions at GnRH Receptors to Impact Memory in Ovariectomized Rats. *eNeuro*, **3**, ENEURO.0321.
- NELSON, L. R. & BULUN, S. E. 2001. Estrogen production and action. *J Am Acad Dermatol*, **45**, 116.
- NELSON, R. J. & TRAINOR, B. C. 2007. Neural mechanisms of aggression. *Nat Rev Neurosci*, **8**, 536.
- NENADOV, D. S., POGRMIC-MAJKIC, K., FA, S., STANIC, B., TUBIC, A. & ANDRIC, N. 2018. Environmental mixture with estrogenic activity increases Hsd3b1 expression through estrogen receptors in immature rat granulosa cells. *J Appl Toxicol*, **38**, 879.
- NEUMANN, I. D., KRÖMER, S. A., TOSCHI, N. & EBNER, K. 2000. Brain oxytocin inhibits the (re)activity of the hypothalamo-pituitary-adrenal axis in male rats: involvement of hypothalamic and limbic brain regions. *Regul Pept*, **96**, 31038.
- NEWMAN, S. W. 1999. The Medial Extended Amygdala in Male Reproductive Behavior A Node in the Mammalian Social Behavior Network. *Ann NY Acad Sci*, **877**, 242.
- NILSEN, J., MOR, G. & NAFTOLIN, F. 2000. Estrogen-regulated developmental neuronal apoptosis is determined by estrogen receptor subtype and the Fas/Fas ligand system. *J Neurobiol*, **43**, 64.
- NILSSON, M. E., VANDENPUT, L., TIVESTEN, A., NORLEN, A. K., LAGERQUIST, M. K., WINDAHL, S. H., BORJESSON, A. E., FARMAN, H. H., POUTANEN, M.,

- BENRICK, A., MALIQUEO, M., STENER-VICTORIN, E., RYBERG, H. & OHLSSON, C. 2015. Measurement of a Comprehensive Sex Steroid Profile in Rodent Serum by High-Sensitive Gas Chromatography-Tandem Mass Spectrometry. *Endocrinology*, **156**, 2492.
- NISHIDA, Y., YOSHIOKA, M. & ST-AMAND, J. 2005. Sexually dimorphic gene expression in the hypothalamus, pituitary gland, and cortex. *Genomics*, **85**, 679.
- NOMIKOS, G. G. & SPYRAKI, C. 1988. Influence of oestrogen on spontaneous and diazepam-induced exploration of rats in an elevated plus maze. *Neuropharmacology*, **27**, 691.
- NOMURA, M., DURBAK, L., CHAN, J., SMITHIES, O., GUSTAFSSON, J. Å., KORACH, K. S., PFAFF, D. W. & OGAWA, S. 2002. Genotype/age interactions on aggressive behavior in gonadally intact estrogen receptor beta knockout (betaERKO) male mice. *Horm Behav*, **41**, 288.
- NUMAN, M., ROSENBLATT, J. S. & KOMISARUK, B. R. 1977. Medial preoptic area and onset of maternal behavior in the rat. *J Comp Physiol Psychol*, **91**, 146.
- NUÑEZ, J. L., ALT, J. J. & MCCARTHY, M. M. 2003. A novel model for prenatal brain damage. II. Long-term deficits in hippocampal cell number and hippocampal-dependent behavior following neonatal GABAA receptor activation. *Exp Neurol*, **181**, 270.
- O'LONE, R., FRITH, M. C., KARLSSON, E. K. & HANSEN, U. 2004. Genomic Targets of Nuclear Estrogen Receptors. *Mol Endocrinol*, **18**, 1859.
- OGAWA, S., CHAN, J., CHESTER, A. E., GUSTAFSSON, J.-Å., KORACH, K. S. & PFAFF, D. W. 1999. Survival of reproductive behaviors in estrogen receptor β gene-deficient (β ERKO) male and female mice. *Proc Natl Acad Sci USA*, **96**, 12887.
- OGAWA, S., CHAN, J., GUSTAFSSON, J. Å., KORACH, K. S. & PFAFF, D. W. 2003. Estrogen increases locomotor activity in mice through estrogen receptor alpha: specificity for the type of activity. *Endocrinology*, **144**, 230.
- OGAWA, S., CHESTER, A. E., HEWITT, S. C., WALKER, V. R., GUSTAFSSON, J. Å., SMITHIES, O., KORACH, K. S. & PFAFF, D. W. 2000. Abolition of male sexual behaviors in mice lacking estrogen receptors α and β ($\alpha\beta$ ERKO). *Proc Natl Acad Sci USA*, **97**, 14737.

- OGAWA, S., LUBAHN, D. B., KORACH, K. S. & PFAFF, D. W. 1997. Behavioral effects of estrogen receptor gene disruption in male mice. *Proc Natl Acad Sci USA*, **94**, 1476.
- OLIVEIRA, A. G., COELHO, P. H., GUEDES, F. D., MAHECHA, G. A. B., HESS, R. A. & OLIVEIRA, C. A. 2007. 5alpha-Androstane-3beta,17beta-diol (3beta-diol), an estrogenic metabolite of 5alpha-dihydrotestosterone, is a potent modulator of estrogen receptor ERbeta expression in the ventral prostate of adult rats. *Steroids*, **72**, 914.
- OLVERA-HERNÁNDEZ, S., CHAVIRA, R. & FERNÁNDEZ-GUASTI, A. 2015. Prenatal letrozole produces a subpopulation of male rats with same-sex preference and arousal as well as female sexual behavior. *Physiol Behav*, **139**, 403.
- ORIKASA, C. & SAKUMA, Y. 2004. Sex and Region-Specific Regulation of Oestrogen Receptor beta in the Rat Hypothalamus. *J Neuroendocrinol*, **16**, 964.
- ORTEGA, I., SOKALSKA, A., VILLANUEVA, J. A., CRESS, A. B., WONG, D. H., STENER-VICTORIN, E., STANLEY, S. D. & DULEBA, A. J. 2013. Letrozole increases ovarian growth and Cyp17a1 gene expression in the rat ovary. *Fertil Steril*, **99**, 889.
- PAK, S., CHOI, G., ROY, J., POON, C. H., LEE, J., CHO, D., LEE, M., LIM, L. W., BAO, S., YANG, S. & YANG, S. 2022. Altered synaptic plasticity of the longitudinal dentate gyrus network in noise-induced anxiety. *iScience*, **25**, 104364.
- PAK, T. R., CHUNG, W. C. J., LUND, T. D., HINDS, L. R., CLAY, C. M. & HANDA, R. J. 2005. The androgen metabolite, 5alpha-androstane-3beta, 17beta-diol, is a potent modulator of estrogen receptor-beta1-mediated gene transcription in neuronal cells. *Endocrinology*, **146**, 147.
- PALERMO-NETO, J. & DORCE, V. A. 1990. Influences of estrogen and/or progesterone on some dopamine related behavior in rats. *Gen Pharmacol*, **21**, 83.
- PAREDES, R. G. 2003. Medial preoptic area/anterior hypothalamus and sexual motivation. *Scand J Psychol*, **44**, 203.
- PARETO, D., BIEGON, A., ALEXOFF, D., CARTER, P., SHEA, C., MUENCH, L., XU, Y., FOWLER, J. S., KIM, S. W. & LOGAN, J. 2013. In Vivo Imaging of Brain Aromatase in Female Baboons: [11 C]Vorzole Kinetics and Effect of the Menstrual Cycle. *Mol Imaging*, **12**, 7290.2013.00068.
- PAWLISCH, B. A. & REMAGE-HEALEY, L. 2015. Neuroestrogen signaling in the songbird auditory cortex propagates into a sensorimotor network via an 'interface' nucleus. *Neuroscience*, **284**, 522.

- PAXINOS, G. & FRANKLIN, B. J. 2001. The mouse brain in stereotaxic coordinates: hard cover edition, Elsevier.
- PAYNE, A. H. & HALES, D. B. 2004. Overview of Steroidogenic Enzymes in the Pathway from Cholesterol to Active Steroid Hormones. *Endocr Rev*, **25**, 947.
- PEDRAM, A., RAZANDI, M., SAINSON, R. C. A., KIM, J. K., HUGHES, C. C. & LEVIN, E. R. 2007. A Conserved Mechanism for Steroid Receptor Translocation to the Plasma Membrane. *J Biol Chem*, **282**, 22278.
- PELLETIER, G. 2010. Steroidogenic enzymes in the brain: morphological aspects. *Prog Brain Res*, **181**, 193.
- PELLETIER, G., LUU-THE, V. & LABRIE, F. 1994. Immunocytochemical localization of 5 alpha-reductase in rat brain. *Mol Cell Neurosci*, **5**, 394.
- PELLETIER, G., LUU-THE, V. & LABRIE, F. 1995. Immunocytochemical localization of type I 17 β -hydroxysteroid dehydrogenase in the rat brain. *Brain Res*, **704**, 233.
- PEREIRA, M. & MORRELL, J. I. 2009. The changing role of the medial preoptic area in the regulation of maternal behavior across the postpartum period: Facilitation followed by inhibition. *Behav Brain Res*, **205**, 238.
- PERETTO, P., SCHELLINO, R., DE MARCHIS, S. & FASOLO, A. 2014. The Interplay between Reproductive Social Stimuli and Adult Olfactory Bulb Neurogenesis. *Neural Plast*, **2014**, 1.
- PÉREZ, A. E., ORTÍZ, E., CABEZA, M., BEYER, C. & PÉREZ-PALACIOS, G. 1975. In vitro metabolism of 3-H-androstenedione by the male rat pituitary, hypothalamus, and hippocampus. *Steroids*, **25**, 53.
- PETERS, P. J., BRONSON, F. H. & WHITSETT, J. M. 1972. Neonatal castration and intermale aggression in mice. *Physiol Behav*, **8**, 265.
- PETERSON, R. S., YARRAM, L., SCHLINGER, B. A. & SALDANHA, C. J. 2005. Aromatase is pre-synaptic and sexually dimorphic in the adult zebra finch brain. *Proc Biol Sci*, **272**, 2089.
- PFAFF, D. 1998. Hormonal and environmental control of lordosis behavior: Neural and molecular mechanisms. *Eur J Neurosci*, **10**, 330.
- PFAFF, D. W. & SAKUMA, Y. 1979. Deficit in the lordosis reflex of female rats caused by lesions in the ventromedial nucleus of the hypothalamus. *J Physiol*, **288**, 203.

- PHAN, A., SUSCHKOV, S., MOLINARO, L., REYNOLDS, K., LYMER, J. M., BAILEY, C. D. C., KOW, L.-M., MACLUSKY, N. J., PFAFF, D. W. & CHOLERIS, E. 2015. Rapid increases in immature synapses parallel estrogen-induced hippocampal learning enhancements. *Proc Natl Acad Sci USA*, **112**, 16018.
- PHOENIX, C. H., GOY, R. W., GERALL, A. A. & YOUNG, W. C. 1959. Organizing action of prenatally administered testosterone propionate on the tissues mediating mating behavior in the female guinea pig. *Endocrinology*, **65**, 369.
- PICAZO, O., ESTRADA-CAMARENA, E. & HERNANDEZ-ARAGON, A. 2006. Influence of the post-ovariectomy time frame on the experimental anxiety and the behavioural actions of some anxiolytic agents. *Eur J Pharmacol*, **530**, 88.
- PINTO, P. I., SINGH, P. B., CONDEÇA, J. B., TEODÓSIO, H. R., POWER, D. M. & CANÁRIO, A. V. 2006. ICI 182,780 has agonistic effects and synergizes with estradiol-17 beta in fish liver, but not in testis. *Reprod Biol Endocrinol*, **4**, 67.
- PISOLATO, R., LOMBARDI, A. P. G., VICENTE, C. M., LUCAS, T. F. G., LAZARI, M. F. M. & PORTO, C. S. 2016. Expression and regulation of the estrogen receptors in PC-3 human prostate cancer cells. *Steroids*, **107**, 74.
- PRANGE-KIEL, J. & RUNE, G. M. 2006. Direct and indirect effects of estrogen on rat hippocampus. *Neuroscience*, **138**, 765.
- PRANGE-KIEL, J., SCHMUTTERER, T., FESTER, L., ZHOU, L., IMHOLZ, P., BRANDT, N., VIERK, R., JARRY, H. & RUNE, G. M. 2013. Endocrine regulation of estrogen synthesis in the hippocampus? *Prog Histochem Cytochem*, **48**, 49.
- PRANGE-KIEL, J., WEHRENBURG, U., JARRY, H. & RUNE, G. M. 2003. Para/autocrine regulation of estrogen receptors in hippocampal neurons. *Hippocampus*, **13**, 226.
- PRIMUS, R. J. & KELLOGG, C. K. 1990. Gonadal hormones during puberty organize environment-related social interaction in the male rat. *Horm Behav*, **24**, 311.
- PROSSNITZ, E. R. & BARTON, M. 2014. Estrogen biology: New insights into GPER function and clinical opportunities. *Mol Cell Endocrinol*, **389**, 71.
- PUGA-OLGUÍN, A., RODRÍGUEZ-LANDA, J. F., ROVIROSA-HERNÁNDEZ, M. D. J., GERMÁN-PONCIANO, L. J., CABA, M., MEZA, E., GUILLÉN-RUIZ, G. & OLMOS-VÁZQUEZ, O. J. 2019. Long-term ovariectomy increases anxiety- and despair-like

behaviors associated with lower Fos immunoreactivity in the lateral septal nucleus in rats. *Behav Brain Res*, **360**, 185.

QIAN, S., YAN, S., PANG, R., ZHANG, J., LIU, K., SHI, Z., WANG, Z., CHEN, P., ZHANG, Y., LUO, T., HU, X., XIONG, Y. & ZHOU, Y. 2022. A temperature-regulated circuit for feeding behavior. *Nat Commun*, **13**, 4229.

QUIÑONES, A. R., CAMACHO-ABREGO, I., RIVERA, N. A., FLORES, G. & PICAZO, O. 2009. Morphological Changes Induced by the Absence of Ovarian Hormones in Nucleus Accumbens of Ovariectomized Rats. *Open Neuroendocrinol J*, **5**, 31.

RAINVILLE, J., POLLARD, K. & VASUDEVAN, N. 2015. Membrane-Initiated Non-Genomic Signaling by Estrogens in the Hypothalamus: Cross-Talk with Glucocorticoids with Implications for Behavior. *Front Endocrinol (Lausanne)*, **6**, 18.

RAJAGOPALAN, A., JINU, K. V., SAILESH, K. S., MISHRA, S., REDDY, U. K. & MUKKADAN, J. K. 2017. Understanding the links between vestibular and limbic systems regulating emotions. *J Nat Sci Bio Med*, **8**, 11.

RAMOS-ORTOLAZA, D. L., DORESTE-MENDEZ, R. J., ALVARADO-TORRES, J. K. & TORRES-REVERON, A. 2017. Ovarian hormones modify anxiety behavior and glucocorticoid receptors after chronic social isolation stress. *Behav Brain Res*, **328**, 115.

REMAGE-HEALEY, L., DONG, S., MAIDMENT, N. T. & SCHLINGER, B. A. 2011. Presynaptic Control of Rapid Estrogen Fluctuations in the Songbird Auditory Forebrain. *J Neurosci*, **31**, 10034.

REMAGE-HEALEY, L., MAIDMENT, N. T. & SCHLINGER, B. A. 2008. Forebrain steroid levels fluctuate rapidly during social interactions. *Nat Neurosci*, **11**, 1327.

RENCZES, E., BORBELYOVA, V., STEINHARDT, M., HOPFNER, T., STEHLE, T., OSTATNIKOVA, D. & CELEC, P. 2020. The Role of Estrogen in Anxiety-Like Behavior and Memory of Middle-Aged Female Rats. *Front Endocrinol (Lausanne)*, **11**, 570560.

REVANKAR, C. M., CIMINO, D. F., SKLAR, L. A., ARTERBURN, J. B. & PROSSNITZ, E. R. 2005. A transmembrane intracellular estrogen receptor mediates rapid cell signaling. *Science*, **307**, 1625.

RISHER, W. C., USTUNKAYA, T., SINGH ALVARADO, J. & EROGLU, C. 2014. Rapid Golgi Analysis Method for Efficient and Unbiased Classification of Dendritic Spines. *PLoS ONE*, **9**, e107591.

- RIVERA, H. M. & STINCIC, T. L. 2018. Estradiol and the control of feeding behavior. *Steroids*, **133**, 44.
- RODRÍGUEZ-LANDA, J. F. 2022. Considerations of Timing Post-ovariectomy in Mice and Rats in Studying Anxiety- and Depression-Like Behaviors Associated With Surgical Menopause in Women. *Front Behav Neurosci*, **16**, 829274.
- RODRIGUEZ-SIERRA, J. F. & TERASAWA, E. 1979. Lesions of the preoptic area facilitate lordosis behavior in male and female guinea pigs. *Brain Res Bull*, **4**, 513.
- ROMANÒ, N., LEE, K., ÁBRAHÁM, M. I., JASONI, C. L. & HERBISON, A. E. 2008. Non-classical estrogen modulation of presynaptic GABA terminals modulates calcium dynamics in gonadotropin-releasing hormone (GnRH) neurons. *Endocrinology*, **149**, 5335.
- ROSAS-ARELLANO, A., VILLALOBOS-GONZÁLEZ, J. B., PALMA-TIRADO, L., BELTRÁN, F. A., CÁRABEZ-TREJO, A., MISSIRLIS, F. & CASTRO, M. A. 2016. A simple solution for antibody signal enhancement in immunofluorescence and triple immunogold assays. *Histochem Cell Biol*, **146**, 421.
- ROSELLI, C. E. 1991. Sex Differences in Androgen Receptors and Aromatase Activity in Microdissected Regions of the Rat Brain. *Endocrinology*, **128**, 1310.
- ROSELLI, C. E. 1995. Subcellular localization and kinetic properties of aromatase activity in rat brain. *J Steroid Biochem Mol Biol*, **52**, 469.
- ROSELLI, C. E., ABDELGADIR, S. E., RØNNEKLEIV, O. K. & KLOSTERMAN, S. A. 1998. Anatomic distribution and regulation of aromatase gene expression in the rat brain. *Biol Reprod*, **58**, 79.
- ROSELLI, C. E., ELLINWOOD, W. E. & RESKO, J. A. 1984. Regulation of brain aromatase activity in rats. *Endocrinology*, **114**, 192.
- ROSELLI, C. E., HORTON, L. E. & RESKO, J. A. 1985. Distribution and regulation of aromatase activity in the rat hypothalamus and limbic system. *Endocrinology*, **117**, 2471.
- ROSELLI, C. E. & KLOSTERMAN, S. A. 1998. Sexual differentiation of aromatase activity in the rat brain: effects of perinatal steroid exposure. *Endocrinology*, **139**, 3193.
- ROY, E. J. & WADE, G. N. 1975. Role of estrogens in androgen-induced spontaneous activity in male rats. *J Comp Physiol Psychol*, **89**, 573.

- RUSSELL, A. J., MCCARTIN, S., CORCAO, G., BURRIDGE, S. M., MCBRIDE, M. W., MCNICOL, A. M., HAWES, C. S., MASON, J. I. & SUTCLIFFE, R. G. 1995. Variation in the expression of human 3 beta-hydroxysteroid dehydrogenase. *Endocr Res*, **21**, 485.
- SALDANHA, C. J., BURSTEIN, S. R. & DUNCAN, K. A. 2013. Induced synthesis of oestrogens by glia in the songbird brain. *J Neuroendocrinol*, **25**, 1032.
- SALDANHA, C. J., REMAGE-HEALEY, L. & SCHLINGER, B. A. 2011. Synaptocrine Signaling: Steroid Synthesis and Action at the Synapse. *Endocr Rev*, **32**, 532.
- SALDANHA, C. J., TUERK, M. J., KIM, Y.-H., FERNANDES, A. O., ARNOLD, A. P. & SCHLINGER, B. A. 2000. Distribution and regulation of telencephalic aromatase expression in the zebra finch revealed with a specific antibody. *The J Comp Neurol*, **423**, 619.
- SANO, K., TSUDA, M. C., MUSATOV, S., SAKAMOTO, T. & OGAWA, S. 2013. Differential effects of site-specific knockdown of estrogen receptor alpha in the medial amygdala, medial pre-optic area, and ventromedial nucleus of the hypothalamus on sexual and aggressive behavior of male mice. *Eur J Neurosci*, **37**, 1308.
- SANTOLLO, J. & DANIELS, D. 2015. Activation of G protein-coupled estrogen receptor 1 (GPER-1) decreases fluid intake in female rats. *Horm Behav*, **73**, 39.
- SATOH, Y., ENDO, S., NAKATA, T., KOBAYASHI, Y., YAMADA, K., IKEDA, T., TAKEUCHI, A., HIRAMOTO, T., WATANABE, Y. & KAZAMA, T. 2011. ERK2 Contributes to the Control of Social Behaviors in Mice. *J Neurosci*, **31**, 11953.
- SCHELLINO, R., TROVA, S., CIMINO, I., FARINETTI, A., JONGBLOETS, B. C., PASTERKAMP, R. J., PANZICA, G., GIACOBINI, P., DE MARCHIS, S. & PERETTO, P. 2016. Opposite-sex attraction in male mice requires testosterone-dependent regulation of adult olfactory bulb neurogenesis. *Sci Rep*, **6**, 36063.
- SCHLINGER, B. A. & ARNOLD, A. P. 1992. Circulating estrogens in a male songbird originate in the brain. *Proc Natl Acad Sci USA*, **89**, 7650.
- SCHLINGER, B. A., PRADHAN, D. S. & SOMA, K. K. 2008. 3 β -HSD activates DHEA in the songbird brain. *Neurochem Int*, **52**, 611.
- SCHLINGER, B. A., REMAGE-HEALEY, L. & RENSEL, M. 2014. Establishing regional specificity of neuroestrogen action. *Gen Comp Endocrinol*, **205**, 235.

- SCHMIDT, L. J., MURILLO, H. & TINDALL, D. J. 2004. Gene Expression in Prostate Cancer Cells Treated With the Dual 5 Alpha-Reductase Inhibitor Dutasteride. *J Androl*, **25**, 944.
- SCHOLL, J. L., AFZAL, A., FOX, L. C., WATT, M. J. & FORSTER, G. L. 2019. Sex differences in anxiety-like behaviors in rats. *Physiol Behav*, **211**, 112670.
- SCHULZ, K. M., MOLENDAS-FIGUEIRA, H. A. & SISK, C. L. 2009. Back to the future: The organizational–activational hypothesis adapted to puberty and adolescence. *Horm Behav*, **55**, 597.
- SCHULZ, K. M., RICHARDSON, H. N., ZEHR, J. L., OSETEK, A. J., MENARD, T. A. & SISK, C. L. 2004. Gonadal hormones masculinize and defeminize reproductive behaviors during puberty in the male Syrian hamster. *Horm Behav*, **45**, 242.
- SCHULZ, K. M. & SISK, C. L. 2006. Pubertal hormones, the adolescent brain, and the maturation of social behaviors: Lessons from the Syrian hamster. *Mol Cell Endocrinol*, **25**, 120.
- SCHULZ, K. M. & SISK, C. L. 2016. The organizing actions of adolescent gonadal steroid hormones on brain and behavioral development. *Neurosci Biobehav Rev*, **70**, 148.
- SCHUMACHER, M., GUENNOUN, R., MERCIER, G., DÉSARNAUD, F., LACOR, P., BÉNAVIDES, J., FERZAZ, B., ROBERT, F. & BAULIEU, E. E. 2001. Progesterone synthesis and myelin formation in peripheral nerves. *Brain Res Brain Res Rev*, **37**, 343.
- SCUDIERO, R. & VERDARAME, M. 2017. Gene expression profile of estrogen receptors alpha and beta in rat brain during aging and following high fat diet. *C R Biol*, **340**, 372.
- SELLAYAH, D., SEK, K., ANTHONY, F. W., HANSON, M. A. & CAGAMPANG, F. R. 2008. Sensitivity of housekeeping genes in the hypothalamus to mismatch in diets between pre- and postnatal periods in mice. *Neurosci Lett*, **447**, 54.
- SELLERS, K., RAVAL, P. & SRIVASTAVA, D. P. 2015. Molecular signature of rapid estrogen regulation of synaptic connectivity and cognition. *Front Neuroendocrinol*, **36**, 72.

- SEREDYNSKI, A. L., BALTHAZART, J., BALL, G. F. & CORNIL, C. A. 2015. Estrogen Receptor β Activation Rapidly Modulates Male Sexual Motivation through the Transactivation of Metabotropic Glutamate Receptor 1a. *J Neurosci*, **35**, 13110.
- SEREDYNSKI, A. L., BALTHAZART, J., CHRISTOPHE, V. J., BALL, G. F. & CORNIL, C. A. 2013. Neuroestrogens rapidly regulate sexual motivation but not performance. *J Neurosci*, **33**, 164.
- SHAY, D. A., VIEIRA-POTTER, V. J. & ROSENFELD, C. S. 2018. Sexually Dimorphic Effects of Aromatase on Neurobehavioral Responses. *Front Mol Neurosci*, **11**, 374.
- SHEPPARD, P. A. S., CHOLERIS, E. & GALEA, L. A. M. 2019. Structural plasticity of the hippocampus in response to estrogens in female rodents. *Mol Brain*, **12**, 22.
- SHEPPARD, P. A. S., KOSS, W. A., FRICK, K. M. & CHOLERIS, E. 2018. Rapid actions of oestrogens and their receptors on memory acquisition and consolidation in females. *J Neuroendocrinol*, **30**, e12485.
- SHIBUYA, K., TAKATA, N., HOJO, Y., FURUKAWA, A., YASUMATSU, N., KIMOTO, T., ENAMI, T., SUZUKI, K., TANABE, N., ISHII, H., MUKAI, H., TAKAHASHI, T., HATTORI, T. A. & KAWATO, S. 2003. Hippocampal cytochrome P450s synthesize brain neurosteroids which are paracrine neuromodulators of synaptic signal transduction. *Biochim Biophys Acta*, **1619**, 301.
- SHOLL, D. A. 1953. Dendritic organization in the neurons of the visual and motor cortices of the cat. *J Anat*, **87**, 387.
- SHUGHRUE, P. J., LANE, M. V. & MERCHENTHALER, I. 1997. Comparative distribution of estrogen receptor-alpha and -beta mRNA in the rat central nervous system. *J Comp Neurol*, **388**, 507.
- SHUGHRUE, P. J. & MERCHENTHALER, I. 2001. Distribution of estrogen receptor beta immunoreactivity in the rat central nervous system. *J Comp Neurol*, **436**, 64.
- SICKEL, M. J. & MCCARTHY, M. M. 2000. Calbindin-D28k immunoreactivity is a marker for a subdivision of the sexually dimorphic nucleus of the preoptic area of the rat: developmental profile and gonadal steroid modulation. *J Neuroendocrinol*, **12**, 397.
- SILVA, A. L., FRY, W. H. D., SWEENEY, C. & TRAINOR, B. C. 2010. Effects of photoperiod and experience on aggressive behavior in female California mice. *Behav Brain Res*, **208**, 528.

- SIMERLY, R. B. & SWANSON, L. W. 1986. The organization of neural inputs to the medial preoptic nucleus of the rat. *J Comp Neurol*, **246**, 312.
- SIMERLY, R. B., SWANSON, L. W., CHANG, C. & MURAMATSU, M. 1990. Distribution of androgen and estrogen receptor mRNA-containing cells in the rat brain: An in situ hybridization study. *J Comp Neurol*, **294**, 76.
- SKARRA, D. V., HERNÁNDEZ-CARRETERO, A., RIVERA, A. J., ANVAR, A. R. & THACKRAY, V. G. 2017. Hyperandrogenemia Induced by Letrozole Treatment of Pubertal Female Mice Results in Hyperinsulinemia Prior to Weight Gain and Insulin Resistance. *Endocrinology*, **158**, 2988.
- SMEJKALOVA, T. & WOOLLEY, C. S. 2010. Estradiol Acutely Potentiates Hippocampal Excitatory Synaptic Transmission through a Presynaptic Mechanism. *J Neurosci*, **30**, 16137.
- SOMA, K. K., ALDAY, N. A., HAU, M. & SCHLINGER, B. A. 2004. Dehydroepiandrosterone metabolism by 3beta-hydroxysteroid dehydrogenase/Delta5-Delta4 isomerase in adult zebra finch brain: sex difference and rapid effect of stress. *Endocrinology*, **145**, 1668.
- SOMA, K. K., SINCHAK, K., LAKHTER, A., SCHLINGER, B. A. & MICEVYCH, P. E. 2005. Neurosteroids and Female Reproduction: Estrogen Increases 3 β -HSD mRNA and Activity in Rat Hypothalamus. *Endocrinology*, **146**, 4386.
- SONG, D., HE, H., INDUKURI, R., HUANG, Z., STEPANAUSKAITE, L., SINHA, I., HALDOSÉN, L.-A., ZHAO, C. & WILLIAMS, C. 2022. ER α and ER β Homodimers in the Same Cellular Context Regulate Distinct Transcriptomes and Functions. *Front Endocrinol (Lausanne)*, **13**, 930227.
- SONNWEBER, R., STEVENS, J. M. G., HOHMANN, G., DESCHNER, T. & BEHRINGER, V. 2022. Plasma Testosterone and Androstenedione Levels Follow the Same Sex-Specific Patterns in the Two Pan Species. *Biology*, **11**, 1275.
- SPITERI, T., OGAWA, S., MUSATOV, S., PFAFF, D. W. & AGMO, A. 2012. The role of the estrogen receptor α in the medial preoptic area in sexual incentive motivation, proceptivity and receptivity, anxiety, and wheel running in female rats. *Behav Brain Res*, **230**, 11.
- SRIVASTAVA, D. P., WOOLFREY, K. M., LIU, F., BRANDON, N. J. & PENZES, P. 2010. Estrogen receptor ss activity modulates synaptic signaling and structure. *J Neurosci*, **30**, 13454.

- STANIC, D., DUBOIS, S., CHUA, H. K., TONGE, B., RINEHART, N., HORNE, M. K. & BOON, W. C. 2014. Characterization of aromatase expression in the adult male and female mouse brain. I. Coexistence with oestrogen receptors alpha and beta, and androgen receptors. *PLoS One*, **9**, e90451.
- STEERS, W. D. 2001. 5alpha-reductase activity in the prostate. *Urology*, **58**, 17.
- STOCCO, C. 2008. Aromatase Expression in the Ovary: Hormonal and Molecular Regulation. *Steroids*, **73**, 473.
- STROBER, W. 2001. Trypan Blue Exclusion Test of Cell Viability. *Curr Protoc Immunol*, **21**, p. A.3B.1-A.3B.2.
- STRÖMSTEDT, M. & WATERMAN, M. R. 1995. Messenger RNAs encoding steroidogenic enzymes are expressed in rodent brain. *Mol Brain Res*, **34**, 75.
- SUNDIN, M., WARNER, M., HAAPARANTA, T. & GUSTAFSSON, J. Å. 1987. Isolation and catalytic activity of cytochrome P-450 from ventral prostate of control rats. *J Biol Chem*, **262**, 12293.
- SUZUKI, K. & HANDA, R. J. 2005. Estrogen receptor-beta, but not estrogen receptor-alpha, is expressed in prolactin neurons of the female rat paraventricular and supraoptic nuclei: comparison with other neuropeptides. *J Comp Neurol*, **484**, 28.
- SZE, Y., GILL, A. C. & BRUNTON, P. J. 2018. Sex-dependent changes in neuroactive steroid concentrations in the rat brain following acute swim stress. *J Neuroendocrinol*, **30**, e12644.
- TABATADZE, N., SATO, S. M. & WOOLLEY, C. S. 2014. Quantitative analysis of long-form aromatase mRNA in the male and female rat brain. *PLoS One*, **9**, e100628.
- TAKASE, M., UKENA, K. & TSUTSUI, K. 2002. Expression and localization of cytochrome P45011 β ,aldo mRNA in the frog brain. *Brain Res*, **950**, 288.
- TAKEO, T., CHIBA, Y. & SAKUMA, Y. 1993. Suppression of the lordosis reflex of female rats by efferents of the medial preoptic area. *Physiol Behav*, **53**, 831.
- TAMRAZI, A., CARLSON, K. E., DANIELS, J. R., HURTH, K. M. & KATZENELLENBOGEN, B. S. 2002. Estrogen Receptor Dimerization: Ligand Binding Regulates Dimer Affinity and Dimer Dissociation Rate. *Mol Endocrinol*, **16**, 2706.
- TANABE, H., MUTAI, H., SASAYAMA, D., SASAMOTO, H., MIYASHIRO, Y., SUGIYAMA, N. & WASHIZUKA, S. 2021. Sex differences in serum levels of 5 α -

- androstane-3 β , 17 β -diol, and androstenediol in the young adults: A liquid chromatography–tandem mass spectrometry study. *PLoS One*, **16**, e0261440.
- TANG, H., ZHANG, Q., YANG, L., DONG, Y., KHAN, M., YANG, F., BRANN, D. W. & WANG, R. 2014. GPR30 mediates estrogen rapid signaling and neuroprotection. *Mol Cell Endocrinol*, **387**, 52.
- TAZIAUX, M., KELLER, M., BAKKER, J. & BALTHAZART, J. 2007. Sexual Behavior Activity Tracks Rapid Changes in Brain Estrogen Concentrations. *J Neurosci*, **27**, 6563.
- TERASHIMA, M., TODA, K., KAWAMOTO, T., KURIBAYASHI, I., OGAWA, Y., MAEDA, T. & SHIZUTA, Y. 1991. Isolation of a full-length cDNA encoding mouse aromatase P450. *Arch Biochem Biophys*, **285**, 231.
- THOMAS, C. N. & GERALL, A. A. 1969. Effect of hour of operation on feminization of neonatally castrated male rats. *Psychon Sci*, **16**, 19.
- THOMAS, M. P. & POTTER, B. V. L. 2013. The structural biology of oestrogen metabolism. *J Steroid Biochem Mol Biol*, **137**, 27.
- THOMAS, P., PANG, Y., FILARDO, E. J. & DONG, J. 2005. Identity of an estrogen membrane receptor coupled to a G protein in human breast cancer cells. *Endocrinology*, **146**, 624.
- TITUS, M. A., LI, Y., KOZYREVA, O. G., MAHER, V., GODOY, A., SMITH, G. J. & MOHLER, J. L. 2014. 5 α -reductase type 3 enzyme in benign and malignant prostate. *Prostate*, **74**, 235.
- TODA, K., SAIBARA, T., OKADA, T., ONISHI, S. & SHIZUTA, Y. 2001. A loss of aggressive behaviour and its reinstatement by oestrogen in mice lacking the aromatase gene (Cyp19). *J Endocrinol*, **168**, 217.
- TOMIHARA, K., SOGA, T., NOMURA, M., KORACH, K. S., GUSTAFSSON, J. Å., PFAFF, D. W. & OGAWA, S. 2009. Effect of ER-beta gene disruption on estrogenic regulation of anxiety in female mice. *Physiol Behav*, **96**, 300.
- TORAN-ALLERAND, C. D. 2004. Minireview: A Plethora of Estrogen Receptors in the Brain: Where Will It End? *Endocrinology*, **145**, 1069.
- TRAINOR, B. C., BIRD, I. M. & MARLER, C. A. 2004. Opposing hormonal mechanisms of aggression revealed through short-lived testosterone manipulations and multiple winning experiences. *Horm Behav*, **45**, 115.

- TRAINOR, B. C., FINY, M. S. & NELSON, R. J. 2008a. Paternal aggression in a biparental mouse: Parallels with maternal aggression. *Horm Behav*, **53**, 200.
- TRAINOR, B. C., GREIWE, K. M. & NELSON, R. J. 2006. Individual differences in estrogen receptor α in select brain nuclei are associated with individual differences in aggression. *Horm Behav*, **50**, 338.
- TRAINOR, B. C., LIN, S., FINY*, M. S., ROWLAND, M. R. & NELSON, R. J. 2007a. Photoperiod reverses the effects of estrogens on male aggression via genomic and nongenomic pathways. *Proc Natl Acad Sci USA*, **104**, 9840.
- TRAINOR, B. C., ROWLAND, M. R. & NELSON, R. J. 2007b. Photoperiod affects estrogen receptor α , estrogen receptor β and aggressive behavior. *Eur J Neurosci*, **26**, 207.
- TRAINOR, B. C., SIMA FINY, M. & NELSON, R. J. 2008b. Rapid effects of estradiol on male aggression depend on photoperiod in reproductively non-responsive mice. *Horm Behav*, **53**, 192.
- TSIEN, J. Z., CHEN, D. F., GERBER, D., TOM, C., MERCER, E. H., ANDERSON, D. J., MAYFORD, M., KANDEL, E. R. & TONEGAWA, S. 1996. Subregion- and Cell Type–Restricted Gene Knockout in Mouse Brain. *Cell*, **87**, 1317.
- TSUDA, M. C. & OGAWA, S. 2012. Long-Lasting Consequences of Neonatal Maternal Separation on Social Behaviors in Ovariectomized Female Mice. *PLoS One*, **7**, e33028.
- TSUNEOKA, Y., MARUYAMA, T., YOSHIDA, S., NISHIMORI, K., KATO, T., NUMAN, M. & KURODA, K. O. 2013. Functional, anatomical, and neurochemical differentiation of medial preoptic area subregions in relation to maternal behavior in the mouse. *J Comp Neurol*, **521**, 1633.
- TSURUO, Y., ISHIMURA, K. & OSAWA, Y. 1995. Presence of estrogen receptors in aromatase-immunoreactive neurons in the mouse brain. *Neurosci Lett*, **195**, 49.
- TUSCHER, J. J., SZINTE, J. S., STARRETT, J. R., KRENTZEL, A. A., FORTRESS, A. M., REMAGE-HEALEY, L. & FRICK, K. M. 2016. Inhibition of local estrogen synthesis in the hippocampus impairs hippocampal memory consolidation in ovariectomized female mice. *Horm Behav*, **83**, 60.

- UBUKA, T., HARAGUCHI, S., TOBARI, Y., NARIHIRO, M., ISHIKAWA, K., HAYASHI, T., HARADA, N. & TSUTSUI, K. 2014. Hypothalamic inhibition of socio-sexual behaviour by increasing neuroestrogen synthesis. *Nat Commun*, **5**, 3061.
- UDDIN, M. M., IBRAHIM, M. M. H. & BRISKI, K. P. 2020. Sex-dimorphic neuroestradiol regulation of ventromedial hypothalamic nucleus glucoregulatory transmitter and glycogen metabolism enzyme protein expression in the rat. *BMC Neurosci*, **21**, 51.
- UKENA, K., HONDA, Y., INAI, Y., KOHCHI, C., LEA, R. W. & TSUTSUI, K. 1999. Expression and activity of 3beta-hydroxysteroid dehydrogenase/Delta5-Delta4-isomerase in different regions of the avian brain. *Brain Res*, **818**, 536.
- UNGER, E. K., BURKE, K. J., JR., YANG, C. F., BENDER, K. J., FULLER, P. M. & SHAH, N. M. 2015. Medial amygdalar aromatase neurons regulate aggression in both sexes. *Cell Rep*, **10**, 453.
- VAHABA, D. M. & REMAGE-HEALEY, L. 2018. Neuroestrogens rapidly shape auditory circuits to support communication learning and perception: Evidence from songbirds. *Horm Behav*, **104**, 77.
- VELÁZQUEZ-ZAMORA, D. A., GONZÁLEZ-TAPIA, D., GONZÁLEZ-RAMÍREZ, M. M., FLORES-SOTO, M. E., VÁZQUEZ-VALLS, E., CERVANTES, M. & GONZÁLEZ-BURGOS, I. 2012. Plastic changes in dendritic spines of hippocampal CA1 pyramidal neurons from ovariectomized rats after estradiol treatment. *Brain Res*, **1470**, 1.
- VERTES, R. P. & HOOVER, W. B. 2008. Projections of the paraventricular and paratenial nuclei of the dorsal midline thalamus in the rat. *J Comp Neurol*, **508**, 212.
- WADE, C. B., ROBINSON, S., SHAPIRO, R. A. & DORSA, D. M. 2001. Estrogen receptor (ER)alpha and ERbeta exhibit unique pharmacologic properties when coupled to activation of the mitogen-activated protein kinase pathway. *Endocrinology*, **142**, 2336.
- WALF, A. A. & FRYE, C. A. 2006. A Review and Update of Mechanisms of Estrogen in the Hippocampus and Amygdala for Anxiety and Depression Behavior. *Neuropsychopharmacology*, **31**, 1097.
- WALLACE, M., LUINE, V., ARELLANOS, A. & FRANKFURT, M. 2006. Ovariectomized rats show decreased recognition memory and spine density in the hippocampus and prefrontal cortex. *Brain Res*, **1126**, 176.

- WANG, A., ZOU, X., WU, J., MA, Q., YUAN, N., DING, F., LI, X. & CHEN, J. 2020. Early-Life Stress Alters Synaptic Plasticity and mTOR Signaling: Correlation With Anxiety-Like and Cognition-Related Behavior. *Front Genet*, **11**, 590068.
- WANG, J., PRATAP, U. P., LU, Y., SAREDDY, G. R., TEKMAL, R. R., VADLAMUDI, R. K. & BRANN, D. W. 2023. Development and Characterization of Inducible Astrocyte-Specific Aromatase Knockout Mice. *Biology (Basel)*, **12**, 621.
- WANG, W., LE, A. A., HOU, B., LAUTERBORN, J. C., COX, C. D., LEVIN, E. R., LYNCH, G. & GALL, C. M. 2018. Memory-Related Synaptic Plasticity Is Sexually Dimorphic in Rodent Hippocampus. *J Neurosci*, **38**, 7935.
- WANG, Z., HU, L., SALARI, K., BECHIS, S. K., GE, R., WU, S., RASSOULIAN, C., PHAM, J., WU, C.-L., TABATABAEI, S., STRAND, D. W. & OLUMI, A. F. 2017. Androgenic to oestrogenic switch in the human adult prostate gland is regulated by epigenetic silencing of steroid 5 α -reductase 2. *The J Pathol*, **243**, 457.
- WARDELL, S. E., MARKS, J. R. & MCDONNELL, D. P. 2011. The turnover of estrogen receptor α by the selective estrogen receptor degrader (SERD) fulvestrant is a saturable process that is not required for antagonist efficacy. *Biochem Pharmacol*, **82**, 122.
- WARTENBERG, P., FARKAS, I., CSILLAG, V., COLLEDGE, W. H., HRABOVSKY, E. & BOEHM, U. 2021. Sexually dimorphic neurosteroid synthesis regulates neuronal activity in the murine brain. *J Neurosci*, **41**, 9177.
- WATAI, K., TSUDA, M., NAKATA, M., TODA, K. & OGAWA, S. 2007. Analyses of running wheel activity (RWA) in aromatase-knockout (ArKO) mice. *Neurosci Res*, **58**, S108.
- WATERS, E. M. & SIMERLY, R. B. 2009. Estrogen Induces Caspase-Dependent Cell Death during Hypothalamic Development. *J Neurosci*, **29**, 9714.
- WATTERS, J. J., CAMPBELL, J. S., CUNNINGHAM, M. J., KREBS, E. G. & DORSA, D. M. 1997. Rapid Membrane Effects of Steroids in Neuroblastoma Cells: Effects of Estrogen on Mitogen Activated Protein Kinase Signalling Cascade and c-fos Immediate Early Gene Transcription. *Endocrinology*, **138**, 4030.
- WEHRENBURG, U., PRANGE-KIEL, J. & RONE, G. M. 2001. Steroidogenic factor-1 expression in marmoset and rat hippocampus: co-localization with StAR and aromatase. *J Neurochem*, **76**, 1879.

- WEI, D., OSAKADA, T., GUO, Z., YAMAGUCHI, T., VARSHNEYA, A., YAN, R., JIANG, Y. & LIN, D. 2023. A hypothalamic pathway that suppresses aggression toward superior opponents. *Nat Neurosci*, **26**, 774.
- WEI, D., TALWAR, V. & LIN, D. 2021. Neural circuits of social behaviors: Innate yet flexible. *Neuron*, **109**, 1600.
- WEI, Y.-C., WANG, S.-R., JIAO, Z.-L., ZHANG, W., LIN, J.-K., LI, X.-Y., LI, S.-S., ZHANG, X. & XU, X.-H. 2018. Medial preoptic area in mice is capable of mediating sexually dimorphic behaviors regardless of gender. *Nat Commun*, **9**, 279.
- WEIHUA, Z., LATHE, R., WARNER, M. & GUSTAFSSON, J. A. 2002. An endocrine pathway in the prostate, ER , AR, 5 -androstane-3 ,17 -diol, and CYP7B1, regulates prostate growth. *Proc Natl Acad Sci USA*, **99**, 13589.
- WEISER, M. J. & HANDA, R. J. 2009. Estrogen impairs glucocorticoid dependent negative feedback on the hypothalamic–pituitary–adrenal axis via estrogen receptor alpha within the hypothalamus. *Neuroscience*, **159**, 883.
- WEISER, M. J., WU, T. J. & HANDA, R. J. 2009. Estrogen Receptor- β Agonist Diarylpropionitrile: Biological Activities of R- and S-Enantiomers on Behavior and Hormonal Response to Stress. *Endocrinology*, **150**, 1817.
- WERSINGER, S. R. & RISSMAN, E. F. 2001. Oestrogen Receptor α is Essential for Female-Directed Chemo-Investigatory Behaviour but is not Required for the Pheromone-Induced Luteinizing Hormone Surge in Male Mice. *J Neuroendocrinol*, **12**, 103.
- WHIRLEDGE, S. & CIDLOWSKI, J. A. 2013. A Role for Glucocorticoids in Stress-Impaired Reproduction: Beyond the Hypothalamus and Pituitary. *Endocrinology*, **154**, 4450.
- WILSON, C. A. & DAVIES, D. C. 2007. The control of sexual differentiation of the reproductive system and brain. *Reproduction*, **133**, 331.
- WISE, P. M. & RATNER, A. 1980. Effect of ovariectomy on plasma LH, FSH, estradiol, and progesterone and medial basal hypothalamic LHRH concentrations old and young rats. *Neuroendocrinology*, **30**, 15.
- WOOD, R. I. & NEWMAN, S. W. 1995. Androgen and estrogen receptors coexist within individual neurons in the brain of the Syrian hamster. *Neuroendocrinology*, **62**, 487.

- WOODWARD, E. M., RINGLAND, A., ACKERMAN, J. & COUTELLIER, L. 2023. Prepubertal ovariectomy confers resilience to stress-induced anxiety in adult female mice. *Psychoneuroendocrinology*, **148**, 105997.
- WOOLLEY, C. & MCEWEN, B. 1992. Estradiol mediates fluctuation in hippocampal synapse density during the estrous cycle in the adult rat [published erratum appears in *J Neurosci* 1992 Oct;12(10):following table of contents]. *J Neurosci*, **12**, 2549.
- WOOLLEY, C. S. & MCEWEN, B. S. 1993. Roles of estradiol and progesterone in regulation of hippocampal dendritic spine density during the estrous cycle in the rat. *J Comp Neurol*, **336**, 293.
- WU, C. & ZETTER, M. A. 2022. Role of the hypothalamic paraventricular nucleus in anxiety disorders. *Stress and Brain*, **2**, 53.
- WU, M. V., MANOLI, D. S., FRASER, E. J., COATS, J. K., TOLLKUHN, J., HONDA, S., HARADA, N. & SHAH, N. M. 2009. Estrogen masculinizes neural pathways and sex-specific behaviors. *Cell*, **139**, 61.
- WU, M. V. & TOLLKUHN, J. 2017. Estrogen receptor alpha is required in GABAergic, but not glutamatergic, neurons to masculinize behavior. *Horm Behav*, **95**, 3.
- XU, Y., THEKKETHIL, ZHU, L., SOBHANI, N., BOMAN, KATHRYN, ZHANG, X., ZOU, F., LANA, LISA, SOHAIB, CAROL, JOEL & DEBORAH 2011. Distinct Hypothalamic Neurons Mediate Estrogenic Effects on Energy Homeostasis and Reproduction. *Cell Metab*, **14**, 453.
- YAMAGUCHI, S., ABE, Y., MAEJIMA, S. & TSUKAHARA, S. 2018. Sexual experience reduces neuronal activity in the central part of the medial preoptic nucleus in male rats during sexual behavior. *Neurosci Lett*, **685**, 155].
- YAMANA, K., LABRIE, F. & LUU-THE, V. 2010. Human type 3 5 α -reductase is expressed in peripheral tissues at higher levels than types 1 and 2 and its activity is potently inhibited by finasteride and dutasteride. *Horm Mol Biol Clin Investig*, **2**, 293.
- YANG, C. F., CHIANG, M., GRAY, D. C., PRABHAKARAN, M., ALVARADO, M., JUNTTI, S. A., UNGER, E. K., WELLS, J. A. & SHAH, N. M. 2013. Sexually dimorphic neurons in the ventromedial hypothalamus govern mating in both sexes and aggression in males. *Cell*, **153**, 896.
- YANG, C. F. & SHAH, N. M. 2014. Representing Sex in the Brain, One Module at a Time. *Neuron*, **82**, 261.

- YI, P., DRISCOLL, M. D., HUANG, J., BHAGAT, S., HILF, R., BAMBARA, R. A. & MUYAN, M. 2002. The Effects of Estrogen-Responsive Element- and Ligand-Induced Structural Changes on the Recruitment of Cofactors and Transcriptional Responses by ER α and ER β . *Mol Endocrinol*, **16**, 674.
- YILMAZ, M. B., WOLFE, A., CHENG, Y. H., GLIDEWELL-KENNEY, C., JAMESON, J. L. & BULUN, S. E. 2009. Aromatase promoter 1.f is regulated by estrogen receptor alpha (ESR1) in mouse hypothalamic neuronal cell lines. *Biol Reprod*, **81**, 956.
- YILMAZ, M. B., WOLFE, A., ZHAO, H., BROOKS, D. C. & BULUN, S. E. 2011. Aromatase promoter 1.f is regulated by progesterone receptor in mouse hypothalamic neuronal cell lines. *J Mol Endocrinol*, **47**, 69.
- YOKOSUKA, M., OKAMURA, H. & HAYASHI, S. 1997. Postnatal development and sex difference in neurons containing estrogen receptor-alpha immunoreactivity in the preoptic brain, the diencephalon, and the amygdala in the rat. *J Comp Neurol*, **389**, 81.
- YOUSEFVAND, S. & HAMIDI, F. 2020. Role of Paraventricular Nucleus in Regulation of Feeding Behaviour and the Design of Intranuclear Neuronal Pathway Communications. *Int J Peptide Res Ther*, **26**, 1231.
- ZEHR, J. L., TODD, B. J., SCHULZ, K. M., MCCARTHY, M. M. & SISK, C. L. 2006. Dendritic pruning of the medial amygdala during pubertal development of the male Syrian hamster. *J Neurobiol*, **66**, 578.
- ZHANG, G.-W., SHEN, L., TAO, C., JUNG, A. H., PENG, B., LI, Z., ZHANG, L. I. & TAO, H. W. 2021. Medial preoptic area antagonistically mediates stress-induced anxiety and parental behavior. *Nat Neurosci*, **24**, 516.
- ZHANG, J.-Q., CAI, W.-Q., ZHOU, D.-S. & SU, B.-Y. 2002. Distribution and differences of estrogen receptor beta immunoreactivity in the brain of adult male and female rats. *Brain Res*, **935**, 73.
- ZHAO, C., FUJINAGA, R., TANAKA, M., YANAI, A., NAKAHAMA, K. & SHINODA, K. 2007. Region-specific expression and sex-steroidal regulation on aromatase and its mRNA in the male rat brain: immunohistochemical and in situ hybridization analyses. *J Comp Neurol*, **500**, 557.
- ZHAO, H., TIAN, Z., HAO, J. & CHEN, B. 2005. Extragonadal aromatization increases with time after ovariectomy in rats. *Reprod Biol Endocrinol*, **3**, 6.

- ZHAO, J., BIAN, C., LIU, M., ZHAO, Y., SUN, T., XING, F. & ZHANG, J. 2018. Orchiectomy and letrozole differentially regulate synaptic plasticity and spatial memory in a manner that is mediated by SRC-1 in the hippocampus of male mice. *J Steroid Biochem Mol Biol*, **178**, 354.
- ZHOU, D., CLARKE, P., WANG, J. & CHEN, S. 1996. Identification of a Promoter That Controls Aromatase Expression in Human Breast Cancer and Adipose Stromal Cells. *J Biol Chem*, **271**, 15194.
- ZHOU, L., FESTER, L., VON BLITTERSDORFF, B., HASSU, B., NOGENS, H., PRANGE-KIEL, J., JARRY, H., WEGSCHEIDER, K. & RUNE, G. M. 2010. Aromatase inhibitors induce spine synapse loss in the hippocampus of ovariectomized mice. *Endocrinology*, **151**, 1153.
- ZHU, Y.-S. & SUN, G.-H. 2005. 5 α -Reductase Isozymes in the Prostate. *J Med Sci*, **25**, 1.
- ZULOAGA, D. G., ZULOAGA, K. L., HINDS, L. R., CARBONE, D. L. & HANDA, R. J. 2014. Estrogen receptor β expression in the mouse forebrain: Age and sex differences. *J Comp Neurol*, **522**, 358.
- ZWAIN, I. H. & YEN, S. S. C. 1999. Neurosteroidogenesis in Astrocytes, Oligodendrocytes, and Neurons of Cerebral Cortex of Rat Brain. *Endocrinology*, **140**, 3843.